The flux of extraterrestrial matter to Earth as recorded in Paleogene and Middle Ordovician marine sediments

Cronholm, Anders

2009

LITHOLUND theses No. 17

DOCTORAL THESIS

The flux of extraterrestrial matter to Earth as recorded in Paleogene and Middle Ordovician marine sediments

Anders Cronholm

LUND UNIVERSITY
DEPARTMENT OF GEOLOGY

Akademisk avhandling som med vederbörligt tillstånd från naturvetenskapliga fakulteten vid Lunds universitet för avläggande av filosofie doktorsexamen, offentligen försvaras i Lund, 3 juni 2009

"Nothing shocks me

- I'm a scientist!"

Dr. H. W. Jones, Jr.

CONTENTS

ABSTRACT

This thesis aims at reconstructing events in the solar system, mainly collisional events in the asteroid belt, by searches for extraterrestrial minerals in Paleogene and Middle Ordovician marine sediments on Earth. Recent empirical evidence show that Earth has experienced a few brief periods during the Phanerozoic when the flux of extraterrestrial matter significantly increased. The most prominent of these occurred at approximately 470 Ma, as a consequence of the massive break-up of the L-chondrite parent body in the asteroid belt. The finds of more than 87 fossil L chondritic meteorites (Ø = 1-21 cm) in mid-Ordovician strata at Thorsberg, Kinnekulle, give testimony to the spectacular flux of meteorites that followed the break-up event. The fossil meteorites are almost completely pseudomorphed, with the exception of chromite, an exceptionally resistant accessory mineral (~0.25 wt%) in ordinary chondrites. Extraterrestrial chromite (EC) is distributed in the immediate surrounding limestones beds of the fossil L chondrites, indicating that most meteorites that reached the sea floor were dissolved, dispersing the EC grains in the contiguous sediments. The distribution of EC has previously been studied at mid-Ordovician sections in Sweden.

The goals of this thesis are threefold: (1) establish the normal background distribution of EC to corroborate the extraordinary circumstances recorded during the mid-Ordovician; (2) investigate the global pattern of the EC distribution during the mid-Ordovician, by studying a remote site; (3) study variations in the marine osmium isotope ($^{187}Os/^{188}Os$) record across the EC-rich interval at Hällekis, Kinnekulle.

The Paleogene marine sediments at Gubbio and Massignano, Italy, were analysed for EC content, yielding 7 EC in a total of 377 kg whole-rock (0.019 EC kg^{-1}). This result is very similar to previously studied mid-Ordovician strata, forming prior to the L-chondritic breaking event, in Sweden and China (0.009-0.013 EC kg^{-1}). In addition, the low EC content at Massignano contradicts a proposed ordinary (L) chondritic meteorite shower in the late Eocene.

The general trend in the distribution of sediment-dispersed EC in Swedish strata during the mid-Ordovician has been reproduced in the coeval stratigraphic interval at Puxi River, central China. At this time, the Chinese section was positioned at mid-latitudes on the southern hemisphere, a few 1000 km east of the Swedish sites. The EC-rich interval at Puxi typically has 1-4 EC grains per kg rock, equivalent to previous results for coeval Swedish limestone. Consequently, a global correlation has been established for the EC distribution across the Arenig-Llanvirn transition. A close temporal correlation has also been suggested for the main phase of the Great Ordovician Biodiversification Event and the disruption of the L-chondrite parent body at ~470 Ma, based on bed-by-bed records of EC, $^{187}Os/^{188}Os$ and invertebrate fossils in Middle Ordovician sediments in Baltoscandia and China. The intense species radiation and level of change in biodiversity of this event changed the biological composition of the Earth's oceans forever. The causes of the event remain elusive, although influences of extraterrestrial origin cannot be excluded, and further studies are warranted. At Hällekis, the first appearance of common EC grains is marked by a negative $^{187}Os/^{188}Os$ excursion in the strata, verifying an increased influence of unradiogenic osmium. This source is most likely extraterrestrial in origin, as corroborated by stable strontium isotope ratios from late Arenig to early Llanvirn.

In all, 665 kg of Paleogene and Middle Ordovician sediments from Italy and China has been searched for EC grains in this thesis work. The composite background material from the Italian and Chinese sections represents 487 kg of rock, and yielded only 8 EC altogether. The EC-rich Ordovician interval, representing the sequential *L. variabilis*, *Y. crassus* and *M. hagetiana* conodont zones, yielded a total of 290 EC grains in 178 kg of limestone, signifying an average 1.63 EC per kg rock. This clearly shows a two orders-of-magnitude increase in the flux of L-chondritic matter during the mid-Ordovician. In conclusion, the largest documented break-up event in the asteroid belt has left a prominent signature in the coeval sediments on Earth, and this thesis corroborates the significance and global consequences of this event.

POPULÄRVETENSKAPLIG SAMMANFATTNING (POPULAR SUMMARY IN SWEDISH)

Denna avhandling behandlar en unik period i jordens historia då det kosmiska inflödet till jorden, under en geologiskt sett kort tid på cirka 1-3 miljoner år, var omkring hundra gånger större än normalt. De konkreta bevisen för en sådan period är exceptionella fynd av fossila meteoriter i kalksten från Kinnekulle.

Under mellan-ordovicium, för cirka 470 miljoner år sedan, inträffade den största explosionen i asteroidbältet under de senaste tre miljarder åren, då den cirka 200 km stora L-kondritiska *föräldra-kroppen* (dvs. källan till alla L-kondriter) splittrades efter en kollision med ett okänt kosmiskt föremål. Resultatet av denna förödande sammanstötning blev att stora mängder materia slungades ut i solsystemet, varpå jorden utsattes för ett intensivt bombardemang av mikrometeoriter, meteoriter och även asteroider under de följande en till tre miljoner åren. Konkreta bevis för att händelsen ägt rum består bl. a. av mer än 87 fossila L-kondritiska meteoriter (diameter: 1-21 cm) funna i ett avgränsat lager av mellan-ordovicisk kalksten i Thorsberg stenbrottet på Kinnekulle. Beräkningar visar att tillförseln av kosmiskt material under denna period var cirka 100 gånger högre än idag.

Den kosmiska katastrofen för cirka 470 miljoner år sedan lämnade distinkta spår efter sig, i form av mängder av fossila meteoriter som bevarats i långsamt avsatta havssediment. Alla meteoriterna har blivit så gott som helt omvandlade till lermineral och kalcit, med undantag av svarta, mikroskopiska korn av kromit (cirka 0,1 mm i diameter). Kromit är ett accessoriskt mineral i vanliga kondriter (cirka 0,25 %) och är väldigt motståndskraftigt mot vittringsprocesser. Man finner även utomjordisk kromit fritt i den kalksten som innehåller de fossila L-kondriterna. Detta tyder på att de flesta meteoriterna inte bevarades, utan löstes snabbt upp och spred utomjordisk kromit i sedimenten.

Under passagen genom jordens atmosfär förångas en stor del av meteoriterna och när dessa gaspartiklar sedan kyls ner igen, bildas nya små partiklar, så kallade *kosmiska sfäruler*. Dessa rundade eller droppformade partiklar kan enkelt skiljas från kantiga utomjordiska kromitkorn på basis av deras kemiska sammansättning. På liknande sätt skiljer man även vanlig kromit på jorden från utomjordisk kromit. Noggranna undersökningar efter utomjordisk kromit har tidigare genomförts i mellan-ordoviciska lagerföljder vid Hällekis och Thorsberg (Kinnekulle, Västergötaland), samt Komstad och Fågelsång (Skåne) av andra forskare inom vår grupp.

METEORIT

Definitionen av en *meteorit* är; en meteorid (dvs. en rymdsten) som lyckas nå jordens yta utan att helt förångas av den värme som uppstår när den passerar genom atmosfären. De flesta meteoriter har sitt ursprung i asteroidbältet mellan Mars och Jupiter. Det består av en mängd olika typer av oregelbundet formade stenblock (diameter: <1 mm till cirka 1000 km) vilka kretsar i en bana runt Solen. Dessa meteorider och asteroider bildades för ungefär 4,6 miljarder år sedan och är den äldst bevarade materian i solsystemet. De flesta tillhör gruppen *vanliga kondriter* vilket också är den vanligaste typen av meteoriter som faller ner på jorden idag (cirka 87 %). De vanliga kondriterna delas vidare in i tre undergrupper, *H*, *L* och *LL*, där innehållet av järn och övriga metaller minskar från H till L till LL. Meteoriter och så kallade *mikrometeoriter* (<1 mm) är småbitar och stoft från kollisioner som fortfarande sker mellan meteorider och asteroider, medan mindre partiklar (<0,02 mm) främst kommer från passerande kometer. Varje år når ungefär 30.000 ton kosmisk materia jordens yta, och största delen av detta består av partiklar <1 mm. Ny forskning visar att det under de senaste 500 miljoner åren funnits några korta perioder med kraftigt ökat inflöde av kosmiskt material till jorden, dvs. under sen eocen (cirka 35 miljoner år sedan), vid krita-paleogen (K-T) gränsen (cirka 65,5 miljoner år sedan) och, som nämnts ovan, under mellan-ordovicium (cirka 470 miljoner år sedan).

Vid undersökningar av den kalksten som bildats före det stora uppbrottet har man funnit sammanlagt 5 utomjordiska kromitkorn i 542 kg sten, medan prover med en total vikt av 282 kg från det ovanliggande, kromit-rika intervallet innehåller mellan 1-5 kromitkorn per kg kalksten. Genom att analysera den kemiska sammansättningen hos utomjordiska kromitkorn, samt hos inklusioner (<0,01 mm stora mineralpartiklar) i kornen, har de lyckats bestämma kornens ursprung som L-kondritiskt. Även andra typer av geokemiska analyser har använts för att härleda de fossila meteoriterna till uppbrottet för cirka 470 miljoner år sedan, som t ex syreisotoper och exponeringstider som kornen varit utsatta för kosmisk strålning.

Denna avhandling är uppdelad i flera delprojekt och nedan följer en sammanfattning av de viktigaste resultat som uppnåtts och de tolkningar som gjorts utifrån dessa.

De första grundläggande studierna bestod i att uppskatta det normala flödet av utomjordisk kromit till jorden, med avsikt att poängtera signifikansen av detta mellan-ordoviciska intervall som är så rikt på utomjordisk kromit. I detta syfte analyserades prover från de klassiska italienska lokalerna vid Gubbio (K-T gränsen) och Massignano (sen eocen), och endast 7 utomjordiska kromitkorn hittades i totalt 377 kg kalksten, vilket motsvarar 0,019 utomjordiska kromitkorn per kg. Detta är likvärdigt med resultat från de svenska (och kinesiska) studierna, där kalksten som bildats precis innan uppbrottet för cirka 470 miljoner år sedan innehåller 0,009-0,013 utomjordiska kromitkorn per kg. De låga värdena av utomjordisk kromit vid Massignano avfärdar därmed också tidigare framlagda hypoteser om skurar av L-kondritiska meteoriter under sen eocen.

Efter Italien följde två fältarbeten i centrala Kina, vid den avlägsna Puxi River sektionen, och målet var att undersöka den globala trenden i distributionen av utomjordisk kromit under mellan-ordovicium. Under denna period befanns sig både Puxi River sektionen och de svenska lokalerna på södra halvklotets mellanlatituder, separerade av ett några 1000 km brett hav. Lagerföljden vid Puxi River visar näst intill identiska värden med de svenska sektionerna, både vad gäller stratigrafisk utbredning, mängd utomjordiska kromitkorn (1-4 korn per kg kalksten) och kemisk sammansättning av dessa. Därmed har en global korrelation upprättats för detta intervall rikt på utomjordisk kromit, vilket bekräftar omfattningen av de spektakulära regn av meteoriter som drabbade iorden efter den massiva uppsplittringen av den L-kondritiska föräldra-kroppen för cirka 470 miljoner år sedan. Detta stöds också av en negativ trend i osmium-isotoperna som sammanfaller med den första anrikningen av utomjordiska kromitkorn vid Hällekis. Denna trend i osmiumsammansättning tolkas nämligen som en ökad andel utomjordiskt osmium, troligen från upplösta meteoriter.

Det kraftigt ökade inflödet av kosmiskt material under mellan-ordovicium sammanfaller även med den stora ordoviciska biodiversifieringen, d.v.s. då livet på allvar började ta fart på jorden, med bland annat en stor mängd nya arter i haven. Forskargruppen har spekulerat kring en direkt koppling mellan dessa två viktiga händelser i jordens historia, eftersom de sammanfaller väl stratigrafiskt, men ytterligare studier krävs för att pröva denna hypotes.

Totalt har 665 kg kalksten från paleogen och mellan-ordovicium genomsökts efter utomjordisk kromit i dessa studier. I det samlade bakgrundsmaterialet från de italienska lokalerna, och i Kina, återfanns endast 8 utomjordiska kromitkorn i sammanlagt 487 kg kalksten (0,016 utomjordiska kromitkorn per kg). I det kromitrika intervallet vid Puxi River fann vi 290 utomjordiska kromitkorn i 178 kg stenprover, vilket innebär ett genomsnitt på 1,63 korn per kg. Detta representerar en klar ökning, med hundra gånger högre inflöde av kosmiskt material till jorden efter den katastrofala explosionen i asteroidbältet för cirka 470 miljoner år sedan. Denna händelse har därmed lämnat en påfallande signatur i samtida sediment på jorden, och denna avhandling bekräftar dess signifikans i den geologiska historien.

1. INTRODUCTION

The main asteroid belt is located in an orbit around the sun, between Mars and Jupiter, and contains a diverse group of irregular-shaped large objects <1 m to ~1000 km in diameter. They are waste of primordial solar nebula matter that remain after an incomplete planetary formation at ~4.6 Ga (billion years ago), caused by the disturbing gravitational (resonance) forces of Jupiter. With time, most of these very large bodies were disrupted and scattered by violent collisions, resulting in the formation of the asteroid families of the belt. Considerable amounts of cosmic material also pulled toward the centre of the system, due to the massive gravitational forces of the sun. Consequently, the inner planets endured an extensive period of heavy bombardment following this development. Throughout the eons, Earth has experienced several periods of significantly increased cosmic flux as well as an unknown number of large to medium-sized impacts (e.g. the Cretaceous-Paleogene (K-T) boundary impact at ~65.5 Ma). Nonetheless, impact craters are extremely rare on Earth today (175 known impact craters; Earth Impact Database, 2009; http://www.unb.ca/passc/ImpactDatabase/), which is explained by the active and destructive nature of Earth's surface, e.g. plate tectonics and the rapid weathering of the continental crust. In addition, more than 70% of Earth's surface is today protected by deep oceans preventing formation and preservation of impact structures (to a certain size-related point). Recent studies show that the extraterrestrial input to Earth today is, however, predominantly delivered in the sub-cm fraction, as shown by e.g. the Long Duration Exposure Facility (LDEF) satellite (Love and Brownlee 1993), radar micrometeor observations in the upper atmosphere (Mathews et al. 2001), concentrations of platinum group elements (PGE) and osmium isotope systematics (Peucker-Ehrenbrink and Ravizza 2000; Peucker-Ehrenbrink 2001; Dalai and Ravizza 2006), ^{3}He in condensed sediments (Farley et al. 1997), iridium concentrations in ice cores (Karner et al. 2003; Gabrielli et al. 2004), micrometeorite abundance in Antarctic ice (Taylor and Lever 2001), meteor sky-watch programs (Halliday 2001), and meteorite searches in deserts (Bland et al. 1996; Bland 2001). This is a consequence of the steady rate of erosion still occurring in the main asteroid belt, as well as the relatively high frequency of passing comets. An estimated 30,000 ± 15,000 tons of extraterrestrial material reaches Earth annually (Peucker-Ehrenbrink and Ravizza 2000), mainly in the form of interplanetary dust particles (IDPs; diameter: < 35 µm) and micrometeorites (diameter: a few mm to sub-mm). Until recently the flux of extraterrestrial matter to the Earth was considered to be relatively constant through time, but new research indicates several periods of significantly enhanced flux of cosmic material to our planet during the Phanerozoic (~540 Ma to present) (e.g. Farley et al. 1998, 2006; Schmitz et al. 1996, 1997, 2003; Schmitz and Häggström 2006).

1.1. The disruption of the L-chondrite parent body at ~470 Ma

The largest documented asteroid disruption event in late solar system history was the break-up of the L-chondrite parent body at ~470 Ma (Haack et al. 1996; Nesvorný et al. 2002; Korochantseva et al. 2007), possibly related to a collision with a comet. Evidence for this cosmic event was presented already in the 1960's, based on K-Ar gas retention ages of ~500 Ma in recent L-chondritic meteorites (Heymann 1967). About 20% of all meteorites that reach Earth today are shocked L chondrites associated with this event. The timing has since then been further constrained by high-precision ^{39}Ar-^{40}Ar to 470±6 Ma (Korochantseva et al. 2007). Additional evidence is presented by the finds of more than eighty fossil meteorites (i.e. the Österplana meteorites; named after a church close to the place of discovery) in a narrow stratigraphic interval, representing the *Lenodus variabilis*, *Yangtzeplacognathus crassus* and *L. pseudoplanus* conodont zones, of mid-Ordovician marine limestone at the Thorsberg quarry, Kinnekulle (southern Sweden). This suggests an enhanced flux of extraterrestrial matter to Earth by two orders-of-magnitude (elevated >100 times) following the break-up event (Schmitz et al. 1996, 2001). The original meteorite structure (fig. 1) and highly resistant chromite grains (an accessory mineral) are the only extraterrestrial features preserved in the sediment-suspended Österplana meteorites, while the original silicates have been completely replaced (pseudomorphosed) by secondary minerals, such as calcite, clays and barite (Nyström et al. 1988; Schmitz

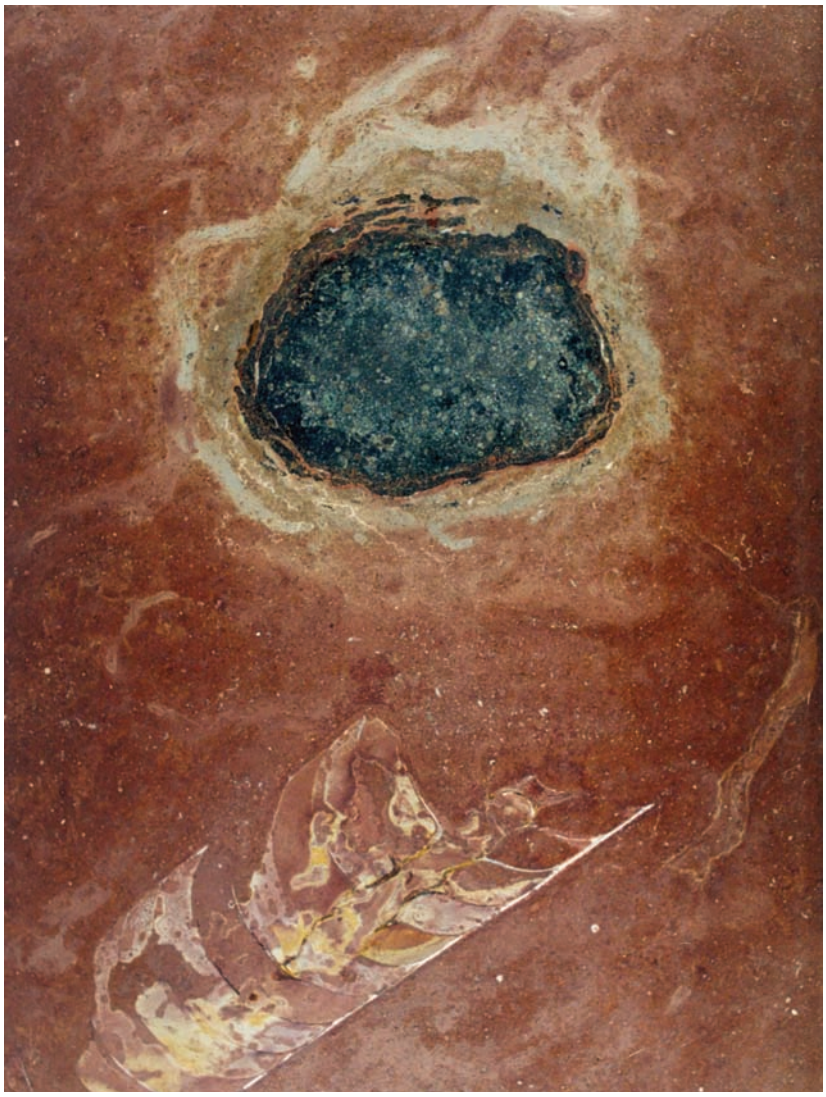

Figure 1. The Österplana Sex 001 meteorite (d. ~8 cm) together with a nautilod shell in a limestone plate sawed parallel to the sea floor surface. Note the relict chondrule structures and partly peeled-off fusion crust (from Schmitz et al. 2001).

et al. 1996, 2001; Bridges et al. 2007; Greenwood et al. 2007). Chondritic chromite is also abundant in the limestone beds surrounding the fossil meteorites, suggesting that only a small fraction of meteorites have been preserved (~10-15%), while most were completely disaggregated with only the chromite grains preserved in the sediments. Systematic searches for sediment-dispersed extraterrestrial chromite (EC) in condensed limestone strata from southern Sweden (i.e. the Hällekis, Thorsberg, Komstad and Fågelsång sections) have provided additional support for an extended period (~1-3 Myr) of major enhanced meteorite flux to Earth during the Middle Ordovician (Schmitz et al. 2003; Schmitz and Häggström 2006; Häggström and Schmitz 2007).

The L-chondritic origin of the Österplana meteorites has been verified by petrographic and textural studies of chondrules (Schmitz et al. 2001; Bridges et al. 2007), and oxygen isotopic analyses of chromite grains (Greenwood et al. 2007). This is further supported by chemical composition (Schmitz et al. 2001, 2003; Schmitz and Häggström 2006; Häggström and Schmitz 2007), inclusion analysis (Alwmark and Schmitz 2009) and (indirectly by) cosmic-ray exposure ages (Heck et al. 2004, 2008) of the sediment-dispersed EC grains and chromite from fossil meteorites.

In the Paleogene Period (65.5-23.0 Ma) Earth experienced at least two additional significant extraterrestrial events (of which one is probably related to a major mass

extinction event), represented by the prominent impact at the Cretaceous-Paleogene (K-T) boundary (65.5 Ma), and the extended period of enhanced flux of cosmic material in the late Eocene (~36-34 Ma). Details regarding these two events will be discussed further in the geological setting section and summary of the relevant papers.

1.2. Ordinary chondritic meteorites

By definition, a meteorite is any meteoroid that reaches Earth's surface in one piece, or in fragments, without being completely vaporized by the intense frictional heat during its passage through the atmosphere (Jackson 1997). All meteorites are divided into three main groups (fig. 2), primarily defined by chemical composition emphasizing on iron content, and include (calculations based on ~36,100 verified meteorites from the Meteoritical Bulletin Database, March 2009; http://tin.er.usgs.gov/meteor/metbull/php): stony (or stones) (~96.7%), stony-iron (~0.6%) and iron meteorites (~2.7%). Stony meteorites are the most common group, and are further divided into chondrites (> 95%) and achondrites (< 5%), based on presence of chondrules in the matrix. Chondrules are small spherical inclusions that represent the oldest solid matter within our solar system, and are believed to have formed as melted or partially melted (presolar) droplets in space, prior to the accretion of their parent bodies. Chondrites retain abundant chondrules (diameter: 0.1 to 4 mm), thus naming the group, whereas all achondrites have either lost their original chondrule structures (due to thermal metamorphism) or they never contained any. The achondrites, which primarily include primitive, HED, Lunar and Martian achondrites, are beyond the scope of this thesis, while attention will be given exclusively to chondrites, specifically the ordinary chondrites.

Chondrites are primitive (undifferentiated) cosmic rocks with a chemical composition that essentially have not changed since their formation at ~4.6 Ga. Thus, chondrites are invaluable sources of information regarding the geological processes of our early solar system.

Individual chondrite meteorites are categorized chemically and petrographically by certain mineralogical and textural criteria (Van Schmus and Wood 1967), and the petrographic classification consists of types 3 to 6 (there is also a type 7, but this type is new and poorly represented, and hence disregarded here) that are primarily based on the gradual reduction of the chondrule definition (texture). This was caused by increasing thermal metamorphic alteration during formation or during violent episodes in the history of the chondrite. In addition,

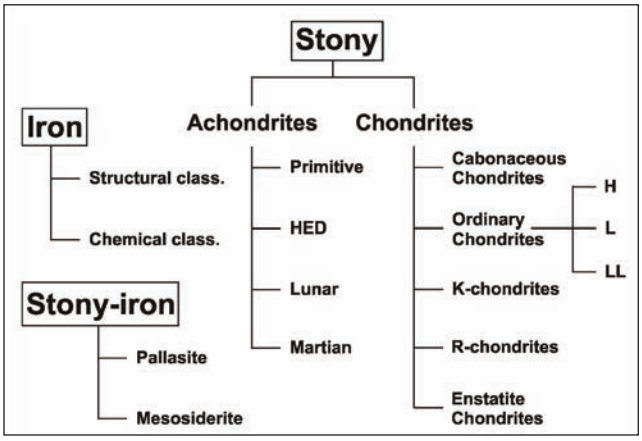

Figure 2. A simple scheme of meteorite groups. The primary groups and classes of chondrites and achondrites are represented in the chart, while only the ordinary chondritic subgroups (H, L and LL) are present. Iron meteorites include more than 20 groups, and is only represented by the basic classification of structural and chemical types.

type 3 is generally separated from type 4 by differences in homogeneity of minerals (Bridges et al. 2007, and references therein).

A few carbonaceous chondrites (see below) belong to petrographic types 1 (CI) and 2 (CM and CR), which indicates various degrees of aqueous alteration (a process in which minerals form or are altered via reactions with water). CI chondrites, for example, contain a high portion of fine-grained hydrous phyllosilicates and associated minerals (~90%), which formed by aqueous alterations (probably from chondrules) during the early formation stages of their parent body (Rubin 1997 and references therein). Thus, with decreasing petrographic type the chondrule definition is reduced. An additional classification parameter is shock metamorphism, and Stöffler et al. (1991) have defined shock stages from S1 (unshocked) to S6 (very strongly shocked) for ordinary chondrite. Shock stages are assigned based primarily on shock effects observed in olivine and plagioclase.

Chondrites are divided into three main classes: ordinary (95.7%), carbonaceous (3.1%) and enstatite (0.7%) chondrites (K- and R-chondrites are minor classes; Fig. 2). The ordinary chondrites represent the majority of all stony meteorite falls, making them the most abundant type of all meteorites that fall on Earth today (~88%). They are aggregates of chondrules, metals and sulphides characterized by olivine and Ca-poor pyroxene. The metal (Fe, Ni) content (e.g. kamacite and taenite) varies between 8-20 wt% and most often occurs as evenly distributed grains (100-200 µm in diameter) throughout the meteorites. Afi-

attalab and Wasson (1980) showed that the morphology and grain shape of these metal grains changes from petrographic type 3 to 6, as the fraction of coarse-grained metal increases at the expense of fine-sized grains (and the abundance of metal and number of metal-bearing chondrules diminishes). Olivine, pyroxene and metal compositions, represent the quantity of fayalite in olivine ($Fa_{mol\%}$), and ferrosilite in pyroxene ($Fs_{mol\%}$), and are used as diagnostic proxies for classification of ordinary chondrites into H, L and LL chondrites (e.g. Bunch et al. 1967; Afiattalab and Wasson 1980; Rubin 1990), as well as the intermediate L/LL group suggested by Rubin (1990).

The H-chondrite group represent the most common type among all meteorites worldwide (~40%), while comprising ~45.5% of the ordinary chondrites. The "H" stands for high total iron (25 to 31 wt%), with regard to the other ordinary chondrites, while this group has least oxidized iron in the silicate mineral phases ($Fa_{16\text{-}20}$ and $Fs_{14.5\text{-}18}$). Nickel-iron metal is also found in its free, reduced form (15 to 19%), making H chondrites strongly magnetic. The primary minerals are olivine and the orthopyroxene bronzite, giving this group of meteorites its former name, i.e. bronzite chondrites. The asteroid, 6 Hebe, is suggested to be casually related to the H chondrites (by reflectance spectrographic analysis), although it is not the direct source of these meteorites (e.g. Migliorini et al. 1997; Gaffey and Gilbert 1998). The H group consists of petrographic types 3 to 6, but is typically dominated by type 5 (Brearley and Jones 1998, and references therein).

The L-chondrite group is the second largest group of both ordinary chondrites (~40%) and of the total assemblage of meteorites (~35%). The "L" defines a relatively low iron content (~20-25 wt%), compared to the H chondrites, while they can also be distinguished by their relative abundance of fayalite in olivine ($Fa_{22\text{-}25}$) and ferrosilite in Ca-poor pyroxene ($Fs_{19\text{-}22}$). The free metal content varies between 4 and 10%. Consequently, the L chondrites have a magnetic attraction, however, inferior to that of the H group. Primary minerals include (besides magnetite) olivine and the orthopyroxene hypersthene, also naming this group in the past, i.e. hypersthene chondrites. Like the previous group, L chondrites range petrographic types 3 to 6, but the majority of meteorites are classified as type 6 (Brearley and Jones 1998, and references therein). The origin of this group has been discussed at length, but Nesvorný et al. (2002) suggest that the L chondrites originate from a ~200 km large parent body, located in the Flora family region in the main asteroid belt, which was probably disrupted by a collision event (with an unknown object) at ~470 Ma. The ramifications of this event have been recognized on Earth from the discovery of numerous fossil meteorites in mid-Ordovician strata at the Thorsberg quarry (Schmitz et al. 1996, 1997, 2001), and common sediment-dispersed EC grains in coeval marine sediments from both Sweden and China (Schmitz et al. 2003; Schmitz and Häggström 2006; Häggström and Schmitz 2007; Paper III).

The LL chondrites constitute only a minor fraction of the ordinary chondritic meteorites (<15%), but are nonetheless more abundant than the total assemblage of iron and stony-iron meteorites (almost four times). The "LL" stands for low iron (19 to 22 wt%) and low free metal content (only 1 to 3%), resulting in weak magnetic properties compared to the H and L chondrites. The iron oxide levels in LL-chondritic olivine ($Fa_{26\text{-}32}$) and pyroxene ($Fs_{22\text{-}26}$) exceeds that of the other OC, indicating that the LL chondrites formed under more oxidizing conditions compared to H and L meteorites. The LL chondrites also contain the largest chondrules of the group, with a mean diameter of ~0.6 mm (Rubin 2000). Petrographic type 5 and 6 dominate, although the LL chondrites range from types 3 to 6 like the other OC (Brearley and Jones 1998, and references therein). The origin of the LL group remain unknown, although a small asteroid, 3628 Boznemcová, in the main asteroid belt has shown geochemical similarities with known LL meteorites, and may represent a fragment of the original LL-chondrite parent body (Binzel et al. 1993).

The petrography of opaque phases in equilibrated ordinary chondrites has been studied in the past by numerous researchers (e.g. Ramdohr 1973; Rubin 1990). The abundance of chromite in ordinary chondrites has been shown to increase with metamorphic grade (from petrographic type 3 to 6), in addition to enhanced size and homogeneity of grains (Snetsinger et al. 1967; Bunch et al. 1967; Bridges et al. 2007). Trends in chromite elemental composition (wt%) signify a general increase in FeO (degree of oxidation), TiO_2 and V_2O_3 content in the order H-L-LL, whereas Cr_2O_3, MgO and MnO concentrations show parallel reduction. Other spinel types previously studied in ordinary chondrites mainly involve assorted compositions of Al-rich spinels (main elements: Al_2O_3: 20-60 wt%, FeO: 12-25 wt%, MgO: 6-20 wt%), but also other accessory minerals like ilmenite and rutile.

1.3. Chromite as a proxy for extraterrestrial flux

Chromite (fig. 3) belongs to a group of highly resistant accessory minerals called spinels, which are the most abundant oxides in equilibrated ordinary chondrites (Rubin 1997), constituting ~0.05-0.5 wt% of the whole-rock (Keil

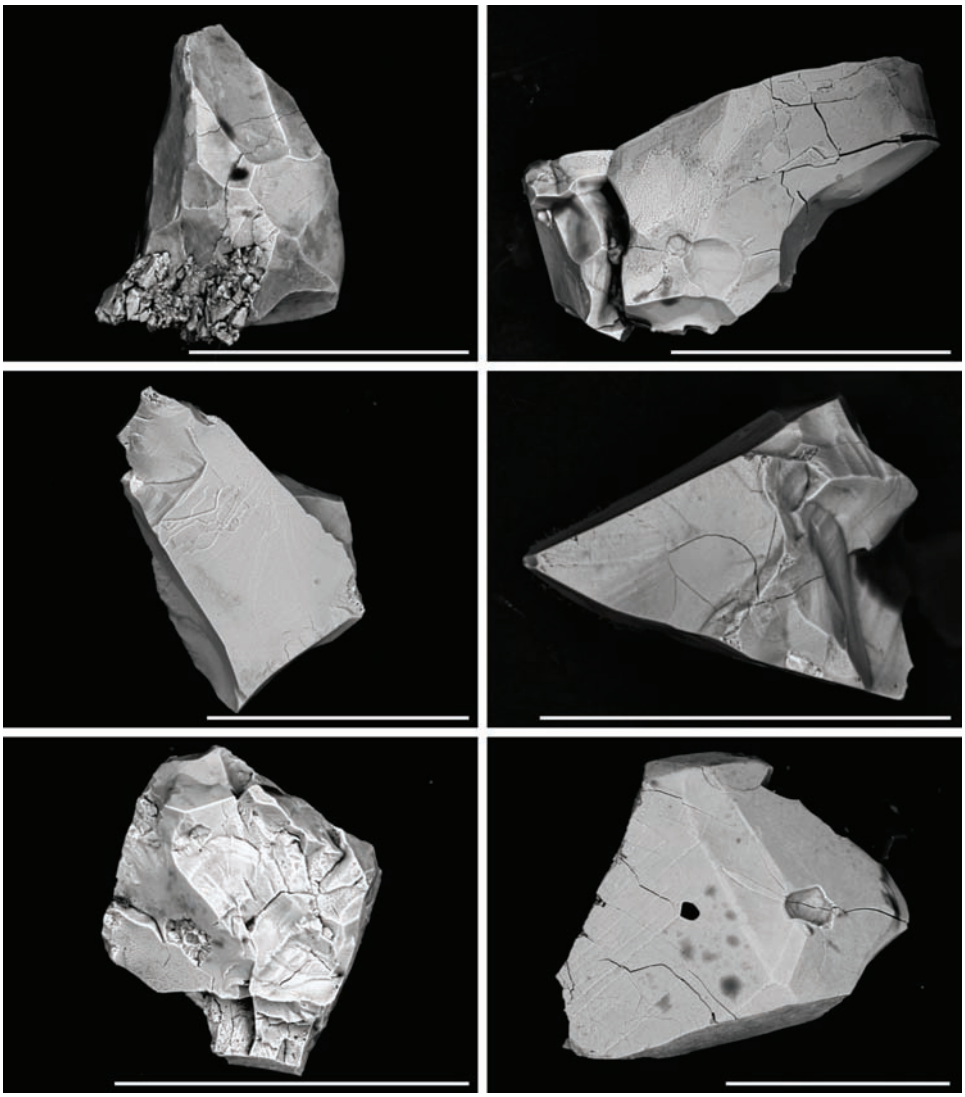

Figure 3. Backscatter images of six characteristic sediment-dispersed extraterrestrial chromite (EC) grains from the Puxi River section, central China. Scale bars are 100 µm. Note the pristine condition and sharp angles of the grains after having been buried in sediments for ~470 Myr.

1962; Nyström et al. 1988; Bridges et al. 2007). Chromite grains studied in this thesis belong to the "coarser" type of chromite (Ramdohr 1967, 1973). It should also be noted that unequilibrated ordinary chondrites, i.e., petrological type 3, contain chromite grains that are usually smaller than 63 µm (Bridges et al. 2007), and consequently falls outside the range of detection (>63 µm) for papers discussed in this thesis. Only <5% of all ordinary chondrites represent petrographic type 3.

Chromium-rich spinels are also a relatively common mineral in terrestrial rocks, often found in relation to peridotite and other layered ultramafic intrusive rocks, as well as metamorphic rocks (Barnes and Roeder 2001). Although extraterrestrial chromite (EC) and terrestrial chromite shares optical similarities, i.e. black opaque appearance and similar size range, they are readily distinguished by elemental composition. Chromite from equilibrated ordinary chondrites is characterized by high titanium content (TiO_2: 1.4-3.5 wt%) and a narrow range of vanadium (V_2O_3: 0.6-0.9 wt%) concentration (Bunch et al. 1967; Nyström et al. 1988; Schmitz et al. 2001; Almark and Schmitz 2007, 2009; Paper III). Table 1. shows a comparison of the elemental compositions of chromite from studies included in this thesis, previous studies of EC and chromite from recent ordinary chondritic meteorites.

The chromite content in other meteorite groups (e.g.

Table 1. The average element concentrations (wt% and 1σ standard deviation) of EC grains from the Puxi River section, China, in comparison with EC grains from previous studies in southern Sweden and chromite from recent meteorites.

Study	Cr_2O_3	Al_2O_3	MgO	TiO_2	V_2O_3	FeO	MnO	ZnO	Fe#[1]	Cr#[2]
Sediment-dispersed EC grains from the Puxi River section, central China, 291 grains, Paper III	57.84 ±1.14	6.00 ±0.36	2.88 ±0.88	2.91 ±0.40	0.71 ±0.08	27.40 ±1.84	0.80 ±0.26	1.09 ±1.12	84.3 ±4.39	86.6 ±0.71
Sediment-dispersed EC grains from Kinnekulle, southern Sweden, 276 grains[3]	57.61 ±1.58	6.07 ±0.76	2.58 ±0.79	3.09 ±0.33	0.75 ±0.07	27.36 ±2.63	0.78 ±0.20	0.53 ±0.50	85.6 ±3.90	86.5 ±1.42
Sediment-dispersed EC grains from Killeröd quarry, Komstad, southern Sweden, 274 grains[4]	56.93 ±1.29	6.08 ±0.73	2.69 ±1.10	2.95 ±0.44	0.74 ±0.07	28.74 ±1.72	0.87 ±0.25	0.71 ±0.84	n.d.[5]	n.d.
26 fossil meteorites from Thorsberg quarry, southern Sweden, 594 grains[6]	57.60 ±1.30	5.53 ±0.29	2.57 ±0.83	2.73 ±0.40	0.73 ±0.03	26.94 ±3.89	1.01 ±0.33	1.86 ±2.43	85.3 ±5.02	87.5 ±0.60
Chromite from 12 recent H5/6 group chondrites[6]	56.64 ±0.37	6.44 ±0.14	2.98 ±0.23	2.20 ±0.17	0.73 ±0.02	29.27 ±0.67	1.00 ±0.08	0.33 ±0.05	84.7 ±1.20	85.5 ±0.30
Chromite from 12 recent L5/6 group chondrites[6]	56.00 ±0.65	5.97 ±0.43	2.93 ±0.97	2.68 ±0.40	0.75 ±0.02	30.22 ±2.23	0.83 ±0.10	0.30 ±0.07	85.3 ±4.92	86.3 ±0.77
Chromite from 13 recent H4-6 group chondrites[7]	57.10 ±1.10	6.64 ±0.41	3.40 ±0.18	1.96 ±0.29	0.65 ±0.03	28.9 ±0.60	0.88 ±0.07	0.28 ±0.14	82.7 ±1.00	85.2 ±1.00
Chromite from 6 recent L4-6 group chondrites[7]	56.1 ±0.80	5.90 ±0.19	2.52 ±0.21	2.67 ±0.44	0.70 ±0.06	30.90 ±0.60	0.63 ±0.08	0.34 ±0.06	87.3 ±0.06	86.5 ±0.30
Chromite from 4 recent LL3-7 group chondrites[7]	55.8 ±0.56	5.52 ±0.17	1.85 ±0.14	3.40 ±0.57	0.67 ±0.10	31.60 ±0.62	0.51 ±0.04	n.d.	90.50 ±0.90	87.22 ±0.20

[1] Fe#: mol% Fe/(Fe+Mg); [2] Cr#: mol% Cr/(Cr+Al); [3] Schmitz and Häggström (2006); [4] Häggström and Schmitz (2007); [5] n.d. = no data; [6] Schmitz et al. (2001), modified by Alwmark and Schmitz (2007); [7] Wlotzka (2005). The numbers associated with H, L and LL chondrites indicate petrographic types.

various chondrites and achondrites (stony), mesosiderites and pallasites (stony-iron), and iron meteorites) is generally less abundant compared to the ordinary chondrites. In addition, chromite from the ordinary chondritic subgroups (H, L and LL) are readily distinguished from other meteorite groups and classes by the same approach used to separate them from terrestrial chromite, i.e. using their elemental composition as a fingerprint. Chromite only shows minor elemental variations within the group, and are mainly separated by iron (FeO) and titanium (TiO_2) content (wt%), with increasing concentrations from H to L to LL (Table 1). These variations are, however, relatively small and liable to overlap, specifically between L and LL types (Bunch et al. 1967, Schmitz et al. 2001; Wlotzka 2005).

The original mineral components of the fossil meteorites at Thorsberg quarry have all, except chromite, been completely replaced through geochemical and diagenetic processes, which make traditional classification unreliable (Nyström et al. 1988; Schmitz et al. 2001). The elemental composition of these preserved chromite grains indicates that all, or almost all, meteorites are of L-chondritic origin, and hence connected to the disruption event of the L-chondrite parent body at ~470 Ma (Schmitz et al. 2001, 2003; Schmitz and Häggström 2006, Häggstrom and Schmitz 2007; Paper III).

Our searches for EC grains should not be confused with previous studies of nickel- and chromium-rich cosmic spinels, e.g. from the Cretaceous-Paleogene (K-T) boundary and the Massignano impact ejecta layer, since these studies primarily investigate spinels (1-50 μm) that were created during atmospheric entry (melting and recondensation) and during impacts of large cosmic objects (ejecta) (Smit and Kyte 1984; Kyte and Smit 1986; Robin et al. 1992; Toppani and Libourel 2003; Ebel and Grossman 2005). The origin and elemental composition of these spinels are quite different from the coarse (>63 μm) and common chromite originally present in equilibrated ordinary chondrites (Keil 1962; Ramdohr 1973; Rubin 1997; Bridges et al. 2007). The sediment-dispersed EC grains of our studies derive from meteorites and micrometeorites that (after surviving atmospheric entry) reached the firm sea floor and rapidly dissolved (~0.1-10 kyr), releasing their chromite grains to the sediments.

Consequently, these grains have maintained their pristine condition and the original chemical composition while harboured in the meteorite.

1.4. The osmium isotope system

The interior of a silicate-dominated planet is usually divided into various layers controlled by differences in chemistry and density, and Earth consists of three such layers: the crust (2.2-2.9 g/cm^3), the mantle (3.4-5.6 g/cm^3) and the core (9.9-13.1 g/cm^3). This separation was initiated by a gravity-driven process, called planetary differentiation, approximately 4.6 Ga, which caused denser matter to sink toward the centre of the planet while the less-dense material was sustained in the crust. Osmium (Os) has major siderophile affinities (iron-loving), like all platinum group elements (PGE; Ru, Rh, Pd, Os, Ir and Pt), and it is estimated that more than 99.5% of all terrestrial Os is contained in Earth's iron-rich core, whereas most of the remaining <0.5% of this element is confined within the mantle (e.g. Peucker-Ehrenbrink 2001). As a result, the continental crust is strongly depleted in PGEs, leaving only minor measurable trace amounts in Os (~31 ppt; Peucker-Ehrenbrink and Jahn 2001). In contrast, meteorites have low rhenium (Re) and high Os abundance (Re/Os: ~0.1), making them less radiogenic ($^{187}Os/^{188}Os$: ~0.13; e.g. Meisel et al. 1996), while terrestrial crustal rocks have a reversed correlation (Re/Os: >10) and are highly radiogenic $^{187}Os/^{188}Os$ ~1.4-1.54 (Levasseur et al. 1999; Peucker-Ehrenbrink and Jahn 2001). Consequently, Os is a sensitive proxy for distinguishing primitive (undifferentiated) extraterrestrial material, from crustal rocks and common marine sediments (e.g. Esser and Turekian 1988, 1993; Koeberl and Shirey, 1997).

The Os isotopic system ($^{187}Os/^{188}Os$) is based on the β-decay of ^{187}Re (rhenium) to ^{187}Os (^{187}Re half-life of 41.6 Gyr), and by comparing the radiogenic ^{187}Os (1.513%) to a non-radiogenic ^{188}Os (13.29%) the ratio can be calculated (Shirey and Walker 1998, and references therein). The abundance of ^{187}Os is directly proportionate to the decay of ^{187}Re, thus increasing with time, and by normalizing the decay to the stable ^{188}Os the following equation is formulated:

$$^{187}Os/^{188}Os = (^{187}Os/^{188}Os)_i + (^{187}Re/^{188}Os)(e^{\lambda t} - 1)$$

where $^{187}Os/^{188}Os$ and $^{187}Re/^{188}Os$ are the measured ratios of these isotopes, $(^{187}Os/^{188}Os)_i$ is the initial isotopic ratio at the time when the system became closed for Re and Os, λ the decay constant for ^{187}Re (1.666×10^{-11} yr^{-1}), and *t* the time elapsed since system closure for Re and Os (Shirey and Walker 1998).

2. AIM OF THE THESIS

The purpose of this thesis is to further investigate the significance of the enhanced content of extraterrestrial matter previously recorded in mid-Ordovician marine sediments of southern Sweden. Sediment-dispersed extraterrestrial chromite (EC) will be evaluated as a proxy for determining variations in accretion rates of ordinary chondritic material on Earth, including periods with suggested enhanced cosmic flux. Issues discussed in this thesis have been formulated accordingly:

I) Search for EC in strata with similarly slow sedimentation rates to the Swedish mid-Ordovician sections, but from other periods, such as in the latest Cretaceous-earliest Paleocene section at Gubbio, to evaluate the significance of the event at ~470 Ma.

II) Investigate the stratigraphic interval proposed to be associated with an (L-chondritic) asteroid or comet shower in late Eocene at Massignano. This issue may be resolved by comparison with the EC-rich strata that formed after the L-chondrite parent body break-up at ~470 Ma.

III) Test the hypothesis that the abundant EC grains in Swedish mid-Ordovician limestone reflect a global event, and not just regional processes, by studying the distribution of EC in coeval strata at a remote location - the Puxi River section, central China.

VI) Evaluate the temporal association between the Great Ordovician Biodiversification Event and the break-up of the L-chondrite parent body in the main asteroid belt at ~470 Myr, by conducting a detailed bed-by-bed study of the distribution of brachiopod species, sediment-dispersed (L-chondritic) EC grains and Os isotopes across Middle Ordovician strata in Baltoscandia.

V) Study potential variations in Os abundances and $^{187}Os/^{188}Os$ in marine mid-Ordovician strata at Hällekis, Kinnekulle, associated with the enhanced flux of meteorites and micrometeorites to Earth that lasted a few million years following the break-up event at ~470 Ma.

3. MATERIALS AND METHODS

3.1. Extraction of chromite grains from marine sediments

The search for chromite grains requires large samples of condensed carbonates, ordinarily ~10-30 kg of limestone each, for recovery of relevant time-area data (grains/kyr/m^2) (see discussion in Peucker-Ehrenbrink and Ravizza 2000). The procedure for extracting and preparing EC grains from carbonate sediments was developed by Schmitz et al. (2003), and only minor improvements have been implemented since then, mainly due to new laboratory conditions. Here follows a detailed sequence of method procedures:

After thorough cleansing, samples are broken up into minor pieces (d. < 10 cm) with a sledgehammer, followed by additional fragmentation (d. ~1 cm) by a Retsch Jaw Crusher BB 200. The crushed material is decalcified in 6 M hydrochloric (HCl) acid at room temperature and subsequently sieved (mesh: 32µm). The residual remainder is leached in 18 M hydrofluoric (HF) acid at room temperature (with occasional stirring), after which the acid-insoluble residue is separated into three size fractions (32-63, 63-355 and >355 µm) and dried. The intermediate fraction (63-355 µm) is systematically scanned for opaque minerals under a stereomicroscope (Nikon SMZ 1500) and potential grains are collected with a fine brush. The unpolished grains are mounted on a carbon tape for preliminarily qualitative scanning electron microscope analyses and backscatter imagery. Subsequently, all Cr-rich grains are mounted in epoxy resin and polished, using a Struers alumina paste (standard quality) mixed with water on a spinning polishing cloth (Buehler), before final quantitative scanning electron microscope analysis is conducted (a minimum of three analyses per grain).

All elemental analyses are performed by an Oxford Inca X-sight energy dispersive spectrometer (EDS) with a Si detector linked to a Hitachi S-3400N scanning electron microscope (SEM). Cobalt is used to standardize the instrument, while providing supervision of potential drift. Accelerating voltage of 15 kV, a sample current of ~1 nA, and counting live-time of 80 seconds were used. Precision (reproducibility) of analyses was typically within 1-4%. Analytical accuracy was controlled by the USNM 117075 chromite (Smithsonian) reference standard (Jarosewich et al., 1980) and three silicate reference standards (Alwmark and Schmitz, 2009)

3.2. The osmium isotope analysis

The procedure for the Os isotopic systematics in this thesis (Paper V) follows Peucker-Ehrenbrink et al. (2003) accordingly:

Samples are granulated with an agate mortar, and ~3-10 g of powdered limestone sediment is mixed with an isotopically enriched spike (including ^{99}Ru, ^{105}Pd, ^{190}Os, ^{191}Ir and ^{198}Pt). After drying at room temperature over night, it is then mixed with borax, nickel and sulfur powder at a typical sample (flux) ratio of two. Following fusion of the mixture (90 minutes at 1000°C in a glazed ceramic crucible), the melt is allowed to cool and the NiS bead is separated from the glass, and consequently dissolved in hydrochloric acid (6.2M HCl) and the residue filtered through cellulose filter paper (0.45 µm). Insoluble acid-resistant PGE-containing particles on the filter paper are dissolved along with the filter in 1 ml concentrated nitritic acid (HNO_3) in a firmly closed Teflon vial at ~100°C for about 60 minutes immediately before the analysis of Os. After dissolution the Teflon vial is chilled in ice water to minimize the escape of volatile OsO_4. Osmium is then extracted from the vial with the sparging method (Hassler et al., 2000) that depend on purging dissolved OsO_4 with inert Ar carrier gas and transferring the gas mixture directly into the torch of a single-collector ICP-MS (Finnigan Element).

The details of the method are described in Hassler et al. (2000). The accuracy and precision of the analytical data has been evaluated in detail by Peucker-Ehrenbrink et al. (2003) using various international reference materials and community standards.

4. GEOLOGICAL SETTINGS

4.1. The Massignano section, Monte Cònero, central Italy

The Massignano section (43°35'N, 13°35'E) is located in an abandoned quarry along the provincial road in the Monte Cònero Park, near Ancona, central Italy (Fig. 4-5). The 23 m thick section spans the upper Eocene and the lowermost Oligocene, exposing a continuous sequence of pelagic marly limestones and calcareous marls, rich in well-preserved benthic and planktonic microfossils. The sediments are furthermore interbedded by several biotite-rich layers of volcanic origin.

In the early 1990's the Massignano section was selected as the Global Stratotype Section and Point (GSSP) for the Eocene-Oligocene boundary, signifying that this stratigraphic section will be used internationally as the

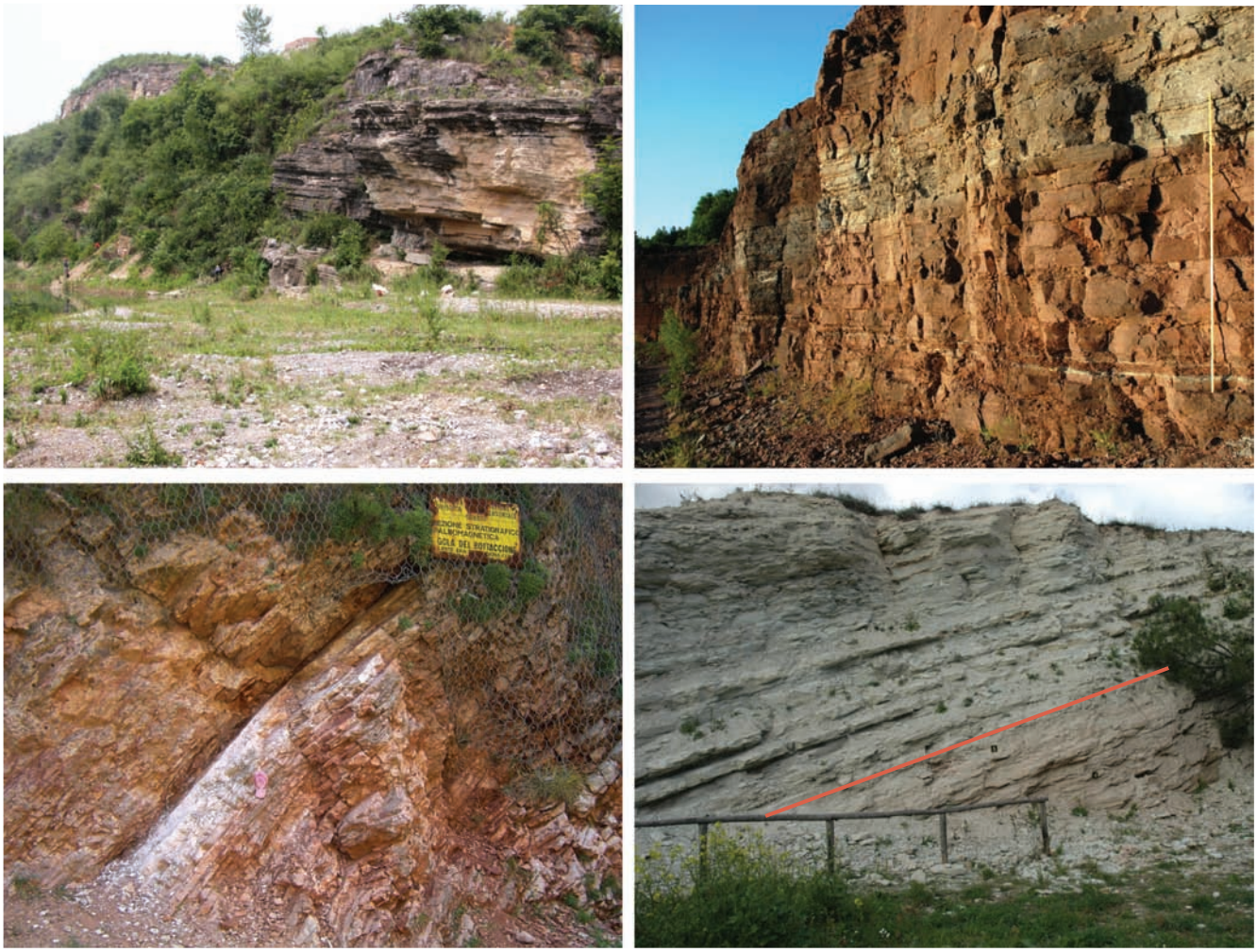

Figure 4. *Upper left*: The Puxi River section, central China. *Upper right:* The Hällekis section, Kinnekulle, southern Sweden. Note the reduced, grey Täljsten interval. *Lower left:* The famous Creataceous-Paleogene (K-T) boundary at the Bottaccione Gorge section, Gubbio, central Italy. Note the excavated nature of K-T boundary clay layer, caused by human activity. *Lower right:* The Massignano section, near Ancona, central Italy. The red line marks the iridium anomaly at 5.61 meter.

reference section for this particular boundary in the geologic time scale. During the first stages of the investigation at Massignano, a thin, marly impact-related (ejecta) layer (dated at 35.5 ± 0.3 Ma) was discovered at 5.61 m (relative to the base of the section), while conducting narrowly spaced iridium analyses across the section. This instigated further studies and soon after two additional minor peaks in iridium were discovered, at 6.20 m and 10.25 m, respectively (e.g. Montanari et al. 1993; Pierrard et al. 1998). These two layers have, however, not yielded any convincing ejecta components (i.e. shocked quartz, impact spherules, etc.), and hence their potential impact-associated origin remains a conundrum (Montanari et al., 1993; Clymer et al., 1996; Bodiselitsch et al., 2004).

The ejecta layer at 5.61 m contains altered microkystites (impact-produced, crystallite-bearing spherules) and nickel-rich spinels (Pierrard et al. 1998), shocked quartz (with multiple sets of planar deformation features or PDFs; Clymer et al. 1996), and enhanced iridium levels (e.g. Montanari et al. 1993; Pierrard et al. 1998). Similar finds have been reported in late Eocene marine sediments worldwide, representing evidence of at least two narrowly spaced ejecta layers (Montanari and Koeberl 2000, and references therein). Distal ejecta from the large Popigai crater, Russia (~35.7 Ma; e.g. Bottomley et al. 1997), has been proposed as a possible source of origin, but this link is primarily based on the approximate coincidence in time.

At Massignano, Farley et al. (1998) have also identified a ~13 m thick interval of late Eocene sediments (dated at 36.3 to 34.3 Ma) enriched in extraterrestrial ^{3}He. This interval includes all three previously mentioned iridium anomalies, while peaking in ^{3}He at 5.61 m, coincident

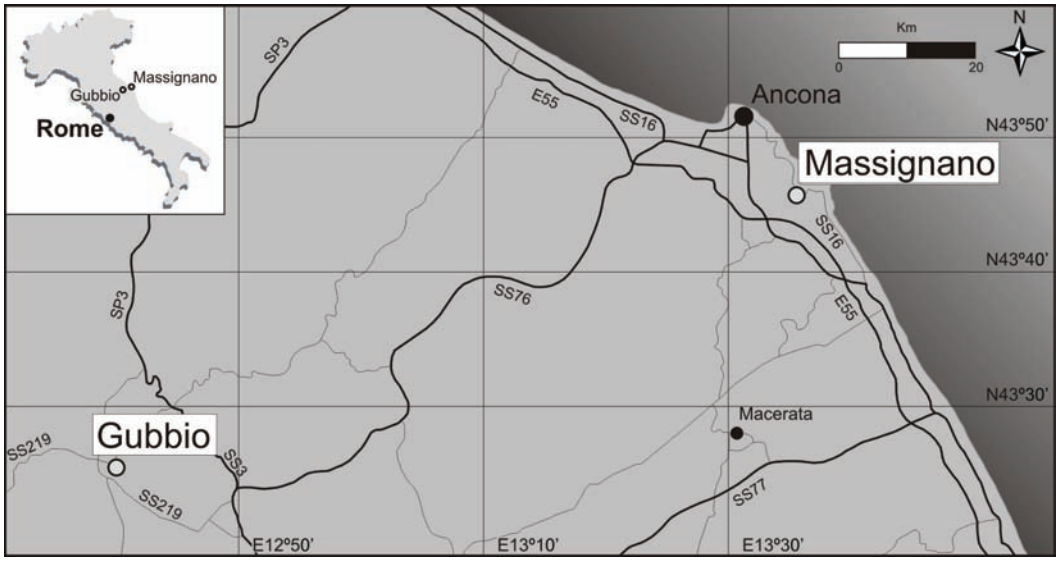

Figure 5. Map of the coastal area around Ancona, eastern central Italy, and the positions of the Gubbio (Bottaccione Gorge) and Massignano sections.

with the confirmed ejecta layer. Helium-3 is a proxy for extraterrestrial dust (<35 μm) and its distribution at Massignano has been interpreted as an extended period of comet activity in the inner solar system, possibly also indicated by an overrepresentation of large impact craters for this period. Presently there are at least two confirmed major impacts in the late Eocene, the previously mentioned Popigai crater, ~100 km in diameter, and the Chesapeake Bay structure, USA (~35.3 Ma; e.g. Koeberl et al. 1995), ~90 km in diameter. In addition, there are several minor craters of comparable ages worldwide that may have been part of the same event (e.g. Crawford and Flaxman, Australia; Wanapitei and Mistastin, Canada; Logoisk, Russia; Montanari and Koeberl 2000).

4.2. The Bottaccione Gorge section, Gubbio, central Italy

The pelagic sequence at the Bottaccione Gorge, Gubbio (central Italy), is probably the most prominent and well-studied section across the Cretaceous-Paleogene (K-T) boundary in the world (e.g. Premoli Silva 1977; Alvarez et al. 1977, 1980, 1990; Lowrie et al. 1990) (Fig. 4-5). It was here that Alvarez et al. (1980) first discovered an iridium anomaly at the K-T boundary, later connected to an impact crater on the Yucatán Peninsula, Mexico, ~65.5 Ma (Hildebrand et al. 1991; Shukolyukov and Lugamir 1998). The iridium anomaly was recorded in a 1-2 cm thick dark clay layer that defines the K-T boundary and is today recognized worldwide.

The Bottaccione Gorge section is located directly north of the medieval town of Gubbio (43°22'N, 12°35'E; along the provincial road (SS298), between Gubbio and Scheggia; Fig. 5), and exposes more than 30 m of the ~325 m thick Scaglia Rossa Formation, which extends from the early Turonian to the middle Eocene (Arthur and Fischer 1977; Monechi and Thierstein 1985). The pink to red homogeneous and marly limestone has been thoroughly bioturbated and compacted before cementation, and appears to be undisturbed by major intrusions and thermal alteration (although flexural slip folding occurs) (Arthur and Fischer 1977). The section is, however, regarded as one of the worst known in the Umbria-Marche region regarding the preservation of the original K-T boundary clay (Montanari and Koeberl 2000). Consequently, we disregarded the thin boundary clay layer in our study, and concentrated on collecting bulky samples in the surrounding unaltered limestones.

The assemblage of agglutinated foraminifera indicates that pelagic conditions (water depth: ~1500-2500 m) prevailed in the Gubbio area during the late Cretaceous and early Paleogene (Kuhnt 1990). This is further supported by abundant calcareous nannofossils and foraminifera, an aeolian clay and silt component, high planktic/benthic ratio in foraminifera, and extremely low concentrations of organic carbon (Arthur and Fischer 1977; Montanari 1991). The estimated sedimentation rates at Gubbio were particularly low, from upper Cretaceous (average 5 mm kyr^{-1}) to the lowermost Paleocene (average 2.5 mm kyr^{-1}) limestone (Arthur and Fischer 1977; Mukhopadhyay et al. 2001b), and helium isotopic data show that the input of extraterres-

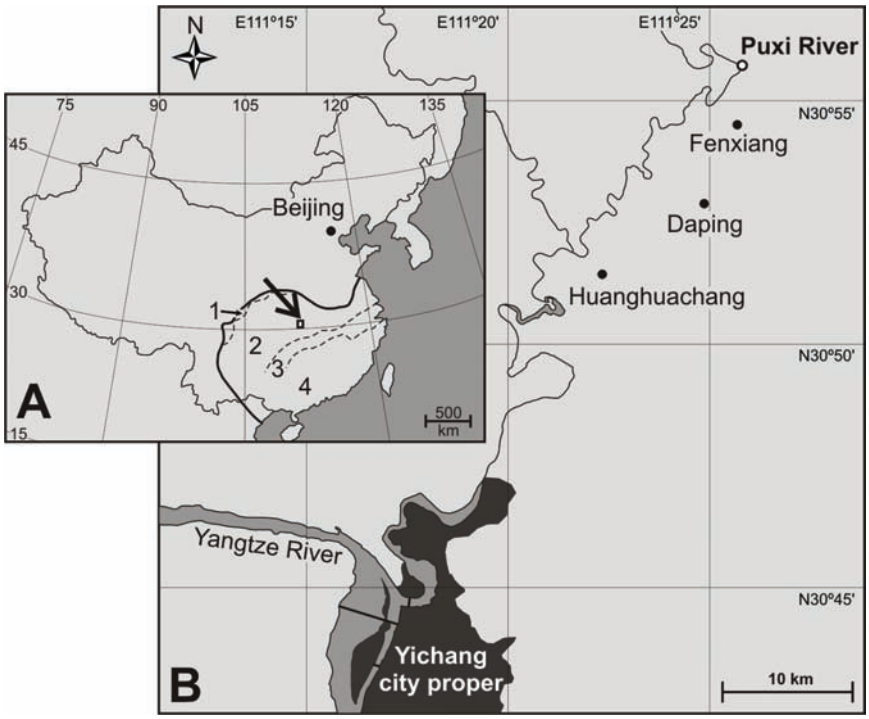

Figure 6. A) Map of China with study area marked. Map also illustrates how the Ordovician South China palaeoplate consisted of four geographic components: 1) old island land masses, 2) the extensive epicontinental sea of the Yangtze Platform, 3) the Zhujiang clastic basin (including the deep Jiangnan Belt) and 4) the Cathaysian landmass (Zhan et al., 2007). B) Study area with the position of the Puxi River site.

trial ^{3}He remained constant (within a factor of ~2) throughout this interval (Mukhopadhyay et al. 2001a, 2001b).

The iridium-rich clay layer at Bottaccione Gorge is sequentially preceded by a 20-50 cm thick zone of white bleached limestone, related to low oxygen conditions. This was likely caused by the rapid increase in delivery of organic material to the sea floor, following the K-T boundary event (Lowrie et al. 1990; Montanari and Koeberl 2000). The Bottaccione Gorge section consists of an essentially complete sequence of biozones across the K-T boundary (Smit 1982), with the exception of the thin (foraminiferal) P0 zone that is absent. This zone is, however, absent or unrecognizable in most of the Umbria-Marche sections, possibly reflecting extremely low sedimentation rates combined with thorough bioturbation.

4.3. The Puxi River section, Hubei Province, central China

Presently, the South China palaeoplate is surrounded by the North China palaeoplate (north), the Chaidam (Qaidam) and Tibet palaeoplates (west), and the Sibumasu and Indo-China palaeoplates (southwest) (Zhou et al., 1995). The core of the South China palaeoplate cratonic basement consists of Precambrian low-grade metamorphic rocks, stretching more than 3000 km from west to east and over 2000 km from north to south. The Ordovician South China palaeoplate consisted of four distinct geographic components from northwest to southeast: 1) old island land masses, 2) the extensive epicontinental sea of the Yangtze Platform, 3) the Zhujiang clastic basin (including the deep Jiangnan Belt) and 4) the Cathaysian landmass (Fig. 6; Zhan et al., 2007). The Yichang area, where our study has been performed, was located in the northeastern Upper Yangtze Platform area, distal from terrigenous sources, which generated primarily condensed conodont-rich carbonates in a moderately shallow, outer shelf environment. During early to middle Darriwilian the Upper Yangtze Platform area was dominated by condensed carbonates which show close facies resemblance to the Baltoscandian "Orthoceratite Limestone" (cf., Kinnekulle, southern Sweden) (Lindström et al., 1991; Zhang, 1996, 1998a,b). Common sedimentary features include frequently occurring burrows and furrows, mineralized discontinuity surfaces, buckled beds (or mini-mounds),

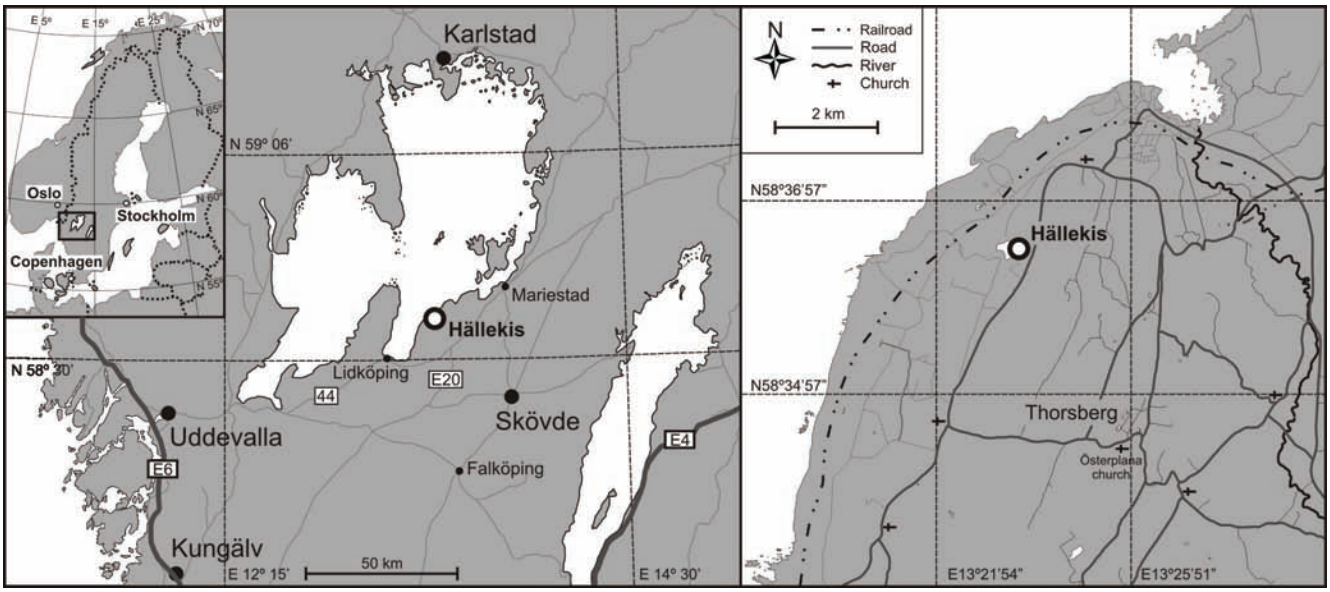

Figure 7. Maps of Scandinavia and parts of Västergötaland. To the right, the geographical location of the Hällekis quarry at Kinnekulle, is positioned. Note the nearby Thorsberg quarry.

suspended cephalopod conchs, thin seams of stromatoids and biocalcarenitic components dominated by arthropods and echinoderms (Lindström et al., 1991).

The Puxi River section (30°55'N, 111°25'E; Fig. 4 and 6) is located in an abandoned limestone quarry, ~30 km north of the city of Yichang in the Hubei Province, next to a minor creek that flow out in the Yangtze river. After crossing a small bridge ~3 km north of the town of Fenxiang, take the first dirt road to the left, down to the water for access to the lowermost part of the section. The section is best studied in the summer months when the water level is low.

At Puxi River, the 19.75 m thick Guniutan Formation is positioned between the Dawan and the Miaopo formations. The lower ~9 m of the formation is a bedded succession mainly consisting of very condensed biocalcarenitic wackestone. Discontinuity surfaces are numerous. Occasionally, the limestone beds are interbedded by thin layers of grey marl or shale, possibly indicating short periods of elevated supply of very fine-grained terrigenous material or reduced biogenic production. The following 1.5 m is represented by a marly interval with a few thin limestone beds. This is followed by the appearance of a very prominent so called "mini-mound" or "buckled bed" structure at +10.5 m. This mound-like structure typically extends 0.5-2 m laterally and 0.2-0.5 m vertically, with subelliptical to subcircular outlining (Zhang 1996, 1998a,b). This lower grey mini-mound appears clayey with a laminated structure, a second much less distinctive, entirely calcareous mini-mound occurs at +11.15 m. At Daping, Lindström et al. (1991) observe a similar thick laminated wavy bedding plane between 10.7-10.9 m relative to the base of the Guniutan Formation, which may represent the discussed mini-mounds. Between and above the two mini-mounds normal bedded limestone occurs. About 0.5 m above the upper mini-mound, the limestone beds are replaced by thick beds of nodular limestone that persist until +14.8 m. The interval across the +15 m mark (samples Y9 to P3) represents a gradual change from nodular to massive, bedded limestone, occasionally intercalating with thin layers of nodular limestone. The compact bedded limestone facies persist until the Miaopo Formation is reached, at +19.75 m. The sedimentary rocks of the Guniutan Formation generally vary from red to reddish grey to grey, although some grey beds may include more distinct red patches. The Dawan Formation below the Guniutan Formation consists of interbedded argillaceous limestone, nodular limestone and some thin- to medium-bedded calcareous mudstone, while the overlying Miaopo Formation is made up of black shales and muddy limestones, rich in graptolites and shells.

4.4. The Hällekis section, Kinnekulle, southern Sweden

Kinnekulle is a 306 m high table mountain situated southeast of Lake Vänern, Västergötaland, formed primarily by sedimentary rocks of Lower Cambrian to Lower Silurian age. The Middle Ordovician succession at Kinnekulle is dominated by the characteristic 'Orthoceratite Limestone' (referring to the occurrence of conchs of or-

thocone endoceroid cephalopods in some beds) deposited in a vast shallow epicontinental sea that covered most of the Baltoscandian shield during this period (Lindström et al. 1971, 1979). The abandoned Hällekis quarry (58°36'N, 13°23'E; Fig. 4 and 7) exposes a ~50 m thick succession of the red homogeneous 'Orthoceratite Limestone', an organic-poor (~0.1%) sediment that formed at very low sedimentation rates (2 ± 1 mm kyr^{-1}) (Lindström et al. 1971, 1979; Schmitz et al. 1996). The color of the massive limestone beds varies from red to brownish red throughout the section, with the exception of the 1.2-1.4 m thick, grey Täljsten interval. The change in color, relatively richness in phosphates and abundant anomalous fossil animals of the Täljsten interval suggest low oxygen conditions in the area, possibly associated with a gradual sea level regression and moderately increasing sedimentation rates, as indicated by observed changes in local conodont fauna (J. Mellgren, personal communication, Lund, 2009). Hard- (or firm-) grounds (mainly corrosional), with varying degree of surface mineralization, are common at Hällekis, suggested to represent extended periods (1-10 kyr) of non-deposition (Lindström 1979). The condensed character of the limestones and small quartz component, suggests deposition distal from terrigenous sources. The condition of well-preserved non-orientated cephalopod shells further support a calm setting, suggesting a water depth of ~100-300 m (or deeper based on the regional structural depression at Kinnekulle) (Chen and Lindström 1991; Schmitz et al. 1996).

5. SUMMARY OF PAPERS

5.1. Paper I

Cronholm A. and Schmitz B. 2007. Extraterrestrial chromite in latest Maastrichtian and Paleocene pelagic limestone at Gubbio, Italy: The flux of unmelted ordinary chondrites. *Meteoritics and Planetary Science* 42:2099-2109.

Summary: This paper we investigate the abundance of sediment-dispersed (chondritic) EC grains (>63 µm) in strata with slow sedimentation rates, similar to the Swedish mid-Ordovician sections, from another period. The marine limestone across the Cretaceous-Paleogene (K-T) boundary in the Bottaccione Gorge section at Gubbio, Italy, is ideal for establishing the accretion rate of EC because of its condensed nature and well-constrained sedimentation rates. In all, 6 EC grains (and possibly one pallasitic chromite grain) were recovered in a total of 210 kg, estimating an average of 0.029 EC grains kg^{-1}. We calculate the average flux of EC to Earth to ~0.26 grains m^{-2} kyr^{-1}, which corresponds to a total flux of ~200 tons of extraterrestrial matter per year, compared to ~30,000 tons per year, as estimated from Os isotopes in deep-sea sediments. The difference is readily explained by the EC grains representing only unmelted equilibrated ordinary chondritic matter, mainly in the cm to sub-mm sized fraction.

The low amounts of EC grains in the Gubbio limestone stands in contrast to the EC-rich mid-Ordovician limestone (1-3 EC grains per kg) at Kinnekulle, southern Sweden, which has been related to the break-up of the L-chondrite parent body ~470 Ma. The sedimentation rates at Kinnekulle and Gubbio are of the same order of magnitude, i.e. a few mm per thousand years, and the difference in EC abundance gives support for an increase by two orders-of-magnitude in the flux of chondritic matter directly after the asteroid break-up. At Kinnekulle limestone that formed prior to the L-chondrite disruption event exhibit similar low EC content (0.013 EC grains kg^{-1}) as the Gubbio limestone. These low concentrations of EC grains probably reflect the normal flux of ordinary chondrites to Earth.

In addition, samples adjacent to the K-T boundary are devoid of ordinary chondritic EC, consistent with an impactor most likely of carbonaceous origin, and thus low in chromite.

5.2. Paper II

Schmitz B., Cronholm A., and Montanari A. 2009a. A search for extraterrestrial chromite in the late Eocene Massignano section, central Italy. *Geological Society of America Special Paper* 452:71-82.

Summary: During the late Eocene Earth may have experienced an extended period of enhanced flux of extraterrestrial matter, possibly related to a comet or asteroid shower at ~36.3-34.3 Ma. The hypothesis is supported by two major and several minor impact craters, at least two microtectite-microkrystite layers, and a stratigraphic interval of ^{3}He-enriched (extraterrestrial) sediments. Tagle and Claeys (2004, 2005) propose that the recorded enrichment of ^{3}He in sediments at Massignano was caused by an asteroid (L-chondritic) shower in the late Eocene, based on platinum group element compositions. Fritz et al. (2007) suggests an asteroid bombardment of the Moon's surface that would have ejected vast amounts of ^{3}He-enriched lunar regolith into space, eventually enrich-

ing sediments on Earth. Any major enrichment of ordinary chondritic matter to Earth of this magnitude is expected to simultaneously enhance the accumulation of extraterrestrial chromite (derived from ordinary chondrites and possibly the Moon) in marine sediments.

In 167 kg of limestone from the ^{3}He-enriched interval at Massignano, only one EC grain was found, which corresponds to 0.006 EC grains kg^{-1}. This is one fifth of the EC content (0.029 EC grain per kg) at Gubbio, Italy, but this difference is explained by an almost threefold higher accumulation rate of the late Eocene sediment at Massignano. Consequently, our results argue against a late Eocene (ordinary chondritic) meteorite or asteroid shower, as no significant increase in the flux of extraterrestrial chromite occurs at this time.

5.3. Paper III

Cronholm A. and Schmitz B. 2009b. Extraterrestrial chromite distribution across the Puxihe section, central China: Evidence for a global major spike in micrometeorite flux during the mid-Ordovician. *Submitted to Icarus*.

Summary: Previous investigations of mid-Ordovician strata in southern Sweden have confirmed that there is a two orders-of-magnitude enrichment in fossil L-chondritic meteorites (∅ = 1-21 cm) and sediment-dispersed extraterrestrial chromite (EC) grains (>63 µm) in a stratigraphic interval across the Arenig-Llanvirn boundary. This extraordinary intensification in the flux of L-chondritic matter to Earth has been connected to the disruption of the L-chondrite parent body in the main asteroid belt at ~470 Ma.

In this paper we demonstrate that the general trend in the distribution of sediment-dispersed EC grains can be reproduced in the Puxi River section, central China. A total of 288 kg of whole-rock was sampled, yielding 291 EC grains with an average chemical composition very similar to chromite from recent L chondrites. In the initial 8 m of the section, representing the *Paroistodus originalis* and *Lenodus antivariabilis* conodont zones, only one EC grain was recovered in a total of 110 kg. Similarly to the Swedish sections, EC grains begin to be common in the overlying *L. variabilis* Zone and remain common all through the upper 9 m of the section, representing the *L. variabilis*, *Yangtzeplacognathus crassus* and *L. pseudoplanus* zones. Most beds across this interval yield 1-4 EC grains per kg limestone, representing a clear two orders-of-magnitude enrichment relative to the lower part of the section. Minor bed-by-bed variations in the EC content over the upper interval most likely reflect variations in sedimentation rates. Terrestrial chrome spinel grains are very rare throughout the Puxi River section, and can be distinguished readily by their rounded, abraded appearance compared to the angular, pristine extraterrestrial chromite.

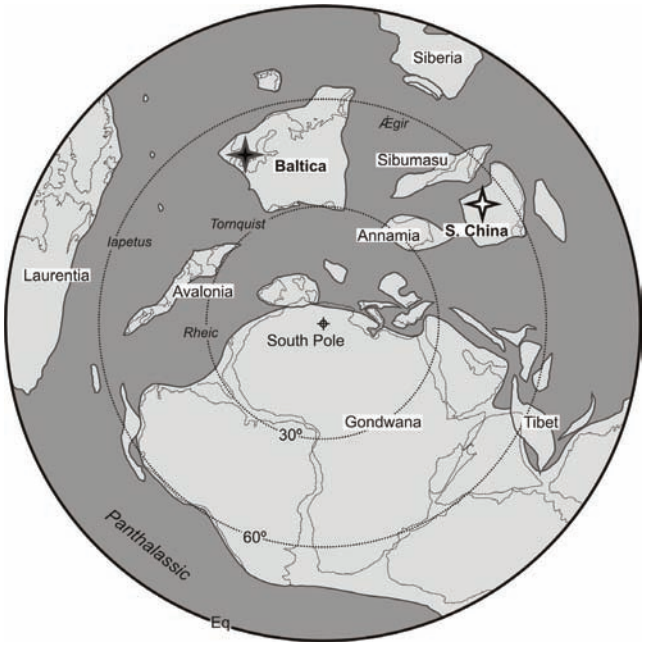

Figure 8. Southern hemisphere paleogeography of Middle Ordovician world, ~470 Ma (modified from Cooks and Torsvik 2002). The paleomaps for 480 respectively 460 Ma in fig. 2 of Cocks and Torsvik (2002) were mainly used for interpolation of position of paleocontinents. Positions of localities studied on the Baltica (black) and South China (white) paleocontinents marked by stars.

In the Middle Ordovician, based on paleoplate reconstructions, the Puxi River section was positioned at mid-latitudes on the southern hemisphere, a few thousand kilometres east of the Swedish sites in Baltica (Fig. 8). The prominent enrichment of EC grains over the same stratigraphic intervals in both China and Sweden constitute strong supporting evidence for a dramatic increase in the flux of L-chondritic matter to Earth shortly after the disruption of the L-chondrite parent-body in the asteroid belt.

5.4. Paper IV

Schmitz B., Harper D.A.T., Peucker-Ehrenbrink B., Stouge S., Alwmark A., Cronholm A., Bergström S.M., Tassinari M. and Wang X. 2008. Asteroid breakup linked to the Great Ordovician Biodiversification Event. *Nature Geoscience* 1:49-53.

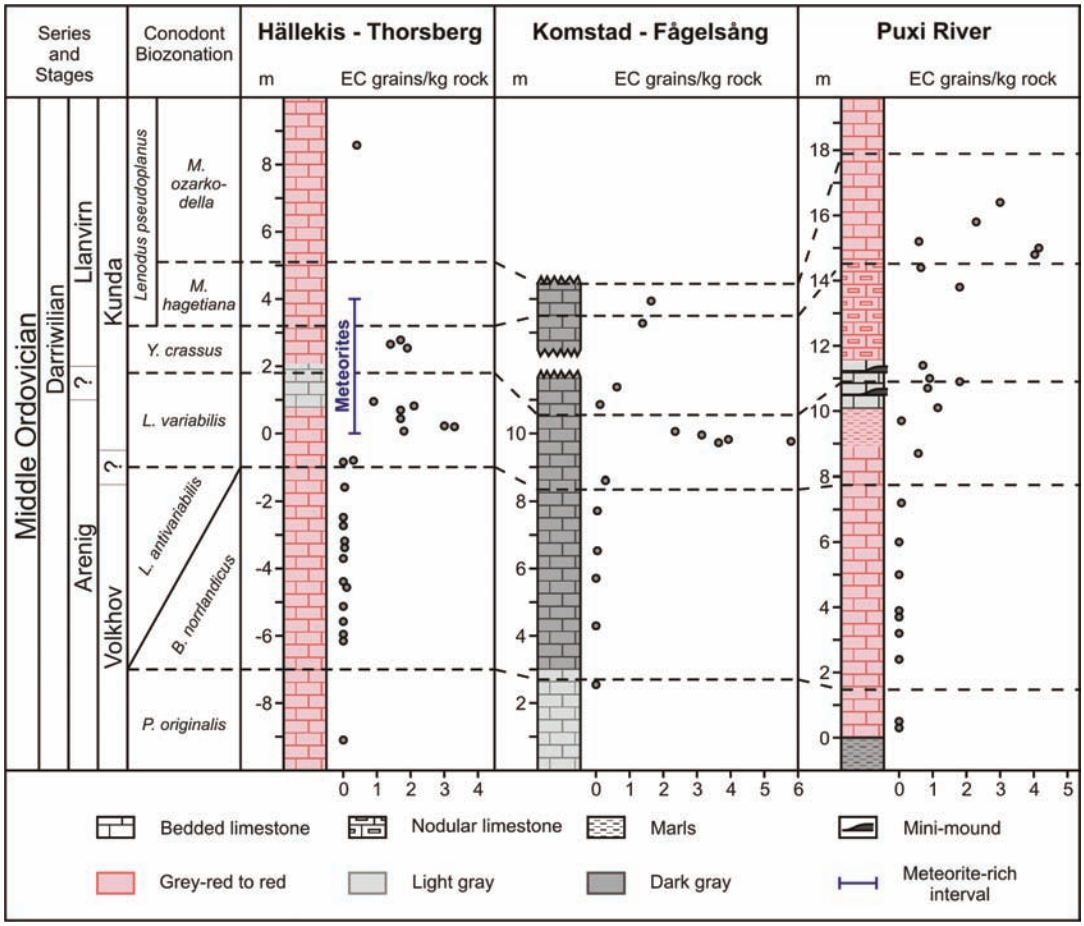

Figure 9. Distribution of extraterrestrial chromite (EC) through Middle Ordovician sections in Sweden and China. Results are shown for sections at Kinnekulle (Hällekis and Thorsberg quarries; Schmitz and Häggström 2006) and southern Scania (Killeröd and Fågelsång sections; Häggström and Schmitz 2007; Paper IV), 350 km apart in southern Sweden, and the Puxi River section, central China (Paper III). The conodont biostratigraphy from S. Stouge in Paper IV, with revisions for the Puxi River section based on re-measured log for this site in 2007. The interval yielding abundant fossil meteorites in the Thorsberg quarry is indicated (Schmitz et al. 2001). *M. ozarkodella=Microzarkodina ozarkodella.*

Summary: During the Great Ordovician Biodiversification Event (GOBE), in the Middle to Late Ordovician, biodiversity experienced a second stage in the major diversification of shelled invertebrates, initiated during the preceding Cambrian explosion (~540 Ma). GOBE was characterized by a period of extreme species radiation, coupled with rapid development in biodiversity at the family, genus and species level. The major changes of this event permanently altered the chemical and biological composition of the global marine environment, while the ulterior triggers of the event remain obscured.

In this paper we show that this major event in Earth's history coincides with the largest disruption event recorded in the main asteroid belt during the past couple of billion years – the break-up of the L-chondrite parent body at ~470 Ma. The close temporal correspondence of the two events has been established by stratigraphical correlation of extraterrestrial chromite, Os isotopes and invertebrate fossils in mid-Ordovician limestone beds of Baltoscandia and China (Fig. 9-10).

The major disruption of the L-chondrite parent body in the early Phanerozoic was recognized already in the 1960's; Today physical evidence include the finds of more than 80 fossil meteorites (d. 1-21 cm) in Middle Ordovician limestone at the Thorsberg quarry, Kinnekulle, and the recovery of abundant extraterrestrial chromite grains in contemporary limestone beds (derived from decomposed meteorites and micrometeorites) at the Kinnekulle, Komstad (Sweden) and Puxi River (China) sections (Fig. 9). Geochemical and petrographic studies have verified

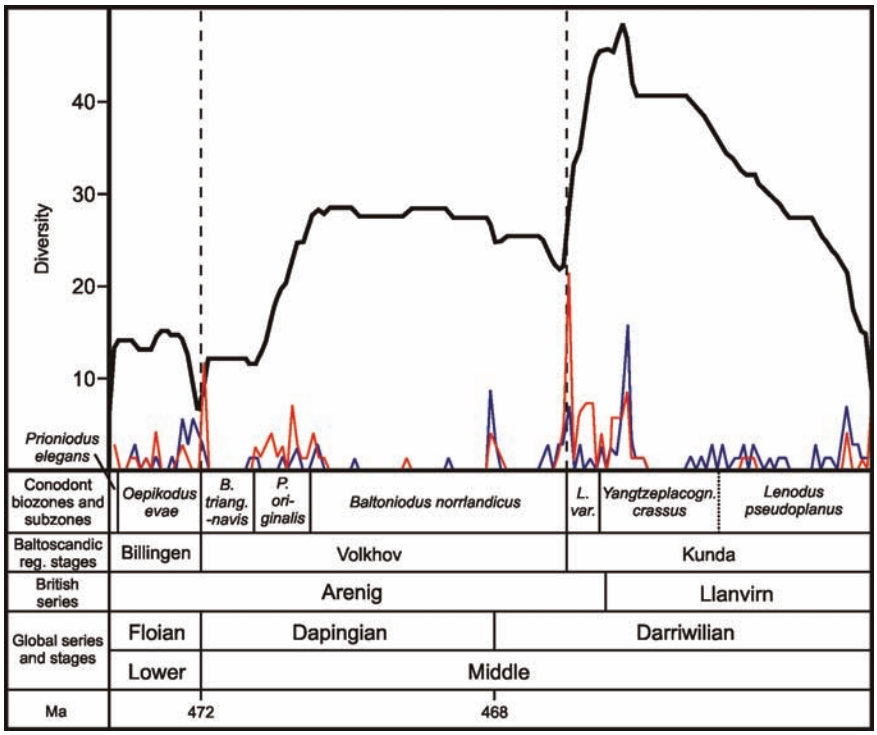

Figure 10. Total diversity of brachiopod species (number of species) through part of the Lower and Middle Ordovician in Baltoscandia. The results are based on bed-by-bed collections at eight localities (see papper IV). Note the dramatic increase in biodiversity (black line) and high extinction (blue line) and origination (red line) levels following the regional Volkhov–Kunda boundary, that is, the same level where extraterrestrial chromite appears in Fig. 9. The dashed lines show the boundaries between the regional states. *B. triang.-navis=Baltoniodus triangulatus-navis.*

the L-chondritic origin of both fossil meteorites and extraterrestrial chromite grains, and confirm that Earth experienced an extended period of enhanced influx of chondritic (cm to km sized) matter to Earth across the Arenig-Llanvirn boundary (middle Darriwilian). This is furthermore supported by a possible overrepresentation of impact craters during this period. In addition, the timing of the break-up event was estimated (by high-precision ^{40}Ar-^{39}Ar dating of recent L-chondritic meteorites) to 470±6 Ma, which correspond to the age of the limestone beds holding the fossil meteorites (467.3±1.6 Ma) according to the 2004 Geological Timescale (Grady 2000; Korochantseva et al. 2007).

Conversely, the global chronological constrains of GOBE is primarily based on regional changes in biodiversity from a range of fossil groups, and can only represent a rough estimation of the timing and pace of the event. A sharp growth in biodiversity is, however, observed at the Arenig-Llanvirn transition, as indicated by brachiopods, cephalopods and echinoderms (Fig. 10). This closely coincidence with the introduction of the extraterrestrial chromite grains and the Os isotopic excursion recorded in mid-Ordovician limestone. In conclusion, we propose that an enhanced influx of extraterrestrial matter, primarily by asteroids in the km-sized fraction, may have accelerated the biodiversification process during the Middle (to Late) Ordovician.

5.5. Paper V

Cronholm A. 2009c. Distribution of Os and ^{187}Os/^{188}Os through the Middle Ordovician Orthoceratite Limestone section at Hällekis, Kinnekulle, Sweden. *In manuscript.*

Summary: This paper presents new Os data for the limestone strata across the Arenig-Llanvirn boundary (middle Darriwilian) at Hällekis, Kinnekulle, coeval to the break-up of the L-chondrite parent body at ~470 Ma. Subsequently, Earth experienced enhanced influx of extraterrestrial matter (by two orders-of-magnitude) for an extended period of time, resulting in the enrichment of extraterrestrial chromite (EC) in the marine sed-

iments, derived from decomposed ordinary chondritic meteorites/micrometeorites. From the first appearance of common sediment-dispersed (EC) grains (in the uppermost *L. antivariabilis* conodont zone), a major reduction is observed in $^{187}Os/^{188}Os$, from 0.7102 to 0.3145, and low ratios are sustained throughout the EC-rich interval (mean 0.46). There is, however, no analogue decline in Os abundance, which would be expected if the radiogenic (terrestrial) Os input was reduced, indicating that the change was primarily caused by an increased unradiogenic Os fraction in the condensed strata. The rational for explanation for this is the increased influence of an extraterrestrial Os component ($^{187}Os/^{188}Os$ ~0.13) surpassing the previously predominating radiogenic (continental and hydrogenous) Os content (modern average ~1.54 and ~1.06, respectively). This corresponds well with the observed distribution of L-chondritic matter in the marine sediments at Kinnekulle during this period. Further support is provided by stable strontium isotope ($^{87}Sr/^{86}Sr$) data measured across the late Arenig to early Llanvirn strata at Hällekis, indicating that the observed increase in unradiogenic Os was not terrestrial in origin.

6. CONCLUSIONS

This thesis deals with the significance and global distribution of sediment-dispersed extraterrestrial chromite (EC) recovered in marine sediments across the Arenig-Llanvirn boundary (corresponding to the Middle Darriwilian and stage slice Dw2) at ~470 Ma. Recovered chromite in Paleogene and Middle Ordovician sediments, i.e. at Massignano and Bottaccione Gorge, Italy, and Puxi River, central China, respectively, was hence applied to reconstruct and evaluate variations in the flux of extraterrestrial matter during related periods. The results of the presented studies are manifold and have positive implications for future applications of EC as tool in interplanetary geology;

I) the normal (average background) distribution of sediment-dispersed (ordinary chondritic) chromite has been determined for early Paleogene pelagic sediments at Gubbio, Italy, at 0.029 EC grains kg^{-1} (Paper I). This is consistent with EC concentrations reported for strata that formed prior to the break-up event at Kinnekulle (0.013 EC grains kg^{-1}; Schmitz and Häggström, 2006), Komstad (<0.006 EC grains kg^{-1}; Häggström and Schmitz, 2007), and Puxi River (0.009 EC grains kg^{-1}; Paper III). Further support is given by low EC content at Massignano, although from less condensed sediments (0.006 EC grains kg^{-1}; Paper II). These results stand in major contrast to the abundances of EC grains recorded in the mid-Ordovician stratigraphic interval, representing the *L. variabilis*, *Y. crassus* and *L. pseudoplanus* conodont zones, in southern Sweden (~1-6 EC grains kg^{-1}; Schmitz and Häggström 2006; Häggström and Schmitz 2007) and central China (~1-4 EC grains kg^{-1}; Paper III) following the disruption of the L-chondrite parent body (~470 Ma). This emphasizes the extraordinary circumstances of this event, and shows an enhanced flux of meteorites and micrometeorites by two orders-of-magnitude for an extended period (~1-3 Myr) in the late Arenig and early Llanvirn.

II) The distribution of sediment-dispersed EC recorded in southern Sweden, has been reproduced at the distal Puxi River section, central China (Paper III). This confirms a global correlation of the extended meteorite and micrometeorite shower on Earth that followed after the break-up of the L-chondrite parent body at ~470 Ma. The EC-rich interval at Puxi River has concentrations of 1-4 EC per kg rock, similar to measured levels at Kinnekulle (1-3 EC per kg) and Komstad (1-6 EC per kg). All in all, our group has prepared and searched 1150 kg of mid-Ordovician limestone from these three localities for chromite (Schmitz et al. 2001, 2003; Schmitz and Häggström 2006; Häggström and Schmitz 2007, Paper III). The lower stratigraphic interval, represented by the *P. originalis* and *L. antivariabilis* conodont zones, have yielded only 8 EC grains in 614 kg of rock, resulting in a mean of 0.013 EC per kg. The sequential overlying *L. variabilis*, *Y. crassus* and *L. pseudoplanus* zones yielded 954 EC grains in a total of 536 kg of limestone, presenting an average of 1.78 EC grains per kg. This readily represents to two orders-of-magnitude increase in the flux of extraterrestrial matter.

III) The Great Ordovician Biodiversification Event (GOBE) and the L-chondrite disruption event seemingly occur at the same time (~470 Ma). Thus, we propose a connection between the sudden increase in extraterrestrial matter (km to sub-mm sized) and the rapid diversification in the marine fauna that coincided during Middle (to Late) Ordovician. Further research is required, specifically to increase the resolution of the GOBE and to find plausible mechanisms that connect the two events.

IV) We have presented strong evidence against a proposed ordinary chondritic meteorite or micrometeorite

shower in the late Eocene (paper II), and consequently suggest that no 'asteroid shower' occurred at this time, even though a minor increase (a factor of a few) in the asteroid flux cannot be ruled out. Only a single EC grains was recovered in 167 kg of limestone samples at Massignano. Considering the sedimentation rates at Massignano, and by comparison with similar studies for other periods in Earth history (see conclusion I) above), this is the approximate EC content to be expected if the flux rate of chondritic matter to Earth was normal or close to normal during the late Eocene.

V) New Os data from Hällekis has shown a correlation between the first appearance of common sediment-dispersed EC, following the break-up event at ~470 Ma, and a major reduction in the marine Os isotopic ($^{187}Os/^{188}Os$) record. The rational explanation for this change in $^{187}Os/^{188}Os$ is the increased influence of a non-radiogenic, extraterrestrial Os component, derived from the decomposition of the meteorites/micrometeorites that enriched sediments in EC. Stable strontium isotope ratios across the late Arenig to early Llanvirn support an extraterrestrial non-radiogenic source, rather than a terrestrial source.

VI) The evaluation of the EC extraction method have shown that it can also be used for the searches of extraterrestrial chromite other than ordinary chondritic, as exemplified by the a probable pallasitic grain recovered at Bottaccione Gorge, Gubbio (Paper I), and a possible grain from an iron meteorite at Puxi River, central China (Paper III).

In conclusion, 665 kg of Paleogene and Middle Ordovician limestone from Italy and China has been searched for EC grains in this thesis work. The composite background material from the Italian and Chinese sections represents 487 kg of rock, and yielded only 8 EC altogether. The EC-rich Ordovician interval, representing the sequential *L. variabilis*, *Y. crassus* and *M. hagetiana* conodont zones, yielded a total of 290 EC grains in 178 kg of limestone, signifying an average 1.63 EC per kg rock. This clearly shows a two orders-of-magnitude increase in the flux of L-chondritic matter during the mid-Ordovician. The largest documented asteroid break-up in the asteroid belt during the past few billion years has left a prominent signature in the coeval sediments on Earth, and this thesis corroborates the significance and global consequences of this event.

7. ACKNOWLEDGMENT

It is exceedingly difficult to write this chapter, since summarizing all contributions and support people have offered during my four years and four months as a Ph.D. student is an impossible task.

I would like begin by thanking my principal supervisor, Birger Schmitz, whom I have had the pleasure of collaborating with for many years now. He started this challenging and innovative project and I think everybody involved agrees that it has been an interesting journey. The highlights of my Ph.D. have been the exciting fieldworks that have brought me to Italy, China and South Africa.

I also want to thank my assistant supervisor Mikael Calner for his support, always making time to discuss various issues. I am grateful to Mario Tassinari, and his inquisitive and passionate nature, without whom the ET project might never have been initiated. Anita Löfgren is thanked for helping with conodont stratigraphy in the various projects. I would also like to thank all my colleagues at the department, but special thanks go out to Carl, with whom it has been a mixed pleasure to share room with over the past four and a half years. Order is not a virtue, my friend, neither is your singing. However, you always lend a helping hand when needed! Thanks!

I want to express my gratitude to all the people in the power lifting crew at Gerda, at the poker and in the gaming group, who made me forget about the 'hardships' of being a Ph.D. student at least for a few hours a every week.

I want to thank all my dear friends who have been very supportive and caring over the last few years, and I will continue to thank them in person. There are, however, a couple of friends who have been essential during these last couple months, and I would like to extend my special gratitude to Åsa Björck (and her loving family) for skilfully making the layout of this synthesis and Paper III and V, and to Erik Uddman, for simply being yourself! You never hesitate to help your friends out, and I admire you for that. Erik has been a harsh, impartial critic of my manuscript drafts over the years, and provided excellent input during the process of this synthesis.

I want to thank my dear parents, Kjell and Birgitta, for always encouraging me to follow my heart and try to be happy. I also want to thank my sister, Marie, and her loving family, Hugo, Hampus, Pontus och Mikael, for all their support! Hopefully I can visit all of you more often now that I have finished my Ph.D.

Financial support was given by the Swedish Research Council, the Crafoord Foundation, the National Geographic Society and The Barringer Crater Company.

8. REFERENCES

Afiattalab F. and Wasson J. T. 1980. Composition of the metal phases in ordinary chondrites: Implications regarding classification and metamorphism. *Geochimica et Cosmochimica Acta* 44:431-446.

Alvarez W., Arthur M. A., Fischer A. G., Lowrie W., Napoleone G., Premoli Silva I., and Roggenthein W. M. 1977. Upper Cretaceous-Paleocene magnetic stratigraphy at Gubbio, Italy: V. Type section for the Late Cretaceous-Paleocene geomagnetic reversal time scale. *Geological Society of America Bulletin* 88: 383–389.

Alvarez L. W., Alvarez W., Asaro F., and Michel H. V. 1980. Extraterrestrial cause for the Cretaceous-Tertiary extinction - Experimental results and theoretical interpretation. *Science* 208: 1095–1108.

Alvarez W., Asaro F., and Montanari A. 1990. Iridium profile for 10 million years across the Cretaceous-Tertiary boundary at Gubbio (Italy). *Science* 250:1700–1702.

Alwmark C. and Schmitz B. 2007. Extraterrestrial chromite in the resurge deposits of the early Late Ordovician Lockne crater, central Sweden. *Earth and Planetary Science Letters* 253:291–303.

Alwmark C. and Schmitz B. 2009. Relict silicate inclusions in extraterrestrial chromite and their use in the classification of fossil chondritic material. *Geochimica et Cosmochimica Acta* 73:1472-1486.

Arthur M. A. and Fischer A. G. 1977. Upper Cretaceous-Paleocene magnetic stratigraphy at Gubbio, Italy: I. Lithostratigraphy and sedimentology. *Geological Society of America Bulletin* 88:367–371.

Barnes S. J. and Roeder P. L. 2001. The range of spinel compositions in terrestrial mafic and ultramafic rocks. *Journal of Petrology* 42:2279–2302.

Binzel R. P., Xu S., Bus S. J., Skrutskie M. F., Meyer M. R., Knezek P., and Barker E. S. 1993. Discovery of a main-belt asteroid resembling ordinary chondrite meteorites. *Science* 262:1541-1543.

Bland P. A. 2001. Quantification of meteorite infall rates from accumulations in deserts, and meteorite accumulations on Mars. In *Accretion of extraterrestrial matter throughout Earth's history*, edited by Peucker-Ehrenbrink B. and Schmitz B. New York: Kluwer Academic/Plenum Publishers. pp. 267–303.

Bland P. A., Smith T. B., Jull A. J. T., Berry F. J., Bevan A. W. R., Cloudt S., and Pillinger C. T. 1996. The flux of meteorites to the Earth over the last 50,000 years. *Monthly Notices of the Royal Astronomical Society* 283:551–565.

Bodiselitsch B., Montanari A., Koeberl C., and Coccioni R. 2004. Delayed climate cooling in the late Eocene caused by multiple impacts: High-resolution geochemical studies at Massignano, Italy. *Earth and Planetary Science Letters* 223 :283–302.

Bottomley R., Grieve R., York D., and Masaitis V. 1997. The age of the Popigai impact event and its relation to the events at the Eocene/Oligocene boundary. *Nature* 388:365-368.

Brearley A. J. and Jones R. H. 1998. Chondritic meteorites. In *Planetary Materials* (ed. J. J. Papike). Mineralogical Society of America, Washington, pp. 3-1--3-398.

Bridges J. C., Schmitz B., Hutchison R., Greenwood R. C., Tassinari M., and Franchi I. A. 2007. Petrographic classification of mid-Ordovician fossil meteorites from Sweden. *Meteoritics & Planetary Science* 43:1781–1789.

Bunch T. E, Keil K., and Snetsinger K. G. 1967. Chromite composition in relation to chemistry and texture of ordinary chondrites. *Geochimica et Cosmochimica Acta* 31:1569–1582.

Chen J. -Y. and Lindström M. 1991. Cephalopod septal strength indices (SSI) and depositional depth of Swedish Orthoceratite limestone. *Geol. Paleontol.* 25:5-18.

Clymer A. K., Bice D.M., and Montanari A., 1996. Shocked quartz from the late Eocene: Impact evidence from Massignano, Italy. *Geology* 24:483–486.

Cocks R. L. and Torsvik T. H. 2002. Earth geography from 500 to 400 million years ago: a faunal and palaeomagnetic review. *Journal of the Geological Society* 159: 631-644.

Dalai T. K. and Ravizza G. 2006. Evaluation of osmium

isotopes and iridium as paleoflux tracers in pelagic carbonates. *Geochimica et Cosmochimica Acta* 70:3928–3942.

Ebel D. S. and Grossman L. 2005. Spinel-bearing spherules condensed from the Chicxulub impact-vapor plume. *Geology* 33:293–296.

Esser B. K. and Turekian K. K. 1988. The accretion rate of extraterrestrial particles determined from osmium isotope systematics of Pacific pelagic clay and manganese nodules. *Geochimica et Cosmochimica Acta* 52:1383-1388.

Esser B. K. and Turekian K. K. 1993. The osmium isotopic composition of the continental crust. *Geochimica et Cosmochimica Acta* 57:3093-3104.

Farley K. A., Love S. G., and Patterson D. B. 1997. Atmospheric entry heating and helium retentivity of interplanetary dust particles. *Geochimica et Cosmochimica Acta* 61:2309–2316.

Farley K. A., Montanari A., Shoemaker E. M., and Shoemaker C. S. 1998. Geochemical evidence for a comet shower in the late Eocene. *Science* 280:1250–1253.

Farley K. A., Vokrouhlicky D., Bottke W. F., and Nesvorny D. 2006. A late Miocene dust shower from the breakup of an asteroid in the main belt. *Nature* 439:295–297.

Fritz J., Tagle R., and Artemieva N. 2007. Lunar helium-3 in marine sediments: Implications for a late Eocene asteroid shower. *Icarus* 189:591–594.

Gabrielli P., Barbante C., Plane J. M. C., Varga A., Hong S., Cozzi G., Gaspari V., Planchon F. A. M., Cairns W., Ferrari C., Crutzen P., Cescon P., and Boutron C. F. 2004. Meteoric smoke fallout over the Holocene epoch revealed by iridium and platinum in Greenland ice. *Nature* 432:1011–1014.

Gaffey M. J. and Gilbert S. L. 1998. Asteroid 6 Hebe: The probable parent body of the H-type ordinary chondrites and of the IIE iron meteorites. *Meteoritics & Planetary Science* 33:1281-1295.

Grady M. M. 2000. *Catalogue of Meteorites*, 5th ed, Cambridge Univiversity Press, New York.

Greenwood R. C., Schmitz B., Bridges J. B., Hutchison R., and Franchi I. A. 2007. Disruption of the L-chondrite parent body: New oxygen isotope evidence from Ordovician relict chromite grains. *Earth and Planetary Science Letters* 262:204–213.

Haack H., Farinella P., Scott E. R. D., and Keil K. 1996. Meteoritic, asteroidal, and theoretical constraints on the 500 Ma disruption of the L chondrite parent body. *Icarus* 119:182-191.

Häggström T. and Schmitz B. 2007. Distribution of extraterrestrial chromite in Middle Ordovician Komstad limestone in the Killeröd quarry, Scania, Sweden. *Bulletin of Geological Society of Denmark* 55:37–58.

Halliday I. 2001. The present-day flux of meteorites to the Earth. In *Accretion of extraterrestrial matter throughout Earth's history*, edited by Peucker-Ehrenbrink B. and Schmitz B. New York: Kluwer Academic/Plenum Publishers. pp. 305–318.

Hassler D. R., Peucker-Ehrenbrink B., and Ravizza G. 2000. Rapid determination of Os isotopic composition by sparging OsO4 into a magnetic-sector ICP-MS. *Chemical Geology* 166:1-14.

Heck P. R., Schmitz B., Baur H., Halliday A. N., and Wieler R. 2004. Fast delivery of meteorites to Earth after a major asteroid collision 480 Myr. *Nature* 430:323–325.

Heck P.R., Schmitz B., Baur H., and Wieler R. 2008. Noble gases in fossil micrometeorites and meteorites from 470 Myr old sediments from southern Sweden and new evidence for the L-chondrite parent body breakup event. *Meteoritics & Planetary Science* 43:517–528.

Heymann, D. 1967. On the origin of hypersthene chondrites: Ages and shock effects of black chondrites. *Icarus* 6:189–221.

Hildebrand A. R., Penfield G. T., Kring D. A., Pilkington M., Camargo A., Jacobsen S. B., and Boynton W. V. 1991. Chicxulub crater: A possible Cretaceous-Tertiary boundary impact crater on the Yucatán Peninsula, Mexico. *Geology* 19:867–871.

Jackson J. A. (ed.).1997. *Glossary of Geology*, Forth edition.

American Geological Institute, Alexandria, Virginia.

Jarosewich E., Nelen J. A., and Norberg J. A. 1980. Reference samples for electron microprobe analysis. *Geostandards Newsletter* 4:43–47.

Karner D. B., Levine J., Muller R. A., Asaro F., Ram M., and Stolz M. R. 2003. Extraterrestrial accretion from the GISP2 ice core. *Geochimica et Cosmochimica Acta* 67:751–763.

Keil K. 1962. On the phase composition of meteorites. *Journal of Geophysical Research* 67:4055–4061.

Keil K., Haack H., Scott E. R. D. 1994. Catastrophic fragmentation of asteroids: Evidence from meteorites. *Planetary and Space Science* 42:1109-1122.

Koeberl C. and Shirey S. B. 1997. Re-Os isotope systematics as a diagnostic tool for the study of impact craters and ejecta. *Paleogeography Paleoclimatology Paleoecology* 132:25-46.

Koeberl C., Reimold W. U., Brandt D. and Poag C. W. 1995. Chesapeake Bay crater, Virginia - Confimation of impact origin. *Meteoritics* 30:528-529.

Korochantseva E. V, Trieloff M., Lorenz C. A., Buykin A. I., Ivanova M. A., Schwartz W. H., Hopp J., and Jessberger E. K. 2007. L-chondrite asteroid breakup tied to Ordovician meteorite shower by multiple isochron ^{40}Ar-^{39}Ar dating. *Meteoritics & Planetary Science* 42:113–130.

Kuhnt W. 1990. Agglutinated foraminifera of western Mediterranean Upper Cretaceous pelagic limestone (Umbrian Apennines, Italy, and Betic Cordillera, southern Spain). *Micropaleontology* 36:297–330.

Kyte F. T. and Smit J. 1986. Regional variations in spinel compositions: An important key to the Cretaceous/Tertiary event. *Geology* 14:485–487.

Levasseur S., Birck J. –L., and Allègre C. J. 1999. The osmium riverine flux and the oceanic mass balance of osmium. *Earth Planet. Sci. Lett.* 174:7-23.

Lindström M. 1971. Vom Anfang, Hochstand und Ende eines Epikontinentalmeeres. *Geologische Rundschau* 60:419–438.

Lindström M. 1979. Diagenesis of Lower Ordovician hardgrounds in Sweden. *Geological Paleontology* 13:9-30.

Lindström M., Chen J.- Y. and Zhang J.- M. 1991. Section at Daping reveals Sino-Baltoscandian parallelism of facies in the Ordovician. *GFF* 113:189-205.

Love S. G. and Brownlee D. E. 1993. A direct measurement of the terrestrial mass accretion rate of cosmic dust. *Science* 262:550–553.

Lowrie W., Alvarez W., and Asaro F. 1990. The origin of the White Beds below the Cretaceous-Tertiary boundary in the Gubbio section, Italy. *Earth and Planetary Science Letters* 98:303–312.

Mathews J. D., Janches D., Meisel D. D., and Zhou Q. H. 2001. The micrometeoroid mass flux into the upper atmosphere: Arecibo results and a comparison with prior estimates. *Geophysical Research Letters* 28:1929–1932.

Meisel T., Biino G. G., and Nägler T. F. 1996. Re-Os, Sm-Nd, and rare earth element evidence for Proterozoic oceanic and possible subcontinental lithosphere in tectonized ultramafic lenses from the Swiss Alps. *Geochimica et Cosmochimica Acta* 60:2583–2593.

Migliorini F., Manara A., Scaltriti F., Farinella P., Cellino A., and Di Martino M. 1997. Surface properties of (6) Hebe: A possible parent body of ordinary chondrites. Icarus 128:104-113.

Monechi S. and Thierstein H. R. 1985. Late Cretaceous-Eocene nannofossil and magnetostratigraphic correlations near Gubbio, Italy. *Marine Micropaleontology* 9:419–440.

Montanari A. 1991. Authigenesis of impact spheroids in the K/T boundary clay from Italy: New constraints for high-resolution stratigraphy of terminal Cretaceous events. *Journal of Sedimentary Petrology* 61:315–339.

Montanari A. and Koeberl C. 2000. Impact Stratigraphy - The Italian Record: Lecture Notes in Earth Sciences, Volume 93: Heidelberg-Berlin, Springer Verlag, p. 1–364.

Montanari A., Asaro F., Michel H.V., and Kennett J.P.

1993. Iridium anomalies of late Eocene age at Massignano (Italy), and ODP Site 689B (Maud Rise, Antarctic). *Palaios* 8:420–437.

Mukhopadhyay S., Farley K. A., and Montanari A. 2001a. A short duration of the Cretaceous-Tertiary boundary event: Evidence from extraterrestrial ^{3}He. *Science* 291:1952–1955.

Mukhopadhyay S., Farley K. A., and Montanari A. 2001b. A 35 Myr record of helium in pelagic limestone from Italy: Implications for interplanetary dust accretion from the early Maastrichtian to the middle Eocene. *Geochimica et Cosmochimica Acta* 65:653–669.

Nesvorný D., Morbidelli A., Vokrouhlický D., Bottke W. F., and Brož M. 2002. The Flora Family: A Case of the Dynamically Dispersed Collisional Swarm? *Icarus* 157:155-172.

Nyström J. O., Lindström M., and Wickman F. E. 1988. Discovery of a second Ordovician meteorite using chromite as a tracer. *Nature* 336:572–574.

Peucker-Ehrenbrink B. 2001. Iridium and osmium as tracers of extraterrestrial matter in marine sediments. In *Accretion of extraterrestrial matter throughout Earth's history*, edited by Peucker-Ehrenbrink B. and Schmitz B. New York: Kluwer Academic/Plenum Publishers. pp. 163–178.

Peucker-Ehrenbrink B. and Ravizza G. 2000. The effects of sampling artifacts on cosmic dust flux estimates: A reevaluation of nonvolatile tracers (Os, Ir). *Geochimica et Cosmochimica Acta* 64:1965–1970.

Peucker-Ehrenbrink B. and Jahn B. –M. 2001. Rhenium-Osmium isotope systematics and platinum group element concentrations: loess and the upper continental crust. *Geochemistry Geophysics Geosystems* 2: paper 2001GC000172.

Peucker-Ehrenbrink B., Bach W., Hart S. R., Blusztajn J. S., and Abbruzzese T. 2003. Rhenium-osmium isotope systematics and platinum group element concentrations in oceanic crust from DSDP/ODP Sites 504 and 417/418. *Geochemisty Geophysics Geosystems* 4: art. no. 8911.

Pierrard O., Robin E., Rocchia R., and Montanari A. 1998. Extraterrestrial Ni-rich spinel in Upper Eocene sediments from Massignano, Italy. *Geology* 26:307–310.

Premoli Silva I. 1977. Upper Cretaceous-Paleocene magnetic stratigraphy at Gubbio, Italy; II. Biostratigraphy. *Geological Society of America Bulletin* 88:371–374.

Ramdohr P. 1967. Chromite and chromite chondrules in meteorites. *Geochimica et Cosmochimica Acta* 31:1961-1967.

Ramdohr P. 1973. *The opaque minerals in stony meteorites.* Amsterdam: Elsevier. 245 p.

Robin E., Bonté Ph., Froget L., Jéhanno C., and Rocchia R. 1992. Formation of spinels in cosmic objects during atmospheric entry: A clue to the Cretaceous-Tertiary boundary event. *Earth and Planetary Science Letters* 108:181–190.

Rubin E. 1990. Kamacite and olivine in ordinary chondrites: Intergroup and intragroup relationships. *Geochimica et Cosmochimica Acta* 54:1217-1232.

Rubin A. E. 1997. Mineralogy of meteorite groups. *Meteoritics & Planetary Science* 32:231–247.

Rubin A. E. 2000. Petrologic, geochemical, and experimental constraints on models of chondrules formation. *Earth Science Reviews* 50:3–27.

Schmitz B. and Häggström T. 2006. Extraterrestrial chromite in Middle Ordovician marine limestone at Kinnekulle, southern Sweden - Traces of a major asteroid breakup event. *Meteoritics & Planetary Science* 41:455–466.

Schmitz B., Lindström M., Asaro F., and Tassinari M. 1996. Geochemistry of meteorite-rich marine limestone strata and fossil meteorites from the Lower Ordovician at Kinnekulle, Sweden. *Earth and Planetary Science Letters* 145:31–48.

Schmitz B., Peucker-Ehrenbrink B., Lindström M., and Tassinari M. 1997. Accretion rates of meteorites and cosmic dust in the Early Ordovician. *Science* 278:88-90.

Schmitz B., Tassinari M., and Peucker-Ehrenbrink B.

2001. A rain of ordinary chondritic meteorites in the early Ordovician. *Earth and Planetary Science Letters* 194:1–15.

Schmitz B., Häggström T., and Tassinari M. 2003. Sediment-dispersed extraterrestrial chromite traces a major asteroid disruption event. *Science* 300:961–964.

Shirey S. B. and Walker R. J. 1998. The Re-Os isotope system in cosmochemistry and high-temperature geochemistry. *Annual Review of Earth and Planetary Sciences* 26:423-500.

Shukolyukov A. and Lugmair G. W. 1998. Isotopic evidence for the Cretaceous-Tertiary impactor and its type. *Science* 282:927–929.

Smit J. 1982. Extinction and evolution of planktonic foraminifera after a major impact at the Cretaceous/Tertiary boundary. GSA Special Paper #190. Boulder, Colorado: Geological Society of America. pp. 329–352.

Smit J. and Kyte F. T. 1984. Siderophile-rich magnetic spheroids from the Cretaceous-Tertiary boundary in Umbria, Italy. *Nature* 310:403–405.

Snetsinger K. G., Keil K., and Bunch T. E. 1967. Chromite from "equilibrated" chondrites. *American Mineralogist* 52:1322-1331.

Stöffler D., Keil K. and Scott E. R. D. 1991. Shock metamorphism of ordinary chondrites. *Geochimica et Cosmochimica Acta* 55:3845-3867.

Tagle R. and Claeys P. 2004. Comet or asteroid shower in the late Eocene? *Science* 305 :492.

Tagle R. and Claeys P. 2005. An ordinary chondrite impactor for the Popigai crater, Siberia. *Geochimica et Cosmochimica Acta* 69:2877–2889.

Taylor S. and Lever J. H. 2001. Seeking unbiased collections of modern and ancient micrometeorites. In *Accretion of extraterrestrial matter throughout Earth's history*, edited by Peucker-Ehrenbrink B. and Schmitz B. New York: Kluwer Academic/Plenum Publishers. pp. 205-219.

Toppani A. and Libourel G. 2003. Factors controlling composition of cosmic spinels: Application to atmospheric entry conditions of meteoritic materials. *Geochimica et Cosmochimica Acta* 67: 4621–4638.

Van Schmus W. R. and Wood J. A. 1967. A chemical-petrologic classification lot the chondritic meteorites. *Geochimica et Cosmochimlca Acta* 31:747-765.

Wlotzka F. 2005. Cr spinel and chromite as petrogenetic indicators in ordinary chondrites: Equilibration temperatures of petrologic types 3.7 to 6. *Meteoritics & Planetary Science* 40:1673–1702.

Zhan R., Jin J., and Chen, P. 2007. Brachiopod diversification during the Early-Mid Ordovician: an example from the Dawan Formation, Yichang area, central China. *Canadian Journal of Earth Sciences* 44:9-24.

Zhang J. 1996. Lithofacies and stratigraphy of the Ordovician Guniutan Formation in its type area, China. *Geological Journal* 31:201-215.

Zhang J. 1998a. Conodonts from the Guniutan Formation (Llanvirnian) in Hubei and Hunan provinces, south-central China. Thesis, University of Stockholm, Stockholm, Sweden. *Stockholm Contributions in Geology* 46:1-161.

Zhang J. 1998b. Middle Ordovician conodonts from the Atlantic Faunal Region and the evolution of key conodont genera. Thesis, Meddelanden från Stockholms Universitets Institution för Geologi och Geokemi 298:1-27.

Zhou D., RU K., and Chen H.-Z. 1995. Kinematics of Cenozoic extension on the South China Sea continental margin and its implications for the tectonic evolution of the region. *Tectonophysics* 251:161-177.

I

The Meteoritical Society

Meteoritics & Planetary Science 42, Nr 12, 2099–2109 (2007)
Abstract available online at http://meteoritics.org

Extraterrestrial chromite in latest Maastrichtian and Paleocene pelagic limestone at Gubbio, Italy: The flux of unmelted ordinary chondrites

Anders CRONHOLM* and Birger SCHMITZ

Department of Geology, Lund University, Sölvegatan 12, SE-22362 Lund, Sweden
*Corresponding author. E-mail: anders.cronholm@geol.lu.se

(Received 17 January 2007; revision accepted 20 June 2007)

Abstract–The distribution of sediment-dispersed extraterrestrial (ordinary chondritic) chromite (EC) grains (>63 μm) has been studied across the latest Maastrichtian and Paleocene in the Bottaccione Gorge section at Gubbio, Italy. This section is ideal for determining the accumulation rate of EC because of its condensed nature and well-constrained sedimentation rates. In a total of 210 kg of limestone representing eight samples of 14–28 kg distributed across 24 m of the Bottaccione section, only 6 EC grains were found (an average of 0.03 EC grains kg^{-1}). In addition, one probable pallasitic chromite grain was found. No EC grains could be found in two samples at the Cretaceous-Tertiary (K-T) boundary, which is consistent with the K-T boundary impactor being a carbonaceous chondrite or comet low in chromite. The average influx of EC to Earth is calculated to ~0.26 grain m^{-2} kyr^{-1}. This corresponds to a total flux of ~200 tons of extraterrestrial matter per year, compared to ~30,000 tons per year, as estimated from Os isotopes in deep-sea sediments. The difference is explained by the EC grains representing only unmelted ordinary chondritic matter, predominantly in the size range from ~0.1 mm to a few centimeters in diameter. Sedimentary EC grains can thus give important information on the extent to which micrometeorites and small meteorites survive the passage through the atmosphere. The average of 0.03 EC grain kg^{-1} in the Gubbio limestone contrasts with the up to ~3 EC grains kg^{-1} in mid-Ordovician limestone that formed after the disruption of the L chondrite parent body in the asteroid belt at ~470 Ma. The two types of limestone were deposited at about the same rate, and the difference in EC abundance gives support for an increase by two orders of magnitude in the flux of chondritic matter directly after the asteroid breakup.

INTRODUCTION

Recent empirical evidence indicates the existence of short periods during the Phanerozoic with significantly increased flux of extraterrestrial matter to Earth (Farley et al. 1998, 2006; Schmitz et al. 1996, 2001, 2003). Such flux increases have been predicted to result from, for example, gravity perturbations of the orbits of comets in the Oort cloud (e.g., Hills 1981; Hut et al. 1987; Matese et al. 1995) or parent body breakup events in the asteroid belt (Zappalà et al. 1998; Nesvorny et al. 2006). The finding of more than fifty fossil meteorites in mid-Ordovician marine limestone at Kinnekulle in southern Sweden supports an increase in the flux of meteorites by one to two orders of magnitude following the disruption of the L chondrite parent body in the asteroid belt ~470 Myr ago (Schmitz et al. 1996, 2001). The fossil meteorites have been shown to be pseudomorphosed L chondrites (Schmitz et al. 2001; Bridges et al. 2007; Greenwood et al. 2007) and their relict chromite grains show cosmic-ray exposure ages that support an origin from an asteroid breakup event (Heck et al. 2004). A mid-Ordovician increase in the meteorite flux is further supported by the distribution of sediment-dispersed extraterrestrial (ordinary chondritic) chromite (EC) grains (63–355 μm) in condensed limestone strata from southern Sweden (Schmitz et al. 2003; Schmitz and Häggström 2006). The search for fossil meteorites is time-consuming and requires screening of thousands of cubic meters of limestone, whereas sediment-dispersed EC grains can be searched in samples of 10–50 kg. Chromite is highly resistant to weathering and it is one of the rare relict minerals of fossil meteorites (Thorslund et al. 1984). The sediment-dispersed EC grains represent residues of primarily small, 0.1 mm to 1–3 cm ordinary chondrites that decomposed on the sea floor (Schmitz et al. 2003; Heck et al., Forthcoming). Recent ordinary chondrites contain on average ~0.25 wt% chromite ($FeCr_2O_4$) (Keil 1962) and constitute ~80% of the total meteoritic influx (Bevan et al. 1998). The EC can be readily distinguished from terrestrial chromite by a

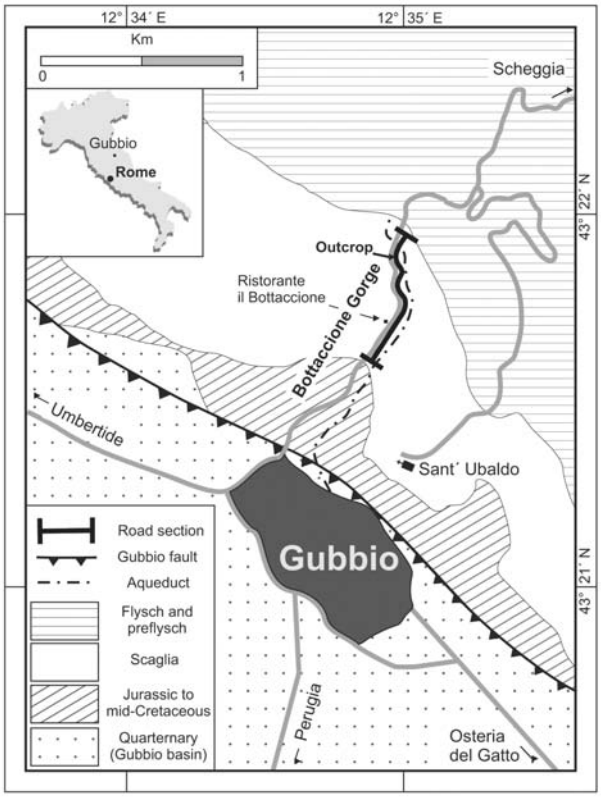

Fig. 1. Geology of Gubbio area and location of Bottaccione Gorge section and outcrop studied. Modified after Alvarez et al. (1977).

characteristic and unique major and trace element composition (Thorslund et al. 1984; Nyström et al. 1988; Roeder 1994; Schmitz et al. 2001). Extraterrestrial chromite shows minor variations in composition related to types H, L, and LL of host meteorite (Bunch et al. 1967; Schmitz et al. 2001; Wlotzka 2005). Hence, EC grains dispersed in sediments can be useful for determining both ancient accretion rates of ordinary chondritic material and variations in the types of ordinary chondrites reaching Earth (Schmitz et al. 2003).

In mid-Ordovician condensed strata in southern Sweden, limestone beds that formed after the disruption of the L chondrite parent body contain typically 1–3 EC grains per kg limestone, whereas in 379 kg of limestone that formed during the ~5 Myr immediately prior to this event, only 5 EC grains were found (Schmitz and Häggström 2006). In order to fully assess the significance of these results, EC accretion rates also for other periods in Earth's history must be determined. In the present study the classic section across the latest Maastrichtian and Paleocene in the Bottaccione Gorge at Gubbio, Italy, was selected for EC searches. The pelagic limestone at this site formed at the same low sedimentation rates, i.e., a few millimeters per 1000 years, as the mid-Ordovician limestone at Kinnekulle (Arthur and Fischer 1977; Schmitz et al. 1996). Detailed bio- and magnetostratigraphies have been established for the Bottaccione Gorge section showing that it is essentially complete over the stratigraphic interval considered here (e.g., Alvarez et al. 1977; Premoli Silva 1977; Monechi and Thierstein 1985; Cresta et al. 1989; Premoli Silva and Sliter 1995), thus making it possible to constrain average sedimentation rates with great confidence. A detailed study of ^{3}He across the section has determined the variations in the flux of interplanetary dust particles to Earth (Mukhopadhyay et al. 2001a, 2001b). Helium-3 records primarily reflect the influx of the smallest extraterrestrial particles, in the size range of ~3–35 μm, with an origin from both comets and asteroids.

The Gubbio section is thus ideal for establishing accretion rates for EC; additionally, light can be shed on whether the Cretaceous-Tertiary (K-T) boundary asteroid or comet impact (Alvarez et al. 1980) was associated with any increase in the flux of ordinary chondritic matter to Earth. It should be noted that our approach differs from previous studies of cosmic spinels at the K-T boundary, mainly since these studies focused on spinels (~1–50 μm) formed during impacts of cosmic objects and/or atmospheric entry of cosmic materials (Smit and Kyte 1984; Kyte and Smit 1986; Robin et al. 1992; Toppani and Libourel 2003; Ebel and Grossman 2005) rather than the coarse (>63 μm) and common chromite originally present in equilibrated ordinary chondrites (Keil 1962; Ramdohr 1973; Rubin 1997; Bridges et al. 2007). In unequilibrated ordinary chondrites, i.e., petrological type 3, the chromite grains are usually smaller than 63 μm (Bridges et al. 2007) and hence lie outside the range of detection in the present study.

GEOLOGICAL SETTING

The Bottaccione Gorge with its famous and well-studied pelagic sequence of the middle Cretaceous to the Eocene (e.g., Arthur and Fischer 1977; Alvarez et al. 1980) is located in the Umbria-Marche Apennines, central Italy, directly north of the medieval town of Gubbio (43°22′N, 12°35′E, along the state road SS298 to Scheggia; see Fig. 1). Our sampled interval belongs to the ~325 m thick Scaglia Rossa Formation, which extends from the early Turonian to the middle Eocene (Arthur and Fischer 1977; Monechi and Thierstein 1985). The upper part of this formation consists predominantly of pink to red homogenous limestone and marly limestone that have been thoroughly bioturbated and compacted prior to cementation. The pristine condition of the Scaglia Rossa is explained by the apparent absence of intrusions and thermal alterations in the area (Arthur and Fischer 1977). Agglutinated foraminifera indicate that during the late Cretaceous and Paleocene, the Gubbio/Umbria-Marche basin had a deep bathyal position with a water depth of 1500–2500 m (Kuhnt 1990). Pelagic conditions are also

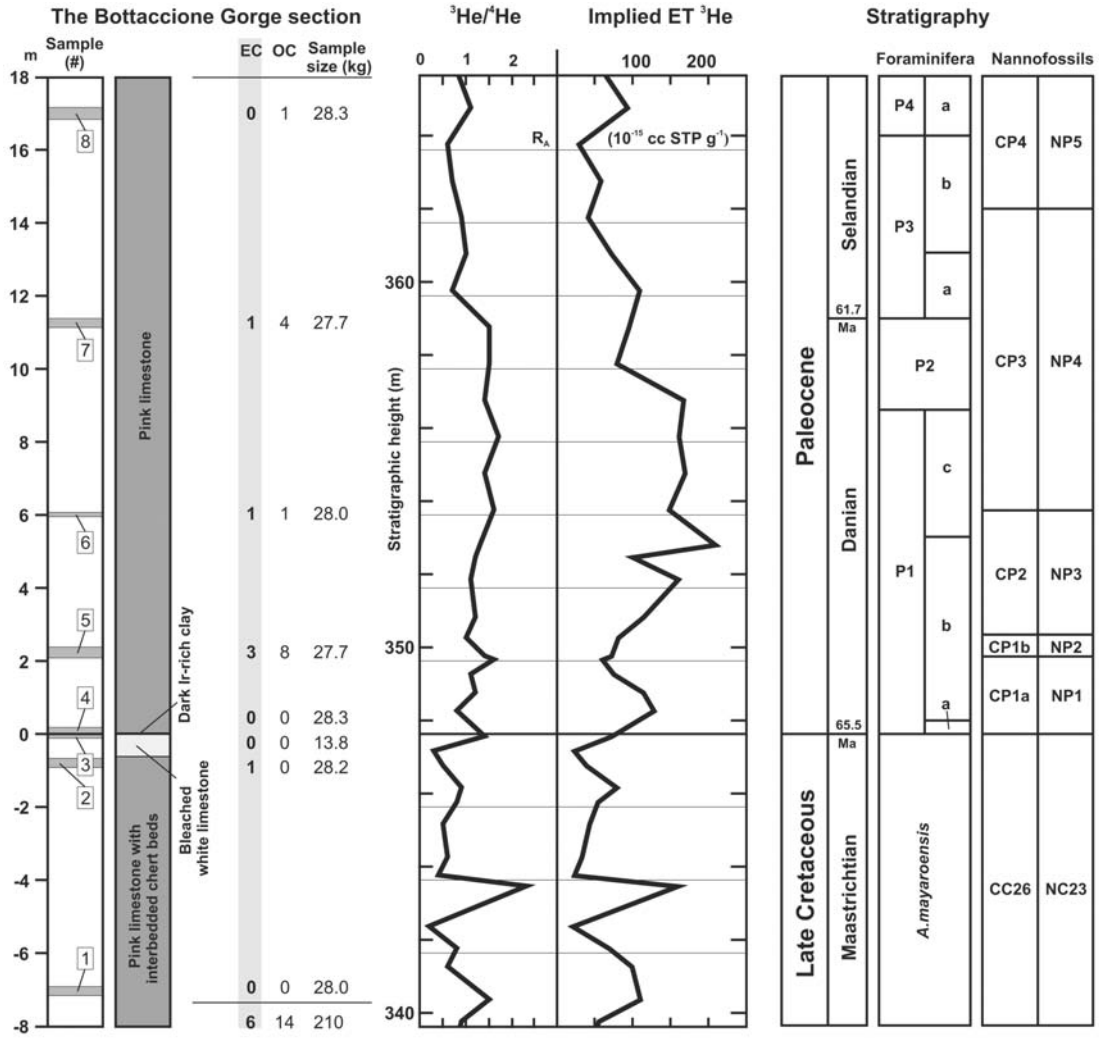

Fig. 2. Distribution of samples studied and number of recovered extraterrestrial (EC) and other (OC) chromite grains across the Bottaccione Gorge section. Lithology after Arthur and Fischer (1977), helium isotopic distribution from Mukhopadhyay et al. (2001), foraminifera stratigraphy from Premoli Silva (1977) and Premoli Silva and Sliter (1995), and nannofossil stratigraphy from Monechi and Thiersten (1985).

indicated by abundant calcareous nannofossils and foraminifera, an aeolian clay and silt component, high planktic/benthic ratio in foraminifera, and extremely low concentrations of organic carbon (Arthur and Fischer 1977; Montanari 1991). In about 50 samples spanning from the Turonian to early Paleocene, Kuhnt (1990) noted the absence of terrigenous detrital material in grain fractions larger than 63 μm.

It is generally considered that the sedimentation rates were extremely low in the Gubbio area from the top Cretaceous (6–10 mm kyr^{-1}) to the lowermost Paleocene limestone (2–5 mm kyr^{-1}) (Montanari and Koeberl 2000). For the Paleocene epoch, Arthur and Fischer (1977) suggest an average sedimentation rate of 2.4 mm kyr^{-1}. Mukhopadhyay et al. (2001b) suggest average sedimentation rates on the order of 4–6 mm kyr^{-1} for the latest Cretaceous and 2–3 mm kyr^{-1} for the early and middle Paleocene. Their helium isotopic data show that the flux of extraterrestrial ^3He to Earth is constant within a factor of ~2 across the K-T boundary and the early and middle Paleocene. Bulk rock ^3He concentrations vary by a factor of ~4, reflecting mainly short-term variations in sedimentation rates (Fig. 2).

The Bottaccione Gorge section became famous as the first section shown to contain enhanced iridium levels (3–6 ppb) at the K-T boundary (Alvarez et al. 1980). The iridium originates from a carbonaceous chondritic asteroid or a comet (diameter of ~10 km) that impacted on the Yucatán Peninsula, Mexico (Hildebrand et al. 1991; Shukolyukov and Lugmair 1998). The K-T boundary in the Bottaccione Gorge section is marked by a 1–2 cm thick dark clay layer underlain by a white bleached limestone zone, ~20–50 cm thick. This zone is related to more reducing sediment conditions when increased

amounts of organic material reached the sea floor during the K-T boundary event (Lowrie et al. 1990; Montanari and Koeberl 2000). With the exception of the thin foraminiferal P0 zone, the Bottaccione Gorge section contains an essentially complete succession of biozones across the K-T transition (Smit 1982). The P0 zone is absent or unrecognizable in most of the Umbria-Marche locations, possibly reflecting slow sedimentation rates combined with thorough bioturbation, which would mix tests from the thin P0 zone and the overlying foraminiferal zones (Montanari and Koeberl 2000). Previous studies of the K-T boundary clay worldwide have located excess amounts of impact-related cosmic spinels and shocked quartz, but according to Montanari and Koeberl (2000), "despite its fame . . . the Bottaccione K-T clay is one of the worst known in the Umbria-Marche region in terms of preservation and suitability for a high-resolution microstratigraphic study." The clay is affected by shearing caused by flexural slip folding and suffers from contamination by the surrounding soil. Common spinel-bearing spherules and shocked quartz have instead been found in the best preserved boundary clay at Petriccio only ~30 km north of Gubbio (Montanari 1991). However, this site is no longer easily accessible.

MATERIALS AND METHODS

Seven large limestone samples ranging from 27.7 to 28.3 kg plus one sample of 13.8 kg, for a total of 210 kg, were collected from 7.15 m below the K-T boundary clay to 17.18 m above it (Fig. 2). One sample of 28.3 kg spanned the 20 cm of section starting 1 cm above the base of the K-T boundary clay; another sample of 13.8 kg spanned the 10 cm of bleached strata immediately underlying the clay. The remaining samples (depths in meters relative to the K-T boundary clay: −7.15 to −6.90, −0.90 to −0.65, +2.10 to +2.40, +5.98 to +6.05, +11.15 to +11.40, +16.85 to +17.18 m) were regarded as representing "background levels" not influenced by the K-T boundary event. The stratigraphically lowest sample is dated to the planktonic foraminifera *Abathomphalus mayaroensis* zone of the latest Maastrichtian (Premoli Silva 1977). The youngest sample at 17 m is dated to the lowest part of the planktonic foraminiferal P4 zone (Premoli Silva 1977) or calcareous nannofossil zone NP5 (Monechi and Thierstein 1985) (Fig. 2).

The eight samples studied were decalcified in 6 M hydrochloric acid at room temperature and then sieved at 32 μm. The residual fractions were leached in 18 M hydrofluoric acid at room temperature and separated into three size fractions (32–63, 63–355, and >355 μm) by sieving and drying. Some samples contained common coal particles and were burned at 550 °C for 24 h to destroy the coal. The coal particles are removed since they resemble the chromite grains. Tests have confirmed that the heating does not affect the major and trace element chemistry of the chromite grains. The middle size fraction (63–355 μm) was scrutinized under a stereomicroscope and suspected chromite grains were collected with a fine brush. The grains were first mounted on carbon tape and preliminarily analyzed in an unpolished state for major and trace elements. The grains were thereafter mounted in epoxy resin and polished before final elemental analysis. For polishing, Struer's alumina paste (standard quality) mixed with water was used on a spinning polishing cloth (Buehler). For a few grains that were destroyed during the polishing phase, we use the results for unpolished grains. Quantitative elemental analyses were conducted with an energy dispersive spectrometer (INCA x-sight, Oxford Instruments) with a Si detector linked to a Hitachi S-3400N scanning electron microscope (SEM). Samples were analyzed at an acceleration voltage of 15 kV, a beam 1–2 μm in diameter, and a counting live-time of 80 s. Cobalt was used as a standard; the precision (reproducibility) of analyses was typically within 1–4%. Analytical accuracy was controlled by repeated analyses of the USNM 117075 chromite (Smithsonian) reference standard (Jarosewich et al. 1980).

DISTRIBUTION AND ORIGIN OF CHROME SPINELS

The distribution of sediment-dispersed chrome-rich spinel grains (63–355 μm) in the Bottaccione Gorge section is shown in Fig. 2 and the chemical composition is shown in Tables 1–4. We follow the procedures outlined by Schmitz and Häggström (2006) and divide the chrome-rich spinels into two groups: extraterrestrial (equilibrated ordinary chondritic) chromite (EC) and "other" chromium-rich spinels (OC). Under the binocular microscope, the EC and OC grains cannot be distinguished from each other, but they differ in chemical composition. The EC grains are characterized primarily by high Cr_2O_3 contents, ~55–60 wt%, FeO concentrations in the range of ~25–30 wt%, low Al_2O_3 at ~5–8 wt%, and low MgO concentrations of ~1.5–4 wt%. The most discriminative feature, however, is that they plot in narrow ranges of V_2O_3 (~0.6–0.9 wt%) and TiO_2 (~2.0–3.5 wt%) concentration. For a grain to be classified as an EC grain, it has to have a composition within or very close to the defined ranges for all the elements listed above. The OC grains, on the other hand, have a wide compositional range. In most cases they have a terrestrial origin, but some grains may represent rare types of extraterrestrial spinels.

In total, only 6 EC and 14 OC grains were retrieved from 210 kg of limestone (Tables 1–4). No chrome-rich spinels were present in the two samples at the K-T boundary (0 to −0.10 m and +0.01 to +0.20 m). Instead, the 6 EC grains were found in 4 samples evenly distributed through the section. The highest concentrations of EC and OC grains were found in the sample at +2.10 m, which contained 3 EC and 8 OC grains. The average EC and OC concentrations in the section are 0.029 and 0.067 grains kg^{-1} limestone,

Table 1. The element concentration (wt%) of extraterrestrial chromite (EC) grains from this study.

Gubbio EC grains[a]		Cr_2O_3	Al_2O_3	MgO	TiO_2	V_2O_3	FeO	MnO	ZnO	Total
–0.90 to –0.65 m	#1	59.53	7.48	3.03	2.20	0.81	22.52	1.05	2.58	99.2
+2.10 to 2.40 m	#1[b]	56.27	5.27	6.08	1.67	0.60	28.45	0.71	0.95	100.0
	#2	59.91	6.30	4.78	1.86	0.51	24.92	n.d.	1.14	99.4
	#3	57.38	4.30	6.94	2.36	0.64	24.14	0.89	2.24	98.9
+5.98 to 6.05 m	#1	59.56	6.14	2.11	3.20	0.65	25.25	0.67	0.51	98.1
+11.15 to 11.40 m	#1	60.96	5.18	3.33	2.83	0.80	23.93	0.75	0.77	98.6
Mean (with s.d.)		58.94 ± 1.75	5.78 ± 1.11	4.38 ± 1.88	2.35 ± 0.58	0.67 ± 0.12	24.87 ± 1.99	0.68 ± 0.36	1.37 ± 0.84	99.0

[a]Depth relative to the K-T boundary in the Bottaccione Gorge section, Gubbio.
[b]The grain was lost during polishing, and is only represented by preliminary pre-polish measurements. The elemental values have been normalized from the original total of 92.8 wt%.
n.d. = not detected.

Table 2. The average element concentration (wt%, with standard deviation) of EC grains from this and previous studies.

	Cr_2O_3	Al_2O_3	MgO	TiO_2	V_2O_3	FeO	MnO	ZnO	Total
Sediment-dispersed EC grains									
Gubbio section, Italy; 6 grains (this study)	58.9 ± 1.75	5.78 ± 1.11	4.38 ± 1.88	2.35 ± 0.58	0.67 ± 0.12	24.9 ± 1.99	0.68 ± 0.36	1.37 ± 0.84	99.0
Thorsberg quarry, Sweden; 276 grains[a]	57.6 ± 1.58	6.07 ± 0.76	2.58 ± 0.79	3.09 ± 0.33	0.75 ± 0.07	27.4 ± 2.63	0.78 ± 0.20	0.53 ± 0.50	98.8
Chromite grains from meteorites[b]									
Mid-Ordovician fossil meteorites, Thorsberg quarry; 26 meteorites	57.6 ± 1.30	5.53 ± 0.29	2.57 ± 0.83	2.73 ± 0.40	0.73 ± 0.03	26.9 ± 3.89	1.01 ± 0.33	1.86 ± 2.43	99.0
Recent H5/6 group chondrites; 11 meteorites	56.6 ± 0.37	6.44 ± 0.14	2.98 ± 0.23	2.20 ± 0.17	0.73 ± 0.02	29.3 ± 0.67	1.00 ± 0.08	0.33 ± 0.05	99.6
Recent L5/6 group chondrites; 10 meteorites	56.0 ± 0.65	5.97 ± 0.43	2.93 ± 0.97	2.68 ± 0.40	0.75 ± 0.02	30.2 ± 2.23	0.83 ± 0.10	0.30 ± 0.07	99.7

[a]Data from Schmitz and Häggström (2006).
[b]Data given is the mean of the average composition of typically 10–20 EC grains from each meteorite. Data from Schmitz et al. (2001), modified by Alwmark and Schmitz (2007).

Table 3. The element concentration (wt%) of other chromium-rich spinel (OC) grains from this study.

Gubbio OC grains[a]		Cr_2O_3	Al_2O_3	MgO	TiO_2	V_2O_3	FeO	MnO	ZnO	Total
+2.10 to 2.40 m	#1	27.61	29.54	15.47	2.08	n.d.	23.80	n.d.	n.d.	98.5
	#2	23.80	32.65	15.21	1.80	n.d.	24.19	n.d.	n.d.	97.7
	#3	26.73	31.07	16.00	1.93	n.d.	22.95	n.d.	n.d.	98.7
	#4	18.06	30.21	9.70	2.50	n.d.	36.91	0.92	n.d.	98.3
	#5	11.73	38.51	14.80	3.05	n.d.	30.91	n.d.	n.d.	99.0
	#6[b]	28.67	38.67	15.96	0.26	n.d.	16.44	n.d.	n.d.	100.0
	#7[c]	(grain lost during polishing)								
	#8[c]	(grain lost during polishing)								
+5.98 to 6.05 m	#1	64.27	5.83	5.42	n.d.	0.56	14.20	0.71	8.11	99.1
+11.15 to 11.40 m	#1	43.46	27.58	12.53	n.d.	n.d.	16.34	n.d.	n.d.	99.9
	#2	26.61	27.16	12.19	1.73	n.d.	30.35	n.d.	n.d.	98.0
	#3	42.13	30.74	12.74	n.d.	n.d.	14.56	n.d.	n.d.	100.2
	#4[d]	(grain lost during polishing)								
+16.85 to 17.18 m	#1	56.79	15.27	8.08	n.d.	n.d.	15.00	n.d.	2.20	97.3

[a]Depth relative to the K-T boundary in the Bottaccione Gorge section, Gubbio.
[b]The grain was lost during polishing, and is only represented by preliminary pre-polish measurements. The elemental values have been normalized from the original total of 96.4 wt%.
[c]Pre-polish measurements of grains #7 and 8 gave similar results as for grains #1, 2, and 3 in the same sample.
[d]Pre-polish measurements of grain #4 gave similar results as for grains #1 and 3 in the same sample.
n.d. = not detected.

Table 4. The element composition (wt%) of average pallasitic chromite compared to the OC grain from +5.98 to 6.05 m above the K-T boundary at Gubbio, Italy.

	Cr_2O_3	Al_2O_3	MgO	TiO_2	V_2O_3	FeO	MnO	ZnO	Total
Average pallasite[a]	64.0	5.6	5.8	0.18	0.54	23.2	0.65	<0.02	99.97
OC grain from +5.98 m	64.3	5.8	5.4	n.d.	0.56	14.2	0.71	8.1	99.1

[a]Data from Bunch and Keil (1971).
n.d. = not detected.

respectively. The EC grains from the Gubbio section are on the whole very similar in composition to both chromite in recent ordinary chondrites and EC grains found in Ordovician limestone and fossil meteorites at Kinnekulle, Sweden (Schmitz et al. 2001, 2003; Schmitz and Häggström 2006) (see Table 2). Some minor but significant differences exist. The Gubbio grains are often high in ZnO (0.5–2.6 wt%) and on average 2–2.5 wt% lower in FeO than Ordovician chondritic chromite. For the Ordovician fossil meteorites, it has been shown that Zn can replace Fe in the chromite structure during diagenesis (Schmitz et al. 2001); hence, the Gubbio grains appear to be more diagenetically altered than most Ordovician EC grains. The Gubbio EC grains on average have a higher MgO (4.4 wt%) concentration than the Ordovician (2.6 wt% MgO) EC grains. However, only the three grains from the sample at +2.10 m have significantly higher MgO than the Ordovician average EC. Single fossil meteorites at Kinnekulle contain chromite grains with MgO concentrations of ~5–6 wt% rather than the normal ~2–4 wt% (Schmitz et al. 2001). Hence, the three EC grains from the +2.10 m level probably derive from the same meteorite or micrometeorite. The TiO_2 concentration of the Gubbio EC grains is on average 0.4–0.7 wt% lower than in Ordovician EC grains. Previous studies have shown that the TiO_2 concentration of sediment-dispersed chromite grains in general is very resistant to weathering and diagenesis (Schmitz et al. 2001; Schmitz and Häggström 2006; Alwmark and Schmitz 2007). Chromite in H chondrites is on average ~0.6–0.7 wt% lower in TiO_2 than in L chondrites (Bunch et al. 1967; Schmitz et al. 2001; Wlotzka 2005). The Ordovician EC grains predominantly originate from the disruption of the L chondrite parent body at this time, which could explain the higher TiO_2. There is no reason to expect that L chondrites dominated the flux in the latest Maastrichtian-Paleocene. Although the majority of the EC grains from Gubbio may derive from H chondrites, the ranges of TiO_2 concentrations in recent H and L chondritic chromite overlap; hence, only the average TiO_2 content of a large number of sediment-dispersed grains is indicative of precursor chondrite type. Moreover, the three grains in the sample at +2.10 m are low in TiO_2 and this affects the average TiO_2 concentration disproportionately. The three EC grains at other levels have typical H or L chondritic TiO_2 contents. In essence, no conclusions about the relative fluxes of H and L chondrites can be drawn from this small data set.

All except 2 of the 14 OC grains originate from the two samples at +2.10 and +11.15 m (Table 3). Most of the OC grains from these samples are similar in composition. They have low Cr/Cr + Al ratios (<0.5), which is in good agreement with a terrestrial origin (Roeder 1994), they are typically high in MgO (12–16 wt%), and they contain no detectable V or Zn. Comparisons of the compositions of the OC grains from Gubbio with chrome spinels from various magmatic provinces as plotted in Barnes and Roeder (2001) indicate an ophiolite provenance, but alternative sources are also plausible. Various magmatic processes, including subduction and possibly plume activity, have occurred in Italy dating back to at least 60–70 Ma (Bell et al. 2004). A more detailed evaluation of the origin of the terrestrial chromite grains from the Gubbio section is beyond the scope of this article.

The two OC grains from the samples at +5.98 and +16.85 m show different compositions compared to those discussed above (Table 3). The origin of the grain from +16.85 m is uncertain and it may be a terrestrial grain. The single OC grain at +5.98 m represents a very special case. It is unusually large (150 × 300 μm) and has a distinct composition almost identical to the average composition of chromites from pallasites (Table 4) (Bunch and Keil 1971). The high Cr_2O_3 (64%), low Al_2O_3 (5.6 wt%), and characteristic V_2O_3 (0.5 wt%) and TiO_2 (0.18 wt%) contents distinguish pallasitic chromite from most terrestrial chromite. The higher ZnO (8.1 wt%) and lower FeO (14.2 wt%) of our OC grain compared to the pallasitic average chromite is readily explained by replacement of Fe by Zn during diagenesis (Schmitz et al. 2001). Pallasitic chromite is also characterized by a larger grain size than in other types of meteorites (Bunch and Keil 1971). The fact that the grain occurs unassociated with any other OC grains in the same sample and the profound difference in composition compared to the terrestrial chrome spinels in the samples above and below also speak in favor of an extraterrestrial origin.

BACKGROUND FLUX OF EXTRATERRESTRIAL CHROMITE

Previous attempts to determine the time-averaged total influx of meteorites and/or smaller extraterrestrial particles to Earth have relied on the density of micrometeoroid hypervelocity impact craters on the Long Duration Exposure Facility (LDEF) satellite (Love and Brownlee 1993), radar micrometeor observations in the upper atmosphere (Mathews et al. 2001), concentrations of platinum group elements, osmium isotopes and ^{3}He in condensed sediments (Farley et al. 1997; Peucker-Ehrenbrink and Ravizza 2000; Peucker-Ehrenbrink 2001; Dalai and Ravizza 2006), iridium concentrations in ice cores (Karner et al. 2003; Gabrielli et al. 2004), micrometeorite abundances in Antarctic ice (Taylor and Lever 2001) and, for meteorites, meteor sky-watch programs (Halliday 2001) and systematic meteorite searches in wind-eroded desert areas (Bland et al. 1996; Bland 2001). The various approaches give flux estimates that sometimes differ significantly. To some extent this can be explained by the different size fractions of the total flux being measured, but methodological problems such as undersampling of larger extraterrestrial particles because of low sample time-area products may in some cases be a problem (see discussion in Peucker-Ehrenbrink and Ravizza 2000). The perhaps best value for the total accreted amount of extraterrestrial matter on the Earth's surface is 30,000 (±15,000) metric tons per year (Peucker-Ehrenbrink and Ravizza 2000). This is based on Os isotopes in deep-sea sediments and agrees with the estimate of 30,000 (±10,000) tons for the flux measured by the LDEF satellite at altitudes of 330 to 480 km (Love and Brownlee 1993; revised estimate in Engrand and Maurette 1998). Desert meteorite search programs show that the total mass flux to the Earth's surface for meteorites over the 10 g to 1 kg interval is between 2.9 and 7.3 tons per year, an estimate that agrees well with estimates from sky-watch networks (Bland et al. 1996; Halliday 2001). The large difference between the total and the meteorite-sized flux illustrates that the bulk of the extraterrestrial matter reaches the Earth surface as very small dust particles or micrometeorites (<300 μm), or occasionally as very large impactors (>1–2 km).

Extraterrestrial chromite grains dispersed in condensed sediments is a new proxy for the influx of extraterrestrial detritus to Earth and has previously only been applied for mid-Ordovician condensed limestone (Schmitz et al. 2003; Schmitz and Häggström 2006). The average EC content of the Gubbio limestone, 0.029 grain kg^{-1}, is similar to that of mid-Ordovician limestone, (0.013 grain kg^{-1} for 379 kg) which formed before the disruption of the L chondrite parent body. Based on the Gubbio data, the average influx of EC to Earth is calculated to be ~0.26 EC grain m^{-2} kyr^{-1}, using average sedimentation rates of 2.5 mm kyr^{-1} for the Paleocene and 5 mm kyr^{-1} for the three Cretaceous samples studied (Arthur and Fischer 1977; Mukhopadhyay et al. 2001b) and a limestone density of 2.7 g cm^{-3}. For the mid-Ordovician, before the asteroid breakup event, the estimated flux is ~0.09 EC grains m^{-2} kyr^{-1} but increases dramatically to an average of ~13 EC grains m^{-2} kyr^{-1} after the event (Schmitz and Häggström 2006). We use a sedimentation rate of 2.5 mm kyr^{-1} for the Ordovician limestone, but this number contains an uncertainty of up to a factor of two. Furthermore, single EC grains can be readily overlooked during the chromite search and coincidental recovery of relict chromite from larger meteorite fragments, such as probably in sample +2.10 m at Gubbio, also adds statistical uncertainty to the flux estimates. We conclude that the normal flux of EC to Earth lies at ~0.1–0.3 grain m^{-2} kyr^{-1}.

The flux of EC grains (0.26 grain m^{-2} kyr^{-1}) reconstructed at Gubbio corresponds to 4.7×10^{-4} g of ordinary chondritic, unmelted debris m^{-2} kyr^{-1}. For this estimate, we assume that the average EC grain is a cube with

a diameter of 100 μm; we use a chromite density of 4.6 g cm^{-3} and an average chromite content for ordinary chondrites of 0.25 wt% (Keil 1962). Many of the EC grains have irregular shapes, but the use of a 100 μm cube in our calculation is reasonable, considering that all grains are >63 μm in at least one dimension and most of the grains have maximum length axes <150 μm. The fact that we only search for chromite grains larger than 63 μm introduces some uncertainty, but for a gross, order-of-magnitude estimate the effect is negligible. Extrapolation to the entire surface of the Earth yields a global flux of ~200 tons of meteoritic matter per year. This is substantially less than the flux of ~30,000 tons based on Os isotopes in deep-sea sediments (Peucker-Ehrenbrink and Ravizza 2000), but significantly more than the 2.9–7.3 tons of meteorites in the 10 g to 1 kg mass spectrum according to desert meteorite abundances (Bland et al. 1996). Based on cosmic spherules from the South Pole Water Well, Taylor and Lever (2001) estimated an annual flux of 2700 ±1400 tons of micrometeorites in the size range 50–700 μm; however, 85% of the spherules were totally melted. Our mass estimate clearly appears realistic in view of these numbers and considering that our EC grains originate predominantly from decomposed unmelted meteorite fragments in the size range of 0.1 mm to a few centimeters (Schmitz et al. 2003; Heck et al., Forthcoming). The full range of the size spectrum and the significance of different size fractions within this spectrum are difficult to assess. Some micrometeorites may have been only marginally larger than the chromite grain itself. At the other end of the mass spectrum, chromite grains were spread over the sea floor by currents and bioturbation from decomposed kilogram-sized meteorites. Some of the chromite grains may derive from bodies 1–100 m in diameter, or even larger, which disrupted in the atmosphere or water column, resulting in micrometeorite and meteorite strewn fields on the sea floor (Lal and Jull 2002; Klekociuk et al. 2005).

Because of atmospheric disintegration of larger meteoroids, the size distribution of objects above the atmosphere is substantially different from that of the material reaching the Earth's surface (Lal and Jull 2002). In order to understand the processes that regulate the extraterrestrial flux through the atmosphere, it is necessary to understand the distribution of extraterrestrial matter over the different size fractions reaching Earth's surface. In flux estimates, the EC distribution in sediments appears to be an important complement to, for example, chemical studies of deep-sea sediments that primarily sample the most fine-grained and/or vaporized and recondensed fractions of the extraterrestrial flux (Lal and Jull 2003).

We stress that the flux of unmelted ordinary chondritic matter of 200 tons per year is a first-order estimate that may be refined as larger samples of limestone will be studied in the future. There are some potential methodological problems that have been considered. With the type of well-preserved limestone like at Gubbio or in the mid-Ordovician at Kinnekulle in Sweden, there is good reason to believe that no EC grains have been destroyed over time by diagenesis or weathering (Schmitz and Häggström 2006). The EC grains found only show evidence of minor alteration, such as replacement of a few percent Fe by Zn. We do not find EC grains with, e.g., zoning that characterizes grains from more aggressive diagenetic environments, like in the Lockne impact crater where EC grains have been affected by hydrothermal activity (Alwmark and Schmitz 2007). Without grains representing intermediate states of alteration, it is not likely that grains were lost entirely because of diagenesis. Redistribution of EC grains by sea-floor currents may bias the EC grain distribution, but with large samples from several stratigraphic levels, the effect of this process will be smoothed out. Tests with individual chromite grains leached in HF and HCl show that the acids do not destroy the grains, but occasionally grains with fragile structure can break into smaller than 63 μm fragments during the wet sieving. Tests with samples "spiked" with EC grains show that this affects at the most a few percent of all grains.

CRETACEOUS-TERTIARY BOUNDARY EVENT

Chemical and isotopic extraterrestrial signatures at the K-T boundary worldwide and coeval species mass extinctions are best explained by the impact of a major extraterrestrial body (~10 km in diameter) at the Yucatán Peninsula, Mexico (e.g., Alvarez et al. 1980; Hildebrand et al. 1991; Arenillas et al. 2006). The globally distributed K-T boundary clay containing iridium, shocked quartz, and spinel-rich microspherules represents compelling evidence for the impact event (Montanari and Koeberl 2000). Chromium isotopic analyses of the boundary clay (Shukolyukov and Lugmair 1998; Trinquier et al. 2006) and studies of a mm-sized weathered meteorite fragment from the K-T boundary in DSDP Hole 576 (Kyte 1998) suggest that the impactor was a carbonaceous chondrite, although a comet can not be ruled out. An important question is whether the K-T boundary impactor was a lone stray object or part of an asteroid or comet shower related to perturbations of solar system gravity (e.g., Hut et al. 1987). An enhanced flux of comets during a few million years can be produced by gravitational perturbations of the Oort Cloud, but the studies by Mukhopadhyay et al. (2001a, 2001b) at Gubbio indicate a near-constant flux of extraterrestrial ^{3}He during the K-T boundary event (Fig. 2), speaking against a comet shower. Varadi et al. (2003) suggest that the K-T impactor may instead have been related to perturbations in the asteroid belt ~65 Myr ago during chaotic transitions in the motions of the inner planets. Any such activity could have increased material transport in the inner solar system, resulting in enhanced accretion rates of cosmic material on Earth. High-resolution Ir analyses across the latest Maastrichtian and earliest

Paleocene strata at Gubbio, show that Ir is only enriched across a narrow interval close to the very K-T boundary, speaking against an extended period with substantially enhanced flux of extraterrestrial matter to Earth (Alvarez et al. 1990). Short vertical tails of enhanced Ir concentrations around the boundary clay most likely reflect redistribution of Ir during bioturbation and diagenesis. To add to this, our chromite searches in samples immediately adjacent to the K-T boundary clay could not find support for any significant increase in the flux of equilibrated ordinary chondritic micrometeorites or meteorites to Earth associated with the K-T event. The absence of >63 μm chromite grains in beds immediately adjacent to the K-T boundary clay at Gubbio also speaks against an equilibrated ordinary chondritic impactor. Although we have not studied the centimeter-thick K-T boundary clay itself, chromite grains in adjacent beds can be expected if they occur in the boundary clay because of the effects of bioturbation and redistribution of material by currents. Alternatively, complete vaporization of an ordinary chondritic impactor during impact could have led to the absence of chromite. Our results are consistent with a carbonaceous chondritic impactor as suggested based on chromium isotopes. Carbonaceous chondrites only contain trace amounts of chromite, and grains larger than 63 μm are entirely absent or extremely rare (Fuchs et al. 1973; El Goresy 1976; Johnson and Prinz 1991; Rubin 1997), hence our data cannot rule out an increased flux of such material over an extended period.

CONCLUSIONS

The influx of extraterrestrial (ordinary chondritic) chromite (>63 μm) to Earth during the latest Maastrichtian and Paleocene has been established at a perfect testing ground, the condensed, pelagic limestones of the Bottaccione Gorge section at Gubbio, Italy. In 210 kg of limestone deposited at ~2.5 to 5 mm kyr^{-1}, we found a total of 6 EC grains, corresponding to an average of 0.03 EC grain kg^{-1}. From well-constrained sedimentation rates, relying on detailed stratigraphic records, we determine the average flux of EC grains to Earth to ~0.26 grain m^{-2} kyr^{-1}. This corresponds to a total influx of ~200 tons of extraterrestrial matter to Earth per year, which is realistic considering that the EC grains only record the flux of unmelted ordinary chondritic matter in the size range from ~0.1 mm up to a few centimeters in diameter. The distribution of EC grains in sediments can give information on the extent to which extraterrestrial matter survives the passage through the atmosphere.

The results in this study confirm the extraordinary circumstances recorded in mid-Ordovician (~470 Ma) limestone at Kinnekulle, Sweden, where an increase in EC grains of two orders of magnitude (from ~0.013 to 1–3 EC grains kg^{-1} limestone) coincides with the coeval disruption of the L chondrite parent body in the asteroid belt.

Large limestone samples collected at Gubbio in the immediate stratigraphic vicinity of the 1 cm thick K-T boundary clay contained no EC grains. This shows that there was no increase in the flux of ordinary chondritic matter to Earth during the K-T boundary transition.

The finding of 6 ordinary chondritic and 1 probable pallasitic chromite grain in 210 kg of condensed limestone from Gubbio shows that our approach has promise for retrieving general knowledge about past variations in the meteorite flux to Earth, particularly if methods could be developed for automatic preparation of limestone samples in the size of 100–200 kg.

Acknowledgments–We are grateful to C. Alwmark for support at different occasions and to T. Häggström and J. Mellgren for field assistance at Gubbio. This study was funded by the Swedish Research Council and the Crafoord Foundation.

Editorial Handling—Dr. Timothy Swindle

REFERENCES

Alvarez L. W., Alvarez W., Asaro F., and Michel H. V. 1980. Extraterrestrial cause for the Cretaceous-Tertiary extinction—Experimental results and theoretical interpretation. *Science* 208: 1095–1108.

Alvarez W., Arthur M. A., Fischer A. G., Lowrie W., Napoleone G., Premoli Silva I., and Roggenthein W. M. 1977. Upper Cretaceous-Paleocene magnetic stratigraphy at Gubbio, Italy: V. Type section for the Late Cretaceous-Paleocene geomagnetic reversal time scale. *Geological Society of America Bulletin* 88: 383–389.

Alvarez W., Asaro F., and Montanari A. 1990. Iridium profile for 10 million years across the Cretaceous-Tertiary boundary at Gubbio (Italy). *Science* 250:1700–1702.

Alwmark C. and Schmitz B. 2007. Extraterrestrial chromite in the resurge deposits of the early Late Ordovician Lockne crater, central Sweden. *Earth and Planetary Science Letters* 253:291–303.

Arenillas I., Arz J. A., Grajales-Nishimura J. M., Murillo-Muñeton G., Alvarez W., Camargo-Zanoguera A., Molina E., and Rosales-Domínguez C. 2006. Chicxulub impact event is Cretaceous/Paleogene boundary in age: New micropaleontological evidence. *Earth and Planetary Science Letters* 249:241–257.

Arthur M. A. and Fischer A. G. 1977. Upper Cretaceous-Paleocene magnetic stratigraphy at Gubbio, Italy: I. Lithostratigraphy and sedimentology. *Geological Society of America Bulletin* 88:367–371.

Barnes S. J. and Roeder P. L. 2001. The range of spinel compositions in terrestrial mafic and ultramafic rocks. *Journal of Petrology* 42: 2279–2302.

Bell K., Castorina F., Lavecchia G., Rosatelli G., and Stoppa F. 2004. Is there a mantle plume below Italy? *Eos* 85:541; 545–547.

Bevan A. W. R., Bland P. A., and Jull A. J. T. 1998. Meteorite flux on the Nullarbor region, Australia. In *Meteorites: Flux with time and impact effects*, edited by Grady M. M., Hutchison R., McCall G. J., and Rothery D. A. Geological Society London Special Publication #140. London: Geological Society of London. pp. 59–73.

Bland P. A. 2001. Quantification of meteorite infall rates from

accumulations in deserts, and meteorite accumulations on Mars. In *Accretion of extraterrestrial matter throughout Earth's history*, edited by Peucker-Ehrenbrink B. and Schmitz B. New York: Kluwer Academic/Plenum Publishers. pp. 267–303.

Bland P. A., Smith T. B., Jull A. J. T., Berry F. J., Bevan A. W. R., Cloudt S., and Pillinger C. T. 1996. The flux of meteorites to the Earth over the last 50,000 years. *Monthly Notices of the Royal Astronomical Society* 283:551–565.

Bridges J. C., Schmitz B., Hutchison R., Greenwood R. C., Tassinari M., and Franchi I. A. 2007. Petrographic classification of mid-Ordovician fossil meteorites from Sweden. *Meteoritics & Planetary Science* 43:1781–1789.

Bunch T. E. and Keil K. 1971. Chromite and ilmenite in non-chondritic meteorites. *American Mineralogist* 56:146–157.

Bunch T. E, Keil K., and Snetsinger K. G. 1967. Chromite composition in relation to chemistry and texture of ordinary chondrites. *Geochimica et Cosmochimica Acta* 31:1569–1582.

Cresta S., Monechi S., and Parisi G. 1989. Mesozoic-Cenozoic stratigraphy in the Umbria-Marche area. *Memorie Descrittive della Carta Geologica d'Italia* 39:1–185.

Dalai T. K. and Ravizza G. 2006. Evaluation of osmium isotopes and iridium as paleoflux tracers in pelagic carbonates. *Geochimica et Cosmochimica Acta* 70:3928–3942.

Ebel D. S. and Grossman L. 2005. Spinel-bearing spherules condensed from the Chicxulub impact-vapor plume. *Geology* 33: 293–296.

El Goresy A. 1976. Opaque oxide minerals in meteorites. In *Oxide minerals*, edited by Rumble D. III. Reviews in Mineralogy, vol. 3. Washington, D.C.: Mineralogical Society of America. pp. EG47–EG72.

Engrand C. and Maurette M. 1998. Carbonaceous micrometeorites from Antarctica. *Meteoritics & Planetary Science* 33:565–580.

Farley K. A., Love S. G., and Patterson D. B. 1997. Atmospheric entry heating and helium retentivity of interplanetary dust particles. *Geochimica et Cosmochimica Acta* 61:2309–2316.

Farley K. A., Montanari A., Shoemaker E. M., and Shoemaker C. S. 1998. Geochemical evidence for a comet shower in the late Eocene. *Science* 280:1250–1253.

Farley K. A., Vokrouhlicky D., Bottke W. F., and Nesvorny D. 2006. A late Miocene dust shower from the breakup of an asteroid in the main belt. *Nature* 439:295–297.

Fuchs L. H., Olsen E., and Jensen K. J. 1973. Mineralogy, mineral-chemistry, and composition of the Murchison (C2) meteorite. *Smithsonian Contributions to the Earth Sciences* 10:1–39.

Gabrielli P., Barbante C., Plane J. M. C., Varga A., Hong S., Cozzi G., Gaspari V., Planchon F. A. M., Cairns W., Ferrari C., Crutzen P., Cescon P., and Boutron C. F. 2004. Meteoric smoke fallout over the Holocene epoch revealed by iridium and platinum in Greenland ice. *Nature* 432:1011–1014.

Greenwood R. C., Schmitz B., Bridges J. B., Hutchison R., and Franchi I. A. 2007. Disruption of the L-chondrite parent body: New oxygen isotope evidence from Ordovician relict chromite grains. *Earth and Planetary Science Letters* 262:204–213.

Halliday I. 2001. The present-day flux of meteorites to the Earth. In *Accretion of extraterrestrial matter throughout Earth's history*, edited by Peucker-Ehrenbrink B. and Schmitz B. New York: Kluwer Academic/Plenum Publishers. pp. 305–318.

Heck P. R., Schmitz B., Baur H., Halliday A. N., and Wieler R. 2004. Fast delivery of meteorites to Earth after a major asteroid collision 480 Myr. *Nature* 430:323–325.

Heck P. R., Schmitz B., Baur H., and Wieler R. Forthcoming. Noble gases in fossil micrometeorites and meteorites from 470 Myr old sediments from southern Sweden and new evidence for the L chondrite parent body breakup event. *Meteoritics & Planetary Science* 43.

Hildebrand A. R., Penfield G. T., Kring D. A., Pilkington M., Camargo A., Jacobsen S. B., and Boynton W. V. 1991. Chicxulub crater: A possible Cretaceous-Tertiary boundary impact crater on the Yucatán Peninsula, Mexico. *Geology* 19: 867–871.

Hills J. G. 1981. Comet showers and the steady-state infall of comets from the Oort cloud. *The Astronomical Journal* 86: 1730–1740.

Hut P., Alvarez W., Elder W. P., Hansen T., Kauffman E. G., Keller G., Shoemaker E. M., and Weissman P. R. 1987. Comet showers as cause of mass extinctions. *Nature* 329:118–126.

Jarosewich E., Nelen J. A., and Norberg J. A. 1980. Reference samples for electron microprobe analysis. *Geostandards Newsletter* 4:43–47.

Johnson C. A. and Prinz M. 1991. Chromite and olivine in type II chondrules in carbonaceous and ordinary chondrites: Implications for thermal histories and group differences. *Geochimica et Cosmochimica Acta* 55:893–904.

Karner D. B., Levine J., Muller R. A., Asaro F., Ram M., and Stolz M. R. 2003. Extraterrestrial accretion from the GISP2 ice core. *Geochimica et Cosmochimica Acta* 67:751–763.

Keil K. 1962. On the phase composition of meteorites. *Journal of Geophysical Research* 67:4055–4061.

Klekociuk A. R., Brown P. G., Pack D. W., ReVelle D. O., Edwards W. N., Spalding R. E., Tagliaferri E., Yoo B. B., and Zagari J. 2005. Meteoritic dust from the atmospheric disintegration of a large meteoroid. *Nature* 436:1132–1135.

Kuhnt W. 1990. Agglutinated foraminifera of western Mediterranean Upper Cretaceous pelagic limestone (Umbrian Apennines, Italy, and Betic Cordillera, southern Spain). *Micropaleontology* 36: 297–330.

Kyte F. T. 1998. A meteorite from the Cretaceous/Tertiary boundary. *Nature* 396:237–239.

Kyte F. T. and Smit J. 1986. Regional variations in spinel compositions: An important key to the Cretaceous/Tertiary event. *Geology* 14:485–487.

Lal D. and Jull A. J. T. 2002. Atmospheric cosmic dust fluxes in the size range 10^{-4} to 10 centimeters. *The Astrophysical Journal* 576: 1090–1097.

Lal D. and Jull A. J. T. 2003. Extraterrestrial influx rates of cosmogenic isotopes and platinum group elements: Realizable geochemical effects. *Geochimica et Cosmochimica Acta* 67: 4925–4933.

Love S. G. and Brownlee D. E. 1993. A direct measurement of the terrestrial mass accretion rate of cosmic dust. *Science* 262:550–553.

Lowrie W., Alvarez W., and Asaro F. 1990. The origin of the White Beds below the Cretaceous-Tertiary boundary in the Gubbio section, Italy. *Earth and Planetary Science Letters* 98: 303–312.

Matese J. J., Whitman P. G., Innanen K. A., and Valtonen M. J. 1995. Periodic modulation of the Oort cloud comet flux by the adiabatically changing galactic tide. *Icarus* 116:225–268.

Mathews J. D., Janches D., Meisel D. D., and Zhou Q. H. 2001. The micrometeoroid mass flux into the upper atmosphere: Arecibo results and a comparison with prior estimates. *Geophysical Research Letters* 28:1929–1932.

Monechi S. and Thierstein H. R. 1985. Late Cretaceous-Eocene nannofossil and magnetostratigraphic correlations near Gubbio, Italy. *Marine Micropaleontology* 9:419–440.

Montanari A. 1991. Authigenesis of impact spheroids in the K/T boundary clay from Italy: New constraints for high-resolution stratigraphy of terminal Cretaceous events. *Journal of Sedimentary Petrology* 61:315–339.

Montanari A. and Koeberl C. 2000. *Impact stratigraphy—The Italian*

record. Lecture Notes in Earth Sciences, vol. 93. Heidelberg: Springer. 364 p.

Mukhopadhyay S., Farley K. A., and Montanari A. 2001a. A short duration of the Cretaceous-Tertiary boundary event: Evidence from extraterrestrial ^{3}He. *Science* 291:1952–1955.

Mukhopadhyay S., Farley K. A., and Montanari A. 2001b. A 35 Myr record of helium in pelagic limestone from Italy: Implications for interplanetary dust accretion from the early Maastrichtian to the middle Eocene. *Geochimica et Cosmochimica Acta* 65:653–669.

Nesvorny D., Vokrouhlicky D., Bottke W. F., and Sykes M. 2006. Physical properties of asteroid dust bands and their sources. *Icarus* 181:107–144.

Nyström J. O., Lindström M., and Wickman F. E. 1988. Discovery of a second Ordovician meteorite using chromite as a tracer. *Nature* 336:572–574.

Peucker-Ehrenbrink B. 2001. Iridium and osmium as tracers of extraterrestrial matter in marine sediments. In *Accretion of extraterrestrial matter throughout Earth's history*, edited by Peucker-Ehrenbrink B. and Schmitz B. New York: Kluwer Academic/Plenum Publishers. pp. 163–178.

Peucker-Ehrenbrink B. and Ravizza G. 2000. The effects of sampling artifacts on cosmic dust flux estimates: A reevaluation of nonvolatile tracers (Os, Ir). *Geochimica et Cosmochimica Acta* 64:1965–1970.

Premoli Silva I. 1977. Upper Cretaceous-Paleocene magnetic stratigraphy at Gubbio, Italy; II. Biostratigraphy. *Geological Society of America Bulletin* 88:371–374.

Premoli Silva I. and Sliter W. V. 1995. Cretaceous planktonic foraminiferal biostratigraphy and evolutionary trends from the Bottaccione section, Gubbio, Italy. *Palaeontographia Italica* 82: 1–89.

Ramdohr P. 1973. *The opaque minerals in stony meteorites*. Amsterdam: Elsevier. 245 p.

Robin E., Bonté Ph., Froget L., Jéhanno C., and Rocchia R. 1992. Formation of spinels in cosmic objects during atmospheric entry: A clue to the Cretaceous-Tertiary boundary event. *Earth and Planetary Science Letters* 108:181–190.

Roeder P. L. 1994. Chromite: From the fiery rain of chondrules to the Kilauea Iki lava lake. *The Canadian Mineralogist* 32:729–746.

Rubin A. E. 1997. Mineralogy of meteorite groups. *Meteoritics & Planetary Science* 32:231–247.

Schmitz B. and Häggström T. 2006. Extraterrestrial chromite in Middle Ordovician marine limestone at Kinnekulle, southern Sweden—Traces of a major asteroid breakup event. *Meteoritics & Planetary Science* 41:455–466.

Schmitz B., Lindström M., Asaro F., and Tassinari M. 1996. Geochemistry of meteorite-rich marine limestone strata and fossil meteorites from the lower Ordovician at Kinnekulle, Sweden. *Earth and Planetary Science Letters* 145:31–48.

Schmitz B., Tassinari M., and Peucker-Ehrenbrink B. 2001. A rain of ordinary chondritic meteorites in the early Ordovician. *Earth and Planetary Science Letters* 194:1–15.

Schmitz B., Häggström T., and Tassinari M. 2003. Sediment-dispersed extraterrestrial chromite traces a major asteroid disruption event. *Science* 300:961–964.

Shukolyukov A. and Lugmair G. W. 1998. Isotopic evidence for the Cretaceous-Tertiary impactor and its type. *Science* 282:927–929.

Smit J. 1982. Extinction and evolution of planktonic foraminifera after a major impact at the Cretaceous/Tertiary boundary. GSA Special Paper #190. Boulder, Colorado: Geological Society of America. pp. 329–352.

Smit J. and Kyte F. T. 1984. Siderophile-rich magnetic spheroids from the Cretaceous-Tertiary boundary in Umbria, Italy. *Nature* 310:403–405.

Taylor S. and Lever J. H. 2001. Seeking unbiased collections of modern and ancient micrometeorites. In *Accretion of extraterrestrial matter throughout Earth's history*, edited by Peucker-Ehrenbrink B. and Schmitz B. New York: Kluwer Academic/Plenum Publishers. pp. 205–219.

Thorslund P., Wickman F. E., and Nyström J. O. 1984. The Ordovician chondrite from Brunflo, central Sweden. I. General description and primary minerals. *Lithos* 17:87–100.

Toppani A. and Libourel G. 2003. Factors controlling composition of cosmic spinels: Application to atmospheric entry conditions of meteoritic materials. *Geochimica et Cosmochimica Acta* 67: 4621–4638.

Trinquier A., Birck J.-L., and Allègre C. J. 2006. The nature of the K-T impactor. A ^{54}Cr reappraisal. *Earth and Planetary Science Letters* 241:780–788.

Varadi F., Runnegar B., and Ghil M. 2003. Successive refinements in long-term integrations of planetary orbits. *The Astrophysical Journal* 592:620–630.

Wlotzka F. 2005. Cr spinel and chromite as petrogenetic indicators in ordinary chondrites: Equilibration temperatures of petrologic types 3.7 to 6. *Meteoritics & Planetary Science* 40: 1673–1702.

Zappalà V., Cellino A., Gladman B. J., Manley S., and Migliorini F. 1998. Asteroid showers on Earth after family breakup events. *Icarus* 134:176–179.

II

The Geological Society of America
Special Paper 452
2009

A search for extraterrestrial chromite in the late Eocene Massignano section, central Italy

Birger Schmitz*
Anders Cronholm
Department of Geology, Lund University, Sölvegatan 12, SE-22362 Lund, Sweden

Alessandro Montanari
Osservatorio di Coldigioco, 62021 Apiro, Italy

ABSTRACT

The late Eocene may have been a period with an enhanced flux of extraterrestrial matter to Earth related either to a comet or an asteroid shower. The evidence comes from two very large and several medium-sized impact craters, at least two microtektite-microkrystite layers, and a stratigraphic interval with enhanced extraterrestrial ^{3}He, all within the period ca. 36.3–34.3 Ma. Here, we show that the distribution of sediment-dispersed extraterrestrial (ordinary chondritic) chromite (EC) grains in the Massignano section, central Italy, can be used to test whether the flux of ordinary chondritic matter to Earth was enhanced in the late Eocene. In twelve limestone samples, each weighing ~12–15 kg, from 1.25 m to 10.25 m above the base of the section, only 1 EC grain was found. Based on the total amount of limestone analyzed, 167 kg, this corresponds to 0.006 EC grain kg^{-1} limestone. This is a factor of five lower than the 0.029 EC grain kg^{-1} recovered in 210 kg of latest Cretaceous–Paleocene limestone from the Bottaccione Gorge section at Gubbio, central Italy. The difference can readily be explained by an approximately threefold higher sedimentation rate in the late Eocene at Massignano. In essence, our results speak against a late Eocene asteroid shower. Apparently, there was no significant increase in the flux of extraterrestrial chromite at this time, such as that after the disruption of the L-chondrite parent body in the mid-Ordovician, when the EC flux was enhanced by two orders of magnitude. We also discuss the potential to search for lunar minerals in the Massignano section in order to test the recent hypothesis that late Eocene ^{3}He enrichments originated from impact-ejected lunar regolith.

Keywords: extraterrestrial chromite, asteroid shower, micrometeorite, impact ejecta, late Eocene.

*birger.schmitz@geol.lu.se

Schmitz, B., Cronholm, A., and Montanari, A., 2009, A search for extraterrestrial chromite in the late Eocene Massignano section, central Italy, *in* Koeberl, C., and Montanari, A., eds., The Late Eocene Earth—Hothouse, Icehouse, and Impacts: Geological Society of America Special Paper 452, p. 71–82, doi: 10.1130/2009.2452(05).

INTRODUCTION

Global changes such as cooling and stepwise floral and faunal turnovers in the late Eocene have been suggested to be at least partially related to either a comet or an asteroid shower (Hut et al., 1987; Bodiselitsch et al., 2004; Tagle and Claeys, 2004). Supporting evidence includes an overrepresentation of impact craters of this age, enhanced extraterrestrial ^{3}He concentrations in sediments over an ~2.2 m.y. period, and, in the same interval, three iridium anomalies, of which, one has associated shocked quartz, and two microtektite-microkrystite layers (Montanari et al., 1993, 1998; Clymer et al., 1996; Farley et al., 1998; Bodiselitsch et al., 2004). The two largest impact craters of the Cenozoic, Popigai, 100 km in diameter, and Chesapeake Bay, 85 km in diameter, formed at 36–35 Ma, and a number of smaller craters with comparable ages may be part of the same event (Montanari and Koeberl, 2000). The sedimentary ^{3}He enrichments have been considered to more likely represent a comet shower (Farley et al., 1998; Bodiselitsch et al., 2004), whereas platinum group element patterns for ejecta melts from the Popigai crater have been related to a stony chondritic projectile, possibly an L chondrite (Tagle and Claeys, 2004, 2005). Recently, Fritz et al. (2007) suggested that an asteroid (L chondrite) shower in the late Eocene led to an increased impact rate on both Earth and the Moon, and that impact-ejected lunar regolith was transported to Earth, resulting in the ^{3}He enrichments in marine sediments.

The question of comet or asteroid shower may be resolved by comparisons with the middle Ordovician, a time when the L-chondrite parent body disrupted, leading to a dramatically enhanced flux of extraterrestrial matter to Earth (Schmitz et al., 2001, 2003, 2008). This is the largest documented asteroid breakup event during the Phanerozoic, and a major fraction of the L-chondritic meteorites that fall onto Earth have argon gas retention ages around 470 Ma attesting to the event (Korochantseva et al., 2007). No other asteroid breakup has left any similar prominent imprint on present-day meteorite argon ages. In marine limestone formed at 470 Ma in the mid-Ordovician, more than 80 fossil L-chondritic meteorites (1–20 cm in diameter) and a two-orders-of-magnitude enrichment in sediment-dispersed L-chondritic chromite grains, mainly from decomposed unmelted micrometeorites, attest to the parent-body breakup (Schmitz et al., 2001; Schmitz, 2008, personal commun.). According to modeling studies, a breakup event of this magnitude should be accompanied by an asteroid shower to Earth (Zappalà et al., 1998). There is some evidence of an enhanced number of impact craters on Earth at this time, and an asteroid shower could have played a role in the coeval rapid diversification of invertebrate life (Schmitz et al., 2001, 2008).

Analogous to the mid-Ordovician, a potential asteroid shower in the late Eocene may have resulted in excess amounts of extraterrestrial (ordinary chondritic) chromite (EC) grains (>63 μm) in sediments. Here, we present results of searches for EC grains in twelve limestone samples, each ~12–15 kg in size, from the late Eocene ^{3}He enriched interval of the Massignano section near Ancona in central Italy (Fig. 1). Nine of the samples represent "background" samples chosen at arbitrary levels throughout the section, and three samples correspond to three levels with enhanced iridium concentrations (see Montanari et al., 1993; Bodiselitsch et al., 2004). One of the Ir-enriched levels, at 5.6 m, is a confirmed impact ejecta layer with abundant shocked quartz, Ni-rich spinels, 200 ppt Ir, and common pancake spherules, representing relics of clinopyroxene-bearing microkrystites

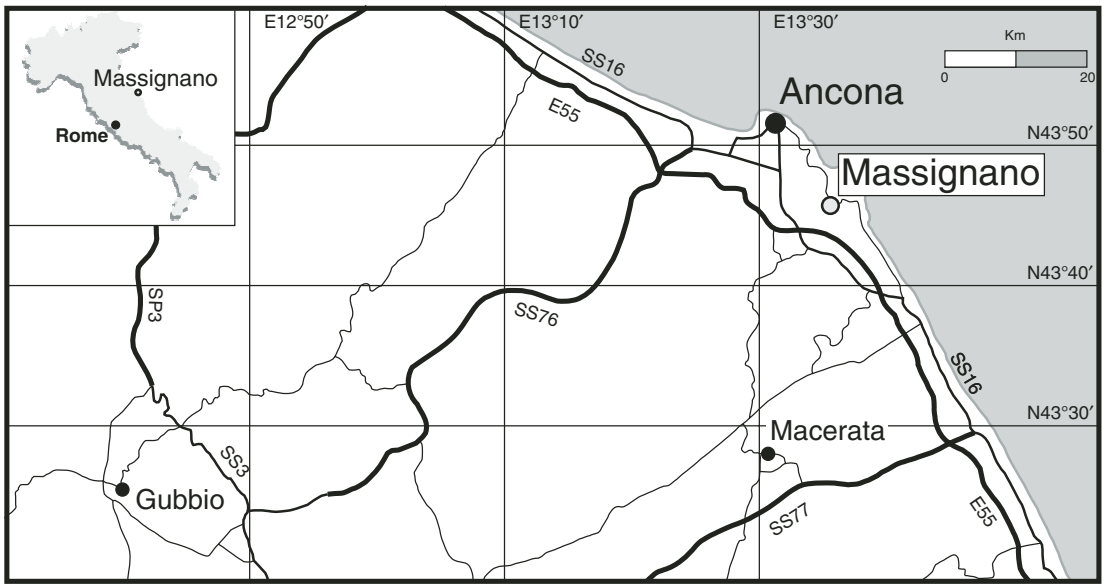

Figure 1. Map of area around Ancona, eastern central Italy, and the position of the Massignano section. Note that the town of Gubbio, where the Bottaccione section is exposed, is also indicated.

(e.g., Montanari and Koeberl, 2000, and references therein). The layer may represent the distal ejecta from the Popigai crater, but this link is mainly based on the approximate coincidence in time. The two other Ir-enriched levels have not yielded any shocked quartz or other compelling impact ejecta constituents, and their possible impact association remains enigmatic (Montanari et al., 1993; Clymer et al., 1996; Bodiselitsch et al., 2004).

We note that the chromite grains discussed here have a quite different origin and composition than the Ni- and Cr-rich spinels in the Massignano impact ejecta layer, dealt with in studies by, for example, Pierrard et al. (1998) and Glass et al. (2004). The latter spinels occur as tiny crystals (a few microns) in fragile stringers on pancake spherules, and formed in the heat during the impact event, whereas the coarse chromite studied here represents an original component (on average 0.25 wt%) in equilibrated ordinary chondrites (Keil, 1962; Bridges et al., 2007).

MATERIALS AND METHODS

Dry weights of the limestone samples studied ranged from 11.6 to 15.1 kg, and the samples were collected from 1.25 m to 10.25 m above the base of the section (Table 1), all within the 13-m-thick ^{3}He enriched interval of Farley et al. (1998). In the Massignano section, meter levels relative to the base of the section are marked by persistent metal plates, and the sample depths in our study refer to this meter scale, like in most previous studies of the section (see, e.g., Montanari et al., 1993). The three samples from Ir-enriched levels were collected at 5.60, 6.15, and 10.25 m. All samples were decalcified in 6 *M* hydrochloric acid at room temperature and then sieved at 32 μm. The samples were readily dissolvable, and there was no need to break them into smaller pieces prior to HCl leaching. The remaining HCl residues were leached with 18 *M* hydrofluoric acid at room temperature for about 2 d, with occasional stirring. The HF residues were recovered with a 32 μm sieve. The acid-insoluble fraction in the size range 63–355 μm was searched under the binocular microscope, and all suspected chromite (i.e., black, opaque) grains were picked with a fine brush for element analyses.

All suspected chromite grains were first mounted on carbon tape and analyzed for elements in an unpolished state. Performed in the right way, these analyses are mostly sufficient to tell whether a grain is extraterrestrial chromite or not. All the confirmed chrome spinel (including chromite) grains were mounted in epoxy resin, polished flat using a 1 μm diamond slurry, and again analyzed for major and trace elements, but with the aim of producing high-quality data. It is unavoidable for a minor fraction of the chrome spinel grains to be lost during the polishing, but by first analyzing all the grains in an unpolished state, we were able to control whether any EC grains were lost. The quantitative element analyses were performed with an Oxford Inca X-sight energy-dispersive spectrometer with a Si detector, mounted on a Hitachi S-3400 scanning electron microscope. Cobalt was used to monitor drift of the instrument. An acceleration voltage of 15 kV, a sample current ~1 nA, and a counting live-time of 80 s were used. Precision of analyses was typically better than 1–4 rel%. Analytical accuracy was controlled by repeated analyses of the USNM 117075 (Smithsonian) chromite reference standard (Jarosewich et al., 1980).

RESULTS

We follow the practice of Schmitz and Häggström (2006) and divide sediment-dispersed Cr-rich spinels into two groups: extraterrestrial (ordinary chondritic) chromite (EC) and "other" Cr-rich spinels (OC). For a grain to be classified as an EC grain, it has to have a composition within narrowly defined ranges for Cr_2O_3 (~55–60 wt%), FeO (~25–30 wt%), Al_2O_3 (~5–8 wt%), TiO_2 (~2.0–3.5 wt%), V_2O_3 (~0.6–0.9 wt%), and MgO (~1.5–4 wt%) (Schmitz and Häggström, 2006). Only grains with compositions that lie within the ranges of all elements listed are considered to be EC grains. The OC grains, on the other hand, have a wide compositional range, and the vast majority has a terrestrial origin, but, in rare cases, they may represent unusual types of extraterrestrial spinels.

In total, 374 chrome spinel grains were found in the 167 kg of limestone analyzed, and of these, only 1 grain can be classified as EC; the remaining are OC grains (Table 1). The single EC grain was found in the sample at 6.15 m (grain no. Cr 12), i.e., from one of the two Ir-enriched levels where supporting evidence for an impact relation is lacking. As shown in Figure 2, the grain is not so well preserved, having some rounded edges and a general abraded appearance, and compared with a typical mid-Ordovician EC grain, the latter has a more fresh appearance. From the analyses of the unpolished chrome spinel grains, it could be ascertained that of the five grains lost during polishing, all were OC grains.

DISCUSSION

The method of extracting EC grains from bulk sediment was originally developed as a complement to the search for mid-Ordovician fossil meteorites (Schmitz et al., 2003; Schmitz and Häggström, 2006). In fossil meteorites, chromite is the only common relict mineral, but much information about the precursor meteorites can be gained from the mineral. For example, with chromite analyses, it is possible to classify the fossil meteorites to group and petrographic type, and to determine their cosmic-ray exposure histories (e.g., Schmitz et al., 2001; Heck et al., 2004; Bridges et al., 2007; Greenwood et al., 2007). The mid-Ordovician sediment-dispersed EC grains contain abundant solar-wind implanted neon, showing that most grains originate from micrometeorites that have undergone decomposition on the seafloor (Heck et al., 2008). In mid-Ordovician condensed strata in southern Sweden, the beds that formed after the L-chondrite disruption event contain one to three EC grains kg^{-1} of limestone, whereas in beds that formed at the same rate during the ~5 m.y. immediately prior to this event, 379 kg of limestone only yielded five EC grains (Schmitz and Häggström, 2006).

TABLE 1. ELEMENT CONCENTRATIONS (WT%) IN CR-RICH SPINELS EXTRACTED FROM LATE EOCENE SEDIMENTS IN THE MASSIGNANO QUARRY, CENTRAL ITALY*

Grains	Cr_2O_3	Al_2O_3	MgO	TiO_2	V_2O_3	FeO	MnO	ZnO	Total†	Fe#§	Cr##
MAS 1.25–1.35 m (13.9 kg)**											
Cr 1	45.11	26.79	10.96	B.D.††	B.D.	16.27	B.D.	B.D.	99.1	45.4	53.0
Cr 2	46.73	21.20	9.44	B.D.	B.D.	21.61	B.D.	0.36	99.3	54.9	59.5
Cr 3	50.05	15.38	9.95	B.D.	B.D.	23.05	B.D.	B.D.	98.4	51.5	68.6
Cr 4	44.04	24.91	12.87	B.D.	B.D.	17.31	B.D.	B.D.	99.1	41.2	54.2
Cr 5	45.37	23.14	12.21	B.D.	B.D.	18.15	B.D.	B.D.	98.9	43.4	56.8
Cr 6	47.55	21.35	12.22	B.D.	B.D.	16.20	B.D.	B.D.	97.3	42.2	59.9
Cr 7	50.12	19.16	11.30	B.D.	B.D.	18.66	B.D.	B.D.	99.2	46.6	63.7
Cr 8	41.97	19.57	9.26	0.72	B.D.	27.27	0.48	B.D.	99.3	56.1	59.0
Cr 9	42.54	27.58	13.95	B.D.	0.34	15.26	B.D.	B.D.	99.7	37.9	50.8
Cr 10	44.54	24.21	12.64	B.D.	B.D.	16.69	B.D.	B.D.	98.1	41.5	55.2
Cr 11	42.54	26.12	13.90	B.D.	B.D.	15.73	B.D.	B.D.	98.3	36.8	52.2
Cr 12	46.21	22.72	12.74	B.D.	0.37	16.70	B.D.	B.D.	98.7	41.4	57.7
Cr 13	50.99	5.61	4.20	B.D.	0.42	35.72	0.66	B.D.	97.6	77.4	85.9
Cr 14	44.74	23.33	12.56	B.D.	B.D.	17.31	B.D.	B.D.	97.9	41.5	56.3
Cr 15	38.29	29.76	13.76	B.D.	B.D.	16.12	B.D.	B.D.	97.9	38.1	46.3
Cr 16	41.93	16.53	8.02	2.53	0.52	27.56	B.D.	B.D.	97.1	62.8	63.0
Cr 17	43.74	25.84	12.27	B.D.	B.D.	18.06	B.D.	B.D.	99.9	44.3	53.2
Cr 18	47.81	23.17	13.59	B.D.	B.D.	16.57	B.D.	B.D.	101.1	38.8	58.0
Cr 19	56.30	12.49	10.90	B.D.	B.D.	18.88	B.D.	B.D.	98.6	46.6	75.1
Cr 20	44.73	24.35	11.39	0.36	B.D.	19.79	B.D.	B.D.	100.6	48.4	55.2
Cr 21	38.27	30.27	12.91	B.D.	B.D.	17.53	0.44	B.D.	99.4	41.8	45.6
Cr 22	50.64	17.79	10.41	B.D.	0.30	19.62	B.D.	B.D.	98.8	50.3	65.6
Cr 23	54.75	14.50	10.33	B.D.	0.40	19.30	B.D.	B.D.	99.3	50.3	71.7
Cr 24	54.86	15.80	8.73	B.D.	B.D.	20.80	B.D.	B.D.	100.2	57.2	70.0
Cr 25	59.92	10.34	8.42	B.D.	B.D.	21.56	0.62	B.D.	100.9	57.7	79.0
Cr 26	50.89	18.68	11.52	B.D.	B.D.	18.08	B.D.	B.D.	99.2	45.5	64.6
Cr 27	29.66	34.89	15.77	0.48	B.D.	16.39	B.D.	B.D.	97.2	31.7	36.3
Cr 28	44.04	23.50	12.21	B.D.	B.D.	17.94	B.D.	B.D.	97.7	43.0	55.7
Cr 29	55.87	11.54	7.84	B.D.	B.D.	23.15	B.D.	B.D.	98.4	60.5	76.5
Cr 30	51.83	17.32	10.47	B.D.	B.D.	19.48	B.D.	B.D.	99.1	49.8	66.7
Cr 31	49.54	16.80	11.22	B.D.	B.D.	21.64	B.D.	B.D.	99.2	46.5	66.4
Cr 32	46.16	23.17	13.10	B.D.	B.D.	16.52	B.D.	B.D.	99.0	39.7	57.2
MAS 1.95–2.20 m (13.9 kg)											
Cr 1	34.41	30.32	11.37	B.D.	0.35	23.44	0.39	B.D.	100.3	49.0	43.2
Cr 2	48.08	22.97	9.61	B.D.	B.D.	18.66	B.D.	0.40	99.7	52.1	58.4
Cr 3	49.31	20.45	12.18	B.D.	B.D.	18.83	B.D.	B.D.	100.8	43.9	61.8
Cr 4	52.41	18.40	10.91	B.D.	B.D.	17.52	B.D.	B.D.	99.2	47.4	65.6
Cr 5	43.74	19.15	11.07	0.37	B.D.	26.01	B.D.	B.D.	100.3	48.7	60.5
Cr 6	44.85	25.99	11.16	B.D.	B.D.	16.16	B.D.	B.D.	98.2	44.8	53.6
Cr 7	56.76	12.72	9.63	B.D.	B.D.	19.28	B.D.	B.D.	98.4	52.3	75.0
Cr 8	50.66	18.79	10.68	B.D.	0.30	19.64	B.D.	B.D.	100.1	49.9	64.4
Cr 9	52.75	16.68	11.33	B.D.	B.D.	19.68	B.D.	B.D.	100.4	46.5	68.8
Cr 10	49.46	21.06	12.35	B.D.	B.D.	16.82	B.D.	B.D.	99.7	42.7	61.2
Cr 11	42.67	27.33	12.53	B.D.	B.D.	18.07	B.D.	B.D.	100.6	43.8	51.1
Cr 12	36.69	26.99	11.43	B.D.	0.31	25.29	B.D.	B.D.	100.7	48.8	47.7
Cr 13	27.09	41.23	16.71	B.D.	B.D.	14.45	B.D.	B.D.	99.5	30.2	30.6
Cr 14	50.59	19.41	11.65	B.D.	B.D.	17.53	B.D.	B.D.	99.2	45.1	63.6
Cr 15	53.06	2.71	1.17	0.47	B.D.	33.74	0.84	0.62	92.6	92.9	92.9
Cr 16	36.14	29.99	13.25	B.D.	B.D.	19.58	B.D.	B.D.	99.0	40.8	44.7
Cr 17	48.57	20.64	11.42	B.D.	B.D.	18.38	B.D.	B.D.	99.0	46.3	61.2
Cr 18	44.75	24.92	14.19	B.D.	B.D.	15.87	B.D.	B.D.	99.7	36.0	54.6
Cr 19	42.20	19.38	8.68	0.46	B.D.	27.19	B.D.	0.32	98.2	58.2	59.4
Cr 20	49.68	20.53	12.34	B.D.	B.D.	17.61	B.D.	B.D.	100.2	42.9	61.9
Cr 21	42.25	22.85	10.11	B.D.	B.D.	23.60	B.D.	B.D.	98.8	52.5	55.4
Cr 22	47.82	21.11	11.74	B.D.	B.D.	17.50	B.D.	B.D.	98.2	44.6	60.3
Cr 23	43.63	26.29	13.01	B.D.	B.D.	17.65	B.D.	B.D.	100.6	41.6	52.7
Cr 24	52.72	15.74	10.78	B.D.	0.33	18.62	B.D.	B.D.	98.2	48.0	69.2
Cr 25	42.40	27.11	12.73	B.D.	B.D.	18.37	B.D.	B.D.	100.6	43.0	51.2
Cr 26	47.42	23.48	12.46	B.D.	B.D.	17.57	B.D.	B.D.	100.9	43.4	57.5
Cr 27	47.23	20.68	12.30	0.29	B.D.	18.87	B.D.	B.D.	99.4	43.1	60.5
Cr 28	46.06	21.72	12.59	B.D.	B.D.	18.84	0.36	B.D.	99.6	41.3	58.7
Cr 29	41.68	26.24	13.30	B.D.	B.D.	17.11	B.D.	B.D.	98.3	39.3	51.6

(*continued*)

TABLE 1. ELEMENT CONCENTRATIONS (WT%) IN CR-RICH SPINELS EXTRACTED FROM LATE EOCENE SEDIMENTS IN THE MASSIGNANO QUARRY, CENTRAL ITALY* (*continued*)

Grains	Cr_2O_3	Al_2O_3	MgO	TiO_2	V_2O_3	FeO	MnO	ZnO	Total†	Fe#§	Cr##
MAS 3.05–3.35 m (15.0 kg)											
Cr 1	51.63	16.96	11.24	B.D.	0.37	20.66	B.D.	B.D.	100.9	47.5	67.1
Cr 2	43.50	21.56	10.28	B.D.	0.39	24.02	0.48	B.D.	100.5	51.8	57.5
Cr 3	40.41	18.96	10.43	2.12	0.36	28.17	B.D.	B.D.	100.5	53.7	58.8
Cr 4	48.81	21.08	11.80	B.D.	B.D.	18.11	B.D.	B.D.	99.8	45.1	60.8
Cr 5	49.12	16.93	10.33	B.D.	0.48	23.07	B.D.	B.D.	99.9	51.2	66.1
Cr 6	42.82	15.12	7.54	0.82	0.66	33.01	B.D.	B.D.	100.0	64.3	65.5
Cr 7	59.86	12.11	11.84	B.D.	B.D.	15.88	B.D.	B.D.	99.7	42.8	76.8
Cr 8	51.46	18.19	11.07	B.D.	B.D.	19.22	B.D.	B.D.	99.9	47.7	65.5
Cr 9	27.93	40.75	15.07	B.D.	B.D.	16.82	B.D.	B.D.	100.6	36.8	31.5
Cr 10	45.48	25.07	13.23	B.D.	B.D.	15.96	B.D.	B.D.	99.7	40.0	54.9
Cr 11	56.92	13.38	10.75	B.D.	B.D.	18.15	B.D.	B.D.	99.2	47.7	74.0
Cr 12	51.27	17.55	10.86	B.D.	B.D.	19.10	B.D.	B.D.	98.8	48.0	66.2
Cr 13	50.38	18.77	11.85	B.D.	B.D.	18.78	B.D.	B.D.	99.8	44.4	54.3
Cr 14	47.74	20.09	9.81	B.D.	B.D.	21.64	B.D.	B.D.	99.3	53.4	61.4
Cr 15	44.25	25.16	12.55	B.D.	0.30	17.54	B.D.	B.D.	99.8	43.2	54.1
Cr 16	20.93	47.48	16.92	B.D.	B.D.	15.24	B.D.	B.D.	100.6	31.5	22.8
Cr 17	45.72	23.96	11.40	B.D.	0.50	17.87	0.42	B.D.	99.9	46.8	56.1
Cr 18	48.82	22.15	13.20	B.D.	B.D.	16.22	B.D.	B.D.	100.4	39.7	59.6
Cr 19	45.65	16.12	7.79	B.D.	B.D.	29.29	B.D.	0.56	99.4	61.5	65.5
Cr 20	39.96	21.62	6.43	B.D.	B.D.	30.02	B.D.	0.46	98.5	68.4	55.3
Cr 21	52.25	14.90	7.82	B.D.	B.D.	23.94	B.D.	B.D.	98.9	61.4	70.2
Cr 22	50.05	17.67	10.91	B.D.	B.D.	19.66	B.D.	B.D.	98.3	47.6	65.5
MAS 4.80–5.10 m (14.6 kg)											
Cr 1	38.61	29.99	14.18	B.D.	B.D.	17.65	0.00	B.D.	100.4	37.7	46.3
Cr 2	54.27	14.11	9.31	B.D.	B.D.	20.69	0.00	B.D.	98.4	54.1	72.1
Cr 3	45.70	19.97	9.58	B.D.	0.37	23.21	0.51	B.D.	99.3	54.1	60.5
Cr 4	47.16	12.26	5.28	0.34	B.D.	32.25	0.74	B.D.	98.0	72.7	72.1
Cr 5	41.21	27.40	13.68	B.D.	B.D.	15.76	B.D.	B.D.	98.0	37.9	50.2
Cr 6	34.31	9.01	2.40	1.75	B.D.	49.83	0.67	0.33	98.3	87.6	71.9
Cr 7	39.70	16.67	8.70	1.54	0.59	31.41	B.D.	B.D.	98.6	59.6	61.5
Cr 8	43.43	25.42	12.61	B.D.	B.D.	17.00	B.D.	B.D.	98.5	42.1	53.4
Cr 9	45.33	22.62	11.74	B.D.	B.D.	18.87	B.D.	B.D.	98.6	45.2	57.3
Cr 10	32.03	10.20	7.26	6.19	B.D.	43.95	B.D.	B.D.	99.6	68.7	67.8
Cr 11	59.39	11.01	10.41	B.D.	B.D.	18.99	B.D.	B.D.	99.8	49.0	78.3
Cr 12	46.84	18.67	9.33	B.D.	B.D.	24.22	0.69	B.D.	99.8	54.7	62.7
Cr 13	46.86	19.64	11.67	B.D.	B.D.	20.47	B.D.	B.D.	98.6	44.9	61.5
Cr 14	52.22	16.45	10.55	B.D.	B.D.	21.25	B.D.	B.D.	100.5	49.9	68.0
Cr 15	52.80	18.05	12.43	B.D.	B.D.	16.59	0.56	B.D.	100.4	41.2	66.2
Cr 16	51.86	17.20	11.56	B.D.	B.D.	19.12	B.D.	B.D.	99.8	45.3	66.9
Cr 17	56.68	13.34	10.32	B.D.	B.D.	18.13	B.D.	B.D.	98.5	49.3	74.0
Cr 18	45.99	23.45	12.61	B.D.	B.D.	16.70	B.D.	B.D.	98.8	41.7	56.8
Cr 19	56.07	13.97	9.60	B.D.	B.D.	19.05	B.D.	B.D.	98.7	52.7	72.9
MAS 5.60–5.65 m (13.9 kg)											
Cr 1	41.88	26.70	13.33	B.D.	B.D.	17.51	B.D.	B.D.	99.4	39.9	51.3
Cr 2	21.56	39.83	15.73	1.00	B.D.	20.99	B.D.	B.D.	99.1	34.9	26.6
Cr 3	31.30	35.83	15.01	B.D.	B.D.	16.47	B.D.	B.D.	98.6	34.9	36.9
Cr 4	59.22	10.45	11.15	B.D.	B.D.	17.93	0.51	B.D.	99.3	44.5	79.2
Cr 5	44.79	19.35	10.72	0.81	B.D.	25.51	B.D.	B.D.	101.2	51.1	60.8
Cr 6	59.44	4.14	3.17	B.D.	0.40	31.04	B.D.	0.19	98.4	83.0	90.6
Cr 7	45.56	23.75	12.33	B.D.	B.D.	18.32	B.D.	B.D.	100.0	43.6	56.3
Cr 8	52.18	18.34	9.63	B.D.	B.D.	18.45	B.D.	B.D.	98.6	51.8	65.6
Cr 9	37.17	11.90	5.20	2.86	0.70	40.92	B.D.	B.D.	98.8	75.7	67.7
Cr 10	46.91	23.00	12.35	B.D.	B.D.	17.93	B.D.	B.D.	100.2	43.4	57.8
Cr 11	31.42	24.04	9.14	B.D.	B.D.	33.77	B.D.	B.D.	98.4	57.0	46.7
Cr 12	35.36	32.76	14.76	B.D.	B.D.	17.00	B.D.	B.D.	99.9	35.8	42.0
Cr 13	46.58	22.16	13.31	B.D.	B.D.	17.10	B.D.	B.D.	99.2	38.7	58.5
Cr 14	59.72	8.43	6.82	B.D.	B.D.	23.39	B.D.	0.70	99.1	64.5	82.6
Cr 15	52.29	15.80	11.63	B.D.	B.D.	18.62	B.D.	B.D.	98.3	44.0	68.9
Cr 16	45.47	22.47	10.08	B.D.	B.D.	21.03	B.D.	0.38	99.4	52.3	57.6
Cr 17	43.94	23.11	13.05	B.D.	B.D.	18.24	B.D.	B.D.	98.3	39.7	56.0
Cr 18	21.05	46.82	17.39	B.D.	B.D.	14.36	B.D.	B.D.	99.6	29.2	23.2
Cr 19	42.29	26.34	11.90	B.D.	B.D.	18.75	B.D.	B.D.	99.3	45.7	51.8
Cr 20	47.43	21.75	10.64	B.D.	B.D.	18.37	B.D.	B.D.	98.2	49.2	59.4
Cr 21	57.36	7.64	0.62	B.D.	B.D.	32.87	1.53	0.54	100.6	96.5	83.4

(*continued*)

TABLE 1. ELEMENT CONCENTRATIONS (WT%) IN CR-RICH SPINELS EXTRACTED FROM LATE EOCENE SEDIMENTS IN THE MASSIGNANO QUARRY, CENTRAL ITALY* (*continued*)

Grains	Cr_2O_3	Al_2O_3	MgO	TiO_2	V_2O_3	FeO	MnO	ZnO	Total†	Fe#§	Cr##
MAS 5.60–5.65 m (13.9 kg) (*continued*)											
Cr 22	36.13	11.30	6.38	2.71	0.57	41.59	B.D.	B.D.	98.7	70.2	68.2
Cr 23	46.94	23.58	12.73	B.D.	B.D.	16.84	B.D.	B.D.	100.1	41.9	57.2
Cr 24	37.16	27.90	13.20	0.34	B.D.	20.05	B.D.	B.D.	98.7	40.8	47.2
Cr 25	45.35	21.28	10.01	B.D.	B.D.	21.56	0.69	B.D.	98.9	51.7	58.8
Cr 26	63.69	7.27	11.10	B.D.	B.D.	16.72	B.D.	B.D.	98.8	44.5	85.5
Cr 27	45.75	22.84	12.65	B.D.	B.D.	17.18	B.D.	B.D.	98.4	41.3	57.3
Cr 28	48.01	12.68	6.24	0.24	B.D.	28.93	2.09	B.D.	98.2	66.6	71.7
Cr 29	45.48	24.25	14.19	B.D.	B.D.	15.21	B.D.	B.D.	99.1	35.5	55.7
Cr 30	31.21	34.06	13.01	B.D.	B.D.	21.42	B.D.	B.D.	99.7	43.0	38.1
Cr 31	44.40	24.96	12.98	B.D.	B.D.	17.26	B.D.	B.D.	99.6	41.0	54.4
Cr 32	38.09	29.70	13.70	B.D.	B.D.	17.47	B.D.	B.D.	99.0	38.8	46.2
Cr 33	39.97	29.58	15.58	B.D.	B.D.	14.06	B.D.	B.D.	99.2	31.3	47.5
Cr 34	46.89	22.29	14.80	B.D.	B.D.	14.51	0.73	1.00	100.2	30.2	58.5
Cr 35	46.90	22.17	12.65	B.D.	B.D.	17.35	B.D.	B.D.	99.1	41.4	58.8
MAS 5.70–5.80 m (13.8 kg)											
Cr 1	43.06	17.03	9.27	0.48	B.D.	28.47	B.D.	B.D.	98.3	55.5	62.9
Cr 2	47.31	20.13	11.35	B.D.	B.D.	19.40	B.D.	B.D.	98.2	46.2	61.2
Cr 3	58.15	7.78	5.14	B.D.	B.D.	26.25	0.68	B.D.	98.0	72.5	83.4
Cr 4	58.48	12.51	12.64	B.D.	B.D.	16.40	B.D.	B.D.	100.0	39.6	75.8
Cr 5	29.81	38.46	15.22	B.D.	B.D.	15.34	B.D.	B.D.	98.8	34.8	34.2
Cr 6	37.28	4.78	0.98	0.16	B.D.	37.10	1.74	0.97	83.0	93.1	83.9
Cr 7	47.81	21.31	12.15	B.D.	B.D.	18.97	B.D.	B.D.	100.2	43.9	60.1
Cr 8	21.56	4.94	1.48	4.69	0.59	64.48	0.60	B.D.	98.3	92.9	74.5
Cr 9	39.64	29.06	12.75	B.D.	B.D.	17.13	B.D.	B.D.	98.6	42.4	47.8
Cr 10	51.61	13.13	9.91	B.D.	B.D.	23.87	B.D.	B.D.	98.5	51.3	72.5
Cr 11	29.50	37.01	17.33	0.34	B.D.	14.05	B.D.	B.D.	98.2	26.6	34.8
Cr 12	42.63	19.00	10.28	0.81	0.47	27.04	B.D.	B.D.	100.2	52.9	60.1
Cr 13	61.42	8.86	5.93	B.D.	B.D.	21.76	0.65	B.D.	98.6	67.3	82.3
Cr 14	57.49	13.67	10.65	B.D.	B.D.	18.84	B.D.	B.D.	100.7	48.9	73.8
Cr 15	46.05	19.31	10.31	0.45	B.D.	23.61	B.D.	B.D.	99.7	51.8	61.5
Cr 16	43.06	17.03	9.27	0.48	B.D.	28.47	B.D.	B.D.	98.3	55.5	62.9
MAS 6.15–6.25 m (14.0 kg)											
Cr 1	48.52	18.39	10.96	B.D.	B.D.	20.66	B.D.	B.D.	98.5	47.7	63.9
Cr 2	45.92	23.97	13.25	B.D.	B.D.	16.12	B.D.	B.D.	99.3	39.4	56.2
Cr 3	35.75	30.22	12.04	B.D.	B.D.	20.90	0.16	0.57	99.6	45.2	44.2
Cr 4	44.86	19.08	9.22	B.D.	B.D.	27.59	B.D.	B.D.	100.8	56.5	61.2
Cr 5	44.26	26.13	13.76	B.D.	B.D.	16.21	B.D.	B.D.	100.4	38.4	53.2
Cr 6	40.17	18.62	6.52	1.63	0.56	29.58	2.01	0.96	100.1	67.4	59.1
Cr 7	43.55	24.20	12.69	B.D.	B.D.	19.85	B.D.	B.D.	100.3	42.4	54.7
Cr 8	44.10	22.70	10.98	B.D.	B.D.	23.01	B.D.	B.D.	100.8	49.5	56.6
Cr 9	53.86	13.03	8.07	B.D.	B.D.	23.59	B.D.	B.D.	98.6	59.8	73.5
Cr 10	37.33	21.88	6.16	0.28	0.35	32.86	0.72	0.26	99.8	70.1	53.4
Cr 11	48.92	21.71	11.16	B.D.	B.D.	18.04	B.D.	B.D.	99.8	47.6	60.2
Cr 12	58.87	5.16	2.42	1.72	0.71	28.85	1.29	0.36	99.4	87.0	88.4
Cr 13	35.65	28.40	12.64	0.53	B.D.	21.42	B.D.	B.D.	98.6	43.5	45.7
Cr 14	30.11	34.25	14.17	0.48	B.D.	19.65	B.D.	B.D.	98.7	38.6	37.1
Cr 15	43.92	25.46	11.97	B.D.	B.D.	19.14	B.D.	B.D.	100.5	45.7	53.6
Cr 16	44.05	25.83	12.38	B.D.	B.D.	18.16	B.D.	B.D.	100.4	44.0	53.3
Cr 17	47.14	19.23	10.74	B.D.	B.D.	22.87	B.D.	B.D.	100.0	49.5	62.2
Cr 18	60.06	6.79	4.91	B.D.	B.D.	26.89	B.D.	B.D.	98.7	74.3	85.6
Cr 19	34.42	33.13	14.70	B.D.	B.D.	15.84	B.D.	B.D.	98.1	35.2	41.1
Cr 20	32.58	34.21	14.23	B.D.	B.D.	17.17	B.D.	B.D.	98.2	37.4	39.0
Cr 21	33.48	36.18	15.68	B.D.	B.D.	15.11	B.D.	B.D.	100.5	33.3	38.3
Cr 22	30.39	37.64	15.28	0.45	B.D.	16.60	B.D.	B.D.	100.4	35.8	35.1
Cr 23	48.15	19.41	11.82	B.D.	B.D.	20.48	0.75	B.D.	100.6	44.0	62.5
MAS 6.70–6.90 m (14.1 kg)											
Cr 1	57.45	15.84	9.19	B.D.	B.D.	16.66	B.D.	B.D.	99.1	50.4	70.9
Cr 2	32.07	37.46	14.83	B.D.	B.D.	15.21	B.D.	B.D.	99.6	36.5	36.5
Cr 3	47.68	19.74	10.77	B.D.	B.D.	21.65	B.D.	B.D.	99.8	49.4	61.8
Cr 4	50.70	19.19	12.01	B.D.	B.D.	18.15	B.D.	B.D.	100.1	43.9	63.9
Cr 5	43.88	25.59	13.54	B.D.	B.D.	16.58	B.D.	B.D.	99.6	38.8	53.5
Cr 6	34.97	33.77	13.76	B.D.	B.D.	17.67	B.D.	B.D.	100.2	40.1	41.0
Cr 7	55.60	22.50	6.98	B.D.	B.D.	15.18	B.D.	B.D.	100.3	55.0	62.4
Cr 8	46.76	22.40	11.94	B.D.	B.D.	18.65	B.D.	B.D.	99.8	44.8	58.3

(*continued*)

TABLE 1. ELEMENT CONCENTRATIONS (WT%) IN CR-RICH SPINELS EXTRACTED FROM LATE EOCENE SEDIMENTS IN THE MASSIGNANO QUARRY, CENTRAL ITALY* (*continued*)

Grains	Cr_2O_3	Al_2O_3	MgO	TiO_2	V_2O_3	FeO	MnO	ZnO	Total†	Fe#§	Cr##
MAS 6.70–6.90 m (14.1 kg) (*continued*)											
Cr 9	33.15	31.18	14.97	0.66	B.D.	19.63	B.D.	B.D.	99.6	35.4	41.6
Cr 10	55.85	14.78	5.52	B.D.	0.28	23.25	B.D.	B.D.	99.7	70.3	71.7
Cr 11	41.63	24.05	11.57	B.D.	B.D.	21.83	B.D.	B.D.	99.1	46.5	53.7
Cr 12	43.92	26.94	13.07	B.D.	B.D.	15.87	B.D.	B.D.	99.8	40.5	52.2
Cr 13	39.53	30.32	13.72	B.D.	B.D.	16.23	B.D.	B.D.	99.8	39.3	46.6
Cr 14	54.37	20.92	9.89	B.D.	B.D.	14.19	B.D.	B.D.	99.4	44.6	63.5
Cr 15	51.13	26.83	8.31	B.D.	0.30	12.79	B.D.	B.D.	99.4	46.3	56.1
Cr 16	48.98	29.21	7.61	B.D.	B.D.	14.53	B.D.	B.D.	100.3	51.7	52.9
Cr 17	45.03	27.52	8.66	B.D.	B.D.	17.03	B.D.	B.D.	98.3	52.5	52.3
Cr 18	46.63	23.82	12.58	B.D.	B.D.	17.67	B.D.	B.D.	100.7	42.9	56.8
Cr 19	41.28	15.41	8.41	0.97	0.39	33.05	B.D.	B.D.	99.5	60.3	64.2
Cr 20	45.81	20.37	12.00	0.62	B.D.	21.89	B.D.	B.D.	100.7	45.4	60.1
Cr 21	55.84	5.77	2.49	B.D.	B.D.	33.01	1.33	0.33	98.8	86.0	86.6
Cr 22	43.20	26.64	13.99	B.D.	B.D.	16.65	B.D.	B.D.	100.5	37.7	52.1
Cr 23	36.54	30.37	12.93	B.D.	B.D.	18.95	B.D.	B.D.	98.8	42.1	44.7
Cr 24	56.81	12.20	8.28	B.D.	B.D.	23.52	B.D.	B.D.	100.8	59.5	75.7
MAS 8.20–8.40 m (14.2 kg)											
Cr 1	61.25	10.64	9.48	B.D.	0.49	16.31	1.77	B.D.	99.9	49.1	79.4
Cr 2	42.08	24.80	12.66	0.74	B.D.	19.93	B.D.	B.D.	100.2	43.5	53.2
Cr 3	30.89	8.69	1.01	2.02	B.D.	56.68	1.09	B.D.	100.4	94.9	70.4
Cr 4	47.22	22.61	12.41	B.D.	B.D.	17.59	B.D.	B.D.	99.8	42.9	58.3
Cr 5	50.31	18.58	10.18	B.D.	B.D.	20.44	B.D.	B.D.	99.5	51.6	64.5
Cr 6	49.93	18.04	10.95	0.27	B.D.	20.15	B.D.	B.D.	99.3	48.3	65.0
Cr 7	46.57	24.38	10.88	B.D.	B.D.	17.59	B.D.	B.D.	99.4	47.6	56.2
Cr 8	46.22	24.67	12.72	B.D.	B.D.	16.03	B.D.	B.D.	99.6	41.4	55.7
Cr 9	46.97	23.07	10.42	B.D.	B.D.	19.59	B.D.	B.D.	100.1	51.3	57.7
Cr 10	45.98	25.80	13.07	B.D.	B.D.	15.96	B.D.	B.D.	100.8	40.7	54.4
Cr 11	45.62	26.18	12.06	B.D.	B.D.	15.84	B.D.	B.D.	99.7	42.4	53.9
Cr 12	51.68	9.42	11.06	0.86	B.D.	27.14	B.D.	B.D.	100.2	47.2	78.6
Cr 13	51.59	12.40	6.95	1.22	0.80	25.88	0.53	B.D.	99.4	66.2	73.6
Cr 14	34.81	28.91	14.20	1.18	B.D.	20.70	B.D.	B.D.	99.8	38.7	44.7
Cr 15	60.68	7.48	12.53	B.D.	B.D.	19.03	B.D.	B.D.	99.7	38.7	84.5
Cr 16	37.42	25.22	9.25	0.37	B.D.	27.28	B.D.	B.D.	99.6	57.4	49.9
Cr 17	41.78	18.23	9.24	0.90	B.D.	28.53	B.D.	B.D.	98.7	56.4	60.6
Cr 18	44.24	23.16	12.51	B.D.	0.19	18.00	0.57	B.D.	98.7	41.4	56.2
Cr 19	48.69	20.61	11.67	B.D.	B.D.	18.05	0.74	B.D.	99.8	44.5	61.3
Cr 20	44.38	17.02	8.90	0.42	B.D.	28.87	B.D.	B.D.	99.6	57.6	63.6
Cr 21	37.06	23.31	9.47	B.D.	0.36	29.22	B.D.	B.D.	99.4	56.0	51.6
Cr 22	50.12	15.23	10.40	0.73	B.D.	22.98	B.D.	B.D.	99.5	50.8	68.8
Cr 23	41.88	26.50	12.65	B.D.	B.D.	18.62	B.D.	B.D.	99.7	42.7	51.5
Cr 24	44.99	22.62	11.52	B.D.	B.D.	19.50	B.D.	B.D.	98.6	46.2	57.2
Cr 25	38.94	22.33	11.67	0.72	0.40	25.03	0.20	B.D.	99.3	46.9	53.9
Cr 26	43.31	26.20	11.99	B.D.	B.D.	18.63	B.D.	B.D.	100.1	45.6	52.6
Cr 27	51.82	11.80	9.06	1.01	0.47	25.13	B.D.	B.D.	99.3	56.7	74.7
Cr 28	44.20	27.67	11.70	B.D.	B.D.	14.43	B.D.	B.D.	98.0	40.9	51.7
Cr 29	40.21	24.94	11.80	B.D.	B.D.	22.37	B.D.	B.D.	99.3	45.9	51.9
Cr 30	42.67	17.24	7.24	0.98	B.D.	31.30	B.D.	B.D.	99.4	65.6	62.4
Cr 31	29.75	12.24	3.88	1.83	0.54	50.72	B.D.	B.D.	99.0	81.3	62.0
Cr 32	27.76	40.72	16.47	B.D.	B.D.	14.32	B.D.	B.D.	99.3	30.8	31.4
Cr 33	56.62	12.29	10.89	B.D.	B.D.	19.51	0.53	B.D.	99.8	46.4	75.5
Cr 34	55.57	11.86	6.99	B.D.	B.D.	24.70	0.74	B.D.	99.9	64.4	75.9
Cr 35	45.29	23.77	12.40	B.D.	B.D.	18.70	B.D.	B.D.	100.2	43.4	56.1
Cr 36	35.76	25.02	13.00	1.67	B.D.	25.15	B.D.	B.D.	100.6	43.7	48.9
MAS 9.00–9.15 m (14.1 kg)											
Cr 1	60.14	4.00	2.28	0.40	0.41	32.20	B.D.	B.D.	99.4	88.0	91.0
Cr 2	51.90	18.19	11.42	B.D.	B.D.	18.25	B.D.	B.D.	99.8	46.1	65.7
Cr 3	46.81	20.81	11.12	B.D.	B.D.	20.73	B.D.	B.D.	99.5	47.9	60.1
Cr 4	30.13	38.11	15.19	B.D.	B.D.	15.54	B.D.	B.D.	99.0	34.9	34.6
Cr 5	49.08	20.97	13.01	B.D.	B.D.	15.97	B.D.	B.D.	99.0	39.6	61.1
Cr 6	39.93	16.76	6.06	1.88	0.58	34.45	B.D.	B.D.	99.7	71.8	61.5
Cr 7	57.07	10.84	7.02	B.D.	B.D.	25.48	B.D.	B.D.	100.4	65.0	77.9
Cr 8	51.90	16.74	11.54	B.D.	B.D.	19.53	B.D.	B.D.	99.7	45.3	67.5
Cr 9	48.58	19.97	11.18	B.D.	B.D.	19.67	B.D.	B.D.	99.4	47.4	62.0
Cr 10	52.76	16.66	12.05	B.D.	B.D.	18.49	B.D.	B.D.	100.0	43.2	68.0

(*continued*)

TABLE 1. ELEMENT CONCENTRATIONS (WT%) IN CR-RICH SPINELS EXTRACTED FROM LATE EOCENE SEDIMENTS IN THE MASSIGNANO QUARRY, CENTRAL ITALY* (*continued*)

Grains	Cr_2O_3	Al_2O_3	MgO	TiO_2	V_2O_3	FeO	MnO	ZnO	Total†	Fe#§	Cr##
MAS 9.00–9.15 m (14.1 kg) (*continued*)											
Cr 11	50.72	18.83	12.15	B.D.	0.42	17.77	B.D.	B.D.	99.9	43.6	64.4
Cr 12	47.60	22.94	12.66	B.D.	B.D.	17.29	B.D.	B.D.	100.5	42.2	58.2
Cr 13	53.83	14.30	9.36	B.D.	B.D.	21.65	B.D.	B.D.	99.1	54.2	71.6
Cr 14	36.82	32.19	14.01	B.D.	B.D.	16.09	B.D.	B.D.	99.1	38.2	43.4
Cr 15	51.57	16.28	11.63	B.D.	0.35	18.71	B.D.	B.D.	98.5	44.5	68.0
Cr 16	40.58	29.88	14.12	B.D.	B.D.	15.75	B.D.	B.D.	100.3	37.8	47.7
Cr 17	49.29	22.06	11.81	B.D.	B.D.	17.09	B.D.	B.D.	100.3	44.8	60.0
Cr 18	47.02	21.64	11.92	B.D.	0.41	18.12	B.D.	B.D.	99.1	44.8	59.3
Cr 19	59.25	11.68	11.03	B.D.	B.D.	18.14	B.D.	B.D.	100.1	46.5	77.3
Cr 20	44.56	23.24	12.36	B.D.	B.D.	18.98	B.D.	B.D.	99.1	43.0	56.3
Cr 21	57.49	11.33	7.74	B.D.	B.D.	22.80	B.D.	B.D.	99.4	61.3	77.3
Cr 22	34.01	33.12	13.60	B.D.	B.D.	19.55	B.D.	B.D.	100.3	40.7	40.8
Cr 23	38.04	15.28	7.84	1.45	0.58	35.56	B.D.	B.D.	98.8	63.2	62.5
Cr 24	37.47	27.29	14.52	0.71	B.D.	18.97	B.D.	B.D.	99.0	36.0	47.9
Cr 25	33.47	33.61	13.90	B.D.	B.D.	17.63	B.D.	B.D.	98.6	38.8	40.0
Cr 26	39.37	10.90	5.21	B.D.	B.D.	43.40	B.D.	0.11	99.0	73.5	70.8
Cr 27	50.29	20.31	11.23	B.D.	B.D.	18.07	B.D.	B.D.	99.9	47.5	62.4
Cr 28	46.60	22.14	11.83	B.D.	B.D.	17.62	B.D.	B.D.	98.2	44.5	58.5
Cr 29	58.00	12.68	8.80	B.D.	B.D.	19.54	B.D.	B.D.	99.0	55.5	75.4
Cr 30	42.91	21.66	6.45	B.D.	B.D.	27.02	0.58	0.90	99.5	67.7	57.1
Cr 31	59.29	7.67	3.30	B.D.	B.D.	27.92	0.83	0.39	99.4	82.1	83.8
Cr 32	46.03	20.66	10.19	0.36	B.D.	22.93	B.D.	B.D.	100.2	52.6	59.9
Cr 33	42.33	25.19	9.91	B.D.	B.D.	21.19	B.D.	B.D.	98.6	53.7	53.0
Cr 34	49.76	20.40	10.27	B.D.	0.34	18.47	B.D.	B.D.	99.2	50.2	62.1
Cr 35	47.05	21.18	11.37	B.D.	0.37	19.46	B.D.	B.D.	99.4	47.2	59.8
Cr 36	48.88	22.47	12.48	B.D.	B.D.	16.85	B.D.	B.D.	100.7	43.0	59.3
Cr 37	37.29	3.52	2.76	B.D.	0.42	55.38	B.D.	B.D.	99.4	85.5	87.7
Cr 38	55.80	2.13	2.92	B.D.	0.57	35.87	0.80	0.42	98.5	83.7	94.6
Cr 39	48.21	20.06	11.12	B.D.	B.D.	19.32	B.D.	B.D.	98.7	47.4	61.7
Cr 40	34.44	34.65	15.22	B.D.	B.D.	15.42	B.D.	B.D.	99.7	34.4	40.0
Cr 41	48.02	21.48	11.81	B.D.	B.D.	17.64	B.D.	B.D.	98.9	44.8	60.0
Cr 42	40.70	28.68	13.15	B.D.	B.D.	17.77	B.D.	B.D.	100.3	41.5	48.8
Cr 43	32.76	33.44	15.14	B.D.	B.D.	18.82	B.D.	B.D.	100.2	34.7	39.6
Cr 44	41.45	27.76	14.16	B.D.	B.D.	16.62	B.D.	B.D.	100.0	37.0	50.0
Cr 45	48.98	19.70	11.14	B.D.	B.D.	18.97	B.D.	B.D.	98.8	47.2	62.5
Cr 46	54.62	14.30	9.80	B.D.	B.D.	21.37	B.D.	B.D.	100.1	52.6	71.9
Cr 47	42.89	25.51	12.10	0.37	B.D.	18.98	B.D.	B.D.	99.8	45.4	53.0
Cr 48	30.70	31.35	8.61	B.D.	0.58	28.97	B.D.	B.D.	100.2	61.4	39.6
Cr 49	43.85	25.43	13.59	B.D.	B.D.	17.27	B.D.	B.D.	100.1	38.8	53.6
Cr 50	47.20	22.57	13.71	B.D.	B.D.	16.97	B.D.	B.D.	100.4	37.8	58.4
Cr 51	40.49	29.26	13.45	B.D.	B.D.	16.63	B.D.	B.D.	99.8	40.1	48.1
Cr 52	53.46	14.62	8.71	B.D.	B.D.	22.07	B.D.	B.D.	98.9	57.2	71.0
Cr 53	44.68	21.71	10.89	B.D.	B.D.	21.70	B.D.	B.D.	99.0	48.9	58.0
Cr 54	64.12	9.62	5.99	B.D.	B.D.	19.12	B.D.	0.47	99.3	64.1	81.7
Cr 55	21.65	48.00	15.82	B.D.	B.D.	14.59	B.D.	B.D.	100.1	34.1	23.2
Cr 56	31.77	36.66	15.52	B.D.	B.D.	15.52	B.D.	B.D.	99.5	33.6	36.8
Cr 57	47.13	18.06	11.76	1.43	B.D.	22.21	B.D.	B.D.	100.6	46.9	63.6
Cr 58	37.19	31.75	15.37	B.D.	B.D.	15.20	B.D.	B.D.	99.5	32.9	44.0
Cr 59	45.47	23.41	12.00	B.D.	B.D.	18.94	B.D.	B.D.	99.8	44.8	56.6
Cr 60	47.85	21.30	10.81	B.D.	B.D.	19.94	B.D.	B.D.	99.9	49.5	60.1
Cr 61	51.34	18.49	9.72	B.D.	0.32	18.55	B.D.	B.D.	98.4	51.7	65.1
Cr 62	45.89	23.22	12.37	B.D.	B.D.	18.36	B.D.	B.D.	99.8	43.2	57.0
Cr 63	46.96	13.69	1.31	0.41	B.D.	35.48	B.D.	0.52	98.4	93.1	69.7
Cr 64	44.70	25.42	10.62	B.D.	B.D.	18.60	B.D.	B.D.	99.4	49.6	54.1
Cr 65	42.61	25.73	12.93	B.D.	B.D.	17.37	B.D.	B.D.	98.6	40.9	52.6
Cr 66	46.62	22.01	11.26	B.D.	B.D.	19.10	B.D.	B.D.	99.0	47.3	58.7
Cr 67	42.23	27.86	13.54	B.D.	B.D.	16.52	B.D.	B.D.	100.2	39.6	50.4
Cr 68	42.22	19.93	7.44	B.D.	B.D.	28.26	B.D.	0.51	98.4	63.4	58.7
Cr 69	43.49	25.13	12.69	B.D.	B.D.	17.44	B.D.	B.D.	98.8	41.8	53.7
Cr 70	46.54	23.04	12.65	B.D.	B.D.	17.05	B.D.	B.D.	99.3	41.7	57.5
Cr 71	48.08	21.61	12.76	B.D.	B.D.	16.44	B.D.	B.D.	98.9	40.7	59.9
MAS 10.00–10.15 m (14.0 kg)											
Cr 1	47.82	18.50	10.20	B.D.	0.32	21.73	B.D.	B.D.	98.6	51.3	63.4
Cr 2	56.02	12.94	9.35	B.D.	0.32	20.19	B.D.	B.D.	98.8	54.1	74.4
Cr 3	55.19	11.90	8.13	B.D.	B.D.	25.22	B.D.	B.D.	100.4	60.0	75.7

(*continued*)

TABLE 1. ELEMENT CONCENTRATIONS (WT%) IN CR-RICH SPINELS EXTRACTED FROM LATE EOCENE SEDIMENTS IN THE MASSIGNANO QUARRY, CENTRAL ITALY* (*continued*)

Grains	Cr_2O_3	Al_2O_3	MgO	TiO_2	V_2O_3	FeO	MnO	ZnO	Total†	Fe#§	Cr##
MAS 10.00–10.15 m (14.0 kg) (*continued*)											
Cr 4	45.63	25.68	14.13	B.D.	B.D.	14.47	B.D.	B.D.	99.9	36.5	54.4
Cr 5	41.88	27.12	12.49	B.D.	0.34	18.42	B.D.	B.D.	100.2	44.1	50.9
Cr 6	45.22	24.20	13.05	B.D.	B.D.	17.10	B.D.	B.D.	99.6	40.5	55.6
Cr 7	40.94	27.20	12.03	B.D.	B.D.	19.46	B.D.	0.25	99.9	45.2	50.2
Cr 8	44.31	25.40	12.89	B.D.	B.D.	18.00	B.D.	B.D.	100.6	41.9	53.9
Cr 9	32.05	34.21	13.81	B.D.	B.D.	18.72	B.D.	B.D.	98.8	38.4	38.6
Cr 10	48.06	22.47	10.84	B.D.	B.D.	17.28	B.D.	B.D.	98.7	47.2	58.9
Cr 11	38.18	30.77	14.07	B.D.	B.D.	16.67	B.D.	B.D.	99.7	37.9	45.4
Cr 12	46.35	15.51	9.93	1.37	B.D.	25.97	B.D.	B.D.	99.1	53.5	66.7
Cr 13	24.99	43.54	17.31	B.D.	B.D.	13.42	B.D.	B.D.	99.3	28.4	27.8
Cr 14	57.20	11.83	8.98	B.D.	B.D.	21.19	B.D.	B.D.	99.2	55.5	76.4
Cr 15	59.69	10.74	11.45	B.D.	B.D.	17.95	B.D.	B.D.	99.8	44.3	78.8
Cr 16	41.85	26.81	12.62	0.25	0.22	18.05	0.48	B.D.	100.3	43.0	51.1
Cr 17	39.07	28.20	13.14	B.D.	B.D.	18.13	B.D.	B.D.	98.5	40.6	48.2
Cr 18	40.88	28.55	14.79	B.D.	B.D.	14.86	B.D.	B.D.	99.1	34.2	49.0
Cr 19	47.14	21.39	11.74	B.D.	B.D.	18.68	B.D.	B.D.	99.0	45.1	59.6
Cr 20	52.55	14.60	9.22	B.D.	0.38	21.60	0.85	B.D.	99.2	54.2	70.7
Cr 21	49.51	19.87	11.80	B.D.	B.D.	18.02	B.D.	B.D.	99.2	44.6	62.6
Cr 22	48.39	21.46	12.68	B.D.	B.D.	16.44	B.D.	B.D.	99.0	41.1	60.2
Cr 23	45.60	23.39	12.76	B.D.	B.D.	16.85	B.D.	B.D.	98.6	41.0	56.7
Cr 24	40.40	26.48	11.30	B.D.	0.26	19.57	B.D.	B.D.	98.0	47.9	50.6
Cr 25	50.47	16.23	9.81	B.D.	B.D.	22.83	B.D.	B.D.	99.3	52.7	67.6
Cr 26	54.62	15.93	10.75	B.D.	B.D.	18.58	B.D.	B.D.	99.9	48.6	69.7
Cr 27	47.88	19.39	11.05	B.D.	B.D.	22.10	B.D.	B.D.	100.4	48.4	62.3
Cr 28	42.77	22.90	9.60	0.25	B.D.	24.09	0.45	B.D.	100.1	54.9	55.6
MAS 10.25–10.35 m (11.6 kg)											
Cr 1	37.32	36.42	13.10	B.D.	B.D.	11.86	B.D.	B.D.	98.7	33.7	40.7
Cr 2	39.84	28.79	13.80	B.D.	B.D.	16.22	B.D.	B.D.	98.7	38.0	48.1
Cr 3	43.38	23.30	11.28	B.D.	B.D.	21.68	B.D.	B.D.	99.6	47.8	55.5
Cr 4	40.09	28.38	12.92	B.D.	B.D.	18.00	B.D.	B.D.	99.4	41.9	48.6
Cr 5	45.93	23.77	15.13	B.D.	0.30	15.20	B.D.	B.D.	100.3	32.5	56.4
Cr 6	40.69	29.64	12.02	B.D.	B.D.	17.88	B.D.	B.D.	100.2	45.5	47.9
Cr 7	39.60	29.86	13.51	B.D.	B.D.	16.95	B.D.	B.D.	99.9	40.1	47.1
Cr 8	47.59	22.19	13.93	B.D.	B.D.	16.36	B.D.	B.D.	100.1	36.6	59.0
Cr 9	40.24	22.24	12.88	0.69	B.D.	22.73	B.D.	B.D.	98.8	41.4	54.8
Cr 10	42.66	26.68	13.89	B.D.	B.D.	16.69	0.57	B.D.	100.5	37.2	51.7
Cr 11	46.75	23.71	11.74	B.D.	0.25	16.41	B.D.	B.D.	98.9	44.0	56.9
Cr 12	41.52	32.36	12.21	B.D.	B.D.	13.98	B.D.	B.D.	100.1	39.1	46.2
Cr 13	41.93	21.59	12.40	0.91	B.D.	22.43	0.57	B.D.	99.8	43.2	56.6
Cr 14	37.97	31.95	14.94	B.D.	B.D.	14.52	B.D.	B.D.	99.4	34.6	44.3
Cr 15	59.32	7.04	3.87	B.D.	0.33	29.18	B.D.	0.60	100.4	79.7	85.0
Cr 16	46.63	16.81	10.82	0.57	B.D.	23.82	B.D.	B.D.	98.7	48.8	65.0
Cr 17	48.57	20.56	11.47	B.D.	B.D.	18.92	B.D.	B.D.	99.5	46.3	61.3
Cr 18	58.93	8.93	6.51	B.D.	0.50	24.16	B.D.	B.D.	99.0	67.0	81.6
Cr 19	42.07	26.71	13.17	B.D.	B.D.	16.11	B.D.	B.D.	98.1	39.8	51.4
Cr 20	45.61	24.16	11.84	B.D.	B.D.	16.87	B.D.	B.D.	98.5	44.4	55.9
Cr 21	50.29	20.53	10.01	B.D.	0.36	19.33	0.41	B.D.	100.9	52.0	62.2
Cr 22	37.79	15.82	6.13	1.33	B.D.	39.36	B.D.	B.D.	100.4	71.0	61.6
Cr 23	50.47	20.32	10.84	B.D.	0.32	18.41	B.D.	B.D.	100.4	48.8	62.5
Cr 24	33.29	36.26	15.62	B.D.	B.D.	14.53	B.D.	B.D.	99.7	33.2	38.1
Cr 25	53.60	18.79	8.12	B.D.	B.D.	18.37	B.D.	B.D.	98.9	55.9	65.7
Cr 26	56.74	6.31	3.44	B.D.	0.42	32.00	0.52	0.50	99.9	81.6	85.8
Cr 27	48.69	15.86	9.99	1.43	0.39	23.15	B.D.	B.D.	99.5	53.8	67.3
Cr 28	36.75	7.16	5.49	5.34	0.77	44.44	B.D.	B.D.	99.9	75.6	77.5
Cr 29	40.57	19.10	9.09	0.36	B.D.	29.99	B.D.	B.D.	99.1	56.9	58.8
Cr 30	47.23	20.93	11.02	B.D.	0.35	20.58	B.D.	B.D.	100.1	48.9	60.2
Cr 31	51.41	17.84	10.96	B.D.	0.36	19.14	B.D.	B.D.	99.7	48.3	65.9
Cr 32	48.81	21.74	10.72	B.D.	B.D.	17.73	B.D.	B.D.	99.0	48.1	60.1
Cr 33	36.64	32.86	14.66	B.D.	B.D.	15.59	B.D.	B.D.	99.8	36.1	42.8
Cr 34	47.51	23.18	12.39	B.D.	B.D.	17.20	B.D.	B.D.	100.3	43.3	57.9

*All analyses were on polished grains. Five grains were lost during polishing.
†The total values represent a mean of a minimum of two analyses.
§Fe#: mole% Fe/(Fe + Mg).
#Cr#: mole% Cr/(Cr + Al).
**Relative to the base of the section; see main text.
††B.D.—below detection limit.

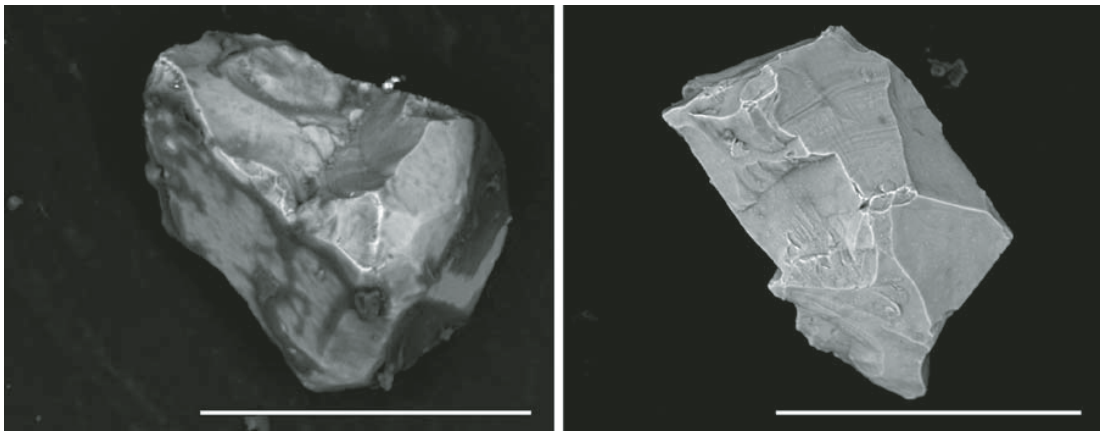

Figure 2. Left: The only EC grain found in this study. It was found in the sample from 6.15 m above the base of the Massignano section. Note the slightly rounded appearance, indicating possibly a reworked origin. Right: For comparison, a mid-Ordovician extraterrestrial chromite grain from the upper part of the Puxi River section in China (Schmitz et al., 2008). Many or most of the extraterrestrial chromite grains recovered from limestone that formed directly after the mid-Ordovician asteroid breakup event are characterized by their sharp edges and often excellent preservation. Scale bar in both images is 100 µm.

Similar trends have been confirmed at several sites in Sweden and now also in the Puxi River section in the Hubei Province in China (Schmitz et al., 2003, 2008; Schmitz and Häggström, 2006). This is strong support for a dramatic increase in the flux of extraterrestrial matter in the submeter size fraction at ca. 470 Ma.

Based on the experience from the mid-Ordovician limestone, it should be possible to test, using quantitative searches for EC grains in late Eocene sediments, whether an asteroid shower, with accompanying increase in the flux of EC-carrying meteorites and micrometeorites, occurred also at that time. Our finding in this study of only one EC grain in 167 kg of limestone from the ^{3}He-enriched part of the Massignano section is a very strong indication that the EC flux was not significantly enhanced at this time. In a previous study, we also searched for extraterrestrial chromite in 210 kg of condensed limestone from the latest Maastrichtian and Paleocene section in the Bottaccione Gorge at Gubbio (Cronholm and Schmitz, 2007). The limestone studied there represents eight levels across 24 m of section. Only six EC grains were found, which is in accord with the predisruption values for similarly condensed limestone in the mid-Ordovician. Using well-established sedimentation rates for the Gubbio section (e.g., Mukhopadhyay et al., 2001), the results indicate an EC flux of ~0.26 grain m^{-2} $k.y.^{-1}$. The sedimentation rate in the late Eocene part of the Massignano section is about three times higher than in the latest Cretaceous–Paleocene at Gubbio (see, e.g., Montanari et al., 1993; Cronholm and Schmitz, 2007). An estimate of the late Eocene EC flux based on the finding of only 1 grain in 167 kg of rock gives 0.16 grain m^{-2} $k.y.^{-1}$, similar to the value for the Gubbio section. This is similar also to the EC flux of 0.09 EC grain m^{-2} $k.y.^{-1}$ for the mid-Ordovician before the asteroid breakup event (based on 5 grains in 379 kg of limestone), but it is two orders of magnitude lower than the 13 EC grains m^{-2} $k.y.^{-1}$ after the event (based on 276 EC grains in 148 kg of limestone) (Schmitz and Häggström, 2006; Cronholm and Schmitz, 2007). We emphasize that flux rates based on a single or a few grains have large statistical uncertainties and are significant for comparison mainly at an order-of-magnitude scale.

Our data thus give no support of a chondritic asteroid shower in the late Eocene as envisioned by Tagle and Claeys (2004, 2005). Their claim was based mainly on studies of Popigai crater impact melts, for which platinum group element profiles indicated an L-chondritic impactor. A chondritic impactor for the Popigai crater agrees with Cr-isotopic measurements of the late Eocene layers with (altered) clinopyroxene-bearing spherules at Massignano and Ocean Drilling Program (ODP) Site 709c (Kyte et al., 2004), but the Cr isotopes cannot distinguish between different groups of ordinary chondrites. The clinopyroxene-spherule layers at the two sites are generally considered to represent the same ejecta event, probably associated with the formation of the Popigai crater (Glass et al., 2004). Similar to Farley (this volume), however, we are skeptical about the use of element signatures to determine impactor types. For example, recently Tagle et al. (2008) suggested, based on Ir and Cr measurements of the mid-Ordovician Lockne crater resurge deposits, that the Lockne impactor was a nonmagmatic iron body, similar to a group of meteorites that is uncommon in recent meteorite collections. This is contradictory to the findings of Alwmark and Schmitz (2007), who showed that the same resurge deposits are extremely rich in L-chondritic chromite grains (>75 grains kg^{-1}), representing relict fragments of the impactor. The approach by Tagle et al. (2008) assumes that Ir is immobile in sediments, which is inconsistent with our experience of Ir behavior in mid-Ordovician fossil meteorites (Schmitz et al., 1996). Other studies have shown that Ir is highly mobile in ejecta layers in marine sediments (e.g.,

Wallace et al., 1990; Colodner et al., 1992). Our recent oxygen isotopic measurements of chromite grains from the Lockne crater resurge deposits confirm an L-chondritic origin (Schmitz et al., 2008, personal commun.).

The fact that the single EC grain found in the present study at 6.15 m is associated with a small Ir-enrichment (~250 ppt) could reflect that it is a preserved fragment of an impactor, perhaps a small body that broke up in the water column, but the grain may as well reflect the normal rain of micrometeorites to Earth. Only studies of additional very large samples can show if the bed at 6.15 m is richer in extraterrestrial chromite than other parts of the section. The slightly rounded edges of the grain may indicate that it was transported on the seafloor for some time before being trapped in the sediment (Fig. 2).

The detailed origin of the many OC grains in the Massignano section is beyond the scope of this study, but there is no doubt that almost all or all of them are terrestrial. Most of the grains are similar in composition to OC grains found by Cronholm and Schmitz (2007) in middle Paleocene sediments in the Bottaccione Gorge section at Gubbio, supporting the existence of a long-term local source for this type of chrome spinel grains. However, OC grains are much more common in the Massignano section, with on average 2.24 grains kg^{-1}, compared to Gubbio limestone, with 0.07 OC grain kg^{-1}. The difference may reflect a more pelagic situation in the Paleocene and development to more hemipelagic conditions in the late Eocene, as indicated also by increasing sedimentation rates.

The hypothesis of Fritz et al. (2007) of a lunar origin of ^3He in late Eocene sediments is testable, for example, by searches for relict minerals from lunar micrometeorites and meteorites in the Massignano sediments. The minerals with greatest potential are ilmenites and chrome spinels because they are common in lunar volcanic rocks, very durable in sedimentary environments on Earth, and can be readily retrieved by different acid-leaching processes. Ilmenites are abundant in the Massignano sediments, but they were mostly destroyed in the strong HF acid used in the present study; otherwise we could have searched for Mg-rich ilmenites with a possible lunar origin (Papike et al., 1998). Any lunar ilmenites, however, would be diluted with large amounts of terrestrial ilmenites, and the compositional differences between the two types of ilmenites are not straightforward; hence, this would be a very tedious and difficult project. With regard to chrome spinels, it cannot be entirely ruled out that one or a few of the OC grains in Table 1 actually originated from the Moon. The problem is that, whereas the dominant type of chromite in equilibrated chondrites has a very narrow compositional range, which also is very unique and different from terrestrial chromite, lunar chrome spinels have a wide range of compositions, and complex overlaps exist with terrestrial chrome spinels (Papike et al., 1998). With the present level of understanding, it is questionable whether a lunar origin of a chrome spinel grain can be ascertained only by its element composition.

The L-chondrite disruption event in the mid-Ordovician is the largest documented asteroid breakup event during the past 3 b.y. (Keil et al., 1994), and it is highly plausible that it led to a dramatic increase in the flux of extraterrestrial matter to Earth. There is no indication in argon gas retention ages from recent meteorites for any major asteroid disruption event during the last 100 m.y., but cosmic-ray exposure ages show that secondary collisional events involving smaller bodies have occurred. In fact, cosmic-ray exposure ages show that a major fraction of the L chondrites falling on Earth today originated from such a meteorite dispersal event at ca. 40 Ma (Wieler and Graf, 2001). The close temporal relation of this event to the Popigai and Chesapeake Bay impact events could be consistent with a slight increase in the flux of chondritic matter to Earth, but such an increase was most likely not larger than a factor of a few, judging from the results in the present study.

CONCLUSIONS

Only one ordinary chondritic chromite grain was found in large limestone samples, totaling at 167 kg and collected at representative levels throughout the late Eocene part of the Massignano section. Considering the sedimentation rates at Massignano, and by comparison with similar studies for other periods in Earth history, this is the approximate number of grains to be expected if the flux rate of chondritic matter to Earth was normal or close to normal during the late Eocene. We thus find no evidence of any chondritic meteorite or micrometeorite shower in the late Eocene, and by implication, suggest that neither was there any "asteroid shower" at this time, although a slight increase (a factor of a few) in the asteroid flux cannot be ruled out.

ACKNOWLEDGMENTS

We thank C. Koeberl for his patience and encouragement in the editorial processing of this paper, L. Ferrière and F.T. Kyte for helpful reviews of a previous, quite different version of the paper, M. Nolvi and G. Thorelli for heroic assistance with the acid leaching, and C. Alwmark for valuable comments and suggestions. The study was supported by the Swedish Research Council.

REFERENCES CITED

Alwmark, C., and Schmitz, B., 2007, Extraterrestrial chromite in the resurge deposits of the early Late Ordovician Lockne Crater, central Sweden: Earth and Planetary Science Letters, v. 253, p. 291–303, doi: 10.1016/j.epsl.2006.10.034.

Bodiselitsch, B., Montanari, A., Koeberl, C., and Coccioni, R., 2004, Delayed climate cooling in the late Eocene caused by multiple impacts: High-resolution geochemical studies at Massignano, Italy: Earth and Planetary Science Letters, v. 223, p. 283–302, doi: 10.1016/j.epsl.2004.04.028.

Bridges, J.C., Schmitz, B., Hutchison, R., Greenwood, R.C., Tassinari, M., and Franchi, I.A., 2007, Petrographic classification of Middle Ordovician fossil meteorites from Sweden: Meteoritics & Planetary Science, v. 42, p. 1781–1789.

Clymer, A.K., Bice, D.M., and Montanari, A., 1996, Shocked quartz from the late Eocene: Impact evidence from Massignano, Italy: Geology, v. 24, p. 483–486, doi: 10.1130/0091-7613(1996)024<0483:SQFTLE>2.3.CO;2.

Colodner, D.C., Boyle, E.A., Edmond, J.M., and Thomson, J., 1992, Post-depositional mobility of platinum, iridium and rhenium in marine sediments: Nature, v. 358, p. 402–404, doi: 10.1038/358402a0.

Cronholm, A., and Schmitz, B., 2007, Extraterrestrial chromite in latest Maastrichtian and Paleocene pelagic limestone at Gubbio, Italy: The flux of unmelted ordinary chondrites: Meteoritics & Planetary Science, v. 42, p. 2099–2109.

Farley, K.A., Montanari, A., Shoemaker, E.M., and Shoemaker, C.S., 1998, Geochemical evidence for a comet shower in the late Eocene: Science, v. 280, p. 1250–1253, doi: 10.1126/science.280.5367.1250.

Farley, K.A., 2008, this volume, Late Eocene and late Miocene cosmic dust events: Comet showers, asteroid collisions, or lunar impacts?, *in* Koeberl, C., and Montanari, A., eds., The Late Eocene Earth—Hothouse, Icehouse, and Impacts: Geological Society of America Special Paper 452, doi: 10.1130/2008.2452(03).

Fritz, J., Tagle, R., and Artemieva, N., 2007, Lunar helium-3 in marine sediments: Implications for a late Eocene asteroid shower: Icarus, v. 189, p. 591–594, doi: 10.1016/j.icarus.2007.03.026.

Glass, B.P., Liu, S., and Montanari, A., 2004, Impact ejecta in upper Eocene deposits at Massignano, Italy: Meteoritics & Planetary Science, v. 39, p. 589–597.

Greenwood, R.C., Schmitz, B., Bridges, J.B., Hutchison, R., and Franchi, I.A., 2007, Disruption of the L chondrite parent body: New oxygen isotope evidence from Ordovician relict chromite grains: Earth and Planetary Science Letters, v. 262, p. 204–213, doi: 10.1016/j.epsl.2007.07.048.

Heck, P.R., Schmitz, B., Baur, H., Halliday, A.N., and Wieler, R., 2004, Fast delivery of meteorites to Earth after a major asteroid collision: Nature, v. 430, p. 323–325, doi: 10.1038/nature02736.

Heck, P.R., Schmitz, B., Baur, H., and Wieler, R., 2008, Noble gases in fossil micrometeorites and meteorites from 470 Myr old sediments from southern Sweden and new evidence for the L-chondrite parent body breakup event: Meteoritics & Planetary Science, v. 43, p. 517–528.

Hut, P., Alvarez, W., Elder, W.P., Hansen, T., Kauffman, E.G., Keller, G., Shoemaker, E.M., and Weissman, P.R., 1987, Comet showers as a cause of mass extinctions: Nature, v. 329, p. 118–126, doi: 10.1038/329118a0.

Jarosewich, E., Nelen, J.A., and Norberg, J.A., 1980, Reference samples for electron microprobe analysis: Geostandards Newsletter, v. 4, p. 43–47, doi: 10.1111/j.1751-908X.1980.tb00273.x.

Keil, K., 1962, On the phase composition of meteorites: Journal of Geophysical Research, v. 67, p. 4055–4061, doi: 10.1029/JZ067i010p04055.

Keil, K., Haack, H., and Scott, E.R.D., 1994, Catastrophic fragmentation of asteroids: Evidence from meteorites: Planetary and Space Science, v. 42, p. 1109–1122, doi: 10.1016/0032-0633(94)90011-6.

Korochantseva, E.V., Trieloff, M., Lorenz, C.A., Buykin, A.I., Ivanova, M.A., Schwarz, W.H., Hopp, J., and Jessberger, E.K., 2007, L-chondrite asteroid breakup tied to Ordovician meteorite shower by multiple isochron ^{40}Ar-^{39}Ar dating: Meteoritics & Planetary Science, v. 42, p. 113–130.

Kyte, F.T., Shukolyukov, A., Hildebrand, A.R., Lugmair, G.W., and Hanova, J., 2004, Initial Cr-isotopic and iridium measurements of concentrates from late-Eocene cpx-spherule deposits: Lunar and Planetary Science Conference XXXV, abstract 1824 2 p.

Montanari, A., and Koeberl, C., 2000, Impact Stratigraphy—The Italian Record: Lecture Notes in Earth Sciences, Volume 93: Heidelberg-Berlin, Springer Verlag, p. 1–364.

Montanari, A., Asaro, F., Michel, H.V., and Kennett, J.P., 1993, Iridium anomalies of late Eocene age at Massignano (Italy), and ODP Site 689B (Maud Rise, Antarctic): Palaios, v. 8, p. 420–437, doi: 10.2307/3515017.

Montanari, A., Campo Bagatin, A., and Farinella, P., 1998, Earth cratering record and impact energy flux in the last 150 Ma: Planetary and Space Science, v. 46, p. 271–281, doi: 10.1016/S0032-0633(97)00130-X.

Mukhopadhyay, S., Farley, K.A., and Montanari, A., 2001, A 35 Myr record of helium in pelagic limestone from Italy: Implications for interplanetary dust accretion from the early Maastrichtian to the middle Eocene: Geochimica et Cosmochimica Acta, v. 65, p. 653–669, doi: 10.1016/S0016-7037(00)00555-X.

Papike, J.J., Ryder, G., and Shearer, C.K., 1998, Lunar samples, *in* Papike, J.J., ed., Planetary Materials, Mineralogical Society of America Reviews in Mineralogy, v. 36, ch. 5, 234 p.

Pierrard, O., Robin, E., Rocchia, R., and Montanari, A., 1998, Extraterrestrial Ni-rich spinel in Upper Eocene sediments from Massignano, Italy: Geology, v. 26, p. 307–310, doi: 10.1130/0091-7613(1998)026<0307:ENRSIU>2.3.CO;2.

Schmitz, B., and Häggström, T., 2006, Extraterrestrial chromite in Middle Ordovician marine limestone at Kinnekulle, southern Sweden—Traces of a major asteroid breakup event: Meteoritics & Planetary Science, v. 41, p. 455–466.

Schmitz, B., Lindström, M., Asaro, F., and Tassinari, M., 1996, Geochemistry of meteorite-rich marine limestone strata and fossil meteorites from the Lower Ordovician at Kinnekulle, Sweden: Earth and Planetary Science Letters, v. 145, p. 31–48, doi: 10.1016/S0012-821X(96)00205-1.

Schmitz, B., Tassinari, M., and Peucker-Ehrenbrink, B., 2001, A rain of ordinary chondritic meteorites in the early Ordovician: Earth and Planetary Science Letters, v. 194, p. 1–15, doi: 10.1016/S0012-821X(01)00559-3.

Schmitz, B., Häggström, T., and Tassinari, M., 2003, Sediment-dispersed extraterrestrial chromite traces a major asteroid disruption event: Science, v. 300, p. 961–964, doi: 10.1126/science.1082182.

Schmitz, B., Harper, D.A.T., Peucker-Ehrenbrink, B., Stouge, S., Alwmark, C., Cronholm, A., Bergström, S.M., Tassinari, M., and Wang, X., 2008, Asteroid breakup linked to the Great Ordovician Biodiversification Event: Nature Geoscience, v. 1, p. 49–53, doi: 10.1038/ngeo.2007.37.

Tagle, R., and Claeys, P., 2004, Comet or asteroid shower in the late Eocene?: Science, v. 305, p. 492, doi: 10.1126/science.1098481.

Tagle, R., and Claeys, P., 2005, An ordinary chondrite impactor for the Popigai crater, Siberia: Geochimica et Cosmochimica Acta, v. 69, p. 2877–2889, doi: 10.1016/j.gca.2004.11.024.

Tagle, R., Schmitt, R.T., and Erzinger, J., 2008, The Lockne impact is not related to the Ordovician L-chondrite shower: Lunar and Planetary Science Conference XXXIX, abstract 1418, 2 p.

Wallace, M.W., Gostin, V.A., and Keays, R.R., 1990, Acraman impact ejecta and host shales: Evidence for low-temperature mobilization of iridium and other platinoids: Geology, v. 18, p. 132–135, doi: 10.1130/0091-7613(1990)018<0132:AIEAHS>2.3.CO;2.

Wieler, R., and Graf, T., 2001, Cosmic ray exposure history of meteorites, *in* Peucker-Ehrenbrink, B., and Schmitz, B., eds., Accretion of Extraterrestrial Matter Throughout Earth's History: New York, Kluwer Academic/Plenum Publishers, p. 221–240.

Zappalà, V., Cellino, A., Gladman, B.J., Manley, S., and Migliorini, F., 1998, Asteroid showers on Earth after family breakup events: Icarus, v. 134, p. 176–179, doi: 10.1006/icar.1998.5946.

Manuscript Accepted by the Society 16 September 2008

III

Extraterrestrial chromite distribution across the Puxi River section, central China: Evidence for a global major spike in flux of L-chondritic matter during the mid-Ordovician

Anders Cronholm* and Birger Schmitz

Department of Geology, Sölvegatan 12, SE-22362 Lund, Sweden
Submitted to Icarus

Index words:
asteroid breakup
chromite
extraterrestrial dust
micrometeorite
Ordovician

* Corresponding author
E-mail: anders.cronholm@geol.lu.se)

A B S T R A C T

Previous studies of mid-Ordovician limestone in Sweden have shown that over a stratigraphic interval representing a few million years there is a two orders-of-magnitude enrichment in fossil L-chondritic meteorites (Ø = 1-21 cm) and sediment-dispersed extraterrestrial chromite (EC) grains (>63 μm). This has been interpreted as a dramatic increase in the flux of L-chondritic matter to Earth following the breakup of the L-chondrite parent body, which based on Ar-Ar gas retention ages (470 ±6 Ma) of recently fallen meteorites occurred at about this time. Here we show that the general trend in the distribution of sediment-dispersed EC grains can be reproduced in the Puxi River section in central China. In this section a total of 288 kg of limestone yielded 291 EC grains, with an average chemical composition very similar to chromite from recent L chondrites. In samples spanning the lower 8 m of the section, representing the *Paroistodus originalis* and *Lenodus antivariabilis* conodont zones, a total of 110 kg of limestone yielded only one EC grain. Similarly to the Swedish sections, EC grains begin to be common in the overlying *L. variabilis* Zone and remain common throughout the upper 9 m of the section, representing the *L. variabilis*, *Yangtzeplacognathus crassus* and *L. pseudoplanus* zones. In most of the beds over this interval one finds 1-4 EC grains per kg rock, a clear two orders-of-magnitude enrichment relative to the lower part of the section. Small bed-by-bed variations in the EC content over the upper interval most likely reflect a factor of a few variation in sedimentation rates. The Puxi River section contains only very rare terrestrial chrome spinel grains, which can be distinguished already by their rounded, abraded appearance compared to the angular, pristine extraterrestrial spinels. In the mid-Ordovician, based on paleoplate reconstructions, the Puxi River site was positioned at mid-latitudes on the southern hemisphere a few thousand kilometres east of the Swedish sites. The prominent enrichment of EC grains over the same stratigraphic intervals in China and Sweden is strong supporting evidence for a dramatic increase in the flux of L-chondritic matter to Earth shortly after the disruption of the L-chondrite parent-body in the asteroid belt.

1. Introduction

The distribution of sediment-dispersed extraterrestrial (chondritic) chromite (EC) grains (>63 μm) in mid-Ordovician marine limestone in Sweden indicates a dramatic increase in the flux of extraterrestrial matter to Earth after the disruption of the L-chondrite parent body in the asteroid belt at ~470 Ma (Schmitz et al., 2003, 2008; Schmitz and Häggström, 2006; Häggström and Schmitz, 2007). The searches for EC grains were initiated subsequent to the discovery of numerous fossil meteorites (Ø = 1-21 cm) in 470 Myr old marine limestone in the Thorsberg quarry at Kinnekulle, southern Sweden (Schmitz et al., 1996, 2001). The meteorites are almost entirely pseudomorphed by calcite and clay minerals, but contain relict chromite grains, an accessory (~0.25 wt%) mineral in ordinary chondrites (Keil, 1962; Nyström et al., 1988; Bridges et al., 2007). Contrary to other common meteoritic minerals chromite is extremely resistant to weathering and diagenesis. Both fossil meteorites and sediment-dispersed EC grains are two orders-of-magnitude more abundant compared to background levels over a part of mid-Ordovician strata corresponding to a few million years of deposition (Schmitz et al., 2001; Schmitz and Häggström, 2006; Alw-

mark and Schmitz, 2009a). Oxygen isotopic and elemental composition of chromite grains, the composition of relict silicate inclusions in chromite grains and chondrule sizes of the fossil meteorites indicates that all or almost all the extraterrestrial matter is of L-chondritic origin (Schmitz et al., 2001, 2003; Bridges et al., 2007; Greenwood et al., 2007; Alwmark and Schmitz, 2009b; Heck et al., 2009). Cosmic-ray exposure ages (cosmogenic ^{21}Ne) of chromite grains from the fossil meteorites increase upward in the strata from ~0.1 to ~1 Myr (Heck et al., 2004). The ages correlate inversely with a similar decrease in sediment ages, consistent with a common origin of the meteorites from one major asteroid breakup event. The disruption of the L-chondrite parent body is the largest documented breakup event in the asteroid belt during the last few billion years (Keil et al., 1994; Bogard, 1995,). The event was initially discovered based on K-Ar gas retention ages of around 500 Ma in a large fraction of recently fallen L chondrites (Anders, 1964; Heymann, 1967). High-precision ^{40}Ar-^{39}Ar dating of recent L chondrites have further constrained the age to 470 ±6 Ma (Korochantseva et al., 2007), which is identical within errors to the age of 466 ±1 Ma of the oldest beds with fossil meteorites, based on conodont biozonation and the 2004 Geological Time Scale (Cooper and Sadler, 2004).

The prime evidence for a dramatic increase in the flux of extraterrestrial matter to Earth around 470 Ma comes from the fossil meteorites. More than 87 fossil meteorites have now been found in the systematic meteorite search project pursued together with quarry workers in the Thorsberg quarry (Schmitz et al., 2001, and unpublished results). The meteorite search, however, is geographically limited, because it requires occurrence of quarries in slowly formed strata of the right age and where the right production methods are used, such as sawing and slicing of rock rather than crushing. The search is also tedious with only a handful of finds per year of quarry operation even under optimal conditions such as in the Thorsberg quarry. Therefore the method to search for sediment-dispersed EC grains in large limestone samples was developed (Schmitz et al., 2003). Abundant solar-wind implanted ^{21}Ne in these grains indicate that they derive mainly from micrometeorites that have decomposed on the ancient sea floor (Heck et al., 2008). The mid-Ordovician limestone in southern Sweden formed at very slow sedimentation rates, a few mm per 1000 years, and provides an ideal setting for searches of relict extraterrestrial components. In post-asteroid-breakup strata at Kinnekulle typically 1-3 EC grains are found per kg limestone, compared with only 5 EC grains in 379 kg of pre-breakup strata (Schmitz and Häggström, 2006). Similar low EC abundances as the latter occur also in strata with similarly slow sedimentation rates from other periods, such as in the latest Cretaceous-earliest Paleocene section at Gubbio (6 EC grains in 210 kg rock) or the late Eocene section at Massignano (1 EC grain in 167 kg of rock), both in central Italy (Cronholm and Schmitz, 2007; Schmitz et al., 2009a).

In order to test the hypothesis that the abundant EC grains reflect a global event, and not just regional processes in southern Sweden, we have now studied the distribution of EC in strata of the same age in the Puxi River (or Puxihe) section of the Yangtze Platform, Hubei Province, central China. This region was chosen for comparison because of the great similarities, in terms of slow sedimentation rates, facies development and biostratigraphy, with the coeval sections in Baltoscandia (Lindström et al., 1991). Through much of the Dapingian and Darriwilian stages (from middle Arenig and throughout Llanvirn) there is a close parallel sediment facies evolution in these areas, supported by a predominantly similar stratigraphic extension of conodont assemblages in relation to lithological variations (Lindström et al., 1991; Zhang, 1996, 1998a,b). During the Middle Ordovician Sweden was part of the Baltica continent positioned at mid latitudes on the southern hemisphere. The South China paleoplate, with the epicontinental sea where the Yangtze Platform sediments formed, lay at about the same latitude, but a few thousand kilometers to the east (Fig. 1; Cocks and Torsvik, 2002, 2005, 2007; Fortey and Cocks, 2003). Here we present the results of searches for EC grains in 288 kg of limestone across the upper Dapingian and lower to middle Darriwilian interval of the Puxi River section, providing a robust foundation for detailed comparison with the Baltoscandian region. Some preliminary results of this study where discussed by Schmitz et al. (2008).

2. Geological setting

Palaeoplates and palaeogeography

Currently, the South China palaeoplate is enclosed by the North China palaeoplate (north), the Chaidam (Qaidam) and Tibet palaeoplates (west), and the Sibumasu and Indo-China palaeoplates (southwest) (Zhou et al., 1995). The formation of the South China palaeoplate has been a hot topic for decades, but today it is generally recognized that ~830 Ma it was still in its oceanic crust phase. Subsequently, the fundamental structure of the plate was outlined in late Precambrian, during the three orogenies of the Yangtze tectonic cycle, approximately 800-570 Ma (Chen and Jahn, 1998; Chen et al., 2001, and references therein). The core of the South China palaeoplate cratonic basement consists of Precambrian low-grade metamorphic rocks, stretching more than 3000 km from west to east and over 2000 km from north to south. The Ordovician South China palaeoplate consisted of four distinct geographic components from northwest to southeast: 1) old island land masses, 2) the extensive epicontinental sea of the Yangtze Platform, 3) the Zhujiang clastic basin (including the deep Jiangnan Belt) and 4) the Cathaysian landmass (Fig. 2; Zhan et al., 2007). The eastern Yangtze

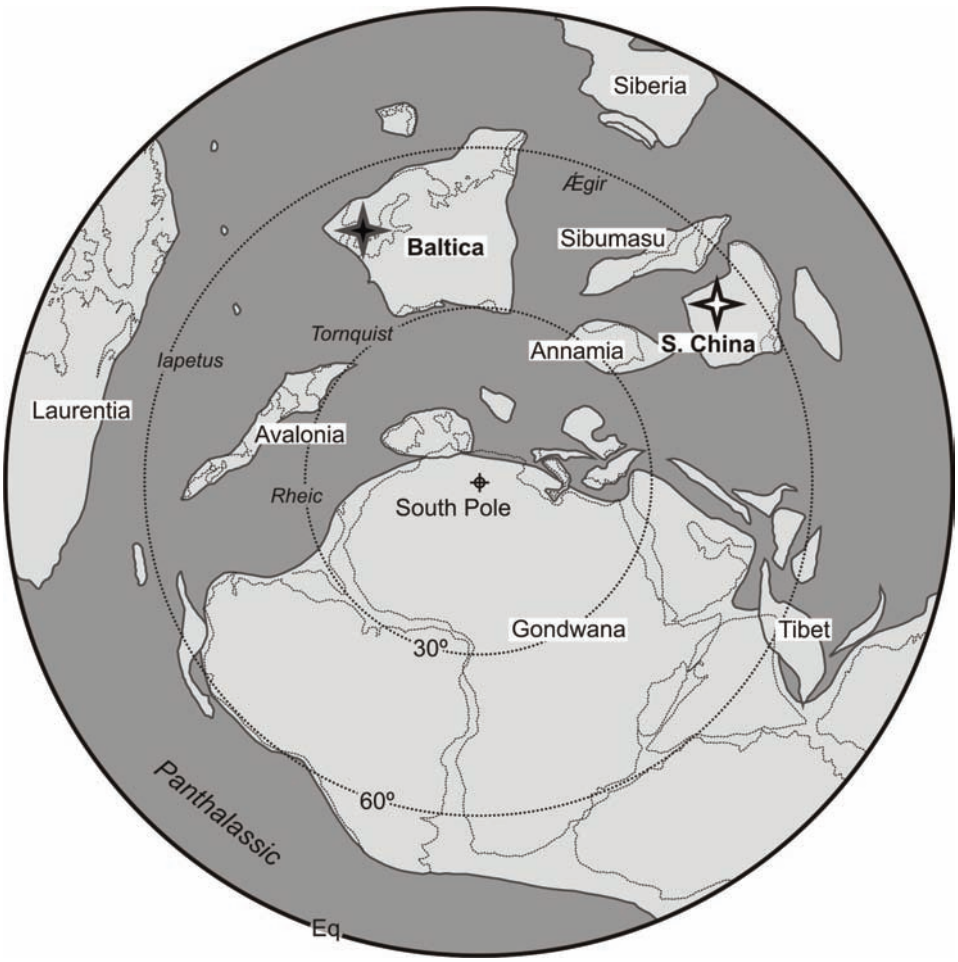

Fig. 1. Southern hemisphere paleogeography of Middle Ordovician world, ~470 Ma, modified from Cooks and Torsvik (2002, 2005, 2007) and Fortey and Cocks (2003). The paleomaps for 480 respectively 460 Ma in fig. 2 of Cocks and Torsvik (2002) were mainly used for interpolation of position of paleocontinents. Positions of localities studied on the Baltica and South China paleocontinents marked by stars.

Gorges, including the Yichang area where our study has been performed, was located in the northeastern Upper Yangtze Platform area, distal from terrigenous sources, which generated primarily condensed conodont-rich carbonates in a moderately shallow, outer shelf environment. Presently, Ordovician rocks are well exposed and easily accessible foremost on the eastern side of the Huangling anticline, represented by among others the Puxi River, Fenxiang, Daping and Huanghuachang sections (Fig. 2). The ~300 m thick fossiliferous Ordovician limestone succession has been subdivided into 11 formations, of which our study focuses on the Guniutan Formation. Throughout much of the Dapingian and early to middle Darriwilian the Upper Yangtze Platform area was dominated by condensed carbonates which show close facies resemblance to the Baltoscandian "Orthoceratite Limestone" (cf., Kinnekulle, southern Sweden) (Lindström et al., 1991; Zhang, 1996). Common sedimentary features include frequently occurring burrows and furrows, mineralized discontinuity surfaces, buckled beds (or mini-mounds), suspended cephalopod conchs, thin seams of stromatoids and biocalcarenitic components dominated by arthropods and echinoderms (Lindström et al., 1991).

The Guniutan Formation at Puxi River

The Puxi River section (30º55' N, 111º 25' E) is situated in an abandoned limestone quarry ~30 km north of the city of Yichang, next to a small river that flows out in the Yangtze river (Fig. 2). After crossing a small bridge ~3

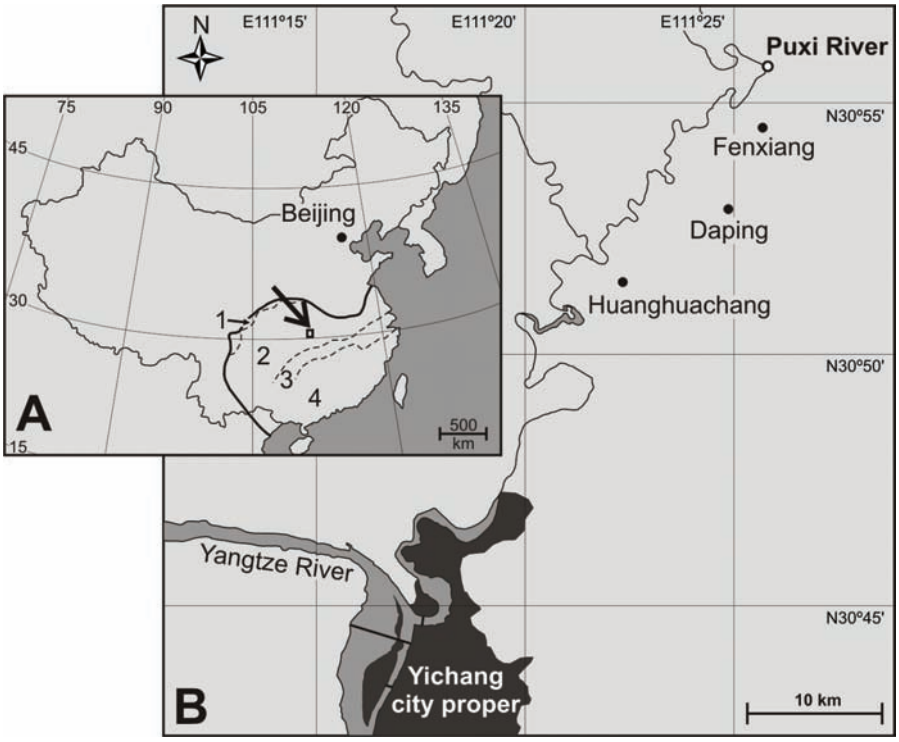

Fig. 2. A) Map of present-day China with study area marked by square and arrow. Map also illustrates how the Ordovician South China palaeoplate consisted of four distinct geographic components that today can be recognized in the geological record from northwest to southeast: 1) old island land masses, 2) the extensive epicontinental sea of the Yangtze Platform, 3) the Zhujiang clastic basin (including the deep Jiangnan Belt) and 4) the Cathaysian landmass (Zhan et al., 2007). B) Study area with positions of the Puxi River site and three other important Ordovician reference sections.

km north of the town of Fenxiang, take the first dirt road to the left, down to the water for access to the lowermost part of the section. The section is best studied in the summer months when the water level is low. The type section for the Guniutan Formation is the Fenxiang section, near Fenxiang. Previous research history of the Guniutan Formation has been well documented by Zhang (1996). At Puxi River, the 19.75 m thick Guniutan Formation is positioned between the Dawan and the Miaopo formations (Fig. 3). The lower ~9 m of the formation is a bedded succession mainly consisting of very condensed biocalc-arenitic wackestone. Discontinuity surfaces are numerous. Occasionally, the limestone beds are interbedded by thin layers of grey marl or shale, possibly indicating short periods of elevated supply of very fine-grained terrigenous material or reduced biogenic production. The following 1.5 m is represented by a marly interval with a few thin limestone beds. This is followed by the appearance of a very prominent so called "mini-mound" or "buckled bed" structure at +10.5 m. This mound-like structure typically extends 0.5-2 m laterally and 0.2-0.5 m vertically, with subelliptical to subcircular outlining, see Zhang (1996, 1998a,b) for further details. This lower grey mini-mound appears clayey with a laminated structure, a second much less distinctive, entirely calcareous mini-mound occurs at +11.15 m. At Daping, Lindström et al. (1991) observe a similar thick laminated wavy bedding plane between 10.7-10.9 m relative to the base of the Guniutan Formation, which may represent the discussed mini-mounds. Between and above the two mini-mounds normal bedded limestone occurs. About 0.5 m above the upper mini-mound the limestone beds are replaced by thick beds of nodular limestone, that persist until +14.8 m. The interval across the +15 m mark (samples Y9 to P3) represents a gradual change from nodular to massive, bedded limestone, occasionally intercalating with thin layers of nodular limestone. The compact bedded limestone facies persist until the Miaopo Formation is reached, at +19.75 m. The sedimentary rocks of the Guniutan Formation generally vary from red to reddish grey to grey, although some grey beds may include more distinct red patches. The Dawan Formation below the Guniutan Formation consists of interbedded argillaceous limestone, nodular limestone and some thin- to medium-bedded calcareous

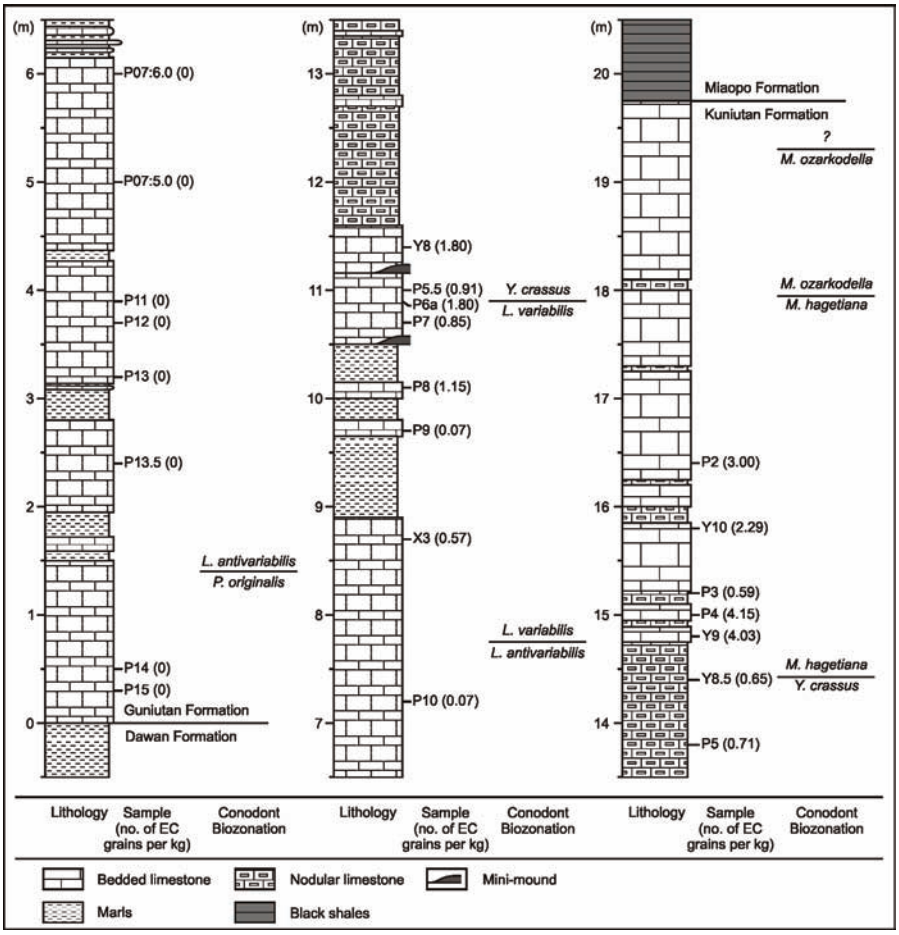

Fig. 3: Detailed log for the Puxi River section studied. Sample numbers are given together with (in parenthesis) number of EC grains found per kilogram of sedimentary rock. Conodont stratigraphy from S. Stouge in Schmitz et al. (2008) with revisions based on the re-measured section in 2007.

mudstone, while the overlying Miaopo Formation is made up of black shales and muddy limestones, rich in graptolites and shells.

Biostratigraphy of Guniutan Formation

Based on studies of the Fenxiang section, Zhang (1998a,b) established a detailed conodont biostratigraphy for the Guniutan Formation in the region. For the part of the formation studied by us, Zhang (1998a,b) recognizes, from top to bottom, the following conodont zones and subzones: *Lenodus antivariabilis*, *L. variabilis*, *Yangtzeplacognathus crassus*, *Microzarkodina hagetiana* and *M. ozarkodella*. This general biostratigraphy has been confirmed at the Puxi River section, where zone boundary levels have been established by Svend Stouge, in Schmitz et al. (2008) (Fig. 3). The development of the conodont species from *L. antivariablilis* to *L. variabilis* during the upper Arenig is generally recognized as a usable global marker, but the complex and similar morphology of this rapidly evolving taxa has created some disagreements regarding the detailed definitions separating the two conodont species (see e.g., Stouge and Bagnoli, 1990; Bagnoli and Stouge, 1996; Löfgren and Zhang, 2003). Therefore there is some uncertainty, at the most a couple of meters, in the exact placement of this boundary according to different authors. At or close to the Arenig-Llanvirn transition, the zone fossil *Y. crassus* appears, a species that has been recognized as very important for global correlations, mainly because of its narrow stratigraphical and wide geographical distribution (Bergström and Wang, 1998). At Kinnekulle in Sweden *Y. crassus* appears approximately 1.3 m above the first level with abundant EC grains (and fossil meteorites) (Schmitz and Häggström, 2006). In the Puxi River section the species has its first appearance between the two mini-mounds, at approximately +10.9 m. In the Fenxiang section Zhang (1996), however, places this faunal change directly above the second mini-mound, at

+12 m. This illustrates some of the uncertainty in correlation by means of conodont zonations by workers using slightly different species concepts or differently measured lithological logs. There are also some minor differences in the log and biostratigraphy for the Puxi River section in the present study and the preliminary study by Schmitz et al. (2008). This is further discussed in the next section.

3. Materials and Methods

Samples and analytical methods

The search for chromite grains requires large (>10 kg) samples of condensed limestone in order to retrieve relevant time-space data (grains/m^2/kyr) and avoid the hazards of undersampling, see e.g. Peucker-Ehrenbrink and Ravizza (2000), and discussion therein. In full, 23 samples were studied across the Puxi River section, spanning a ~16.4 m interval above the base of the Guniutan Formation. The samples ranged between 7-15 cm in thickness and 7.7-14.8 kg in weight, accumulating at a total mass of 287.8 kg. Samples were collected during two field trips, in June 2005 and October 2007. Although river water levels were lower in 2005 allowing easier access to the section, very thick vegetation covered some parts of it. This vegetation had been cleared in 2007 allowing a more detailed lithological log to be established also over the intervals not readily accessible in 2005. The section was remeasured leading to some significant changes relative to the preliminary log published by Schmitz et al. (2008). The main difference is the thickness of the lower interval dominated by limestone, which was estimated to ~ 7 m in 2005, but re-measured to ~9 m in 2007. The position of each sample in this study is given relative to the base of the Guniutan Formation, in accordance with the most recent lithological log (Fig. 3).

For extraction of chrome spinels limestone samples were first thoroughly washed and cleaned. Thereafter the samples were split into minor pieces (∅ < 10 cm) with a sledgehammer, followed by further fragmentation (∅ < 1 cm) by a Retsch Jaw Crusher BB 200. The crushed samples were decalcified in 6 M hydrochloric acid at room temperature and subsequently sieved (32 µm mesh). The remaining residues were leached in 18 M hydrofluoric acid at room temperature (with occasional stirring), after which the acid-insoluble remains were separated into three size fractions (32-63, 63-355 and >355 µm) and dried. The 63-355 µm fraction was searched for opaque minerals under a stereomicroscope (Nikon SMZ 1500) and all potential chromite grains were picked with a fine brush. The unpolished grains were mounted on carbon tape for roundness and size analyses in the scanning electron microscope (SEM) using backscatter imagery and semi-quantitative chemical analyses (see below). Subsequently, relevant Cr-rich grains were mounted in epoxy resin and polished, using a Struers alumina paste (standard quality) mixed with water on a spinning polishing cloth (Buehler), before final quantitative chemical analysis. The semi-quantitative analyses of the unpolished grains are made as a backup in case grains get lost during the polishing. In this study, however, only one grain was lost, which lacks significance. All elemental analyses were performed (minimum of three analyses per grain) by an Oxford Inca X-sight energy dispersive spectrometer (EDS) with a Si detector linked to a Hitachi S-3400N SEM. Cobalt was used to standardize the measurements, while controlling potential drift. Accelerating voltage of 15 kV, a sample current of ~1 nA, and counting live-time of 80 seconds were used. Precision (reproducibility) of analyses was typically within 1-4%. Analytical accuracy was controlled by the USNM 117075 chromite (Smithsonian) reference standard (Jarosewich et al., 1980) and three silicate reference standards (Alwmark and Schmitz, 2009b). Back-scatter images were evaluated according to the "Pettijohn" system for roundness, with the subdivision: very angular, angular, sub-angular, sub-rounded, rounded and very rounded (Pettijohn, 1957). The survey was performed independently by three instructed persons and each grain was labeled according to the collective perception of the grains. The individual size, length and width, of each grain while mounted on carbon tape was also measured in the SEM.

Definitions of EC and OC grains

Based on their chemical composition recovered chrome spinel grains have been divided into two groups: extraterrestrial (equilibrated chondritic) chromite (EC) grains and other Cr-rich spinel (OC) grains. The definition of the EC grains follows the standards established by Schmitz and Häggström (2006). These grains have similar chemical composition as the dominant chromite type of recent ordinary chondritic meteorites (petrographic types 4-6) and are more or less identical in elemental composition to the chromite grains retrieved from the fossil meteorites at Thorsberg quarry. Following Schmitz and Häggström (2006) the EC grains are characterized by high Cr_2O_3 content of ~55-60 wt%, FeO in the range of ~25-30 wt%, low Al_2O_3 at ~5-8 wt% and MgO concentrations of ~1.5-4 wt%. A most distinguishing feature is the typical TiO_2, ~2.0-3.5 wt%, and V_2O_3, ~0.6-0.9 wt% concentrations. Alwmark and Schmitz (2009b), however, showed that chromite of recent, partly unequilibrated, meteorites of the L4 type typically have low TiO_2 (~1.4-2.1 wt%) concentrations compared to more equilibrated L4-L6 meteorites (~2.0-3.5 wt%). Consequently, we revise the "accepted" EC range for TiO_2 to ~1.4-3.5 wt%. Because L4 grains make up only a minor fraction of all the EC grains this has no major implications for the overall distribution of EC grains in previous studies. We stress that for a grain to be classified as an EC grain, it has to have a composition within the defined ranges for all elements listed above, except when obvious,

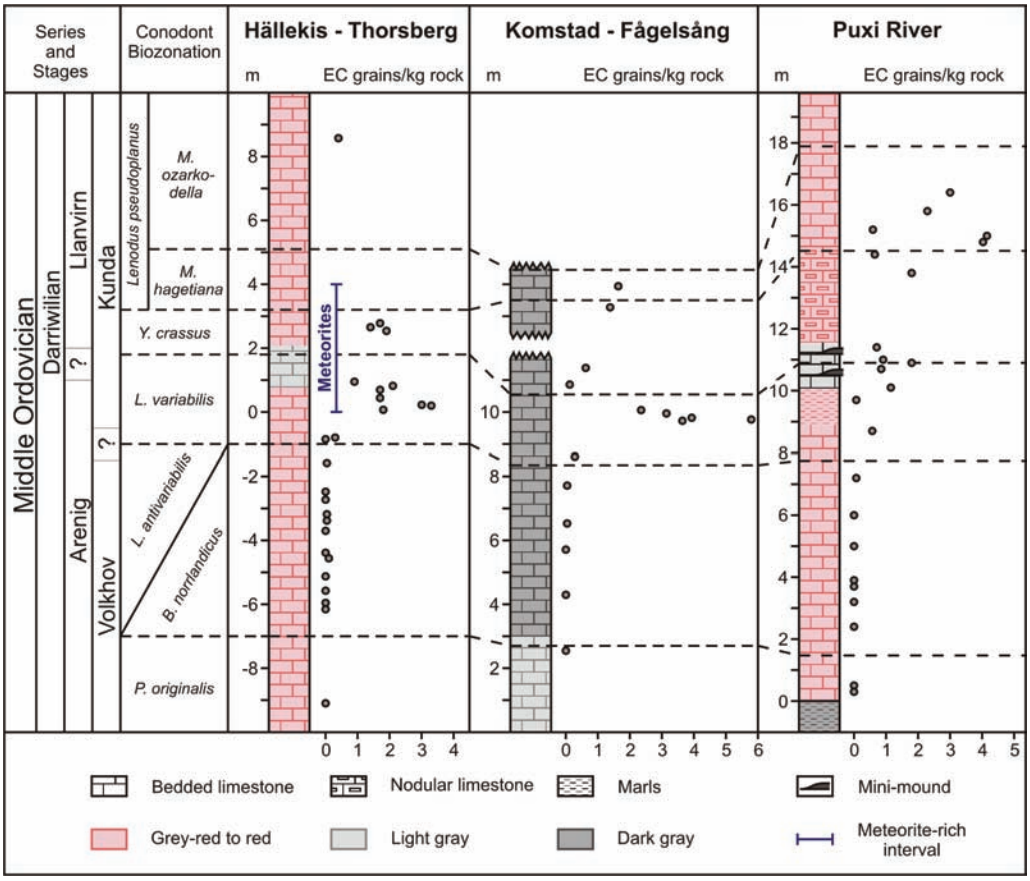

Fig. 4. Distribution of EC grains through Middle Ordovician sections in Sweden and China. Results are shown for sections at Kinnekulle (Hällekis and Thorsberg quarries; Schmitz and Häggström, 2006) and southern Scania (Killeröd and Fågelsång sections; Häggström and Schmitz, 2007, Schmitz et al., 2008), 350 km apart in southern Sweden, and the Puxi River section, central China, this study. The conodont biostratigraphy from S. Stouge in Schmitz et al. (2008) with revisions for the Puxi River section, based on a re-measured log for this site in 2007.

minor diagenetic changes have occurred (Schmitz et al., 2001; Schmitz and Häggström, 2006). All grains that fall outside the defined EC ranges for one or more elements are classified as "other" Cr-rich spinel (OC) grains. These grains typically display a wide compositional range, and most have a terrestrial origin. A few may be more unusual types of extraterrestrial grains, such as pallasitic chromite (Cronholm and Schmitz, 2007), rare types of ordinary chondritic chrome spinels (Thorslund et al., 1984) or even of lunar origin (see discussion in Schmitz et al., 2009a).

4. Results

Distribution of EC and OC grains

In the 288 kg of limestone studied across the Guniutan Formation at total of 317 Cr-spinel grains were found (Table 1; Appendix Table 1; Fig. 3-4). Of these grains, 291 are here classified as EC and the remaining 26 as OC. A few of the OC grains have compositions close to those of the EC grains and are most likely diagenetically altered EC grains. Only one single EC grain and no OC grains were found in the eight samples of in total 110 kg spanning the lower 8 m of the Guniutan Formation. In the interval from +8.7 m to the highest sample studied at +16.4 m relative to the base of the Guniutan Formation, all samples contain EC grains, but there is considerable variation between the samples, in the range 0.07 to 4.15 EC grains per kg. From +8.7 m to +14.4 m, including the strata with nodular limestone and mini-mounds, intermediate EC grain concentrations prevail, typically in the range 0.6 to 1.8 EC grains per kg, but also one sample at +9.7 m with only 0.07 EC grain per kg. The generally highest EC concentrations are found in the five samples in the uppermost two meters of the section studied, from +14.4 to +16.4 m. Four of these

Table 1. The distribution of extraterrestrial chromite (EC) and other Cr-rich spinel (OC) grains in mid-Ordovician limestone at the Puxi River section, China.

Sample depth[1]	Sample name	Sample weight (kg)	No. EC grains	EC grains (kg^{-1})	No. OC grains	OC grains (kg^{-1})
+16.4	P2	14.0	42	3.00	11	0.79
+15.8	Y10	14.0	32	2.29	4	0.29
+15.2	P3	8.5	5	0.59	1	0.12
+15.0	P4	13.0	54	4.15	1	0.08
+14.8	Y9	11.9	48	4.03	5	0.42
+14.4	Y8.5	13.9	9	0.65	0	0.00
+13.8	P5	12.8	23	1.80	3	0.23
+11.4	Y8	14.0	10	0.71	0	0.00
+11.0	P5.5	11.0	10	0.91	0	0.00
+10.9	P6a	12.8	23	1.80	0	0.00
+10.7	P7	13.0	11	0.85	0	0.00
+10.1	P8	13.0	15	1.15	0	0.00
+9.7	P9	13.4	1	0.07	0	0.00
+8.7	X3	12.3	7	0.57	1	0.08
+7.2	P10	14.8	1	0.07	0	0.00
+6.0	P07:6.0	14.0	0	0.00	0	0.00
+5.0	P07:5.0	7.7	0	0.00	0	0.00
+3.9	P11	13.0	0	0.00	0	0.00
+3.7	P12	10.7	0	0.00	0	0.00
+3.2	P13	14	0	0.00	0	0.00
+2.4	P13.5	14.3	0	0.00	0	0.00
+0.5	P14	12.1	0	0.00	0	0.00
+0.3	P15	9.6	0	0.00	0	0.00
Total		287.8	291		26	

[1] Meters relative to the base of the Guniutan Formation.

samples contain 2.29 to 4.15 EC grains per kg, whereas a fifth sample contains 0.59 EC grain per kg. The samples at +14.8 m and +15.0 m in this interval show a peak in concentration, 4.03-4.15 EC grains per kg, representing more than a third (102 of 291) of all EC grains recovered in this study. In the upper 8 m of the section, 178 kg of limestone held on average 1.63 EC grains per kg, compared with one grain in 110 kg of limestone in the lower 8 m of the section.

The predominantly terrestrial OC grains are rare throughout most of the section. Most samples (19 of 23) contain no OC grains at all or only a single OC grain (Table 1; Appendix Table 1). A sizable number of OC grains occur only in the uppermost sample at +16.4 m, which contains 11 of the in total 26 OC grains found. Three other samples in the upper three meters of the section contain in the range 3 to 5 OC grains. The average number of OC grains per kg limestone for the EC-rich interval (+8.7 to +16.4 m) is 0.15 grain per kg, less than a tenth of the average EC concentration. Based on chemical composition most of the OC grains have a terrestrial origin, a fact that is further supported by a completely different appearance of these grains in terms of roundness compared to the EC grains (see later section). At least four of the OC grains are most likely diagenetically altered chondritic chromite grains.

The distribution of EC grains in relation to the conodont biozonation in the Puxi River section and two previously studied composite sections 350 km apart in Sweden are shown in Figure 4. At all three sites the lower 7 to 8 meters of the section, representing the *Paroistodus originalis* and *L. antivariabilis/B. norrlandicus* zones, is devoid or almost devoid in EC grains. In the lower *L. variabilis* Zone a small increase in EC grains first occurs, then in the middle to upper part of this zone and in the superjacent *Y. crassus* and *M. hagetiana* zones EC grains are two orders-of-magnitude more common than in the lower part of the section.

Chemistry of EC and OC grains

The chemical composition of individual EC and OC grains is shown in Fig. 5 and Appendix Table 1, while the average composition of EC grains from respective sample is shown in Table 2. The average elemental composition of all the 291 EC grains from the Puxi River section is compared in Table 3 and Fig. 6 with the average compositions of sediment-dispersed EC grains from two localities

Table 2. The average element concentrations (wt% and 1σ standard deviation) of the sediment-dispersed EC grains from the Puxi River section, China.

Sample depth[1]	No. of grains	Cr_2O_3	Al_2O_3	MgO	TiO_2	V_2O_3	FeO	MnO	ZnO	Total[2]
+16.4	42	57.60 ±1.18	6.01 ±0.38	2.86 ±0.74	2.92 ±0.46	0.71 ±0.07	27.68 ±1.80	0.82 ±0.24	0.87 ±0.85	99.47 ±0.82
+15.8	32	57.86 ±1.00	5.94 ±0.34	3.09 ±1.14	3.08 ±0.39	0.70 ±0.09	27.31 ±1.78	0.72 ±0.26	0.79 ±1.08	99.48 ±0.63
+15.2	5	57.27 ±0.96	6.10 ±0.36	2.44 ±0.55	2.91 ±0.38	0.70 ±0.04	28.48 ±1.56	0.74 ±0.16	1.28 ±1.40	99.92 ±0.74
+15.0	54	57.71 ±0.98	5.90 ±0.28	2.77 ±0.67	2.91 ±0.33	0.71 ±0.07	28.01 ±2.03	0.85 ±0.17	1.09 ±0.97	99.93 ±0.68
+14.8	48	58.03 ±0.81	6.13 ±0.34	3.32 ±0.94	2.99 ±0.34	0.75 ±0.10	26.66 ±1.63	0.80 ±0.29	0.87 ±1.05	99.54 ±0.75
+14.4	9	58.00 ±0.98	5.81 ±0.34	2.34 ±0.28	2.49 ±0.55	0.70 ±0.06	27.58 ±1.80	1.26 ±0.45	1.42 ±1.09	99.61 ±0.64
+13.8	23	58.17 ±1.43	6.04 ±0.45	2.57 ±0.64	2.83 ±0.43	0.69 ±0.07	27.07 ±2.00	0.90 ±0.22	1.82 ±1.53	100.09 ±0.76
+11.4	10	57.73 ±0.89	5.91 ±0.38	3.40 ±1.47	2.89 ±0.29	0.70 ±0.07	27.58 ±2.12	0.82 ±0.16	0.59 ±0.48	99.61 ±1.13
+11.0	10	58.54 ±1.36	6.24 ±0.55	2.84 ±0.96	2.56 ±0.55	0.73 ±0.07	26.07 ±1.19	0.42 ±0.34	2.54 ±1.59	99.90 ±0.85
+10.9	23	57.85 ±1.68	5.92 ±0.30	2.80 ±0.88	3.00 ±0.27	0.73 ±0.07	26.95 ±1.61	0.81 ±0.19	1.09 ±1.18	99.14 ±0.98
+10.7	11	57.73 ±1.69	5.89 ±0.33	2.95 ±1.05	2.67 ±0.54	0.63 ±0.10	27.66 ±2.17	0.71 ±0.18	1.31 ±0.78	99.54 ±0.96
+10.1	15	57.62 ±0.70	6.11 ±0.37	2.46 ±0.68	2.91 ±0.31	0.71 ±0.07	27.71 ±1.52	0.73 ±0.19	1.29 ±1.15	99.55 ±0.69
+9.7	1	61.19	6.03	1.50	2.98	0.72	26.67	0.72	0.49	100.29
+8.7	7	57.39 ±0.62	5.95 ±0.13	2.74 ±0.26	2.95 ±0.47	0.68 ±0.08	28.35 ±0.96	0.78 ±0.13	0.54 ±0.47	99.38 ±0.60
+7.2	1	58.12	5.97	2.48	2.95	0.79	28.66	0.84	0.56	100.36

[1] Meters relative to the base of the Guniutan Formation; [2] Represents the average total (wt%) for the totals of a minimum of three separate analyses per grain.

in southern Sweden and chromite from mid-Ordovician fossil L chondrites and different types of recently fallen chondrites (H, L, and LL). The mean compositions of the EC grains from the different Puxi River samples are very homogeneous and there is no significant variation within the section (Table 2). The grains show a narrow range also for the Cr/(Cr + Al) values (84.0-90.1 mol%), with a mean of 86.6 ±0.71 mol%, a strong evidence for the chondritic origin of the grains. The EC grains from Puxi River are also identical, within narrow standard deviations, in mean composition to 276 sediment-dispersed EC grains from Kinnekulle and 274 grains from the Killeröd quarry, the two localities studied in most detail in southern Sweden (Table 3). Particularly significant is the fact that the Puxi River grains have similar high average TiO_2 (2.9 ±0.4 wt%) contents as the grains from southern Sweden (3.1 ±0.3 and 3.0 ±0.4 wt%, respectively). This strongly favors an L chondritic origin of most or all of the grains found, because H-chondritic chromite on average holds around 2.1 ±0.4 wt% TiO_2 compared to 2.7 ±0.4 wt% for L chondrites (Table 3). The Puxi River EC grains also show very similar or identical compositions to the chromite grains from mid-Ordovician fossil L chondrites and recently fallen L or LL chondrites. The fact that relict olivine inclusions in chromites from mid-Ordovician sediments and fossil meteorites in Sweden have a fayalite content representative of L rather than LL chondrites (Alwmark and Schmitz, 2009b), makes it likely that also the Puxi River EC grains are predominantly L rather than LL chondritic.

In this study we have refined our approach slightly following the discovery by Alwmark and Schmitz (2009a) that chromite from many L4 chondrites has lower TiO_2 contents than L5 and L6 chondrites. Although the L4 chondrites are generally considered to be "equilibrated", they actually represent a transitional series between the unequilibrated (L3) and fully equilibrated meteorites (L5 and L6) (Alwmark and Schmitz, 2009a; Grossman et al., 2009). At Puxi River we found 12 grains with equilibrated L-chondritic composition, except for lower TiO_2, ranging between 1.4-2.0 wt%. For the Killeröd quarry, Häggström and Schmitz (2007) also reported 10 grains of generally characteristic EC composition (among in total 274), but with TiO_2 concentrations in the range 1.5-2.0 wt%. The TiO_2 concentrations of chromite in type L3 meteorites range as low as 0.25-0.6 wt% (Bunch et al., 1967), type L4 may have intermediate values between 1.4-2.8 wt%, whereas L5/6 chondrites have an EC "typical" range of 2.5-3.4 wt% (Alwmark and Schmitz, 2009b). Chromite grains in L3 chondrites generally have a diameter <63 μm (Bridges et al., 2007), and are not recovered in our approach. The 12 EC grains with lower than normal TiO_2 content represent 4.1 % of the total EC content in the Puxi River section. This is similar to the Killeröd quarry where this type of grain makes up 3.6 % of the total EC grain assemblage. The recent flux of L4 meteorites to Earth comprises ~7% of all L chondrites (Grady, 2000), which is in reasonable agreement with the amount of EC with lower TiO_2 at Puxi River if the proportions in the flux of different petrographic types was the same as today. Some of the difference can be accounted for by the fact that not all recent L4 chondrites have lower TiO_2 content in chromite than L5/6 meteorites (Alwmark and Schmitz, 2009b).

The EC assemblage from the Guniutan Formation displays a wide range in ZnO contents (0-6.3 wt%), similar to the results for Kinnekulle (0-4.8 wt%; Schmitz and Häggström, 2006) and the Killeröd quarry (0-6.7 wt%; Häggström and Schmitz, 2007). Chromite of recently fallen chondrites usually holds less than 0.4 wt% ZnO (Table 3). Chromite from the fossil meteorites at Thorsberg discloses an invert relationship between FeO and ZnO, and Schmitz et al. (2001) suggest that the Fe is replaced by Zn

Table 3. The average element concentrations (wt% and 1σ standard deviation) of EC grains from the Puxi River section, China, in comparison with EC grains from previous studies in southern Sweden and chromite from recent meteorites.

Study	Cr_2O_3	Al_2O_3	MgO	TiO_2	V_2O_3	FeO	MnO	ZnO	Fe#[1]	Cr#[2]
Sediment-dispersed EC grains from the Puxi River section, central China, 291 grains, this study	57.84 ±1.14	6.00 ±0.36	2.88 ±0.88	2.91 ±0.40	0.71 ±0.08	27.40 ±1.84	0.80 ±0.26	1.09 ±1.12	84.3 ±4.39	86.6 ±0.71
Sediment-dispersed EC grains from Kinnekulle, southern Sweden, 276 grains[3]	57.61 ±1.58	6.07 ±0.76	2.58 ±0.79	3.09 ±0.33	0.75 ±0.07	27.36 ±2.63	0.78 ±0.20	0.53 ±0.50	85.6 ±3.90	86.5 ±1.42
Sediment-dispersed EC grains from Killeröd quarry, Komstad, southern Sweden, 274 grains[4]	56.93 ±1.29	6.08 ±0.73	2.69 ±1.10	2.95 ±0.44	0.74 ±0.07	28.74 ±1.72	0.87 ±0.25	0.71 ±0.84	n.d.[5]	n.d.
26 fossil meteorites from Thorsberg quarry, southern Sweden, 594 grains[6]	57.60 ±1.30	5.53 ±0.29	2.57 ±0.83	2.73 ±0.40	0.73 ±0.03	26.94 ±3.89	1.01 ±0.33	1.86 ±2.43	85.3 ±5.02	87.5 ±0.60
Chromite from 12 recent H5/6 group chondrites[6]	56.64 ±0.37	6.44 ±0.14	2.98 ±0.23	2.20 ±0.17	0.73 ±0.02	29.27 ±0.67	1.00 ±0.08	0.33 ±0.05	84.7 ±1.20	85.5 ±0.30
Chromite from 12 recent L5/6 group chondrites[6]	56.00 ±0.65	5.97 ±0.43	2.93 ±0.97	2.68 ±0.40	0.75 ±0.02	30.22 ±2.23	0.83 ±0.10	0.30 ±0.07	85.3 ±4.92	86.3 ±0.77
Chromite from 13 recent H4-6 group chondrites[7]	57.10 ±1.10	6.64 ±0.41	3.40 ±0.18	1.96 ±0.29	0.65 ±0.03	28.9 ±0.60	0.88 ±0.07	0.28 ±0.14	82.7 ±1.00	85.2 ±1.00
Chromite from 6 recent L4-6 group chondrites[7]	56.1 ±0.80	5.90 ±0.19	2.52 ±0.21	2.67 ±0.44	0.70 ±0.06	30.90 ±0.60	0.63 ±0.08	0.34 ±0.06	87.3 ±0.06	86.5 ±0.30
Chromite from 4 recent LL3-7 group chondrites[7]	55.8 ±0.56	5.52 ±0.17	1.85 ±0.14	3.40 ±0.57	0.67 ±0.10	31.60 ±0.62	0.51 ±0.04	n.d.	90.50 ±0.90	87.22 ±0.20

[1] Fe#: mol% Fe/(Fe+Mg); [2] Cr#: mol% Cr/(Cr+Al); [3] Schmitz and Häggström (2006); [4] Häggström and Schmitz (2007); [5] n.d. = no data; [6] Schmitz et al. (2001), modified by Alwmark and Schmitz (2007); [7] Wlotzka (2005).

during diagenesis. Furthermore, it appears that Zn substitution is favored to the surface of the spinels, explaining the occasional findings of exceedingly high ZnO content during preliminary analysis of unpolished EC grains.

The OC grains from the Puxi River section show wide ranges in composition: Cr_2O_3: 22.1-67.8 wt%; Al_2O_3: 5.0-22.5 wt%; MgO: 0-15.3 wt%; TiO_2: 0-4.1 wt%; V_2O_3: 0-0.62 wt%; FeO: 7.0-51.3 wt%; MnO: 0-2.9 wt%; and ZnO: 0-14.9 wt%. The majority of these spinels are almost certainly of terrestrial origin; however, some may represent more uncommon types of extraterrestrial material. Four of the OC grains may represent altered or anomalous EC grains (see Appendix Table 1), for example, two grains classified as OC in samples +15.2 and +16.4 m have typical EC grain composition for most elements, but 12-15 wt% ZnO, and reduced FeO of ~20-22 wt% compared with the accepted EC range of 25-30 wt% FeO.

Roundness and size of EC and OC grains

The roundness analysis of the recovered EC and OC grains shows a clear trend with more than 99 % of the EC grains having a subangular to very angular shape, whereas 62% (16/26) of the OC grains instead are subrounded to very rounded in shape (Fig. 7-8; Appendix Table 2). None of the EC grains are rounded or very rounded, and only 1 % are subrounded. This clearly indicates different modes of origin of the two types of grains. It shows that the EC grains can not have been drifting around on the sea floor for particularly long periods. Special attention has been given to the chemical composition of the seven OC grains with angular or very angular shape, because the similar appearance as the confirmed EC grains could indicate a meteoritic origin also for these grains. The four OC grains discussed based on chemical composition in the previous section to be diagenetically altered or anomalous EC grains fall in this group (Fig. 5; Appendix Table

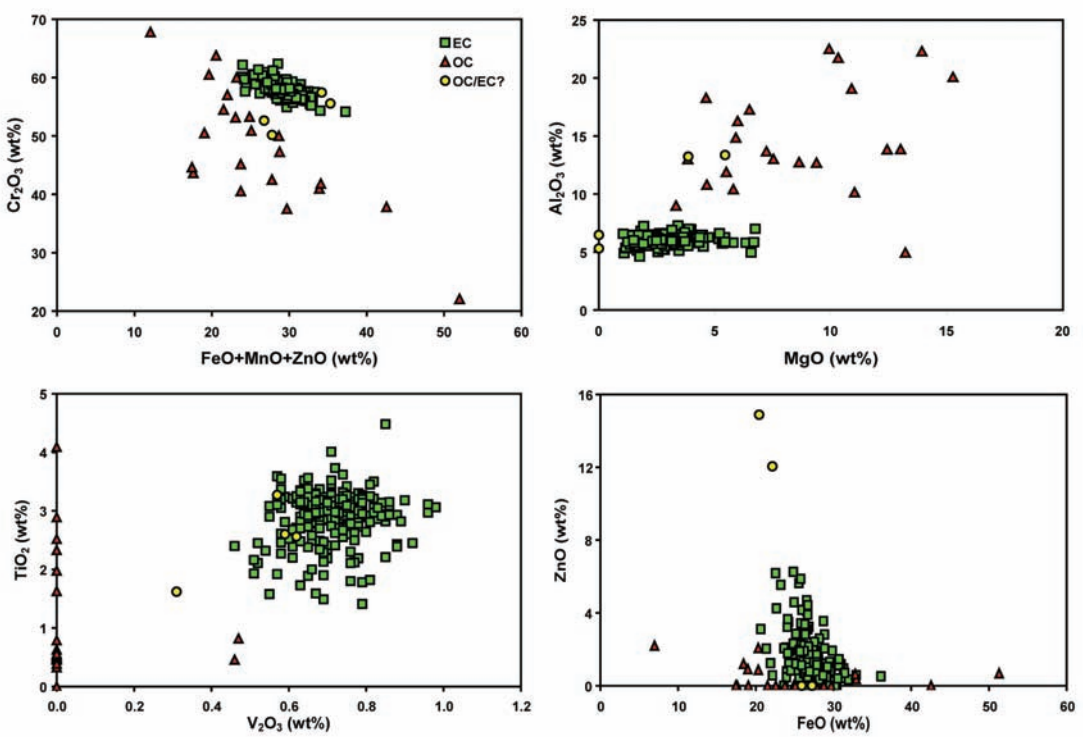

Fig. 5. The chemical composition of individual sediment-dispersed EC and OC grains in the Puxi River section. The definition of an EC grain is that it has a composition within the narrowly defined ranges for all elements analyzed. There may be overlaps between EC and OC grains for single elements, but not for the full range of elements. Four OC grains with a composition indicating they are diagenetically altered or anomalous EC grains are marked with yellow circles, see further main text.

Fig. 6. Comparison of the average composition with one sigma standard deviation of EC grains from this study and previous studies in southern Sweden, as well as chromite grains from recently fallen H and L chondrites, see further Table 3.

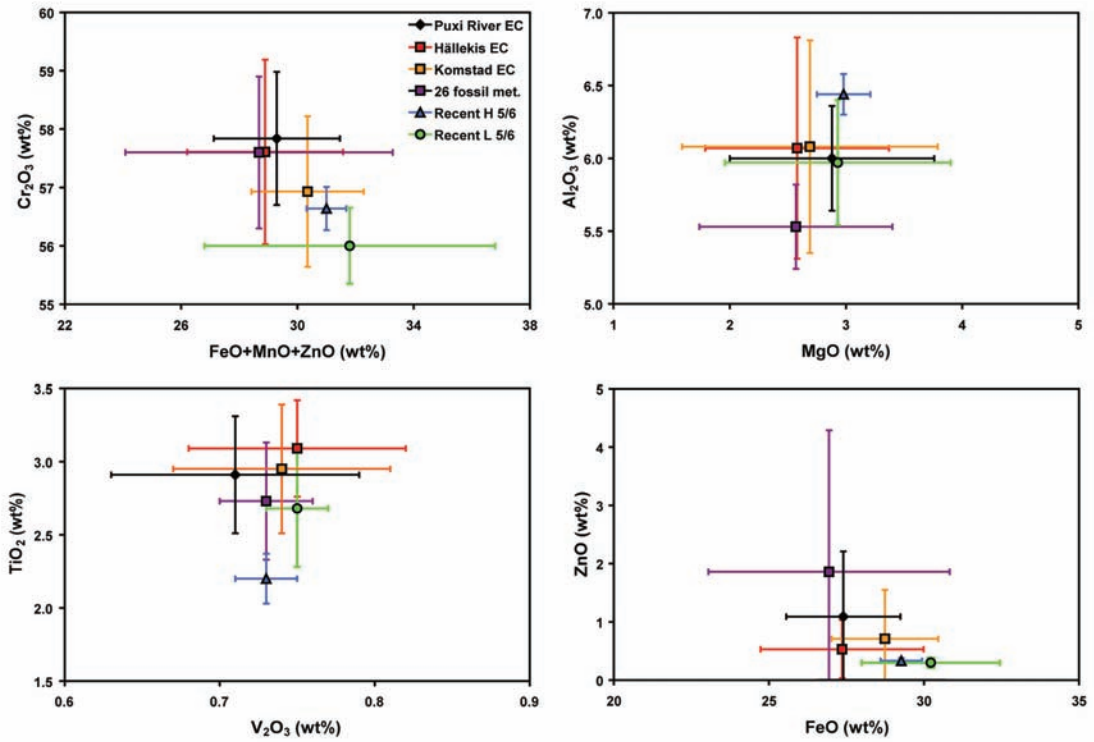

1). Of the remaining three angular OC grains one grain in sample +16.4 m shows Cr_2O_3 as high as 67.8 wt%, which is typical for chromite from iron meteorites. The grain is very similar in overall composition to chromite from the Mundrabilla iron meteorite (western Australia, IIICD group; El Goresy, 1976). Disregarding the five OC grains that based on chemical composition most likely are extraterrestrial, gives a revised number of 81 % of the remaining OC grains being subrounded to very rounded.

The average size, measured in the SEM, of all the chrome spinel grains is 102 x 73 μm (Appendix Table 2). There is no significant difference in size between EC and OC grains. The largest EC grain found measured 200 x 190 μm.

5. Discussion

For the first time we show that the main trend in the distribution of L-chondritic chromite grains across mid-Ordovician condensed sediment sequences can be reproduced at sites from different paleocontinents. Previously it has been shown that at two sites 350 km apart in southern Sweden the EC content increases from only 1-2 grains per 100 kg of rock to 1-6 grains per kg, i.e. a two orders-of-magnitude increase, starting in the *L. variabilis* conodont zone and continuing through at least the two overlying conodont zones, *Y. crassus* and *M. hagetiana* (Schmitz and Häggström, 2006; Häggström and Schmitz, 2007). The same general pattern can be seen in the Puxi River section, with 110 kg of rock spanning the lower 8 m of the section yielding only one EC grain, whereas 290 EC grains were found in the 178 kg of rock representing the upper part of the section (Fig. 4). Just as in Sweden the first common EC grains occur in the middle or upper part of the *L. variabilis* zone and high concentrations prevail upwards through the same biostratigraphic interval as in Sweden. There is nothing in the lithology or biostratigraphy that indicates that the upper EC-rich intervals, both in China and in Sweden, could have formed at substantially lower rates and that this could explain the EC distribution. For example, if the upper EC-rich interval at Puxi River had formed at a sedimentation rate about a hundred times lower than the underlying EC-poor interval (which would be required to account for the EC increase), this would have been apparent by many more and much more condensed biostratigraphic zones in the upper than the lower interval, which is not seen (Fig. 4). The abundance of conodont elements in a sediment may give an indication about sedimentation rate. Detailed such data exist for the nearby, very similar Fenxiang section (Zhang, 1996). These data show no major difference in conodont element abundances betweeen the corresponding lower EC-poor and upper EC-rich parts of the section. The only clear trend is that the limestone intervals both in the lower and upper part of the Fenxiang section are somewhat richer in conodont elements than the middle more marly interval, which could mean that the limestone intervals are more condensed. Alternatively, this could reflect that fewer of the conodont elements were preserved when calcite concentrations were lower at the sea floor.

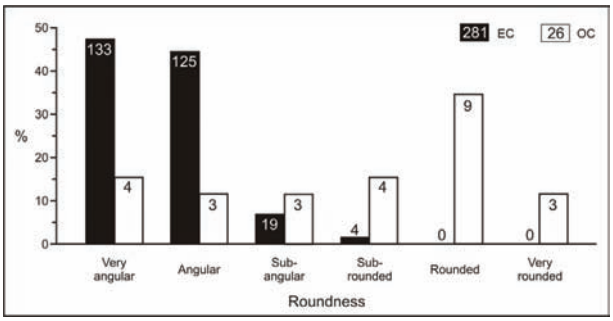

Fig. 7. Results of roundness analyses of chrome spinel grains recovered from the Puxi River section (of in total 291 EC grains recovered 10 were polished before the roundness analyses were performed).

Although the general trend in EC distribution can be reproduced between China and Sweden, there are also some differences. The Swedish sections show highest concentrations of EC grains, 3-6 grains per kg, in the lower part of the EC-rich interval, whereas in the Chinese section concentrations appear to generally increase slightly upwards in the section, reaching a maximum of 4 grains per kg at +15 m. However at all three sites studied there is substantial bed-by-bed variations in the EC content in the EC-rich interval, reflecting small variations in sedimentation rate rather than variations in the flux of extraterrestrial matter. From strict lithological considerations the limestones in the lower and upper part of the Guniutan Formation probably represent the most condensed interval, indicated for example by the occurrence of abundant hard (or firm) ground surfaces. It is likely that the more marly middle interval of the section formed at slightly higher rates, which is also consistent with the conodont element abundances. In the uppermost two meters of the section a marly bed at +15.2 m gave only 0.59 EC grains per kg, compared with concentrations of 2.3-4.1 EC grains per kg in the immediately surrounding limestones (Fig. 3). The marly bed probably formed significantly faster, perhaps because of admixture of occasional storm-transported material.

Another difference is that the EC grains in Sweden in some beds occur together with common terrestrial chrome spinel grains, whereas in China terrestrial grains are very rare, except in a single sample. Schmitz and Häggström (2006) noted that the co-occurrence of EC

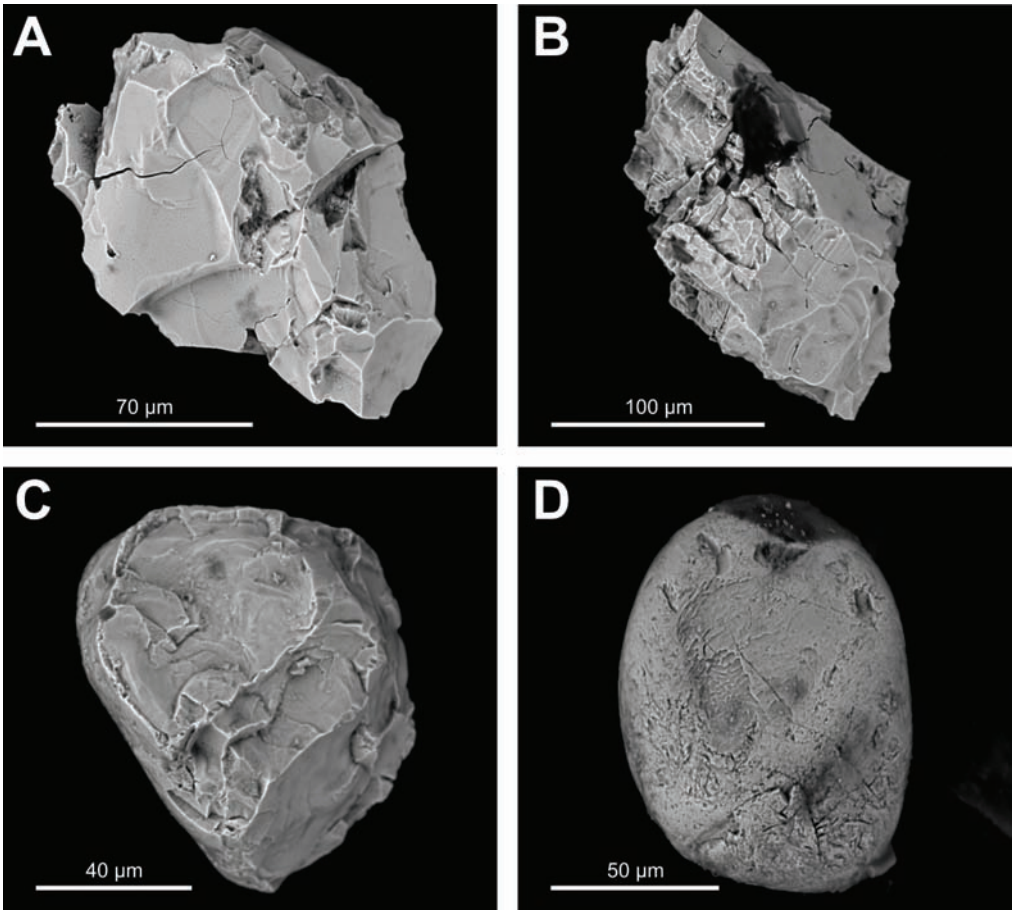

Fig. 8. Examples of roundness of chrome spinel grains recovered from the Puxi River section. A) Very angular EC grain. B) Very angular OC grain. C. Subangular OC grain. D) Rounded to very rounded OC grain.

grains with terrestrial grains in the sections at Kinnekulle may indicate that heavy spinel grains became enriched on the sea-floor because of hydrodynamic sorting, however, the Chinese results show that only the EC-abundance trend can be reproduced worldwide, and that the OC distribution at Kinnekulle is a strictly regional or local feature.

The most simple (Occam's razor) explanation to our results is that the increase in EC grains beginning in the *L. variabilis* Zone reflects the time for the disruption of the L-chondrite parent body, when dust from this event became very abundant in the solar system. The high concentrations of EC grains and common fossil meteorites in the sediments that formed during the succeeding few million years indicate that the flux of L-chondritic matter was enhanced by two orders-of-magnitude for this time interval. In sediments that formed about three to five million years after the time for the *L. variabilis* zone there is a tailing off in the EC content, but the flux was probably still enhanced by one order-of-magnitude (Alwmark and Schmitz, 2009a). Still today, L-chondritic matter from the breakup event represents a major fraction of the extraterrestrial matter reaching Earth, as shown by low K-Ar gas retention ages of recently fallen L chondrites (Heymann, 1967; Korochantseva et al., 2007). Together with a plethora of other data from fossil meteorites and mid-Ordovician EC grains (see references in Introduction), the Puxi River results provide a robust case for that the L-chondrite parent body breakup left a prominent coeval signature in the Earth's geological record. A challenge in the future is to find the ejecta beds from the many larger L-chondritic impactors that also must have struck Earth at this time, according to models for major breakup events (Zappalà et al., 1998). Schmitz et al. (2008) show that the mid-Ordovician increase in EC grains in the Baltic region correlates with a major burst in biodiversity among brachiopods, possibly related to the environmental effects of an asteroid shower. Parnell (2009) pointed out that the mid-Ordovician interval rich in fossil meteorites and EC grains is also characterized by a higher than normal frequency of mega-breccia deposits, that may be related to earthquakes triggered by impacting L-chondritic asteroids. One of the breccias listed by Parnell (2009), the Osmussaar breccia in Estonia, was recently shown by Al-

wmark et al. (personal communication, 2009) to contain abundant L-chondritic chromite from an impactor, just like the resurge deposits of the 458 Myr old Lockne crater in central Sweden (Alwmark and Schmitz, 2007; Schmitz et al., 2009b). Systematic searches for impact ejecta beds in mid-Ordovician strata may reveal to what extent also the flux of asteroid-sized L-chondritic objects was enhanced at this time. There is some indication for that impact craters are more abundant for the Middle and Late Ordovician (~470-440 Ma) (Schmitz et al., 2001; Korochantseva et al., 2007; http://www.unb.ca/passc/ImpactDatabase/). For instance the following craters are dated to this period: Granby, Hummeln, Tvären and Lockne (Sweden), Kärdla (Estonia), Pilot and Slate Islands (Canada), and Calvin (USA). The impactor types for these craters are presently undetermined, with the exception of the Lockne Crater, caused by an L-chondritic impactor (Alwmark and Schmitz, 2007; Schmitz et al., 2009b). Furthermore, many Late Cambrian to Early Ordovician craters retain poor age constrains, and it is possible that some of these may have formed after the L-chondritic breakup

6. Conclusions

For three localities, two of them 350 km apart on the Baltica paleoplate, and one on the South China paleoplate, a few thousand kilometers from Baltica, the distribution of extraterrestrial chromite grains with L-chondritic composition shows the same trend through mid-Ordovician strata. From the three localities altogether 1150 kg of mid-Ordovician limestone has been dissolved and searched for chrome spinel grains in our group. Of this limestone 614 kg comes from the stratigraphic interval represented by the older *P. originalis* and *L. antivariabilis* conodont zones, and has only yielded 8 EC grains altogether. The 536 kg of limestone from the successively overlying *L. variabilis*, *Y. crassus* and *L. pseudoplanus* zones, on the other hand, has yielded altogether 954 EC grains. Concentrations of EC grains in the upper EC-rich interval lie typically at 1-4 grains per kg at all sites. The magnitude of the enrichment compared to background can not possibly be explained by changes in sedimentation rate. Only a prominent increase in the flux of L-chondritic matter can explain the results. The abundance also of larger fossil meteorites of L-chondritic composition in the interval rich in EC grains provides independent evidence for this. The coincidence in time of these features with the gas retention age, ~470 Ma, of recently fallen L chondrites indicates that the breakup of the L-chondrite parent body, the largest documented breakup event in the asteroid belt, left a prominent signal in coeval sediments on Earth.

Acknowledgments

The field expeditions in 2005 and 2007 to the Yichang area, Hubei, would not have been possible without the guidance and logistic support of Wang Xiaofeng. We thank Stig Bergström, Maurits Lindström and Anita Löfgren for valuable advice in the initiation stage of the project. The fieldtrips were sponsored by the National Geographic Society and the Swedish Research Council.

References

Alwmark, C., Schmitz, B. 2007. Extraterrestrial chromite in the resurge deposits of the early Late Ordovician Lockne crater, central Sweden. Earth Planet. Sci. Lett. 253, 291–303.

Alwmark, C., Schmitz, B. 2009a.The origin of the Brunflo fossil meteorite and extraterrestrial chromite in mid-Ordovician limestone from the Gärde quarry (Jämtland, central Sweden). Meteorit. Planet. Sci. 44, 95-106.

Alwmark, C., Schmitz, B. 2009b. Relict silicate inclusions in extraterrestrial chromite and their use in the classification of fossil chondritic material. Geochim. Cosmochim. Acta 73, 1472-1486.

Anders, E. 1964. Origin, age and composition of meteorites. Space Sci. Rev. 3, 583-714.

Bagnoli, G., Stouge, S. 1996 (1997). Lower Ordovician (Billingenian-Kunda) conodont zonation and provinces based on sections from Horns Udde, north Oland, Sweden. Bol. Soc. Paleontol. Ital. 35, 109-163.

Bergström, S. M., Wang, Z-H. 1998. Biostratigraphic significance of the Ordovician conodont *Eoplacognathus crassus* Chen & Zhang, 1993. GFF 120, 91-93.

Bogard, D. D. 1995. Impact ages of meteorites – A synthesis. Meteoritics 30, 244-268.

Bridges, J. C., Schmitz, B., Hutchison, R., Greenwood, R. C., Tassinari, M., Franchi, I. A. 2007. Petrographic classification of Middle Ordovician fossil meteorites from Sweden. Meteorit. Planet. Sci. 42, 1781-1789.

Bunch, T. E., Keil, K., Snetsinger, K. G. 1967. Chromite composition in relation to chemistry and texture of ordinary chondrites. Geochim. Cosmochim. Acta 31, 1569-1582.

Chen, J., Jahn, B.-M. 1998. Crustal evolution of southeastern China: Nd and Sr isotopic evidence. Tectonophysics 284, 101-133.

Chen, X., Rong, J., Zhou, Z., Zhang, Y., Zhan, R., Liu, J., Fan, J. 2001. The central Guizhou and Yichang uplifts, Upper Yangtze region, between Ordovician and Silurian. Chinese Sci. Bull. 46, 1580-1584.

Cocks, R. L., Torsvik, T. H. 2002. Earth geography from 500 to 400 million years ago: a faunal and palaeomagnetic review. J. Geol. Soc. London 159, 631-644.

Cocks, R. L, Torsvik T. H. 2005. Baltica from the late Precambrian to mid-Palaeozoic times: The gain and loss of a terrane's identity. Earth-Sci. Rev. 72, 39–66.

Cocks, R. L., Torsvik T. H. 2007. Siberia, the wandering northern terrane, and its changing geography through the Palaeozoic. Earth-Sci. Rev. 82, 29–74.

Cooper, R. A., Sadler, P. M. 2004. The Ordovician period. In: Gradstein, F.M., Ogg, J. G., Smith, A. G. (EDs), A Geological Time Scale 2004. Cambridge University Press, 2004, pp. 165-187.

Cronholm, A., Schmitz, B. 2007. Extraterrestrial chromite in latest Maastrichtian and Paleocene pelagic limestone at Gubbio, Italy: The flux of unmelted ordinary chondrites. Meteorit. Planet. Sci. 42, 2099–2109.

El Goresy, A. 1976. Opaque oxide minerals in meteorites. In: Rumble III, D. (Ed.) Reviews in Mineralogy, Vol. 3, Oxide Minerals, Mineralogical Society of America, Washington, DC, pp. EF47-EG72.

Fortey, R. A., Cocks, L. R. M. 2003. Palaeontological evidence bearing on global Ordovician–Silurian continental reconstructions. Earth-Sci. Rev. 61, 245–307.

Grady, M. M. 2000. Catalogue of Meteorites, 5th ed, Cambridge Univ. Press, New York.

Greenwood, R. C., Schmitz, B., Bridges, J., Hutchison, R., Franchi, I. A. 2007. Disruption of the L chondrite parent body. New oxygen isotope evidence from Ordovician relict chromite grains. Earth Planet. Sci. Lett. 262, 204–213.

Grossman, J. N., Rubin, A. E., Sears, D. W. G. 2009. The mineral composition and classification of high type-3 and type-4 ordinary chondrites. Lunar Planet. Sci. XL, 1679 (abstract).

Häggström, T., Schmitz, B. 2007. Distribution of extraterrestrial chromite in Middle Ordovician Komstad limestone in the Killeröd quarry, Scania, Sweden. Bull. Geol. Soc. Den. 55, 37–58.

Heck, P. R., Schmitz, B., Baur, H., Halliday, A. N., Wieler, R. 2004. Fast delivery of meteorites to Earth after a major asteroid collision. Nature 430, 323–325.

Heck, P. R., Schmitz, B., Baur, H., Wieler, R. 2008. Noble gases in fossil micrometeorites and meteorites from 470 Myr old sediments from southern Sweden, and new evidence for the L-chondrite parent body breakup event. Meteorit. Planet. Sci. 43, 517-528.

Heck, P. R., Ushikubo, T., Schmitz, B., Kita, N. T., Spicuzza, M. J., Valley, J. W. 2009. High-precision oxygen three-isotope sims analyses of Ordovician extraterrestrial chromite grains from Sweden and China: debris of the L chondrite parent asteroid breakup. Lunar Planet. Sci. XL, 1119 (abstract).

Heymann, D. 1967. On the origin of hypersthene chondrites: Ages and shock effects of black chondrites. Icarus 6, 189-221.

Jarosewich, E., Nelen, J. A., Norberg, J. A. 1980. Reference samples for electron microprobe analysis. Geostand. Newslett. 4, 43–47.

Keil, K. 1962. On the phase composition of meteorites. J. Geophys. Res. 67, 4055–4061.

Keil, K., Haack, H., Scott, E. R. D. 1994. Catastropic fragmentation of asteroids – Evidence from meteorites. Planet. Space Sci. 42, 1109-1122.

Korochantseva, E. V., Trieloff, M., Lotenz, C. A., Buykin, A. I., Ivanova, M. A., Schwarz, W.H., Hopp, J., Jessberger, E. K. 2007. L-chondrite asteroid breakup tied to Ordovician meteorite shower by multiple isochron ^{40}Ar-^{39}Ar dating. Meteorit. Planet. Sci. 42, 113-130.

Lindström, M., Chen, J.- Y., Zhang J.- M. 1991. Section at Daping reveals Sino-Baltoscandian parallelism of facies in the Ordovician. GFF 113, 189-205.

Löfgren, A., Zhang J. 2003. Element association and morphology in some middle Ordovician platform-equipped conodonts. J. Paleontol. 77, 721-737.

Nyström, J. O., Lindström, M., Wickman, F. E. 1988. Discovery of a second Ordovician meteorite using chromite as a tracer. Nature 336, 572-574.

Parnell, J. 2009. Global mass wasting at continental margins during Ordovician high meteorite influx. Nature Geocience 2, 57-61.

Pettijohn, F. J. 1957. Sedimentary Rocks, 2nd ed, New York, Harper. 718 pp.

Peucker-Ehrenbrink, B., Ravizza, G. 2000. The effects of sampling artifacts on cosmic dust flux estimates: A reevaluation of nonvolatile tracers (Os, Ir). Geochim. Cosmochim. Acta 64, 1965–1970.

Schmitz, B., Häggström, T. 2006. Extraterrestrial chromite in Middle Ordovician marine limestone at Kinnekulle, southern Sweden – Traces of a major asteroid breakup event. Meteorit. Planet. Sci. 41, 455-466.

Schmitz, B., Tassinari, M., Peucker-Ehrenbrink, B. 2001. A rain of ordinary chondritic meteorites in the early Ordovician. Earth Planet. Sci. Lett. 194, 1–15.

Schmitz, B., Häggström, T., Tassinari, M. 2003. Sediment-dispersed extraterrestrial chromite traces a major asteroid disruption event. Science 300, 961–964.

Schmitz, B., Harper, D. A., Peucker-Ehrenbrink, B., Stouge, S., Alwmark, C., Cronholm, A., Bergström, S. M., Tass-

inari, M., Wang, X. 2008. Asteroid breakup linked to the Great Ordovician Biodiversification Event. Nature Geoscience 1, 49-53.

Schmitz, B., Cronholm, A., Montanari, A. 2009a. A search for extraterrestrial chromite in the late Eocene Massignano section, central Italy. Geol. Soc. Am. Sp. 452, 71-82.

Schmitz, B., Heck, P. R., Alwmark, C., Kita, N. T., Peucker-Ehrenbrink, B., Ushikubo, T., Valley, J. W. 2009b. Determining the impactor of the Ordovician Lockne crater : oxygen isotopes in chromite versus sedimentary PGE signatures. Lunar Planet. Sci. XL, 1161 (abstract).

Stouge, S., Bagnoli G. 1990. Lower Ordovician (Volkovian-Kundan) conodonts from Hagudden, northern Oland, Sweden. Palaeontographia Ital. 77, 1-54.

Thorslund, P., Wickman, F. E., Nyström, J. O. 1984. The Ordovician chondrite from Brunflo, central Sweden. 1. General description and primary minerals. Lithos 17, 87-100.

Wlotzka, F. 2005. Cr spinel and chromite as petrogenetic indicators in ordinary chondrites: equilibration temperatures of petrologic types 3.7 to 6. Meteorit. Planet. Sci. 40, 1673-1702.

Zappalà, V., Cellino, A., Gladman, B. J., Manely, S., Migliorini, F. 1998. Asteroid showers on Earth after family breakup events. Icarus 134, 176-179.

Zhan, R., Jin, J., Chen, P. 2007. Brachiopod diversification during the Early-Mid Ordovician: an example from the Dawan Formation, Yichang area, central China. Can. J. Earth Sci. 44, 9-24.

Zhang, J. 1996. Lithofacies and stratigraphy of the Ordovician Guniutan Formation in its type area, China. Geol. J. 31, 201-215.

Zhang, J. 1998a. Conodonts from the Guniutan Formation (Llanvirnian) in Hubei and Hunan provinces, south-central China. Thesis, University of Stockholm, Stockholm, Sweden, Stockholm Contributions in Geology 46, 1-161.

Zhang, J. 1998b. Middle Ordovician conodonts from the Atlantic Faunal Region and the evolution of key conodont genera. Thesis, Meddelanden från Stockholms Universitets Institution för Geologi och Geokemi 298, 1-27.

Zhou, D., RU, K., Chen, H.-Z. 1995. Kinematics of Cenozoic extension on the South China Sea continental margin and its implications for the tectonic evolution of the region. Tectonophysics 251, 161-177.

SUPPLEMENTARY INFORMATION

Extraterrestrial chromite ditribution across the Puxi River section, central China: Evidence for a global major spike in flux of L-chondritic matter during the mid-Ordovician

Appendix Table 1. Element concentration (wt%) in sediment-dispersed extraterrestrial chromite (EC) and other Cr-rich spinels (OC) (>63 μm) extracted from the Puxi River section, China.

Level[1]/Sample	Cr_2O_3	Al_2O_3	MgO	TiO_2	V_2O_3	FeO	MnO	ZnO	Total[2]
EC grains									
+16.4 m/P2	58.48	5.84	3.65	3.24	0.59	26.59	0.78	1.02	100.19
	57.53	5.78	1.97	1.49	0.69	31.30	1.01	0.95	100.72
	59.87	6.51	2.56	1.80	0.76	24.90	1.23	1.29	98.93
	56.95	5.87	3.15	3.04	0.68	28.30	0.93	0.50	99.43
	58.69	6.02	2.88	3.23	0.76	28.73	0.79	0.46	101.56
	57.08	6.50	2.40	2.73	0.78	28.05	0.81	1.89	100.24
	58.69	5.84	2.61	3.18	0.69	28.19	0.85	n.d.[3]	100.05
	57.93	6.01	2.63	2.92	0.71	27.83	0.80	0.49	99.32
	60.01	6.14	2.81	3.18	0.71	25.04	0.68	1.26	99.81
	60.55	6.97	3.97	2.23	0.70	20.63	1.53	3.11	99.71
	57.58	6.00	3.12	3.00	0.75	27.99	0.85	0.75	100.04
	57.25	5.89	3.10	2.91	0.73	28.59	0.96	0.52	99.95
	58.34	5.93	2.62	2.74	0.75	28.18	0.53	1.24	100.33
	55.40	5.77	3.56	4.01	0.71	28.83	0.45	0.37	99.08
	56.47	5.70	2.42	3.31	0.68	29.32	0.78	0.32	98.99
	57.78	6.27	4.20	2.34	0.70	25.66	0.90	0.57	98.43
	57.42	5.58	2.16	2.88	0.70	28.82	0.66	0.38	98.60
	56.70	6.40	3.47	2.89	0.67	27.22	0.81	0.98	99.13
	56.71	5.58	3.37	3.20	0.65	28.07	0.74	0.52	98.84
	56.76	6.34	2.42	2.67	0.77	26.80	0.96	1.89	98.61
	57.28	5.19	2.82	3.24	0.76	27.57	1.05	0.90	98.79
	58.31	5.11	3.45	2.93	0.88	25.02	1.18	1.56	98.43
	57.88	5.78	2.43	2.94	0.66	28.82	0.93	1.01	100.45
	57.03	6.22	2.79	3.09	0.67	27.87	0.82	0.33	98.82
	56.22	6.49	2.56	2.41	0.70	28.50	0.92	1.00	98.81
	57.59	5.91	2.42	3.01	0.70	27.21	0.78	0.61	98.24
	57.68	6.19	2.63	3.02	0.66	25.72	0.94	1.31	98.15
	56.86	5.66	2.67	3.24	0.67	29.19	0.90	0.69	99.88
	56.13	5.87	2.23	3.46	0.71	30.43	0.79	n.d.	99.61
	56.28	6.13	2.87	3.21	0.66	28.45	0.84	0.42	98.86
	57.54	5.82	2.7	3.11	0.72	26.95	0.69	0.36	97.89
	55.50	5.71	1.28	3.16	0.65	28.70	0.43	3.55	98.98
	59.12	6.03	2.69	3.08	0.55	27.19	0.76	0.63	100.05
	57.66	6.30	1.87	1.78	0.79	26.83	0.87	3.24	99.33
	54.93	7.01	3.88	2.61	0.58	27.35	0.82	1.51	98.69
	57.83	5.99	2.41	2.90	0.82	28.60	1.00	0.39	99.93
	57.92	6.35	2.99	2.82	0.85	28.35	1.00	0.55	100.84
	58.95	6.19	2.77	3.21	0.82	27.36	0.85	n.d.	100.15
	57.77	6.03	2.82	2.86	0.66	30.26	n.d.	n.d.	100.39
	58.31	5.88	2.56	3.16	0.77	28.46	0.75	n.d.	99.90
	58.34	5.81	5.78	3.19	0.62	25.69	0.55	n.d.	99.97
	58.00	5.77	2.25	3.10	0.75	29.11	0.69	n.d.	99.68
+15.8 m/Y10	57.62	5.99	3.00	2.99	0.70	28.65	0.87	n.d.	99.82
	58.20	6.27	5.42	3.14	0.62	25.66	0.69	0.47	100.48
	56.63	5.81	3.04	3.05	0.58	28.77	0.71	0.40	98.99

	58.22	6.04	4.01	3.73	0.72	25.56	0.86	0.62	99.75
	57.62	5.79	3.05	3.37	0.58	27.53	0.90	n.d.	98.84
	56.11	6.35	3.46	2.78	0.66	27.49	1.20	0.71	98.75
	57.82	6.12	3.25	3.20	0.58	28.48	0.93	n.d.	100.38
	58.98	6.24	2.37	3.03	0.65	25.81	0.63	0.87	98.57
	58.96	6.19	2.45	3.21	0.68	26.94	0.61	1.06	100.10
	57.65	6.24	2.98	2.84	0.77	28.50	0.74	0.50	100.22
	57.99	6.27	2.18	2.81	0.81	26.80	0.70	1.51	99.07
	56.42	5.58	1.76	2.71	0.62	31.10	0.74	0.41	99.34
	57.80	6.12	5.17	3.08	0.65	26.48	0.51	n.d.	99.80
	57.56	5.83	2.15	3.02	0.77	27.61	0.77	1.83	99.55
	59.51	5.75	2.53	3.50	0.82	27.74	n.d.	n.d.	99.84
	58.22	5.74	3.76	3.59	0.57	27.43	0.77	n.d.	100.06
	58.66	5.65	2.36	3.18	0.79	27.11	0.77	n.d.	98.53
	59.72	6.15	3.20	3.09	0.72	23.89	1.11	2.10	99.97
	56.41	5.86	1.26	3.04	0.70	28.84	0.54	2.81	99.46
	60.04	4.96	6.56	2.78	0.78	23.97	n.d.	0.79	99.89
	57.28	6.27	2.61	2.90	0.69	27.89	0.70	0.58	98.92
	57.17	5.81	3.37	2.94	0.68	28.07	0.82	0.52	99.39
	57.41	5.47	4.50	4.48	0.85	26.73	0.62	0.40	100.46
	57.30	6.31	3.08	2.49	0.66	28.46	0.88	0.91	100.09
	58.14	6.05	2.90	2.45	0.92	28.01	0.94	0.48	99.90
	58.53	5.98	1.40	2.89	0.66	23.22	0.44	5.54	98.66
	58.81	6.39	2.86	3.55	0.58	27.02	0.60	0.35	100.16
	58.59	6.06	2.55	3.16	0.76	26.74	0.76	0.31	98.94
	57.55	5.76	3.53	3.06	0.64	27.54	0.97	0.47	99.52
	57.04	5.86	3.85	2.87	0.76	26.67	1.13	0.46	98.64
	57.50	6.02	2.75	2.99	0.75	27.19	0.55	0.76	98.51
	55.99	5.12	1.65	2.68	0.61	31.92	0.53	0.34	98.84
+15.2 m/P3	58.64	6.50	2.34	2.63	0.72	25.80	0.75	3.43	100.82
	57.30	5.90	2.93	3.24	0.69	28.61	0.81	0.62	100.09
	55.98	6.47	1.55	2.38	0.65	29.84	0.49	1.92	99.29
	56.92	5.89	2.51	3.12	0.75	29.12	0.73	n.d.	99.04
	57.49	5.73	2.85	3.18	0.70	29.04	0.92	0.44	100.36
+15.0 m/P4	57.09	5.72	2.86	3.00	0.64	29.41	0.83	0.49	100.04
	57.46	5.95	2.93	3.15	0.75	27.77	0.94	1.05	100.01
	57.04	5.77	2.56	3.04	0.69	28.60	0.57	0.65	98.93
	56.59	5.88	2.74	3.11	0.76	29.66	0.89	0.33	99.96
	57.63	5.66	3.13	3.14	0.69	28.93	0.73	0.41	100.33
	58.02	5.73	5.32	3.13	0.68	25.74	0.64	0.52	99.79
	58.09	6.07	3.32	2.88	0.78	22.66	1.08	4.25	99.13
	56.72	5.75	2.77	3.14	0.68	28.80	0.76	0.61	99.22
	57.53	6.08	3.23	3.15	0.57	27.43	0.85	1.28	100.13
	56.62	5.83	3.19	2.82	0.76	28.15	0.98	0.74	99.09
	56.66	5.96	3.63	2.84	0.70	25.76	1.07	2.27	98.88
	57.46	5.75	2.71	2.86	0.70	29.39	0.63	0.55	100.06
	56.28	6.07	2.20	2.85	0.74	27.14	0.81	1.92	98.02
	57.18	5.73	2.20	3.09	0.78	29.70	0.78	0.77	100.23
	58.36	5.94	2.90	3.08	0.71	27.76	0.94	0.62	100.30
	56.97	5.90	2.86	2.87	0.73	29.14	1.04	0.83	100.33
	57.58	6.23	2.54	2.80	0.66	28.77	0.94	0.80	100.32
	59.28	6.58	3.36	2.30	0.76	26.51	0.75	0.46	100.00
	57.39	6.10	2.81	2.99	0.69	27.43	1.32	1.32	100.06
	58.10	6.05	3.34	2.95	0.66	28.15	0.86	0.58	100.69
	57.66	6.07	2.84	3.20	0.63	27.57	0.73	0.85	99.54
	57.39	5.54	2.64	3.26	0.67	27.91	0.72	0.39	98.51
	57.47	5.98	2.91	3.08	0.68	28.78	0.80	0.50	100.19
	58.29	6.12	3.63	3.17	0.73	24.35	1.22	1.91	99.41

	56.91	5.76	2.93	3.37	0.68	28.41	0.94	0.86	99.86
	57.22	6.11	3.00	3.10	0.79	24.14	0.99	3.50	98.85
	56.83	6.03	3.33	2.86	0.70	28.56	0.78	0.59	99.67
	58.24	5.99	2.84	3.07	0.67	28.23	0.93	0.73	100.70
	58.53	5.99	2.64	3.30	0.78	28.55	1.01	n.d.	100.80
	57.58	6.24	2.51	2.98	0.69	28.79	0.78	0.72	100.31
	57.37	6.00	3.16	2.86	0.72	28.97	0.88	0.43	100.39
	57.98	5.89	2.16	2.95	0.75	28.71	0.78	0.36	99.58
	58.47	5.85	2.90	3.03	0.67	28.40	0.88	0.58	100.80
	58.91	6.23	3.43	2.97	0.78	26.47	0.94	1.25	100.97
	57.47	5.82	2.80	2.82	0.89	28.92	0.79	0.72	100.23
	58.29	6.02	2.96	2.99	0.64	26.70	0.61	1.54	99.75
	57.02	5.59	2.09	2.60	0.75	30.34	0.64	1.11	100.13
	58.22	5.86	3.07	2.75	0.64	26.22	1.06	1.72	99.55
	56.83	5.69	3.26	3.13	0.73	29.46	0.77	n.d.	99.86
	57.94	6.21	2.44	2.90	0.66	25.15	1.05	2.85	99.20
	58.36	5.56	2.71	1.89	0.65	27.71	0.99	1.16	99.05
	56.15	5.65	2.08	1.58	0.55	30.98	0.86	1.18	99.03
	54.15	4.90	1.09	2.32	0.54	36.11	0.64	0.52	100.27
	60.06	6.21	1.86	3.32	0.74	26.70	0.59	0.53	100.01
	59.32	6.02	2.98	2.86	0.83	27.16	0.82	1.15	101.15
	58.71	5.56	3.10	3.26	0.75	28.88	0.80	0.45	101.52
	58.02	5.84	3.10	2.89	0.80	28.39	0.92	0.64	100.58
	59.07	5.90	2.53	3.21	0.61	27.89	0.61	0.53	100.35
	58.80	6.28	2.95	2.64	0.80	24.90	0.96	2.31	99.63
	56.94	6.11	2.86	2.27	0.58	29.51	1.07	0.83	100.18
	58.34	5.78	1.95	2.89	0.75	24.93	0.52	4.59	99.75
	58.83	5.31	1.18	2.98	0.68	28.17	0.71	2.59	100.46
	59.13	6.44	1.42	2.93	0.76	29.01	0.62	n.d.	100.30
	57.64	5.39	1.60	2.58	0.66	30.46	0.81	1.18	100.33
+14.8 m/Y9	60.09	7.01	6.74	2.19	0.78	22.15	1.23	0.57	100.75
	58.65	5.79	3.91	3.10	0.64	26.79	0.80	0.99	100.67
	57.51	6.03	2.90	2.62	0.77	27.48	0.80	1.08	99.19
	57.08	5.94	3.70	3.10	0.66	27.61	0.92	0.52	99.52
	58.03	6.05	3.18	3.12	0.74	27.25	0.79	n.d.	99.17
	57.73	6.27	4.72	3.11	0.63	25.97	0.77	0.67	99.87
	57.36	6.30	2.86	2.99	0.68	27.48	0.70	0.61	98.99
	57.20	5.92	2.58	2.97	0.73	28.55	0.91	0.48	99.32
	57.84	5.77	3.28	3.04	0.64	27.57	0.83	0.47	99.44
	58.63	6.51	2.88	1.73	0.63	24.22	0.96	3.49	99.06
	58.54	5.80	6.34	2.90	0.63	23.95	n.d.	0.46	98.63
	58.00	6.11	2.53	2.99	0.64	27.45	0.96	n.d.	98.67
	57.93	6.48	4.46	2.66	0.74	25.74	1.13	0.78	99.92
	56.89	6.55	2.59	2.45	0.52	29.19	n.d.	1.07	99.26
	57.77	6.11	3.27	3.24	0.65	26.96	0.77	0.47	99.24
	58.51	6.64	2.86	3.00	0.79	25.69	1.08	0.71	99.28
	58.82	6.14	2.44	3.02	0.69	27.41	0.67	0.69	99.88
	57.57	5.81	3.42	2.99	0.64	26.56	0.85	0.67	98.51
	57.65	6.01	3.37	2.91	0.80	27.78	0.89	0.60	100.01
	57.40	5.77	4.12	3.30	0.67	27.25	0.87	n.d.	99.38
	56.80	5.88	2.55	3.06	0.82	24.83	0.62	6.26	100.82
	57.70	6.25	3.67	2.92	0.74	24.83	1.22	2.31	99.64
	58.85	6.19	3.37	3.30	0.71	25.48	1.07	n.d.	98.97
	58.66	6.10	4.16	3.52	0.64	26.04	0.87	0.51	100.50
	57.55	6.17	2.87	3.27	0.79	27.48	0.84	0.49	99.45
	57.89	7.29	3.41	3.06	0.83	25.88	1.25	1.26	100.88
	58.57	6.16	4.24	3.25	0.81	25.14	0.92	0.84	99.94
	58.98	5.96	3.06	2.80	0.71	25.64	0.79	1.19	99.12
	58.89	6.61	5.20	2.90	0.85	25.63	n.d.	n.d.	100.08

	58.54	6.00	2.42	3.04	0.77	28.12	0.78	0.83	100.51
	57.99	6.13	2.87	3.24	0.79	26.97	0.62	0.38	99.00
	59.68	6.62	2.93	2.97	0.96	21.36	0.79	2.04	97.34
	57.60	6.30	3.46	2.21	0.85	28.10	0.94	1.34	100.79
	57.80	5.96	2.90	3.09	0.86	27.02	0.88	n.d.	98.51
	58.64	6.45	3.78	2.92	0.80	26.71	0.89	n.d.	100.18
	57.52	5.74	2.66	2.43	0.88	29.35	0.00	1.06	99.64
	56.89	5.84	2.73	3.45	0.81	28.65	0.94	n.d.	99.29
	56.73	5.89	2.37	3.06	0.98	28.62	0.42	1.21	99.29
	57.70	5.71	3.08	3.15	0.86	26.70	0.82	0.61	98.63
	58.56	6.35	2.44	3.11	0.96	25.57	0.81	1.97	99.76
	58.14	6.07	2.70	3.18	0.90	27.34	1.01	0.78	100.12
	56.83	5.93	3.45	2.97	0.82	27.64	0.68	0.54	98.86
	57.54	6.55	2.61	2.94	0.84	26.51	1.03	1.90	99.92
	58.62	5.84	3.25	3.25	0.62	27.59	0.68	0.55	100.41
	59.76	5.91	3.42	3.15	0.73	25.57	0.88	0.39	99.82
	56.57	5.73	2.46	3.05	0.69	28.84	0.73	n.d.	98.08
	58.35	5.94	2.71	3.1	0.74	27.19	0.9	0.81	99.74
	58.74	5.75	2.34	3.56	0.65	28.01	0.88	n.d.	99.93
+14.4 m/Y8.5	57.11	5.51	2.01	3.00	0.67	26.69	0.98	3.09	99.07
	59.70	5.51	2.67	1.41	0.79	24.07	1.89	3.24	99.28
	58.65	5.71	2.54	2.00	0.66	27.93	1.12	0.80	99.41
	58.23	5.53	2.16	2.88	0.65	27.61	1.21	1.25	99.52
	57.47	5.74	2.27	2.82	0.63	29.63	0.91	0.44	99.93
	56.97	5.90	2.35	2.37	0.68	28.03	1.12	1.14	98.56
	58.28	5.88	1.88	2.12	0.77	30.22	0.65	n.d.	99.81
	58.83	5.93	2.52	2.87	0.71	26.49	2.04	1.41	100.78
	56.78	6.61	2.62	2.98	0.74	27.59	1.41	1.38	100.12
+13.8 m/P5	56.42	6.00	1.85	2.39	0.61	28.84	0.78	2.05	98.94
	57.91	6.27	3.17	3.42	0.75	27.39	0.74	0.46	100.12
	57.33	5.60	2.52	2.90	0.55	27.39	0.81	2.11	99.20
	59.18	6.16	3.31	2.19	0.70	23.62	1.42	2.06	98.63
	58.04	6.33	2.58	1.90	0.69	29.36	0.99	0.70	100.59
	57.54	6.73	3.70	2.48	0.63	28.91	0.73	0.61	101.32
	56.94	5.69	2.92	3.16	0.70	28.46	0.99	0.44	99.31
	57.19	6.50	3.28	2.81	0.59	26.86	1.02	1.35	99.60
	58.09	6.52	3.32	2.11	0.76	27.37	1.24	1.37	100.77
	57.44	6.42	3.13	2.78	0.76	22.54	1.37	6.18	100.63
	57.24	5.83	2.37	2.49	0.68	29.55	0.80	0.80	99.77
	57.76	5.96	3.45	3.52	0.71	26.77	1.16	1.91	101.24
	57.93	5.97	2.07	3.35	0.63	28.37	0.77	0.62	99.71
	57.53	5.38	1.16	3.01	0.67	25.53	0.91	5.64	99.83
	58.20	5.91	2.74	3.10	0.57	28.78	0.80	0.83	100.93
	57.25	6.25	2.40	2.72	0.72	27.54	0.75	2.41	100.03
	56.90	6.07	2.16	2.81	0.81	30.67	0.62	1.13	101.18
	58.34	5.91	2.54	3.23	0.75	27.19	0.83	1.26	100.06
	57.36	6.03	1.71	3.14	0.74	26.54	0.85	4.12	100.49
	60.09	6.49	2.34	3.05	0.71	24.49	0.70	1.12	98.99
	60.07	6.12	2.30	2.70	0.68	25.80	0.89	1.41	99.97
	60.90	6.25	2.41	3.27	0.71	24.81	0.67	1.27	100.30
	62.36	4.61	1.76	2.58	0.66	25.76	0.84	1.93	100.49
+11.4 m/Y8	56.65	5.01	2.55	2.52	0.60	31.45	0.66	0.70	100.14
	57.74	6.53	2.91	2.29	0.69	29.19	0.84	0.49	100.68
	58.29	5.94	2.54	3.16	0.79	28.17	0.65	0.40	99.94
	57.27	6.15	2.43	2.95	0.64	28.36	0.85	0.41	99.05
	57.63	5.85	6.68	2.83	0.68	23.61	0.69	tr.[4]	97.97
	59.52	6.05	2.25	3.28	0.67	27.51	0.75	0.65	100.68

	58.23	5.87	3.16	3.04	0.70	28.34	1.14	0.55	101.04
	57.30	5.84	5.37	2.85	0.72	25.47	0.73	n.d.	98.28
	58.21	5.91	3.56	2.91	0.84	26.61	1.01	1.01	100.05
	56.47	5.92	2.56	3.04	0.69	27.06	0.87	1.66	98.27
+11.0/P5.5	58.82	6.27	2.45	3.11	0.67	28.10	0.37	0.89	100.67
	60.46	6.47	4.40	2.55	0.74	24.25	n.d.	1.22	100.10
	57.35	6.83	1.81	1.82	0.81	25.78	tr.	5.87	100.27
	60.38	6.21	4.49	2.39	0.88	24.10	0.66	1.78	100.65
	57.00	5.88	2.74	3.38	0.65	26.16	0.68	1.78	98.25
	59.03	5.20	2.75	2.50	0.77	26.83	0.31	2.09	99.49
	59.17	6.56	2.78	2.76	0.68	26.19	0.52	2.22	100.86
	56.39	6.51	2.19	3.00	0.70	25.94	n.d.	4.16	98.89
	58.93	6.91	3.15	1.59	0.67	26.62	1.01	1.47	100.35
	57.90	5.52	1.66	2.47	0.69	26.68	0.63	3.90	99.46
+10.9 m/P6a	56.04	5.95	2.18	2.74	0.71	26.55	0.79	4.69	99.65
	57.14	5.62	2.73	3.01	0.78	28.58	0.70	0.32	98.87
	55.68	6.10	3.04	2.11	0.52	28.40	1.03	1.03	97.89
	58.21	6.25	3.41	3.21	0.74	27.34	0.67	0.75	100.59
	57.35	5.27	2.55	3.14	0.84	26.84	1.09	1.75	98.83
	57.36	5.71	3.24	3.20	0.78	27.37	0.89	0.44	98.99
	56.26	6.46	2.47	2.66	0.74	26.53	0.54	3.09	98.75
	56.08	6.04	2.44	2.93	0.86	27.57	0.77	0.50	97.19
	61.35	6.17	2.32	3.20	0.73	24.50	0.67	0.84	99.79
	59.30	5.97	1.65	3.13	0.64	28.83	0.61	0.95	101.08
	59.67	5.63	1.35	2.94	0.67	27.92	0.40	1.31	99.89
	59.31	5.56	1.71	3.09	0.75	24.10	0.73	3.65	98.90
	58.71	5.82	2.43	2.62	0.72	28.24	0.70	0.75	100.00
	56.87	5.80	3.61	3.12	0.64	27.11	1.03	0.51	98.69
	56.91	6.01	3.44	3.20	0.79	27.00	0.87	0.55	98.77
	57.10	5.81	3.59	2.70	0.68	27.20	1.23	0.59	98.90
	62.16	6.48	1.71	3.13	0.79	21.90	0.84	1.24	98.26
	58.06	5.88	5.44	3.31	0.74	26.25	0.63	n.d.	100.32
	58.07	5.73	3.15	3.14	0.75	28.35	0.79	0.32	100.29
	56.36	5.57	3.59	3.19	0.68	27.52	0.88	n.d.	97.79
	56.46	6.33	2.40	2.96	0.73	28.41	0.95	0.35	98.60
	58.87	6.07	3.05	3.17	0.71	26.45	0.93	0.66	99.92
	57.21	6.01	2.84	3.09	0.71	26.91	0.85	0.68	98.29
+10.7 m/P7	57.75	6.26	3.13	3.14	0.70	27.45	0.93	1.30	100.66
	58.09	5.82	4.32	2.41	0.72	26.18	0.43	0.69	98.67
	58.17	5.72	2.80	3.25	0.74	26.80	0.90	2.15	100.54
	57.91	6.27	4.35	2.67	0.74	26.60	0.64	0.68	99.87
	59.18	5.50	2.83	2.16	0.51	26.37	0.55	2.82	99.90
	58.30	5.78	3.68	3.15	0.63	26.23	0.91	1.91	100.58
	55.19	5.86	1.92	1.93	0.51	30.7	0.68	1.46	98.24
	54.32	6.57	1.05	2.40	0.46	32.91	0.50	0.58	98.79
	57.05	5.76	2.32	2.46	0.58	27.82	0.79	1.69	98.46
	58.81	5.78	2.16	3.62	0.74	26.39	0.61	0.67	98.79
	60.21	5.52	3.84	2.20	0.61	26.85	0.82	0.43	100.48
+10.1 m/P8	57.89	6.10	3.03	3.14	0.79	28.64	0.91	0.51	101.01
	58.18	6.10	2.51	3.15	0.64	27.68	0.64	0.65	99.56
	57.35	6.12	2.65	2.94	0.78	28.49	0.80	0.49	99.62
	57.65	7.24	1.93	2.13	0.69	25.70	0.68	1.88	97.90
	58.16	5.87	1.24	2.98	0.68	26.31	0.38	3.37	98.97
	56.84	5.80	1.52	3.06	0.76	26.69	0.66	4.42	99.76
	57.80	6.15	2.56	2.97	0.79	28.08	0.70	0.62	99.66
	57.99	5.96	2.70	2.97	0.67	27.81	0.67	1.29	100.07

	57.21	5.69	2.44	3.15	0.63	29.01	0.64	0.84	99.61
	56.94	5.74	1.92	2.73	0.65	30.55	0.71	0.40	99.64
	57.33	6.21	2.57	3.26	0.75	28.51	0.60	0.55	99.79
	59.20	6.01	2.41	3.05	0.83	25.15	0.81	1.21	98.67
	56.30	6.43	2.10	2.70	0.63	29.51	0.79	1.31	99.77
	58.09	6.30	3.64	2.34	0.68	25.89	1.26	1.13	99.33
	57.34	5.93	3.71	3.05	0.75	27.70	0.72	0.68	99.88
+9.7 m/P9	61.19	6.03	1.5	2.98	0.72	26.67	0.72	0.49	100.29
+8.7 m/X3	56.88	5.70	2.70	3.33	0.63	29.10	0.93	0.47	99.73
	56.90	5.92	2.92	3.16	0.67	27.87	0.89	1.15	99.47
	57.84	6.10	2.85	2.92	0.65	26.92	0.84	0.78	98.91
	58.08	5.97	2.57	3.20	0.74	27.63	0.67	tr.	98.86
	56.50	6.05	2.69	1.92	0.57	29.22	0.65	1.04	98.64
	57.59	5.95	2.32	3.00	0.78	29.55	0.63	tr.	99.82
	57.95	5.95	3.14	3.09	0.75	28.19	0.86	0.33	100.26
+7.2 m/P10	58.12	5.97	2.48	2.95	0.79	28.66	0.84	0.56	100.36

Level/Sample	Cr_2O_3	Al_2O_3	MgO	TiO_2	V_2O_3	FeO	MnO	ZnO	Total
OC grains									
+16.4 m/P2	57.44	5.31	n.d.	2.56	0.62	22.14	n.d.	12.05	100.12
	57.01	16.30	5.98	n.d.	n.d.	20.32	0.82	0.87	101.30
	43.64	22.31	13.92	n.d.	n.d.	17.60	n.d.	n.d.	97.46
	60.50	10.15	11.02	n.d.	n.d.	18.42	n.d.	1.20	101.28
	49.99	13.03	7.52	0.79	n.d.	28.66	n.d.	n.d.	99.99
	45.17	19.09	10.89	0.33	n.d.	23.73	n.d.	n.d.	99.21
	42.50	13.87	13.00	2.52	n.d.	27.77	n.d.	n.d.	99.65
	67.77	4.96	13.21	0.46	0.46	6.97	2.89	2.20	98.91
	50.16	13.23	3.85	3.27	0.57	27.23	0.55	n.d.	98.88
	50.49	13.85	12.42	1.98	n.d.	19.04	n.d.	n.d.	97.78
	47.29	14.86	5.90	0.46	n.d.	28.75	n.d.	n.d.	97.27
+15.8 m/Y10	44.62	20.09	15.26	2.33	n.d.	17.43	n.d.	n.d.	99.73
	54.51	12.75	8.63	0.47	n.d.	21.51	n.d.	n.d.	97.86
	53.29	11.90	5.49	0.39	n.d.	24.87	n.d.	n.d.	95.93
	50.89	12.70	9.38	0.50	n.d.	25.09	n.d.	n.d.	98.57
+15.2 m/P3									
	55.54	6.47	n.d.	2.60	0.59	20.43	n.d.	14.88	100.52
+15.0 m/P4	60.00	10.81	4.65	0.82	0.47	20.31	0.82	2.07	99.94
+14.8 m/Y9	40.53	21.75	10.31	1.63	n.d.	23.73	n.d.	n.d.	97.95
	53.16	13.68	7.22	n.d.	n.d.	22.57	0.48	n.d.	97.11
	40.99	17.28	6.49	0.63	n.d.	32.91	0.61	0.37	99.27
	22.08	13.00	3.83	4.09	n.d.	51.31	n.d.	0.68	94.99
	37.84	9.01	3.32	2.89	n.d.	42.56	n.d.	n.d.	95.62
+13.8 m/P5	41.83	18.29	4.62	0.53	n.d.	32.80	0.63	0.64	99.34
	37.51	22.51	9.92	0.56	n.d.	29.70	n.d.	n.d.	100.20
	63.77	10.42	5.79	n.d.	n.d.	18.97	0.66	0.91	100.54
+8.7 m/X3	52.62	13.36	5.44	1.62	0.31	25.90	0.86	n.d.	100.10

[1] Meters relative to the base of the Guniutan Formation; [2] Represents the average Total (wt%) for a minimum of three separate analyses per grain. [3] n.d. = not detected; [4] tr.=trace amounts, but not represented due to poor precision (i.e. <0.30 wt%), hence considered statistically unreliable.

Appendix Table 2. Results of the roundness and size analysis of individual Cr-rich grains from the Puxi River section, China.

Level[1]/Samples	Grain	Roundness analysis[2]							Size analysis (μm)	
		VA	A	SA	SR	R	VR	Definition	Length	Width
+16.4 m/P2	Cr 1	3	-	-	-	-	-	VA	150	83
	Cr 2	2	1	-	-	-	-	VA	106	58
	Cr 3[3]	3	-	-	-	-	-	VA	86	84
	Cr 4	3	-	-	-	-	-	VA	104	79
	Cr 5	3	-	-	-	-	-	VA	86	66
	Cr 6	2	1	-	-	-	-	VA	109	68
	Cr 7	3	-	-	-	-	-	VA	141	69
	Cr 8	3	-	-	-	-	-	VA	108	90
	Cr 9[3]	-	3	-	-	-	-	A	162	109
	Cr 10	-	3	-	-	-	-	A	89	56
	Cr 11[3]	2	1	-	-	-	-	VA	88	55
	Cr 12	-	-	1	2	-	-	SR	135	69
	Cr 13	3	-	-	-	-	-	VA	125	60
	Cr 14	-	-	-	2	1	-	SR	94	82
	Cr 15	-	2	1	-	-	-	A	118	91
	Cr 16	-	3	-	-	-	-	A	96	94
	Cr 17	3	-	-	-	-	-	VA	98	63
	Cr 18	1	2	-	-	-	-	A	82	46
	Cr 19	3	-	-	-	-	-	VA	116	80
	Cr 20	3	-	-	-	-	-	VA	82	56
	Cr 21	2	1	-	-	-	-	VA	114	103
	Cr 22	3	-	-	-	-	-	VA	109	80
	Cr 23	1	2	-	-	-	-	A	134	57
	Cr 24	-	2	1	-	-	-	A	104	66
	Cr 25[3]	-	-	-	-	3	-	R	124	108
	Cr 26	3	-	-	-	-	-	VA	118	80
	Cr 27[3]	-	-	-	-	1	2	VR	121	77
	Cr 28	3	-	-	-	-	-	VA	90	59
	Cr 29[3]	-	-	-	1	2	-	R	110	65
	Cr 30	-	2	1	-	-	-	A	124	84
	Cr 31	2	1	-	-	-	-	VA	122	68
	Cr 32[3]	3	-	-	-	-	-	VA	112	83
	Cr 33	2	1	-	-	-	-	VA	73	51
	Cr 34[3]	-		-	-	2	1	R	153	134
	Cr 35	-	3	-	-	-	-	A	78	74
	Cr 36	3	-	-	-	-	-	VA	83	67
	Cr 37[3]	-	-	1	1	1	-	SR	183	100
	Cr 38[3]	-	1	2	-	-	-	SA	141	72
	Cr 39	-	3	-	-	-	-	A	92	74
	Cr 40	-	3	-	-	-	-	A	91	57
	Cr 41	2	1	-	-	-	-	VA	82	59
	Cr 42	2	1	-	-	-	-	VA	72	68
	Cr 43[3]	-	-	1	2	-	-	SR	87	75
	Cr 44	-	2	1	-	-	-	A	86	69
	Cr 45	2	1	-	-	-	-	VA	96	83
	Cr 46		3	-	-	-	-	A	74	60
	Cr 47	2	1	-	-	-	-	VA	79	77
	Cr 48	3	-	-	-	-	-	VA	104	62
	Cr 49	3	-	-	-	-	-	VA	89	83
	Cr 50	-	2	1	-	-	-	A	88	86
	Cr 51	2	1		-	-	-	VA	99	58
	Cr 52		2	1	-	-	-	A	84	83
	Cr 53	2	1	-	-	-	-	VA	95	60

+15.8 m/Y10	Cr 1	-	3	-	-	-	-	A	99	88
	Cr 2	-	-	3	-	-	-	SA	219	139
	Cr 3	1	2	-	-	-	-	A	169	133
	Cr 4	2	1	-	-	-	-	VA	93	69
	Cr 5	-	3	-	-	-	-	A	156	93
	Cr 6	-	3	-	-	-	-	A	126	89
	Cr 7[3]	-	-	-	-	3	-	R	104	67
	Cr 8	3	-	-	-	-	-	VA	113	62
	Cr 9	3	-	-	-	-	-	VA	89	77
	Cr 10[3]	-	-	-	1	2	-	R	78	71
	Cr 11	3	-	-	-	-	-	VA	126	87
	Cr 12	-	3	-	-	-	-	A	81	62
	Cr 13	1	2	-	-	-	-	A	67	65
	Cr 14	2	1	-	-	-	-	VA	79	71
	Cr 15	-	2	1	-	-	-	A	95	64
	Cr 16	3	-	-	-	-	-	VA	174	73
	Cr 17	3	-	-	-	-	-	VA	143	87
	Cr 18	3	-	-	-	-	-	VA	101	61
	Cr 19	3	-	-	-	-	-	VA	112	73
	Cr 20	2	1	-	-	-	-	VA	51	39
	Cr 21	2	1	-	-	-	-	VA	104	83
	Cr 22	-	2	1	-	-	-	A	105	67
	Cr 23	3	-	-	-	-	-	VA	96	69
	Cr 24	-	3	-	-	-	-	A	96	64
	Cr 25[3]	-	-	3	-	-	-	SA	82	64
	Cr 26	-	2	1	-	-	-	A	132	78
	Cr 27[3]	-	-	-	-	2	1	R	93	85
	Cr 28	3	-	-	-	-	-	VA	110	62
	Cr 29	3	-	-	-	-	-	VA	111	61
	Cr 30	3	-	-	-	-	-	VA	101	51
	Cr 31	2	1	-	-	-	-	VA	102	74
	Cr 32	3	-	-	-	-	-	VA	102	76
	Cr 33	3	-	-	-	-	-	VA	92	69
	Cr 34	-	3	-	-	-	-	A	82	63
	Cr 35	3	-	-	-	-	-	VA	123	64
	Cr 36	-	2	1	-	-	-	A	79	66
+15.2 m/P3	Cr 1	-	3	-	-	-	-	A	133	83
	Cr 2	3	-	-	-	-	-	VA	88	75
	Cr 3[3]	-	3	-	-	-	-	A	97	76
	Cr 4	3	-	-	-	-	-	VA	132	107
	Cr 5	1	2	-	-	-	-	A	147	84
	Cr 6	-	3	-	-	-	-	A	79	61
+15.0 m/P4	Cr 1	3	-	-	-	-	-	VA	102	84
	Cr 2	2	1	-	-	-	-	VA	126	91
	Cr 3	1	2	-	-	-	-	A	124	86
	Cr 4	3	-	-	-	-	-	VA	231	148
	Cr 5	-	3	-	-	-	-	A	82	63
	Cr 6	-	1	2	-	-	-	SA	102	69
	Cr 7	1	2	-	-	-	-	A	92	75
	Cr 8	2	1	-	-	-	-	VA	158	69
	Cr 9	1	2	-	-	-	-	A	69	67
	Cr 10	1	2	-	-	-	-	A	93	71
	Cr 11	-	2	1	-	-	-	A	98	77
	Cr 12	1	2	-	-	-	-	A	96	67
	Cr 13	-	3	-	-	-	-	A	77	74
	Cr 14	2	1	-	-	-	-	VA	162	132
	Cr 15	2	1	-	-	-	-	VA	152	67
	Cr 16	-	3	-	-	-	-	A	120	82

	Cr 17	1	2	-	-	-	-	A	136	87
	Cr 18	3	-	-	-	-	-	VA	94	83
	Cr 19	-	3	-	-	-	-	A	86	79
	Cr 20	2	1	-	-	-	-	VA	140	93
	Cr 21	1	2	-	-	-	-	A	115	62
	Cr 22	3	-	-	-	-	-	VA	188	85
	Cr 23	-	3	-	-	-	-	A	126	83
	Cr 24	1	2	-	-	-	-	A	137	86
	Cr 25	2	1	-	-	-	-	VA	128	71
	Cr 26	2	1	-	-	-	-	VA	131	91
	Cr 27	1	2	-	-	-	-	A	152	103
	Cr 28	1	2	-	-	-	-	A	97	84
	Cr 29	1	2	-	-	-	-	A	93	82
	Cr 30	-	1	2	-	-	-	SA	98	70
	Cr 31	-	3	-	-	-	-	A	95	77
	Cr 32	3	-	-	-	-	-	VA	126	55
	Cr 33	3	-	-	-	-	-	VA	108	74
	Cr 34	1	2	-	-	-	-	A	75	72
	Cr 35	2	1	-	-	-	-	VA	67	63
	Cr 36	1	2	-	-	-	-	A	83	67
	Cr 37	-	3	-	-	-	-	A	101	76
	Cr 38	-	3	-	-	-	-	A	66	58
	Cr 39	-	-	3	-	-	-	SA	163	83
	Cr 40	1	2	-	-	-	-	A	107	70
	Cr 41	1	2	-	-	-	-	A	82	72
	Cr 42	-	2	1	-	-	-	A	111	78
	Cr 43	2	1	-	-	-	-	VA	79	62
	Cr 44	3	-	-	-	-	-	VA	94	65
	Cr 45	-	3	-	-	-	-	A	79	67
	Cr 46	1	1	1	-	-	-	A	99	75
	Cr 47	-	2	1	-	-	-	A	95	60
	Cr 48	3	-	-	-	-	-	VA	121	60
	Cr 49	2	1	-	-	-	-	VA	102	98
	Cr 50	1	2	-	-	-	-	A	83	73
	Cr 51	1	2	-	-	-	-	A	161	66
	Cr 52	-	3	-	-	-	-	A	97	71
	Cr 53[3]	-	3	-	-	-	-	A	80	78
	Cr 54	-	3	-	-	-	-	A	91	72
	Cr 55	2	1	-	-	-	-	VA	114	88
+14.8 m/Y9	Cr 1	2	1	-	-	-	-	VA	108	71
	Cr 2[3]	-	-	3	-	-	-	SA	141	84
	Cr 3	-	3	-	-	-	-	A	108	61
	Cr 4	3	-	-	-	-	-	VA	77	75
	Cr 5	1	2	-	-	-	-	A	97	64
	Cr 6	2	1	-	-	-	-	VA	92	76
	Cr 7	-	2	1	-	-	-	A	71	65
	Cr 8	2	1	-	-	-	-	VA	90	72
	Cr 9	2	1	-	-	-	-	VA	110	75
	Cr 10	2	1	-	-	-	-	VA	85	45
	Cr 11	-	3	-	-	-	-	A	99	66
	Cr 12	-	3	-	-	-	-	A	116	84
	Cr 13	2	1	-	-	-	-	VA	95	74
	Cr 14[3]	-	-	-	2	1	-	SR	85	63
	Cr 15	3	-	-	-	-	-	VA	85	56
	Cr 16	1	2		-	-	-	A	82	62
	Cr 17	-	2	1	-	-	-	A	81	79
	Cr 18	2	1	-	-	-	-	VA	104	62
	Cr 19	3	-	-	-	-	-	VA	134	69
	Cr 20	-	2	1	-	-	-	A	76	60

	Cr 21	3	-	-	-	-	-	VA	80	74
	Cr 22	3	-	-	-	-	-	VA	74	74
	Cr 23	3	-	-	-	-	-	VA	80	56
	Cr 24	1	2	-	-	-	-	A	104	47
	Cr 25	-	3	-	-	-	-	A	95	58
	Cr 26	1	2	-	-	-	-	A	70	55
	Cr 27[3]	-	-	-	-	2	1	R	60	55
	Cr 28	1	1	-	1	-	-	A	128	120
	Cr 29	-	2	1	-	-	-	A	122	64
	Cr 30	1	2	-	-	-	-	A	84	53
	Cr 31	3	-	-	-	-	-	VA	89	59
	Cr 32	3	-	-	-	-	-	VA	104	72
	Cr 33	1	2	-	-	-	-	A	79	73
	Cr 34[3]	-	-	-	3	-	-	SR	118	60
	Cr 35	2	1	-	-	-	-	VA	73	62
	Cr 36	2	1	-	-	-	-	VA	105	69
	Cr 37	-	1	2	-	-	-	SA	77	60
	Cr 38	2	1	-	-	-	-	VA	63	61
	Cr 39	1	2	-	-	-	-	A	109	72
	Cr 40[3]	-	-	-	-	1	2	VR	82	80
	Cr 41	2	1	-	-	-	-	VA	69	63
	Cr 42	3	-	-	-	-	-	VA	108	73
	Cr 43	3	-	-	-	-	-	VA	141	59
	Cr 44	3	-	-	-	-	-	VA	75	69
	Cr 45	3	-	-	-	-	-	VA	83	66
	Cr 46	3	-	-	-	-	-	VA	94	65
	Cr 47	2	1	-	-	-	-	VA	164	93
	Cr 48	3	-	-	-	-	-	VA	87	76
	Cr 49	3	-	-	-	-	-	VA	91	57
	Cr 50	2	1	-	-	-	-	VA	89	75
	Cr 51	-	3	-	-	-	-	A	108	60
	Cr 52	3	-	-	-	-	-	VA	123	72
	Cr 53	3	-	-	-	-	-	VA	85	67
+14.4 m/Y8.5	Cr 1	-	2	1	-	-	-	A	85	62
	Cr 2	-	3	-	-	-	-	A	83	70
	Cr 3	-	3	-	-	-	-	A	77	73
	Cr 4	2	1	-	-	-	-	VA	120	81
	Cr 5	1	2	-	-	-	-	A	96	79
	Cr 6	2	1	-	-	-	-	VA	85	61
	Cr 7	-	1	2	-	-	-	SA	206	111
	Cr 8	-	2	1	-	-	-	A	67	63
	Cr 9	2	1	-	-	-	-	VA	81	71
+13.8 m/P5	Cr 1	-	3	-	-	-	-	A	84	60
	Cr 2	3	-	-	-	-	-	VA	113	71
	Cr 3	-	-	3	-	-	-	SA	103	98
	Cr 4[3]	-	-	-	1	1	1	R	70	61
	Cr 5	3	-	-	-	-	-	VA	68	62
	Cr 6	3	-	-	-	-	-	VA	96	52
	Cr 7	1	2	-	-	-	-	A	112	88
	Cr 8	-	2	1	-	-	-	A	80	78
	Cr 9[3]	-	-	-	-	-	3	VR	84	76
	Cr 10	1	2	-	-	-	-	A	100	60
	Cr 11	-	1	2	-	-	-	SA	96	69
	Cr 12	1	2	-	-	-	-	A	76	62
	Cr 13	2	1	-	-	-	-	VA	123	87
	Cr 14	3	-	-	-	-	-	VA	96	66
	Cr 15	3	-	-	-	-	-	VA	141	95
	Cr 16	2	1	-	-	-	-	VA	94	64

	Cr 17	1	2	-	-	-	-	A	77	63
	Cr 18	-	3	-	-	-	-	A	68	50
	Cr 19	1	2	-	-	-	-	A	139	115
	Cr 20	-	1	2	-	-	-	SA	201	193
	Cr 21	-	2	1	-	-	-	A	126	102
	Cr 22	-	1	2	-	-	-	SA	97	76
	Cr 23	-	-	3	-	-	-	SA	102	95
	Cr 24[3]	-	-	-	1	2	-	R	66	60
	Cr 25	-	-	3	-	-	-	SA	94	62
	Cr 26	1	2	-	-	-	-	A	85	60
+11.4 m/Y8	Cr 1	1	2	-	-	-	-	A	66	58
	Cr 2	-	2	1	-	-	-	A	85	64
	Cr 3	2	1	-	-	-	-	VA	53	41
	Cr 4	3	-	-	-	-	-	VA	84	81
	Cr 5	-	1	2	-	-	-	SA	83	58
	Cr 6	2	1	-	-	-	-	VA	70	69
	Cr 7	2	1	-	-	-	-	VA	85	75
	Cr 8	3	-	-	-	-	-	VA	95	55
	Cr 9	3	-	-	-	-	-	VA	99	70
	Cr 10	3	-	-	-	-	-	VA	113	81
+10.9 m/P6a	Cr 1	-	3	-	-	-	-	A	117	86
	Cr 2	-	2	1	-	-	-	A	84	57
	Cr 3	3	-	-	-	-	-	VA	97	57
	Cr 4	-	2	1	-	-	-	A	86	69
	Cr 5	-	1	2	-	-	-	SA	61	46
	Cr 6	-	-	2	1	-	-	SA	102	77
	Cr 7	-	3	-	-	-	-	A	82	63
	Cr 8	2	1	-	-	-	-	VA	64	63
	Cr 9	1	1	1	-	-	-	A	73	49
	Cr 10	2	1	-	-	-	-	VA	84	81
	Cr 11	3	-	-	-	-	-	VA	82	75
	Cr 12	-	3	-	-	-	-	A	75	62
	Cr 13	2	1	-	-	-	-	VA	107	48
	Cr 14	3	-	-	-	-	-	VA	84	82
	Cr 15	2	1	-	-	-	-	VA	70	66
	Cr 16	-	2	1	-	-	-	A	73	68
	Cr 17	-	2	1	-	-	-	A	106	61
	Cr 18	3	-	-	-	-	-	VA	102	51
	Cr 19	1	2	-	-	-	-	A	140	83
	Cr 20	2	1	-	-	-	-	VA	78	59
	Cr 21	-	3	-	-	-	-	A	103	85
	Cr 22	-	3	-	-	-	-	A	107	83
	Cr 23	-	-	3	-	-	-	SA	90	75
+10.7 m/P7	Cr 1	1	2	-	-	-	-	A	76	61
	Cr 2	-	1	2	-	-	-	SA	115	81
	Cr 3	-	-	2	1	-	-	SA	79	64
	Cr 4	2	1	-	-	-	-	VA	109	98
	Cr 5	-	2	1	-	-	-	A	99	65
	Cr 6	-	1	2	-	-	-	SA	94	72
	Cr 7	-	3	-	-	-	-	A	116	56
	Cr 8	1	2	-	-	-	-	A	103	81
	Cr 9	2	1	-	-	-	-	VA	140	99
	Cr 10	1	1	1	-	-	-	A	89	83
	Cr 11	1	2	-	-	-	-	A	98	75
+10.1 m/P8	Cr 1	-	3	-	-	-	-	A	129	68
	Cr 2	-	3	-	-	-	-	A	167	66

	Cr 3	-	2	1	-	-	-	A	58	56
	Cr 4	-	-	-	3	-	-	SR	103	68
	Cr 5	-	3	-	-	-	-	A	176	129
	Cr 6	-	3	-	-	-	-	A	96	62
	Cr 7	-	2	1	-	-	-	A	85	74
	Cr 8	2	1	-	-	-	-	VA	121	71
	Cr 9	2	1	-	-	-	-	VA	110	87
	Cr 10	-	3	-	-	-	-	A	117	99
	Cr 11	-	3	-	-	-	-	A	96	67
	Cr 12	3	-	-	-	-	-	VA	98	62
	Cr 13	1	2	-	-	-	-	A	91	55
	Cr 14	3	-	-	-	-	-	VA	74	68
	Cr 15	2	1	-	-	-	-	VA	73	63
+9.7 m/P9	Cr 1	-	-	-	3	-	-	SR	96	85
+8.7 m/X3	Cr 1[3]	3	-	-	-	-	-	VA	122	72
	Cr 2	2	1	-	-	-	-	VA	86	63
	Cr 3	1	2	-	-	-	-	A	94	60
	Cr 4	-	3	-	-	-	-	A	64	62
	Cr 5	3	-	-	-	-	-	VA	121	74
	Cr 6	1	2	-	-	-	-	A	80	74
	Cr 7	-	3	-	-	-	-	A	71	62
	Cr 8	3	-	-	-	-	-	VA	86	79
+7.2 m/P10	Cr 1[4]	2	1	-	-	-	-	VA	-	-

[1] Meters relative to the base of the Guniutan Formation; [2] According to the "Pettijon" system (Pettijohn 1957): VA = Very angular; A = Angular; SA = Sub-angular; SR = Sub-rounded; R = Rounded; VR = Very rounded; [3] Other Cr-rich grains; [4] The scale in the photo is incorrect, i.e. no size analysis. Sample P 5.5 (10 EC grains) is not represented by photos during preliminary analysis, and are hence disregarded from roundness and size analysis.

IV

Asteroid breakup linked to the Great Ordovician Biodiversification Event

BIRGER SCHMITZ[1]*, DAVID A. T. HARPER[2], BERNHARD PEUCKER-EHRENBRINK[3], SVEND STOUGE[2], CARL ALWMARK[1], ANDERS CRONHOLM[1], STIG M. BERGSTRÖM[4], MARIO TASSINARI[1] AND WANG XIAOFENG[5]

[1]Department of Geology, University of Lund, Sölvegatan 12, SE-22362 Lund, Sweden
[2]Natural History Museum of Denmark, Geological Museum, University of Copenhagen, Øster Voldgade 5-7, DK-1350 Copenhagen K, Denmark
[3]Department of Marine Chemistry and Geochemistry, Woods Hole Oceanographic Institution, MS 25, Woods Hole, Massachusetts 02543, USA
[4]School of Earth Sciences, The Ohio State University, 125 South Oval Mall, Columbus, Ohio 43210, USA
[5]Yichang Institute of Geology and Mineral Resources, Yichang, Hubei 443003, China
*e-mail: birger.schmitz@geol.lu.se

Published online: 16 December 2007; doi:10.1038/ngeo.2007.37

The rise and diversification of shelled invertebrate life in the early Phanerozoic eon occurred in two major stages. During the first stage (termed as the Cambrian explosion), a large number of new phyla appeared over a short time interval ~540 Myr ago. Biodiversity at the family, genus and species level, however, remained low until the second stage marked by the Great Ordovician Biodiversification Event in the Middle Ordovician period[1–3]. Although this event represents the most intense phase of species radiation during the Palaeozoic era and led to irreversible changes in the biological make-up of Earth's seafloors, the causes of this event remain elusive. Here, we show that the onset of the major phase of biodiversification ~470 Myr ago coincides with the disruption in the asteroid belt of the L-chondrite parent body—the largest documented asteroid breakup event during the past few billion years[4,5]. The precise coincidence between these two events is established by bed-by-bed records of extraterrestrial chromite, osmium isotopes and invertebrate fossils in Middle Ordovician strata in Baltoscandia and China. We argue that frequent impacts on Earth of kilometre-sized asteroids—supported by abundant Middle Ordovician fossil meteorites and impact craters[6]—accelerated the biodiversification process.

Evidence for an early Palaeozoic major asteroid breakup was already established in the 1960s when recent ordinary chondrites of the L type were shown to commonly have K–Ar gas retention or shock ages of about 450–500 Myr (refs 4,5). About 20% of the meteorites reaching Earth today are shocked L chondrites from this event. The finds of more than 50 fossil L-chondritic meteorites (1–20 cm in diameter) in Middle Ordovician limestone in southern Sweden show that the meteorite flux was enhanced by one to two orders of magnitude for at least a few million years after the disruption event[6,7]. The L-chondritic origin of the fossil meteorites is demonstrated by element and oxygen isotope analyses of relict chromite grains as well as by petrographic studies of chondrule textures[6–8]. Chromite is the only common mineral in chondrites that survives extensive weathering on the wet Earth surface. In the limestone beds containing common meteorites, abundant chromite grains from decomposed meteorites and micrometeorites are also found[9–11]. Cosmic-ray-induced ^{21}Ne in chromite from the fossil meteorites increases upwards in the strata, supporting a common origin from an asteroid breakup event[12]. High-precision ^{40}Ar–^{39}Ar dating of recent L chondrites has constrained the timing of their parent-body disruption to 470 ± 6 Myr ago, which is identical within uncertainties to the age of 467.3 ± 1.6 Myr ago for the beds with fossil meteorites according to the latest geologic timescale[13].

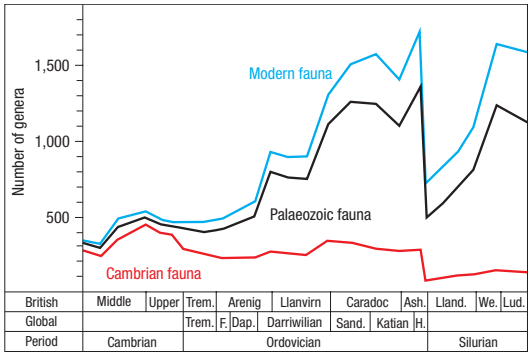

Figure 1 Global biodiversity change at family level through the early Palaeozoic era. Although this diagram from Sepkoski (1995; ref. 15) gives a good representation of the overall biodiversity trend, the resolution is too crude for correlation with field data. Trem. = Tremadocian (Global) and Tremadoc (British), Ash. = Ashgill, Lland. = Llandovery, We. = Wenlock, Lud. = Ludlow, F. = Floian, Dap. = Dapingian, Sand. = Sandbian, H. = Hirnantian.

During the Great Ordovician Biodiversification Event (GOBE), in the Middle to Late Ordovician, biodiversity at the family level increased from a Phanerozoic all-time-low in the Cambrian and Early Ordovician to levels approximately three times higher in the Late Ordovician[1–3,14,15] (Fig. 1). The new biodiversity levels of marine life were matched by an increase in biocomplexity, and were sustained until the end of the Palaeozoic except for short-term declines in connection with extinction events in

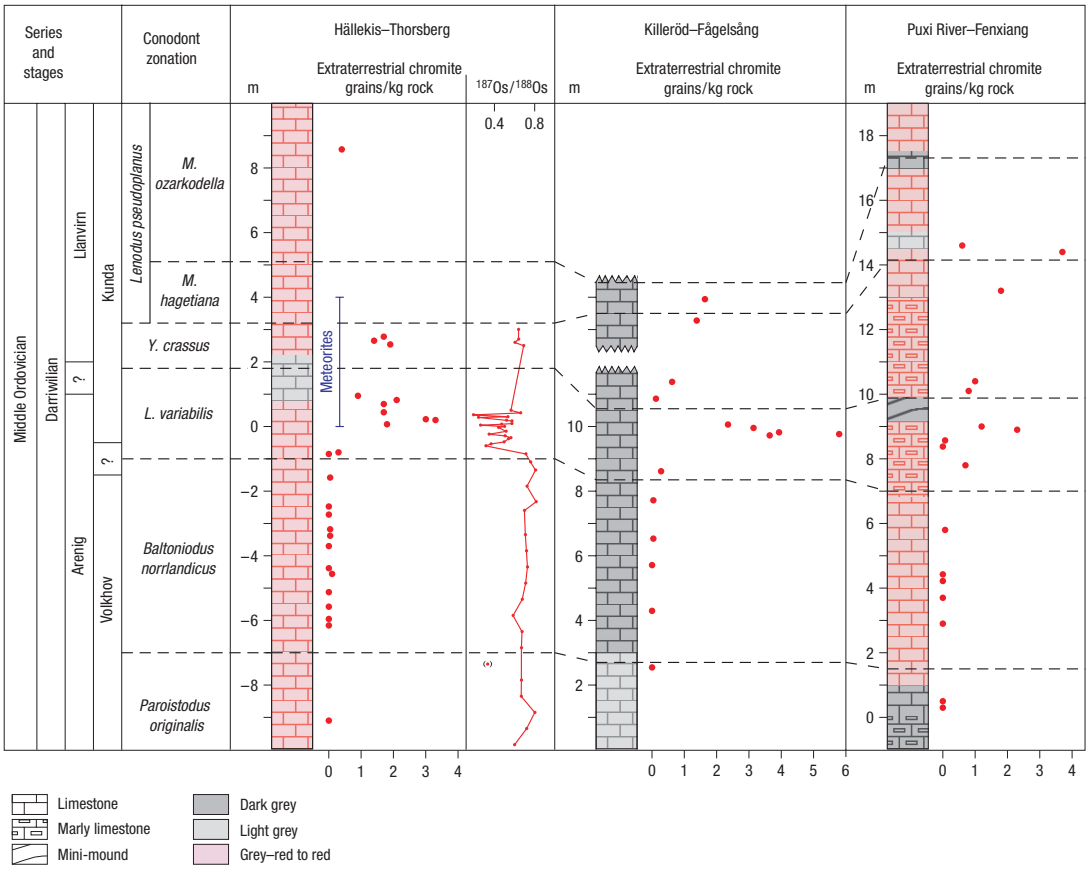

Figure 2 Distribution of extraterrestrial (chondritic) chromite and osmium isotopes through Middle Ordovician sections in Sweden and China. Results are shown for sections at Kinnekulle (Hällekis and Thorsberg quarries) and southern Scania (Killeröd and Fågelsång sections), 350 km apart in southern Sweden, and the Puxi River and Fenxiang sections, 4 km apart in south-central China. The distribution of Os isotopes across the Hällekis section is also shown. The stratigraphic interval yielding abundant fossil meteorites in the Thorsberg quarry is indicated[6]. The conodont biostratigraphy shown has been produced specifically for this study, using consistent taxonomic concepts for the different sections. *M. ozarkodella* = *Microzarkodina ozarkodella*.

the latest Ordovician and Late Devonian periods. The GOBE generated few new higher taxa, for example phyla, but witnessed a staggering increase in biodiversity at, for example, species level among a wide variety of groups of skeletal invertebrates[2,3,15]. Diagrams of changes in global or regional biodiversity during the GOBE give only a crude representation of the timing and pace of the faunal change[15,16]. The global signal represents a combination of many regional diversity changes across a range of fossil groups[2,3]. The most focused global compilation through the early Palaeozoic, shown in Fig. 1, demonstrates a sharp rise in biodiversity at about the Arenig–Llanvirn boundary (about 466 Myr ago). This signal is evident across a number of groups, such as the brachiopods, cephalopods and echinoderms, but less clear in some members of the Cambrian fauna (trilobites) and the modern fauna (gastropods)[15]. It also corresponds to the second-cycle diversity peak in conodonts recognized by Sweet[17]. The causes of the GOBE, and its relation to both intrinsic (biological) and extrinsic (environmental) factors are not known[2]. Many authors have suggested a link to increasing levels of atmospheric oxygen, favouring the radiation of aerobic metazoan life together with an expansion of the phyto and zooplankton[18,19].

Although biodiversity diagrams such as in Fig. 1 show the broad outline of change, at a higher resolution they suffer from the effects of poor correlation and poor preservation of faunas, focus on a particular horizon or group of fossils and data binning. To relate biological change to physical events, detailed high-resolution multiparameter records across complete and fossil-rich sections are required. Here, we have constrained the precise stratigraphic level for the L-chondrite disruption event by searches for sediment-dispersed extraterrestrial (chondritic) chromite grains and Os isotopic studies in Middle Ordovician sections with condensed limestone (Fig. 2). These results are matched by the most detailed bed-by-bed studies of the distribution of brachiopod species across Middle Ordovician strata in Baltoscandia (Fig. 3) conducted until now.

The sections studied for extraterrestrial chromite grains occur at Kinnekulle and in southern Scania, 350 km apart in southern Sweden, and at Puxi River (Puquie) and Fenxiang, 4 km apart in south-central China near Yichang, Hubei province. The extraterrestrial chromite grains (>63 μm) have been retrieved from about 10–30-kg-sized limestone samples that were dissolved in HCl and HF acid[10]. The extraterrestrial chromite can be readily

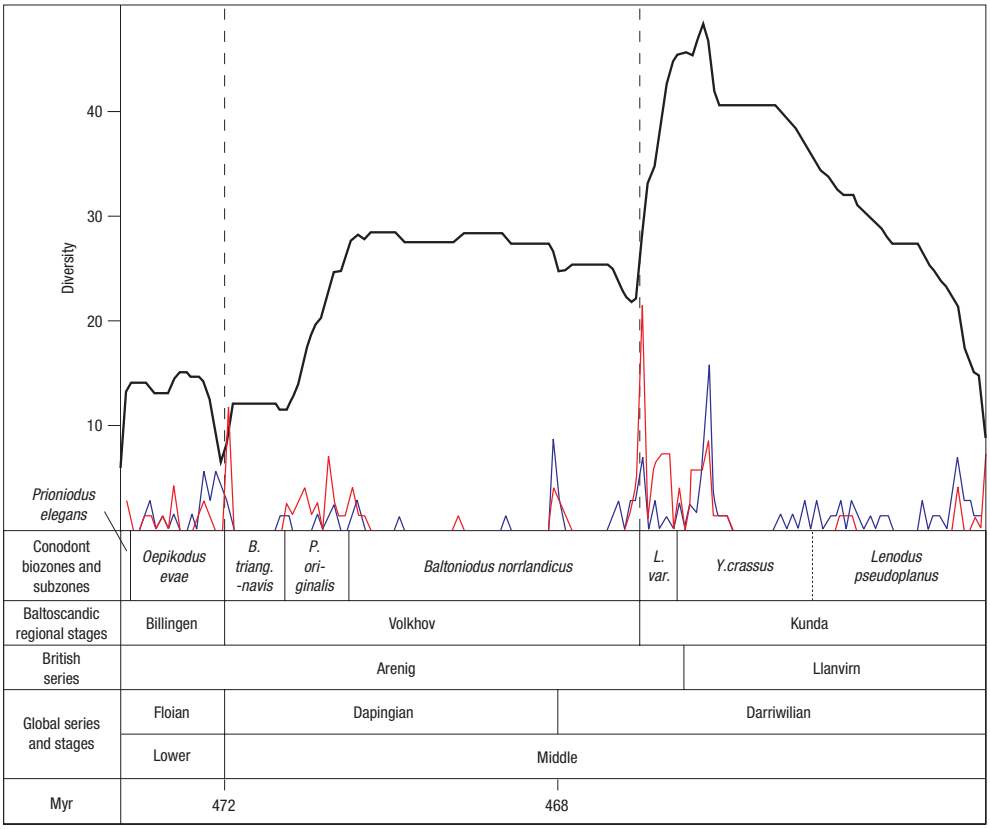

Figure 3 Total diversity of brachiopod species (number of species) through part of the Lower and Middle Ordovician in Baltoscandia. The results are based on bed-by-bed collections at eight localities[22]. Note the dramatic increase in biodiversity (black line) and high extinction (blue line) and origination (red line) levels following the regional Volkhov–Kunda boundary, that is, the same level where extraterrestrial chromite appears and Os isotopes change in Fig. 2. *B. triang.-navis* = *Baltoniodus triangulatus-navis*. The dashed lines show the boundaries between the regional states.

distinguished from terrestrial chromite by its distinct element composition[6,10]. The results of the extraterrestrial chromite searches are shown in Fig. 2 and in the Supplementary Information. In the section studied in greatest detail, at Kinnekulle, in 379 kg of limestone from 14 levels across 9 m of strata below the *Lenodus variabilis* zone, only 5 extraterrestrial chromite grains were found[10] (Fig. 2). The values then increased dramatically to typically 1–3 extraterrestrial chromite grains per kilogram of rock in the *L. variabilis, Yangtzeplacognathus crassus* and *Microzarkodina hagetiana* zones. In this interval, a total of 332 extraterrestrial chromite grains were found in 174 kg of rock. In southern Scania and in China, the distribution trends of extraterrestrial chromite grains are very similar to that at Kinnekulle. In southern Scania, some beds in the *L. variabilis* zone contain up to 6 extraterrestrial chromite grains per kilogram of rock, whereas only 2 grains were found in 125 kg in the beds spanning 7 m below[11]. In the Chinese sections, 89 kg of limestone below the *L. variabilis* zone yielded only 1 extraterrestrial chromite grain compared with 117 extraterrestrial chromite grains in 89 kg in the overlying beds (Fig. 2).

The first appearance of common extraterrestrial chromite grains in the lower *L. variabilis* zone in the three sections is a strong indication of the precise timing of the disruption of the L-chondrite parent body. The data also represent strong support for an increase by two orders of magnitude in the flux of micrometeorites and meteorites to Earth following the disruption event, as previously suggested on the basis of studies of the Swedish sections alone[9–11]. There is no indication that changes in sedimentation rates, on average a few millimetres per thousand years, can explain the observed major trend in extraterrestrial chromite concentrations, although individual beds may have formed at different rates. That the disruption event occurred in the lower *L. variabilis* zone is consistent with cosmic-ray-induced ^{21}Ne ages of chromite grains from the fossil meteorites[12]. In 5–10-Myr-old younger condensed limestone in the Gärde quarry, central Sweden, we found 9 extraterrestrial chromite grains in 23 kg of rock. This indicates that the extraterrestrial chromite flux is still enhanced compared with that before the asteroid breakup. The low pre-breakup concentrations of extraterrestrial chromite grains are similar to concentrations measured in similarly condensed sediments from much younger periods. For example, in 210 kg of pelagic limestone (average sedimentation rate about 2.5 mm kyr^{-1}) from the famous Late Cretaceous–Paleocene Gubbio section in Italy we found only 6 extraterrestrial chromite grains[20].

Our analyses of ^{187}Os/^{188}Os ratios in whole-rock limestone samples through the Kinnekulle section show a relatively stable

trend with ratios around 0.6–0.8 through the lower 11 m of section, but from the same bed where the extraterrestrial chromite grains become common and further up, ratios mainly lie in the range 0.3–0.5 (Fig. 2; Supplementary Information). The simplest explanation for this prominent change is an increasing influence of an extraterrestrial component ($^{187}Os/^{188}Os \sim 0.12$) at the expense of a detrital/hydrogenous Os component ($^{187}Os/^{188}Os \sim 0.8$) (ref. 21), well in line with conclusions based on extraterrestrial chromite trends.

Some of the best sections for studies of Ordovician invertebrate diversification occur in Baltoscandia[22]. We have established the Middle Ordovician biodiversity trends for brachiopods on the basis of bed-by-bed sampling of more than 30,000 fossils from 8 sections in Baltoscandia (Fig. 3). The phylum Brachiopoda dominated the benthos of the Palaeozoic evolutionary fauna both in abundance and diversity and formed a pivotal part of the suspension-feeding food chains of the era. The phylum was widely dispersed across shallow to deep-water environments around all of the palaeocontinents. We show here that there are two intervals in the succession when the Baltoscandian brachiopod fauna suffered dramatic changes—one within the lower part of the regional Volkhov stage and one at the base of the Kunda stage (Fig. 3). The largest change occurs during exactly the same interval when the L-chondritic extraterrestrial flux peaks at the base of the Kunda stage, and when brachiopods more typical of the Palaeozoic evolutionary fauna, that is, orthides and strophomenides, diversified.

Modelling studies suggest an enhanced flux of extraterrestrial matter, including large asteroids, during 10–30 million years after major asteroid disruption events[23]. The L-chondrite parent-body breakup at 470 Myr ago is thought to have created the Flora family of asteroids[24]. These asteroids were particularly prone to enter Earth-crossing orbits because of their position relative to an important orbital resonance[23,24]. Apparently, the Middle Ordovician interval with enhanced extraterrestrial flux is broadly coincident with the main phase of the GOBE[1–3,15]. At least in Baltoscandia, the onset of the two events seems to coincide precisely (Figs 2, 3). Albeit speculative, the best explanation for the coincidence is that frequent impacts on Earth of large asteroids, fragments of the L-chondrite parent body, generated changes in the biota. Impact-related environmental perturbations may have accelerated a process driven also by intrinsic biological mechanisms. Although much contemporary research has focused on the negative effects of large impacts, such as in the Cretaceous–Tertiary boundary case[25], more minor and persistent impacts could generate diversity by creating a range of new niches across a mosaic of more heterogeneous environments. Such diversity increases are predicted by the well-established intermediate disturbance hypothesis, initially applied to diversity changes in coral reefs and tropical rainforests[26]. Frequent impacts may also have destabilized ecological communities, allowing invasive species to take over and displace incumbent communities. The ecological and taxonomic amplitudes of the Middle Ordovician biodiversification may be decoupled and there are important feedback loops in the process. This phase of the diversification is marked by a brachiopod takeover from trilobites in benthic communities, and the establishment of recumbent life modes and size increases in many brachiopod clades. However, in contrast to the carnivores and detritus feeders of the modern fauna, the Palaeozoic fauna was then dominated by a suspension-feeding benthos with low metabolic rates better equipped to deal with and benefit from major environmental disruptions.

There are about 170 known impact craters on Earth and their record shows that impacts may have been more common by a factor of 5–10 during the Middle Ordovician compared with other periods of the Phanerozoic[6,13]. Four of seventeen known impact craters in Baltoscandia (Granby, Lockne, Kärdla and Tvären craters) are of Middle to early Late Ordovician age. For only very few of Earth's craters has it been possible to determine the impactor type, but for at least the 458-Myr-old Lockne crater in central Sweden, chromite in resurge deposits has implicated an L-chondritic impactor[27].

The strata in China and Baltoscandia that we show are rich in fossil meteorites and/or extraterrestrial chromite grains have long been known to include horizons with unusual lithologies. Over several hundred thousand square kilometres in southern Sweden, the succession of homogeneous red orthoceratite limestone is interrupted by a 1-m-thick anomalous grey, clay-rich interval with a peculiar fauna. During deposition of this bed, centimetre-sized cystoids seem to have literally covered the sea floor of a major part of the Baltic Basin. In west Russia, peculiar ooid horizons characterize the interval, and in China, unusual mini-mounds interrupt the normal succession of nodular marl and limestone[28] (Fig. 2). The possible relationship of these anomalous lithologies and structures to asteroid impacts or other astronomical perturbations, such as Solar System gravity disturbances, certainly warrants further studies. As shown here, at least on a regional scale, there is a close temporal coincidence between major biological change and the disruption of the L-chondrite parent body.

Recently, the impactor at the Cretaceous–Tertiary boundary has been tied by modelling to an asteroid disruption event at 160 Myr ago (ref. 29), but this event may not have led to a pronounced asteroid shower as focused in time as the one in the Middle Ordovician, and it has not left any obvious signal in the collision history of present-day meteorites.

METHODS

For chromite searches, samples of typically 10–30 kg of limestone were crushed and decalcified first in 6 M HCl and then in 18 M HF at room temperature. The acid-insoluble fraction, 63–355 μm, was searched for opaque minerals under the binocular microscope. Picked grains were mounted in epoxy resin and polished to a flat surface using a 1 μm diamond slurry. Element analyses were carried out with a scanning electron microscope–energy dispersive spectrometer[9–11,27]. The extraterrestrial chromite grains are characterized first by high Cr_2O_3 contents of ~55–60 wt%, FeO concentrations in the range of ~25–30 wt%, low Al_2O_3 at ~5–8 wt% and MgO concentrations of ~1.5–4 wt%. The most discriminative feature, however, is narrow ranges of V_2O_3, ~0.6–0.9 wt%, and TiO_2, ~2.0–3.5 wt%, concentrations. For a grain to be classified as an extraterrestrial chromite grain, it has to have a composition within the defined ranges for all elements listed[10].

For Os analyses, whole-rock limestone samples were ground in an agate mortar. Between 3–10 g of powdered sediment was weighed, mixed with an isotopically enriched spike containing ^{190}Os, dried at room temperature over night and then mixed with borax, nickel and sulphur powder. After fusing the mixture for 90 min at 1,000 °C, the NiS bead was separated and dissolved in 6.2 M HCl and the residue filtered at 0.45 μm. Insoluble platinum-group-element-containing particles were dissolved in concentrated HNO_3 in a tightly closed Teflon vial at ~100 °C. After dissolution, the Teflon vial was chilled in ice water to minimize the escape of volatile OsO_4. Osmium was then extracted from this vial with the sparging method directly into the torch of a single-collector inductively coupled plasma mass spectrometer (Finnigan Element). Typical Os blanks are < 1 pg g^{-1}. Depending on the Os concentration, the precision in $^{187}Os/^{188}Os$ is between 0.5% and a few per cent. The details of the method and an evaluation of the accuracy and precision of the data have been published elsewhere[30].

Received 25 July 2007; accepted 24 October 2007; published 16 December 2007.

References

1. Sepkoski, J. J. Jr. A factor analytic description of the Phanerozoic marine fossil record. *Paleobiology* **7**, 36–53 (1981).
2. Webby, B. D., Paris, F., Droser, M. L. & Percival, I. G. (eds) *The Great Ordovician Biodiversification Event* (Columbia Univ. Press, New York, 2004).

3. Harper, D. A. T. The Ordovician biodiversification: Setting an agenda for marine life. *Palaeogeogr. Palaeoclimatol. Palaeoecol.* **232**, 148–166 (2006).
4. Heymann, D. On the origin of hypersthene chondrites: Ages and shock effects of black chondrites. *Icarus* **6**, 189–221 (1967).
5. Keil, K., Haack, H. & Scott, E. R. D. Catastrophic fragmentation of asteroids: Evidence from meteorites. *Planet. Space Sci.* **42**, 1109–1122 (1994).
6. Schmitz, B., Tassinari, M. & Peucker-Ehrenbrink, B. A rain of ordinary chondritic meteorites in the early Ordovician. *Earth Planet. Sci. Lett.* **194**, 1–15 (2001).
7. Bridges, J. C. *et al*. Petrographic classification of mid-Ordovician fossil meteorites from Sweden. *Meteorit. Planet. Sci.* (2007, in the press).
8. Greenwood, R. C., Schmitz, B., Bridges, J., Hutchison, R. & Franchi, I. A. Disruption of the L chondrite parent body. New oxygen isotope evidence from Ordovician relict chromite grains. *Earth Planet. Sci. Lett.* **262**, 204–213 (2007).
9. Schmitz, B., Häggström, T. & Tassinari, M. Sediment-dispersed extraterrestrial chromite traces a major asteroid disruption event. *Science* **300**, 961–964 (2003).
10. Schmitz, B. & Häggström, T. Extraterrestrial chromite in Middle Ordovician marine limestone at Kinnekulle, southern Sweden—Traces of a major asteroid breakup event. *Meteorit. Planet. Sci.* **41**, 455–466 (2006).
11. Häggström, T. & Schmitz, B. Distribution of extraterrestrial chromite in Middle Ordovician Komstad Limestone in the Killeröd quarry, Scania, Sweden. *Bull. Geol. Soc. Den.* **55**, 37–58 (2007).
12. Heck, P. R., Schmitz, B., Baur, H., Halliday, A. N. & Wieler, R. Fast delivery of meteorites to Earth after a major asteroid collision. *Nature* **430**, 323–325 (2004).
13. Korochantseva, E. V. *et al*. L-chondrite asteroid breakup tied to Ordovician meteorite shower by multiple isochron ^{40}Ar–^{39}Ar dating. *Meteorit. Planet. Sci.* **42**, 113–130 (2007).
14. Droser, M. L. & Sheehan, P. M. Palaeoecology of the Ordovician radiation; resolution of large-scale patterns with individual clade histories, palaeogeography and environments. *Geobios* **30** (suppl. 1), 221–229 (1997).
15. Sepkoski, J. J. Jr. in *Ordovician Odyssey: Short Papers for the Seventh International Symposium on the Ordovician System* (eds Cooper, J. D., Droser, M. L. & Finney, S. C.) (Pacific Section Society for Sedimentary Geology, Book 77, Fullerton, California, 1995).
16. Hammer, Ø. Biodiversity curves for the Ordovician of Baltoscandia. *Lethaia* **36**, 305–314 (2003).
17. Sweet, W. C. *The Conodonta. Morphology, Taxonomy, Palaeoecology, and Evolutionary History of a Long-Extinct Animal Phylum* (Clarendon, Oxford, 1988).
18. Peterson, K. J. Macroevolutionary interplay between planktic larvae and benthic predators. *Geology* **33**, 929–932 (2005).
19. Vecoli, M., Lehnert, O. & Servais, T. The role of marine microphytoplankton in the Ordovician Biodiversification Event. *Notebooks Geol. Memoir* **2005/02**, 69–70 (2005).
20. Cronholm, A. & Schmitz, B. Extraterrestrial chromite in latest Maastrichtian and Paleocene pelagic limestone at Gubbio, Italy: The flux of unmelted ordinary chondrites. *Meteorit. Planet. Sci.* (in the press).
21. Peucker-Ehrenbrink, B. & Ravizza, G. The marine osmium isotope record. *Terra Nova* **12**, 205–219 (2000).
22. Rasmussen, C. M. Ø., Hansen, J. & Harper, D. A. T. Baltica: A mid Ordovician diversity hotspot. *Hist. Biol.* **19**, 255–261 (2007).
23. Zappalà, V., Cellino, A., Gladman, B. J., Manley, S. & Migliorini, F. Asteroid showers on Earth after family breakup events. *Icarus* **134**, 176–179 (1998).
24. Nesvorny, D., Vokrouhlicky, D., Bottke, W. F., Gladman, B. & Häggström, T. Express delivery of fossil meteorites from the inner asteroid belt to Sweden. *Icarus* **188**, 400–413 (2007).
25. Alvarez, L. W., Alvarez, W., Asaro, F. & Michel, H. V. Extraterrestrial cause for the Cretaceous–Tertiary extinction. *Science* **208**, 1095–1108 (1980).
26. Connell, J. H. Diversity in tropical rain forests and coral reefs. *Science* **199**, 1302–1310 (1978).
27. Alwmark, C. & Schmitz, B. Extraterrestrial chromite in the resurge deposits of the early Late Ordovician Lockne crater, central Sweden. *Earth Planet. Sci. Lett.* **253**, 291–303 (2007).
28. Zhang, J. *Middle Ordovician Conodonts from the Atlantic Faunal Region and the Evolution of Key Conodont Genera*. Thesis, Univ. Stockholm (1998).
29. Bottke, W. F., Vokrouhlicky, D. & Nesvorny, D. An asteroid breakup 160 Myr ago as the probable source of the K/T impactor. *Nature* **449**, 48–53 (2007).
30. Peucker-Ehrenbrink, B., Bach, W., Hart, S. R., Blusztajn, J. S. & Abbruzzese, T. Rhenium-osmium isotope systematics and platinum group element concentrations in oceanic crust from DSDP/ODP Sites 504 and 417/418. *Geochem. Geophys. Geosyst.* **4**, 8911 (2003).

Acknowledgements

This study was supported by financial support to B.S. from the National Geographic Society, Swedish Research Council (VR) and Crafoord Foundation and to D.A.T.H. from the Carlsberg Foundation. This is a contribution to International Geological Correlation Programme project 503.
Correspondence and requests for materials should be addressed to B.S.
Supplementary Information accompanies this paper on www.nature.com/naturegeoscience.

SUPPLEMENTARY INFORMATION

Asteroid breakup linked to Great Ordovician Biodiversification Event

Table 1. The distribution of extraterrestrial chromite (EC) in mid-Ordovician limestone.

Location and depth of sample (m)	Sample size (kg)		EC grains (kg^{-1})
Kinnekulle, south[1]			
+8.50 to +8.65	28.0	11	0.4
	12.6	21	1.7
+2.58 to +2.73	19.0	26	1.4
+2.50 to +2.58	10.7	20	1.9
+0.87 to +1.05	24.6	23	0.9
	13.3	28	2.1
+0.62 to +0.77	17.7	30	1.7
+0.32 to +0.56	24.0	41	1.7
+0.14 to +0.31	7.3	22	3.0
+0.08 to +0.32	26.0	87	3.3
0.00 to +0.14	18.7	34	1.8
- -0.82	22.8	6	0.3
-0.82 to -0.97	25.4	0	0
-1.47 to -1.69	28.0	1	0.04
-2.35 to -2.60	31.7	0	0
-2.60 to -2.85	30.2	0	0
-3.12 to -	28.1	1	0.04
-3.27 to -3.45	27.7	1	0.04
-3.45 to -3.95	31.3	0	0
-4.30 to -4.50	28.1	0	0
-4.50 to -	20.6	2	0.1
-5.00 to -5.25	30.5	0	0
-5.45 to -5.70	28.0	0	0
-5.88 to -	23.1	0	0
-6.08 to -6.18	20.0	0	0
-9.05 to -9.15	26.4	0	0
South Scania, south Sweden[2]			
Fågelsång			
6.85 to 6.95	8.9	16	1.8
6.65 to 6.75	10.4	17	1.6
Killeröd			
11.25 to 11.40	27.4	17	0.6

10.81 to 10.90		3	0.1
	23.8	56	2.4
9.88 to 10.02	23.6	74	3.1
	13.5	53	3.9
9.73 to 9.79	17.8		
9.71 to 9.73		12	
8.50 to 8.72	28.4	8	0.3
7.67 to 7.75	28.4	1	0.04
6.45 to 6.60	27.2	1	0.04
5.63 to 5.78	16.6	0	0
4.21 to 4.35	24.4	0	0
2.49 to 2.59	28.4	0	0
Puxi River-Fenxiang, Hubei, China[3]			
14.6	8.5	5	0.6
14.4	13.0	48	3.7
13.2	12.8	23	1.8
10.4	11.0	11	1.0
10.1	13.0	11	0.8
9.0	13.0	15	1.2
8.9 (F)	0.8	2	2.3
8.6	13.4	1	
8.4 (F)		0	0
7.8 (F)	1.5	1	0.7
5.8	14.8	1	0.07
4.4	13.0	0	0
4.2	10.7	0	0
3.7	14.0	0	0
2.9	14.3	0	0
0.5	12.1	0	0
0.3	9.6	0	0
Gärde quarry, central Sweden[4]			
2.70 to 3.00	22.8	9	0.4

[1] Composite section across the Thorsberg and Hällekis quarries. The depths are relative to the base of the Arkeologen bed, for further details, see Schmitz and Häggström (2006).
[2] Depths for the Fågelsång section according to log in Stouge and Nielsen (2006), and for Killeröd section the log of Nielsen (1995), see further Häggström and Schmitz (2007).
[3] Depths relative to the base of the Guniutan Formation, see Zhang (1998). F = sample from Fenxiang section.
[4] Depth according to log in Löfgren (1978).

Table 2. The distribution of Os and $^{187}Os/^{188}Os$ through the Hällekis section at Kinnekulle

Depth (m)[1]	Os (pg/g)	2σ	Os	2σ
+3.00	14.6	0.70		0.0096
+2.70	9.1	0.04	0.6398	0.0050
+2.60		0.06	0.6032	
+2.50	7.9	0.04	0.6810	0.0078
+0.50	9.0	0.04	0.5641	0.0069
+0.42	9.0	0.22	0.6600	0.0245
+0.36	35.7	0.17		0.0032
+0.30	10.2		0.5331	0.0068
+0.28	22.1	0.17	0.2381	0.0060
+0.19	7.2	0.11	0.5295	0.0129
+0.17	4.9	0.11	0.5730	0.0279
+0.09	6.6	0.11	0.5727	0.0231
+0.07	5.6	0.12	0.4710	0.0237
+0.04	25.1	0.17	0.2413	0.0063
+-0.00	17.2	0.16	0.4995	0.0112
-0.03	27.1	0.28	0.4401	0.0089
-0.15	5.1	0.11	0.5150	0.0215
-0.24	15.0	0.17	0.3460	0.0083
-0.29	14.2	0.12	0.5043	0.0093
-0.35	13.0	0.07	0.5630	0.0103
-0.38	6.2	0.12	0.5390	0.0174
-0.48	7.3	0.10	0.5452	0.0149
-0.54	7.7	0.13	0.3657	0.0150
-0.60	15.7	0.34	0.3145	0.0227
-0.85	12.9	0.07	0.7118	0.0063
-1.10	4.6	0.10	0.7588	0.0319
-1.35	10.1	0.06	0.8081	0.0081
-1.85	14.8	0.06	0.7233	0.0035
-2.33	13.4	0.07	0.8141	0.0110
-2.60	8.6	0.05	0.6979	0.0095
-3.35	11.0	0.05	0.7072	0.0075
-3.85	9.7	0.11	0.7180	0.0199
-4.35	16.7	0.10	0.7278	0.0097
-4.85	11.7	0.08	0.7097	0.0106
-5.35	14.7	0.10	0.6760	0.0096
-5.85	16.5	0.06	0.5849	0.0037
-6.35	15.4	0.13	0.6740	0.0116
-6.85	16.0	0.16	0.6675	0.0141
-7.35	16.7	0.10	0.3336	0.0061
-7.85	14.0	0.07	0.6678	0.0080
-8.35	13.6	0.09	0.6661	0.0086
-8.85	9.8	0.08	0.8013	0.0141
-9.35	5.3	0.05	0.7192	0.0129
-9.85	6.6	0.05	0.5995	0.0083
-10.35	8.9	0.06	0.6237	0.0080

-10.85	9.7	0.05	0.6964	0.0063
-11.35	5.5	0.05	0.7729	0.0102
-11.90	5.8	0.07	0.6835	0.0117

[1] Depth relative to the base of the Arkeologen bed, see Schmitz *et al.* (2001) and Schmitz and Häggström (2006).

References for Supplementary Information

Häggström, T. & Schmitz, B., *Bull. Geol. Soc. Den.* **55**, 37 (2007).

Löfgren, A., *Fossils and Strata* **13**, 1 (1978).

Nielsen, A. T., *Fossils and Strata* **38**, 1 (1995).

Schmitz, B. & Häggström, T., *Meteorit. Planet. Sci.* **41**, 455 (2006).

Schmitz, B., Tassinari, M. & Peucker-Ehrenbrink, B., *Earth Planet. Sci. Lett.* **194**, 1 (2001).

Stouge, S. & Nielsen, A. T., *Bull. Geol. Soc. Den.* **50**, 75 (2003).

Zhang, J., thesis, Stockholm University (1998).

V

Distribution of Os and $^{187}Os/^{188}Os$ through the Middle Ordovician Orthoceratite Limestone at Hällekis, Kinnekulle, Sweden

Anders Cronholm

Department of Geology, GeoBiosphere Science Centre, Sölvegatan 12, SE-223 62 Lund, Sweden
E-mail: anders.cronhom@geol.lu.se

In manuscript

Index words:
osmium
osmium isotopes
extraterrestrial chromite
meteorite
Arenig-Llanvirn

Abstract

New osmium (Os) abundance and isotopic ($^{187}Os/^{188}Os$) data is reported for the Middle Ordovician Orthoceratite Limestone at the Hällekis quarry, Kinnekulle, southern Sweden. In all, 48 whole-rock samples were analysed from a 14.9 m thick interval of the upper part of the homogenous condensed section representing the Lanna, Täljsten, and lower Holen Limestones. Particular focus was given to Os in relation to the first appearance of sediment-dispersed extraterrestrial chromite (EC) grains at -1.59 m below the base of the Täljsten interval. The abundance of EC and fossil meteorites in these beds have been related to the major break-up of the L-chondrite parent body in the main asteroid belt at ~470 Ma. The $^{187}Os/^{188}Os$ ratios throughout the initial ~11 m of the succession demonstrate a relatively stable trend, with an average ratio of 0.71 (ranging 0.60–0.81), which represent normal background levels, dominated by continent-derived Os. At the first appearance of common EC grains, $^{187}Os/^{188}Os$ ratios are abruptly reduced from 0.71 to 0.31, and less radiogenic ratios are thereafter maintained in the ascending limestone beds (mean 0.46). It is hypothesized that this change is due to an increased influence of an extraterrestrial Os component ($^{187}Os/^{188}Os$ ~0.13) at the expense of radiogenic continental and hydrogenous Os (average ~1.54 and ~1.06, respectively), which corresponds with observed trends in the flux of fossil meteorites and EC at Kinnekulle during the Middle Ordovician. This is corroborated by stable $^{87}Sr/^{86}Sr$ data across the Arenig-Llanvirn boundary at Hällekis.

1. INTRODUCTION

The Middle Ordovician Orthoceratite Limestone at the Hällekis quarry, Kinnekulle, southern Sweden (Fig. 1), has been the target for several studies on sedimentology (e.g. Lindström et al. 1971, 1979) and biostratigraphy (e.g. Zhang 1998; Tinn and Meidla 2001; Villumsen et al. 2001; Löfgren 2003). Additionally, Schmitz et al. (2003) and Schmitz and Häggström (2006) have detected a major contribution of particulate extraterrestrial (ET) material at Hällekis, characterized by high abundances of sediment-dispersed chondritic chromite (EC) across the Arenig-Llanvirn boundary (Fig. 2), corresponding to the Middle Darriwilian and stage slice Dw2 (Bergström et al. 2009). These coarse opaque grains (>63μm) originate from dissolved meteorites/micrometeorites, as weathering-resistant accessory minerals. The survey was instigated by the discovery of numerous fossil meteorites in coeval strata in the Thorsberg quarry (Schmitz et al. 1996, 1997, 2001), located only ~4 km southeast of the Hällekis quarry. The elevated accretion rates of ET material at Hällekis are related to the break-up of the L-chondrite parent body in the main asteroid belt at 470 ±6 Ma (Haack et al. 1996; Korochantseva et al. 2007), readily verified by chemical composition (Schmitz et al. 2003; Schmitz and Häggström 2006), inclusion analysis (Alwmark and Schmitz 2009) and cosmic-ray exposure ages (Heck et al. 2004, 2008) of sediment-dispersed EC grains and EC from the fossil meteorites, respectively. Additional affirmation is provided by oxygen isotopic (Greenwood et al. 2007), petrographic and textural analyses (Schmitz et al. 2001; Bridges et al. 2007) of the relict meteorites. The enhanced accumulation rates of ET matter (by a minimum of two orders-of-magnitude) recorded in the limestone beds at Kinnekulle have recently been correlated on a global scale, based on EC-enrichments in sediments at the

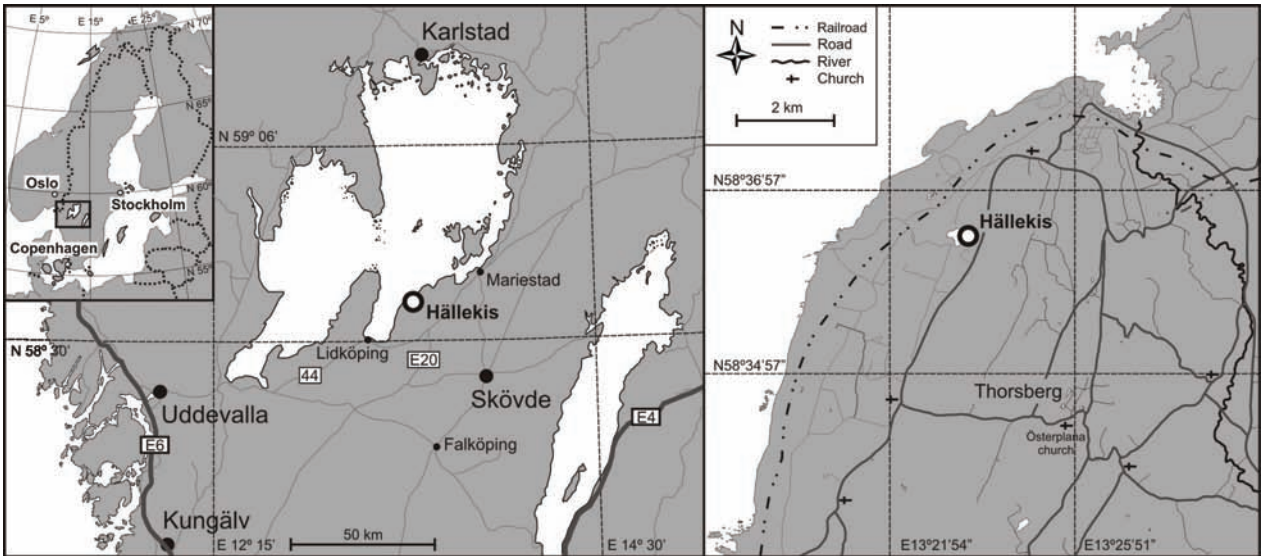

Fig. 1. Map of Scandinavia and parts of Västergötaland, with the geographical location of the Hällekis quarry at Kinnekulle.

Puxi River section, Hubei Province, central China (Cronholm and Schmitz, 2009), and at the Baltic-Ladoga Klint section, Russia (Korochantsev et al. 2009).

The purpose of this paper is to investigate potential changes in the marine osmium (Os) isotope record at Hällekis, associated with the meteorite bombardment of Earth (lasting a few million years) subsequent to the break-up of the L-chondrite parent body at ~470 Ma. This new Os data supplements previous EC studies and will constrain the timing of the first appearance of common EC in the marine sediments. It will thus reinforce our understanding of the events on Earth following the massive disruption event.

2. THE OSMIUM ISOTOPE SYSTEMATICS

Osmium is a recognized, highly sensitive proxy for distinguishing primitive (undifferentiated) ET material, enriched in platinum group elements (PGE; by a factor of 10^2-10^5), from continent-derived crustal rocks (e.g. Esser and Turekian 1988, 1993; Koeberl and Shirey, 1997; Peucker-Ehrenbrink 2001). Furthermore, recent studies show that global changes in seawater/ocean compositions, and related changes in input from sources, can be traced in the marine Os isotopic ($^{187}Os/^{188}Os$) record. This system is based on the decay of ^{187}Re (rhenium-187; half-life: 41.6 Gyr; Smoliar et al. 1996) to radiogenic ^{187}Os. As a result of continued decay, the amount of ^{187}Os increases with time. The initial $^{187}Os/^{188}Os$ ratio (at the time when the system became closed for Re and Os) can be calculated by associating the measured ^{187}Os and ^{187}Re values with the non-radiogenic ^{188}Os. It is believed that the $^{187}Os/^{188}Os$ ratio of oceans is governed by a three-component mixture of continental (rivers, groundwater, aeolian dust), oceanic crust (hydrothermal fluids and submarine alterations) and extraterrestrial (cosmic dust and micrometeorites) Os (e.g. Esser and Turekian 1988). Riverine particulate matter ($^{187}Os/^{188}Os$ ~1.4; Levasseur et al. 1999) and aeolian loess ($^{187}Os/^{188}Os$ ~1.54; Peucker-Ehrenbrink and Jahn 2001) represent eroded continental crust, and are the primary sources of radiogenic Os in the oceans, contributing ~70 to 80% of the total Os budget in the oceans (Sharma et al. 1999). In contrast to the ratios of radiogenic Os sources, the average oceanic crust (mantle-derived) and ET matter have uniformly low (unradiogenic) $^{187}Os/^{188}O$ signatures, of ~0.13 (e.g. Meisel et al. 1996, 2001). The differentiation between crustal and mantle $^{187}Os/^{188}Os$ ratios can be used as a powerful isotopic tracer of material cycling in the surface environment (Ravizza et al. 1996; Sharma et al. 1997). The average $^{187}Os/^{188}Os$ composition of seawater (average modern: ~1.06: e.g. Sharma et al. 1997; Levasseur et al. 1998; Woodhouse et al. 1999) depends on the varying contribution of dissolved Os from its sources (see above), and its composition has varied significantly during the late Phanerozoic, exemplified by the wide range in ratios registered during the Jurassic and Cretaceous Periods ($^{187}Os/^{188}O$: ~0.20-0.80; e.g. Cohen and Coe, 1999; Peucker-Ehrenbrink et al. 1995; Peucker-Ehrenbrink 1996; Peucker-Ehrenbrink and Ravizza 2000a; Ravizza 2007). Widom et al. (2004) have calculated the initial $^{187}Os/^{188}Os$ of Middle to Late Ordovician seawater to ~0.53 (±0.04), and propose that the low value may reflect relatively low continental weathering rates during this period. The slow reduction of seawater strontium isotope ($^{87}Sr/^{86}Sr$) ratios recorded during the Ordovician may support this, possibly related to declining Pan African orogenesis (Qing et al. 1998). Furthermore, there are several terrigenous processes that may result in the enrichment of Os in marine sediments, such as scavenging of dissolved Os from seawater (Ravizza and Turekian 1992), intervention by microfauna (Dyer et al. 1989), and redistribution caused by physiochemical changes during post-burial processes in sediments (Colodner et al. 1992).

3. STUDY AREA

During the Middle Ordovician, most of Baltoscandia, including southern Sweden, was covered by a vast shallow epicontinental sea, in which the characteristic Orthoceratite Limestone was formed (Lindström et al. 1971, 1979). The Hällekis section (58°36'N, 13°23'E; Fig. 1) exposes a ~50 m thick succession of homogeneous Orthoceratite Limestone beds that was deposited at low net sedimentation rates (2 ± 1 mm kyr^{-1}), resulting in the condensed nature of the section (Lindström et al. 1971,1979). The contribution of organic matter in the sediments is generally exceedingly low (~0.1%; Schmitz et al. 1996). The massive limestone beds shade from red to brownish red throughout the section, with the exception of the 1.2-1.4 m thick, grey Täljsten interval at +0.77 m above the base of the Arkeologen bed (Fig. 2). The shift in color, relative enrichment in phosphates, and fossil abundance of this bed indicate an episode with low oxygen conditions (Lindström et al. 1979; Schmitz et al. 1996), possibly associated with a gradual sea level regression and enhanced sedimentation rates, as suggested by changes in the conodont fauna (J. Mellgren, personal communication, 2009). Hard- (or firm-) grounds (primarily corrosional) with a varying degree of surface mineralization are common at Hällekis, probably representing extended periods (1-10 kyr) of non-deposition (Lindström 1979). The condition of well-preserved non-orientated cephalopod shells further supports a calm setting, suggesting a water depth of ~100-300 m (or deeper based on the regional structural depression at Kinnekulle) (Chen and Lindström 1991).

Meteorites that survived atmospheric entry and reached the firm sea floor, would rapidly dissolve in this environment (time for dissolution in a dry terrestrial setting: 20-30 kyr; Bevan et al. 1998; Bland 2001), and subsequently disperse the EC content in the contiguous sediments. Consequently, EC-rich sediments may also have experienced enrichment in meteoritic Os and tiny insoluble PGE-rich inclusions.

4. MATERIALS AND METHODS

The $^{187}Os/^{188}Os$ ratios, Os abundance (ppt) and elemental concentrations (wt%) have been analysed in 48 whole-rock samples from the Hällekis section, Kinnekulle, collected in a span representing the *Paroistodus originalis* to *Yangtzeplacognathus crassus* conodont zones (from 11.90 m below to 3.00 m above the base of the Arkeologen bed; Fig. 2). The focal point of the 14.9 m thick limestone succession was the first appearance of common EC grains, between -0.85 m and -0.60 m representing the uppermost *Lenodus antivariabilis* zone, and related variations in the geochemical record. The sequential, grey Täljsten interval (in the *L. variabilis* zone) was intently circumvented, due to its conspicuous reduced nature and reports of highly radiogenic $^{187}Os/^{188}Os$ values (3.719; Schmitz et al. 1997). Sampling was resumed from +2.5 m to +3.0 m (in the lower *Y. crassus* zone), and was investigated exclusively for $^{187}Os/^{188}Os$ compositions and Os concentrations (4 samples; Fig. 2 and 3 A-B).

For Os analyses, whole-rock samples were ground into a fine powder with an agate mortar. Between 3-10 g of powdered sample was mixed with an isotopically enriched spike (containing ^{99}Ru, ^{105}Pd, ^{190}Os, ^{191}Ir and ^{198}Pt), dried at room temperature over night and then mixed with borax, nickel and sulfur powder at a typical sample/flux ratio of two. After fusing the mixture for 90 minutes at 1000°C in a glazed ceramic crucible, the melt was allowed to cool and the NiS bead was separated from the glass. The bead was then dissolved in hydrochloric acid (6.2M HCl) and the residue filtered through 0.45 µm cellulose filter paper. Insoluble PGE-containing particles on the filter paper were dissolved together with the filter in 1 ml concentrated nitritic acid (HNO_3) in a tightly closed Teflon vial at ~100°C for about 60 minutes immediately before the analysis of Os. After dissolution the Teflon vial was chilled in ice water to minimize the escape of volatile OsO_4. Osmium was then extracted from this vial with the sparging method (Hassler et al. 2000) that relies on purging dissolved OsO_4 with inert Ar carrier gas and transferring the gas mixture directly into the torch of a single-collector ICP-MS (Finnigan Element). The details of the method are described in Hassler et al. (2000), and the accuracy and precision of the analytical data have been evaluated in detail by Peucker-Ehrenbrink et al. (2003) using various international reference materials and community standards. In addition, all samples (with the exception of the four located above the Täljsten) were analysed for major elements with an inductively coupled plasma-atomic emission spectrometer (ICP-AES) at Svensk Grundämnesanalys AB in Luleå, Sweden (for details, see Schmitz et al. 2004). The relative reproducibility (2σ) of these analyses is generally in the range 0.5–6%.

5. RESULTS

The Os concentrations and $^{187}Os/^{188}Os$ results from this study are summarized in Table 1, with elemental plots shown in Figures 2-4. The $^{187}Os/^{188}Os$ ratio in whole-rock samples ranges from 0.1883 to 0.8141, with an average of 0.5898. The initial 11 m of the succession (from upper *P. originalis* to uppermost *L. antivariabilis* conodont zones) and the EC-rich interval (uppermost *L. antivariabilis* zone and further up) present diverging average $^{187}Os/^{188}Os$ values of 0.7102 (0.5995-0.8141) and 0.4602 (0.1883-0.6600), respectively. Although the results are significantly below the $^{187}Os/^{188}Os$ ratio of radiogenic modern seawater (~1.06; Sharma et al. 1997; Levasseur et al. 1998; Woodhouse et al. 1999), the overall average is comparable to the suggested composition of the Ordovician oceans, 0.53 ± 0.04 (Widom et al. 2004). The values of the more radiogenic background strata (i.e. below -0.85 m) correspond better to average late Cenozoic ratios, of 0.6-0.8 (e.g. Peucker-Ehrenbrink and Ravizza 2000b), while the EC-rich interval reflects an increased influence of unradiogenic Os. This is indicated by the results from three separate sam-

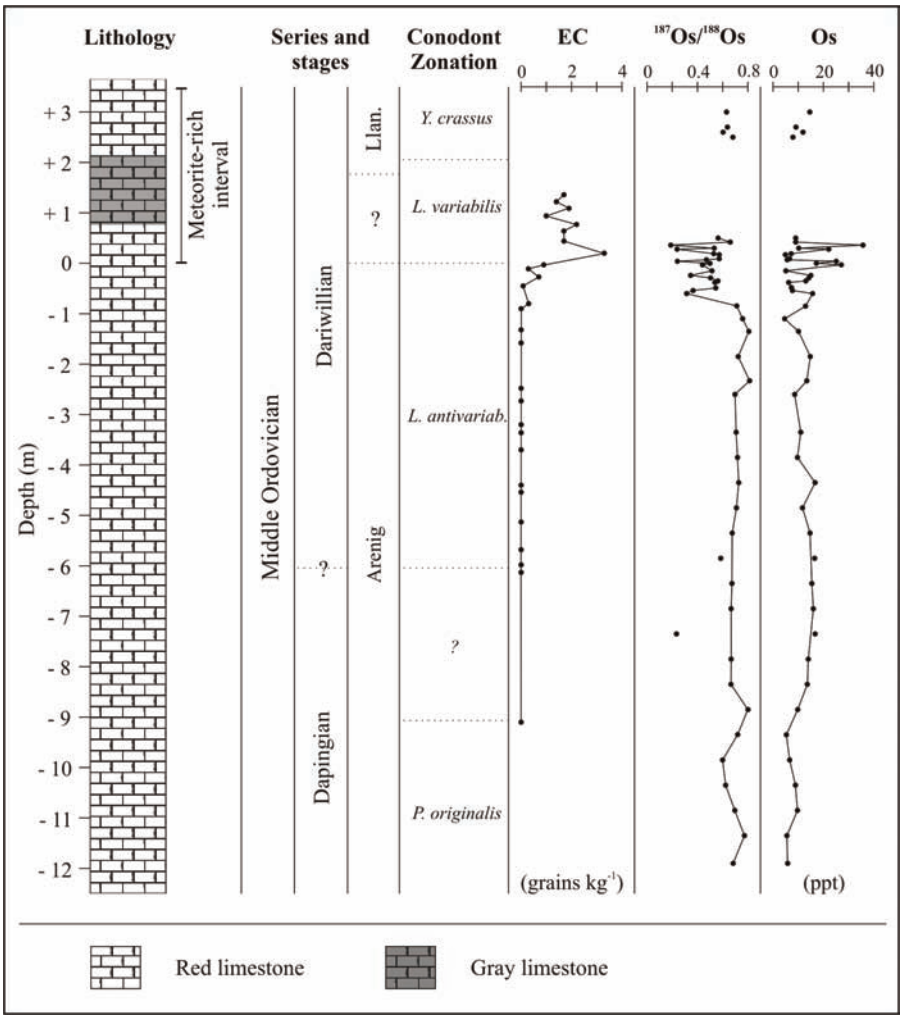

Fig. 2. The variation of EC content (grains per kg; Schmitz and Häggström 2006), $^{187}Os/^{188}Os$ ratio and Os content (ppt) across the Arenig-Llanvirn (early to middle Darriwilian) sequence at Hällekis, Kinnekulle, Sweden. Main trends are marked by solid lines, while the outliners in Os data (at -7.85 m and -5.85 m) are only represented by individual points. The scale gives the distance (in m) in the section from the base of the Arkeologen bed.

ples from this inteval (at +0.04, +0.28 and +0.36, respectively) that present ratios below 0.25, while having relatively elevated Os content (25.1, 22.1 and 35.7 ppt). Whole-rock Os concentrations range from 4.6 to 35.7 ppt, with a mean of 12.1 ppt. The distinction between the background and EC-rich intervals is not as well-pronounced in Os abundance, with the exception of a few high peaks in the upper strata. The average background Os concentration is somewhat lower than for the EC-rich interval (10.85 ppt and 13.20 ppt, respectively), whereas all measured Os concentrations may be considered slightly low compared to the content of modern pelagic carbonates (~42-87 ppt; Dalai and Ravizza 2006).

The strata at Hällekis is predominantly biogenic ($CaCO_3$: 71.8-91.4 wt%) with a minor contribution from lithogenic sources (SiO_2: 3.92-15.9 wt%; Al_2O_3: 1.25-5.56 wt%; K_2O: 0.35-1.49 wt%; Fe_2O_3: 0.89-2.49 wt%), and the carbonate abundance displays a close inverted correlation to (primarily) the silica component, most likely reflecting the balance between marine and continental detritus sources in the marine sediments. The influence of the lithogenic Os fraction is possibly shown through the casual relationship between variations in the abundance of Os and continental-derived elements (Si, Al, K, Fe), but the changes in Os abundance appears decoupled from the $^{187}Os/^{188}Os$ system in the strata that formed prior to the break-up event (Fig. 3 A-F). Moderate bed-by-bed variations in Os abundance and isotopic composition are observed in the EC-yielding interval, most likely caused by heterogeneity of powdered samples.

Table 1. The $^{187}Os/^{188}Os$ ratio, Os abundance (ppt) and elemental concentration (wt%) of whole-rock samples from the Hällekis section, Kinnekulle, Sweden.

Depth[a]	$^{187}Os/^{188}Os$	2σ	[Os][b]	2σ	Al_2O_3	$CaCO_3$	SiO_2	Fe_2O_3	K_2O	MgO	MnO_2	P_2O_5	TiO_2
+3.00	0.6391	0.0096	14.6	0.70	n.a.[c]	n.a.	n.a.	n.a.	n.a.	n.a.	n.a.	n.a.	n.a.
+2.70	0.6398	0.0050	9.1	0.04	n.a.	n.a.	n.a.	n.a.	n.a.	n.a.	n.a.	n.a.	n.a.
+2.60	0.6032	0.0069	11.9	0.06	n.a.	n.a.	n.a.	n.a.	n.a.	n.a.	n.a.	n.a.	n.a.
+2.50	0.6810	0.0078	7.9	0.04	n.a.	n.a.	n.a.	n.a.	n.a.	n.a.	n.a.	n.a.	n.a.
+0.50	0.5641	0.0069	9.0	0.04	1.83	88.57	5.62	1.01	0.527	0.614	0.300	0.044	0.069
+0.42	0.6600	0.0245	9.0	0.22	1.96	88.57	6.08	1.52	0.558	0.599	0.286	0.071	0.069
+0.36	0.1883	0.0032	35.7	0.17	1.42	91.43	4.54	1.22	0.390	0.590	0.294	0.170	0.058
+0.30	0.5331	0.0068	10.2	0.08	1.25	90.89	3.92	1.14	0.354	0.551	0.335	0.063	0.054
+0.28	0.2381	0.0060	22.1	0.17	1.51	91.07	4.68	0.90	0.427	0.585	0.402	0.047	0.067
+0.19	0.5295	0.0129	7.2	0.11	1.62	90.53	4.96	1.07	0.498	0.600	0.288	0.096	0.071
+0.17	0.5730	0.0279	4.9	0.11	1.92	88.39	5.80	1.75	0.534	0.606	0.290	0.092	0.094
+0.09	0.5727	0.0231	6.6	0.11	1.89	88.57	5.89	1.18	0.527	0.613	0.272	0.069	0.083
+0.07	0.4710	0.0237	5.6	0.12	1.77	89.11	5.48	1.85	0.524	0.594	0.265	0.051	0.076
+0.04	0.2413	0.0063	25.1	0.17	2.83	85.18	8.39	1.51	0.798	0.668	0.251	0.060	0.129
±0.00	0.4995	0.0112	17.2	0.16	2.54	86.61	7.55	1.12	0.697	0.662	0.248	0.060	0.106
-0.03	0.4401	0.0089	27.1	0.28	4.49	77.86	12.8	1.77	1.190	0.840	0.236	0.083	0.229
-0.15	0.5150	0.0215	5.1	0.11	1.83	90.53	5.70	1.24	0.514	0.602	0.254	0.115	0.080
-0.24	0.3460	0.0083	15.0	0.17	3.00	84.29	9.00	1.54	0.807	0.691	0.248	0.044	0.140
-0.29	0.5043	0.0093	14.2	0.12	5.07	75.89	14.2	2.19	1.370	0.896	0.202	0.088	0.260
-0.35	0.5630	0.0103	13.0	0.07	2.33	86.79	7.11	1.33	0.671	0.647	0.268	0.054	0.109
-0.38	0.5390	0.0174	6.2	0.12	2.07	86.96	6.41	1.06	0.584	0.565	0.248	0.052	0.105
-0.48	0.5452	0.0149	7.3	0.10	3.54	82.32	10.6	1.83	0.993	0.790	0.230	0.085	0.160
-0.54	0.3657	0.0150	7.7	0.13	1.85	88.93	5.72	1.23	0.534	0.599	0.252	0.077	0.078
-0.60	0.3145	0.0227	15.7	0.34	2.40	86.25	7.54	1.49	0.659	0.708	0.274	0.047	0.116
-0.85	0.7118	0.0063	12.9	0.07	4.77	76.07	13.3	1.83	1.310	0.837	0.202	0.070	0.234
-1.10	0.7588	0.0319	4.6	0.10	2.79	86.07	8.28	1.31	0.755	0.713	0.255	0.049	0.126
-1.35	0.8081	0.0081	10.1	0.06	3.78	80.18	11.0	1.72	1.030	0.797	0.217	0.073	0.171
-1.85	0.7233	0.0035	14.8	0.06	4.07	78.75	11.4	1.52	1.090	0.773	0.233	0.055	0.184
-2.33	0.8141	0.0110	13.4	0.07	3.84	80.18	10.7	2.16	1.010	0.755	0.230	0.058	0.160
-2.60	0.6979	0.0095	8.6	0.05	2.89	84.11	8.35	1.75	0.774	0.684	0.355	0.062	0.130
-3.35	0.7072	0.0075	11.0	0.05	3.01	83.21	8.94	1.43	0.818	0.750	0.261	0.057	0.132
-3.85	0.7180	0.0199	9.7	0.11	3.12	83.75	9.11	1.27	0.832	0.727	0.251	0.054	0.136
-4.35	0.7278	0.0097	16.7	0.10	3.29	82.68	9.93	1.48	0.892	0.754	0.217	0.046	0.149
-4.85	0.7097	0.0106	11.7	0.08	3.62	81.43	10.8	1.63	0.935	0.823	0.178	0.044	0.156
-5.35	0.6760	0.0096	14.7	0.10	5.00	74.82	14.1	1.92	1.380	0.913	0.160	0.054	0.245
-5.85	0.5849	0.0037	16.5	0.06	4.24	78.04	12.2	1.62	1.140	0.799	0.175	0.039	0.186
-6.35	0.6740	0.0116	15.4	0.13	5.56	71.79	15.9	2.24	1.490	0.943	0.156	0.111	0.283
-6.85	0.6675	0.0141	16.0	0.16	5.29	73.57	15.1	2.07	1.410	0.870	0.168	0.052	0.264
-7.35	0.3336	0.0061	16.7	0.10	3.05	84.11	9.32	1.48	0.803	0.680	0.209	0.039	0.143
-7.85	0.6678	0.0080	14.0	0.07	5.14	74.29	14.7	2.49	1.350	0.832	0.169	0.084	0.264
-8.35	0.6661	0.0086	13.6	0.09	4.22	79.11	12.3	1.72	1.120	0.777	0.175	0.049	0.184
-8.85	0.8013	0.0141	9.8	0.08	3.55	81.96	10.6	1.89	0.971	0.696	0.172	0.052	0.147
-9.35	0.7192	0.0129	5.3	0.05	3.02	85.71	9.21	1.53	0.783	0.729	0.161	0.036	0.139
-9.85	0.5995	0.0083	6.6	0.05	2.68	86.96	7.98	1.33	0.675	0.666	0.171	0.041	0.112
-10.35	0.6237	0.0080	8.9	0.06	3.12	84.82	9.31	1.45	0.856	0.722	0.164	0.044	0.138
-10.85	0.6964	0.0063	9.7	0.05	4.76	77.86	13.7	1.94	1.230	0.921	0.147	0.068	0.242
-11.35	0.7729	0.0102	5.5	0.05	3.10	85.18	9.42	1.41	0.813	0.743	0.154	0.031	0.135
-11.90	0.6835	0.0117	5.8	0.07	2.64	86.43	8.26	1.26	0.706	0.677	0.150	0.034	0.126

[a] Meters relative to the base of the Arkeologen bed; [b] ppt or pg Os g^{-1}; [c] Not available.

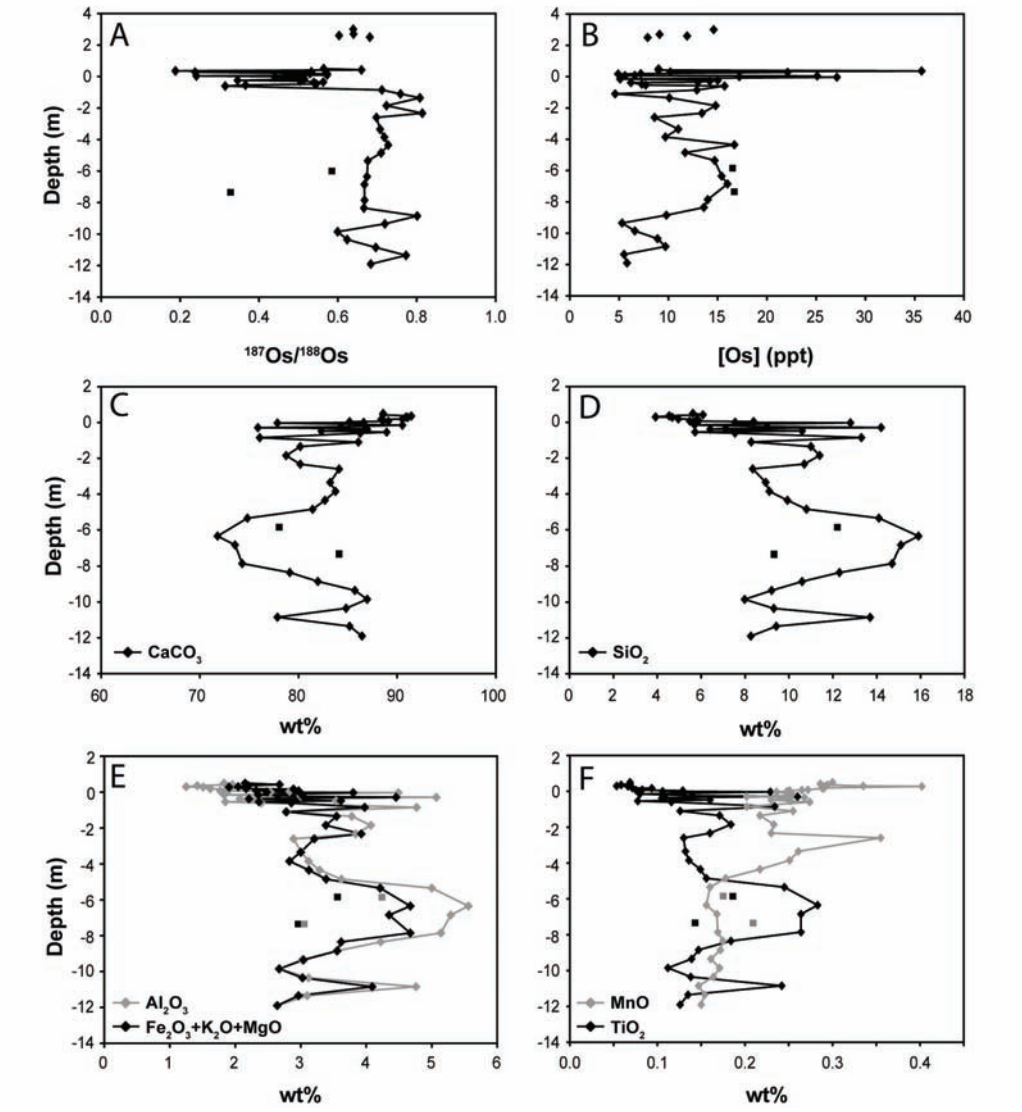

Fig. 3 A-D. Distribution of $^{187}Os/^{188}Os$ ratios, Os content (ppt) and main whole-rock elements (wt%) in the Hällekis section, Kinnekulle, Sweden. Main trends are marked by solid lines in element plots. The outliners at -7.85 m and -5.85 m are only represented by squares. The scale gives the distance (in m) in the section from the base of the Arkeologen bed. Note the negative $^{187}Os/^{188}Os$ excursion at -0.6 m (A).

6. DISCUSSION

6.1 Interpretation of Os data

During the Middle Ordovician, Earth experienced an extended period of enhanced flux of ordinary chondritic matter (e.g. Schmitz et al. 1997, 2001, 2003; Häggström and Schmitz 2007; Cronholm and Schmitz. 2009), and Os isotopic data from the Hällekis section clearly displays a gain in unradiogenic Os at the first appearance of common sediment-dispersed EC in the condensed limestone beds. The interval from -0.85 m and -0.60 m is marked by a major reduction in $^{187}Os/^{188}Os$, from 0.7118 to 0.3145, and relatively low (less radiogenic) values prevail in the following EC-rich strata. Interestingly, no corresponding significant change is observed in Os concentrations; however, a minor increase is instigated approximately at the base of the meteorite-rich interval (at ~0 m). If the observed decline in $^{187}Os/^{188}Os$ was related to a decrease in continental-derived (radiogenic) Os, an analogue negative trend in Os abundance would be expected in the marine record, which is not seen. The observed reduction in $^{187}Os/^{188}Os$ is consistent with previously reported periods of major enhanced ET flux during the Paleogene, i.e. the prolonged asteroid/meteorite or comet shower (and two verified major impacts) in the late Eocene (e.g. Dalai et al. 2006), and the impact event at the Cretaceous-Paleogene (K-T) bound-

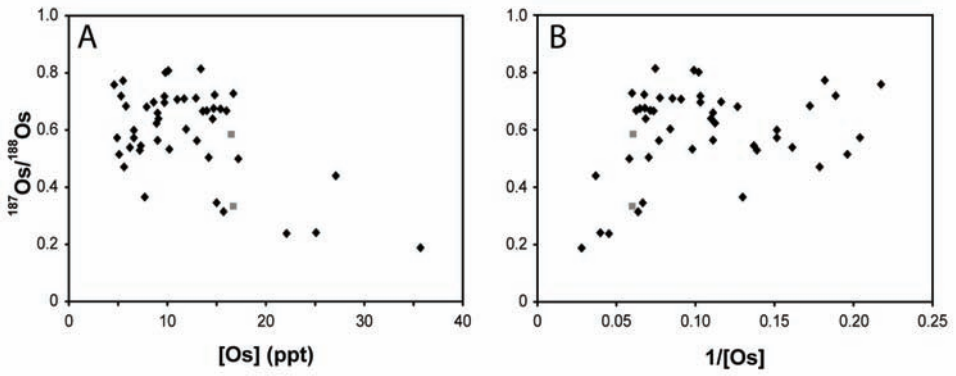

Fig. 4 A-B. Variation in (A) $^{187}Os/^{188}Os$ vs. Os content (in ppt) and (B) $^{187}Os/^{188}Os$ vs. inverse of Os content, respectively, for whole-rock samples from the Hällekis section, Kinnekulle, Sweden. The outliners at -7.85 m and -5.85 m are only represented by grey squares.

ary (e.g. Ravizza 2007). The $^{187}Os/^{188}Os$ excursion at Hällekis is, however, not as distinct in the marine record as the two episodes during the Paleogene. The Os concentrations (4.6 to 16.7 ppt) and radiogenic $^{187}Os/^{188}Os$ values (0.5995-0.8141) of strata below the EC-rich interval, most likely represents typical background values controlled by natural variations in the (low) continental Os input. This is supported by Os abundances and $^{187}Os/^{188}Os$ compositions studied in Middle to Late Ordovician (carbonate and shale) core samples from Serpent Mound, Ohio (USA), reporting about normal crustal Os values of 5-99 ppt and 0.714-6.083, respectively (Widom et al. 2004).

Peucker-Ehrenbrink and Ravizza (2000a) indicate that the modern input of ET Os (~200 mol yr^{-1}; Peucker-Ehrenbrink 1996) is to be considered negligible in the total Os budget, which is related to the increasing radiogenic contribution from the weathering of continents (e.g. the Himalayas). Sharma et al. (2007b) have calculated the modern flux of ET Os (cosmic dust and micrometeorites) in the oceans to 102 ±51 mol yr^{-1}, based on the estimated total delivery of ET matter to Earth (4±2 x 10^7 kg yr^{-1}; Love and Brownlee 1993) and the average Os content in meteorites (CI meteorite: 486 ng Os g^{-1}; Anders and Grevesse 1989), not including Os contributed by vaporization, melting and fragmentation of larger meteorites during atmospheric entry. Lal and Jull (2003) have estimated the Os contribution from these processes to between 161-413 mol yr^{-1}, resulting in a total ET Os of 263-515 (±51) mol yr^{-1}. Schmitz et al. (2001) have previously established that Earth experienced a two orders-of-magnitude increase in the flux of chondritic material across the Arenig-Llanvirn transition, corroborated by recent EC studies in Sweden (Schmitz et al. 2003; Schmitz and Häggström 2006; Häggström and Schmitz 2007) and China (Cronholm and Schmitz 2009). This would suggest that the ET Os contribution was amplified by a similar factor, giving an input of approximately 26-51 (±5) kmol yr^{-1}. This stands in strong contrast to the estimated annual riverine flux of ~1.5-1.7 kmol (Sharma and Wasserburg 1997; Levasseur et al. 1999), which is supposed to constitute ~70-80% of the total Os budget of the oceans. The estimated high contribution of ET Os to the oceans following the disruption event is, however, inconsistent with the relatively low Os concentrations (13.2-35.7 ppt) preserved in the EC-rich interval, and additional geochemical studies of this strata are required for further evaluation (possible Os loss during burial diageneis?).

6.2 Comparison with previous data

Evaluation of the new $^{187}Os/^{188}Os$ composition and Os abundance of whole-rock samples require a comparison with existing geochemical data for Hällekis (Schmitz et al. 1996, 1997). Schmitz et al. (1997) have previously introduced Os isotope data from three levels in the meteorite-yielding interval of the section (at approximately +0.40, +1.30 and +2.25 m), although their interpretations were based on a two-component mixture of Os, which excluded the significant hydrogenous component, and thus overestimated the ET contribution in the sediments. Peucker-Ehrenbrink and Ravizza (2000a) have further suggested that these samples only correspond to an average 'time-area product' of ~0.25 m^2 yr^{-1}, and should thus be regarded as undersampled. The results of Schmitz et al. (1996, 1997) illustrate, however, the sedimentary and geochemical complexity of the reduced, grey Täljsten interval (Fig. 2), as represented by facies changes and a high radiogenic $^{187}Os/^{188}Os$ value of 3.719. Decay correlations of the measured Re in the reduced interval resulted in negative initial $^{187}Os/^{188}Os$ values, suggesting an open-system behavior. The association of Os and Re in reducing environments is well-known, typically reflecting elevated enrichments correlated to the amount of total organic carbon of sediments (e.g. Ravizza and Turekian 1992; Cohen et al. 1999). It should, however, be noted that Os removal from seawater still occurs in organic-poor sediment under oxic condition, while Re is not easily removed under similar circumstances (possibly due to slow kinetics) (Yamashita et al. 2007). The two remaining

Os samples (at approximately +2.25 and +0.40 m), collected in red limestone above (Rödkarten) and below (Arkeologen) the grey Täljsten, present low Os isotopic compositions and concentrations comparable with the data presented in this paper, ranging from 0.2189 to 0.3934 and 17.1 to 51.4, respectively (Schmitz et al. 1997). Peucker-Ehrenbrink (2001) briefly discussed the low Os concentration in the pure carbonates throughout the Hällekis section, and suggested a negligible aeolian Os end member as a possible cause. This is in accordance with the proposed calm marine setting at Kinnekulle during the Middle Ordovician, as part of a shallow epicontinental sea constrained by a fine relief (Lindström et al. 1971, 1979). Furthermore, Schmitz et al. (1997) used $^{87}Sr/^{86}Sr$ as a proxy for coeval $^{187}Os/^{188}Os$, and hypothesized that these two isotopic systems were coupled, based on their observed coupling during late Cenozoic (Peucker-Ehrenbrink et al. 1995). This partial coupling of the Os and Sr isotopic systems is provided by continental inputs (Sharma et al. 1999), and Peucker-Ehrenbrink et al (1995) can show a rough positive correlation between the isotopic records of these two elements for the past ~40 Myr. It is commonly believed that this past coupling has been regulated by an increasing supply of more radiogenic Os and Sr from the weathering of the Himalayas (e.g. Peucker-Ehrenbrink et al. 1995), although Sharma et al. (1999) oppose a direct connection between the weathering of the Himalayas and the increasingly radiogenic Os composition of seawater. The $^{87}Sr/^{86}Sr$ values measured for the mid-Ordovician (0.70879-0.70886; Schmitz et al. 1997) are very similar to ratios reported by Quing et al. (1998) for the Arenig and Llanvirn Stages (0.7086-0.7089). These $^{87}Sr/^{86}Sr$ compositions are also comparable to the modern ocean ratio of ~0.70917 (Andersson et al. 1992; Dia et al. 1992). If the $^{87}Sr/^{86}Sr$ and $^{187}Os/^{188}Os$ systematics were coupled during the Middle Ordovician, one would expect higher, more radiogenic $^{187}Os/^{188}Os$ values at Hällekis, which is not supported by the current Os dataset of the condensed limestone beds. Apart from their similar overall performance, two major distinctions separate the behavior of the marine $^{187}Os/^{188}Os$ and $^{87}Sr/^{86}Sr$ systems; (1) seawater receives an additional non-radiogenic Os contribution from ET material, i.e. the non-radiogenic input of Os and Sr to oceans is partially decoupled (Peucker-Ehrenbrink and Ravizza 2000b; Sharma et al. 2007b); (2) the global residence time of Sr in seawater (~2-5 Myr; e.g. Faure 1986, Hodell et al. 1990) is about two orders-of-magnitude longer than for Os (37±14 kyr; Sharma et al. 2007a). The seawater record is thus too heavily buffered in Sr to detect short-term changes, while Os has the ability to recognize very rapid shifts in the marine environment (even suggested at glacial-interglacial timescales, i.e. ~3 kyr; Oxburgh 1998). The stable $^{87}Sr/^{86}Sr$ record at Hällekis is represented by a ~7.4 m thick interval across the Arenig-Llanvirn boundary, corresponding to ~3.7 Myr (calculated at sedimentation rate of 2 mm kyr^{-1}). If terrestrial sources were responsible for the enhanced non-radiogenic Os component recorded in the marine record, then a similar decline should have occurred in $^{87}Sr/^{86}Sr$ compositions. This supports the presence of an ET Os component during the recorded negative Os excursion at Hällekis.

6.3 Influence of extraterrestrial particles on $^{187}Os/^{188}Os$ records

The inconsistencies in bed-by-bed Os data from the EC-rich interval at Hällekis suggest that the powdered samples most likely are heterogeneous in nature, containing randomly distributed minute particles enriched in ET Os. As demonstrated in Fig. 4 A, samples with relatively high Os concentrations show direct correlation with decreasing $^{187}Os/^{188}Os$, most likely indicating the presence of an ET non-radiogenic component. Six samples from the EC-rich interval have relatively elevated Os concentrations (15.0-35.7 ppt) accompanied by the least radiogenic $^{187}Os/^{188}Os$ ratios recorded in the section, ranging 0.188-0.346. Conversely, the remaining samples from the EC-rich interval have intermediate Os values, between the typical terrestrial background levels and the small less radiogenic group just mentioned.

Dalai and Ravizza (2006) also reported sample heterogeneity in sample powders, and attribute this to unevenly distributed undissolved ET particles in samples. Recent studies have shown that during the passage through Earth´s atmosphere, friction heat of micrometeorites will cause ET Os to concentrate into small (~1 μg) Fe-Ni nuggets (Chen et al. 2005). After reaching the ocean, the nuggets sink rapidly in the water column, and may avoid dissolution before deposition due to the refractory nature of PGE. This is supported by the recovery of cosmic spherules (with chondritic Os/Ir of 1) in pelagic sediments, reported to contain minute (<10 μm) PGE-rich nuggets (Brownlee et al. 1984). Furthermore, Sharma et al. (1997) have estimated that as much as 75% of the ET Os budget may be deposited as undissolved cosmic particles on Earth. Future geochemical studies at Kinnekulle will thus be conducted on larger samples to avoid undersampling, as well as ensuring more representative samples. Furthermore, samples will be analysed in a minimum of triplicates to circumvent problems with inter-sample heterogeneity.

7. CONCLUSIONS

This study presents a succession of Os data across the Arenig-Llanvirn (lower and middle Darriwilian) sequence at Hällekis, Kinnekulle, coeval to the largest recorded disruption event in the main asteroid belt during the past 3 billion years – the break-up of the L-chondrite parent body at ~470 Ma. Following this event, Earth experienced a period of enhanced flux of meteorites/micrometeorites (by two orders-of-magnitude) that is distinctly marked in the marine record by a negative $^{187}Os/^{188}Os$ excursion. At the first appearance of common sediment-dispersed extraterrestrial chromite (EC) grains, a major decrease is observed in $^{187}Os/^{188}Os$ ratios, from 0.7102 to 0.3145, indicating enhanced non-radiogenic Os input to the marine environment. The stable $^{87}Sr/^{86}Sr$ record across the Arenig-Llanvirn transition, representing ~3.7 Myr of

sedimentation, corroborates an extraterrestrial unradiogenic Os origin for the negative $^{187}Os/^{188}Os$ excursion at Hällekis.

ACKNOWLEDGMENTS

I am thankful to Birger Schmitz for generously providing the osmium data from the Hällekis quarry, Kinnekulle, southern Sweden, and for comments assuring the completion of this study. Bernard Peucker-Eherenbrink helped with the analyses of the samples at Woods hole Oceanographic Institution, Woods Hole (MA). I also extend my gratitude to Sanna Holm and Erik Uddman for giving invaluable advice in the writing process of this paper.

REFERENCES

Alwmark C. and Schmitz B. (2009) Relict silicate inclusions in extraterrestrial chromite and their use in the classification of fossil chondritic material. *Geochim. Cosmochim. Acta* **73**, 1472-1486.

Anders E. and Grevesse N. (1989) Abundances of the elements – meteoritic and solar. *Geochim. Cosmochim. Acta* **53**, 197-214.

Andersson P. S., Wasserburg G. J. and Ingri J. (1992) The sources and transport of Sr and Nd isotopes in the Baltic sea. *Earth Planet. Sci. Lett.* 113, 459-472.

Bergström S. M., Chen X., Gutiérrez.Marco J. C. and Dronov A. (2009) The new chronostratigraphic classification of the Ordovician System and its relations to major regional series and stages and to $\delta^{13}C$ chemostratigraphy. *Lethaia* 42, 97-107.

Bevan A. W. R., Bland P. A. and Jull A. J. T. (1998) Meteorite flux on the Nullarbor region, Australia. *Geol. Soc. London Spec. Publ.* 140, 59-73.

Bland P. A. (2001) Quantification of meteorite infall rates from accumulations in deserts, and meteorite accumulations on Mars. In *Accretion of extraterrestrial matter throughout Earth's history* (eds. B. Peucker-Ehrenbrink and B. Schmitz). Kluwer Academic/Plenum Publishers, New York, pp. 267-303.

Bridges J. C., Schmitz B., Hutchison R., Greenwood R. C., Tassinari M. and Franchi I. A. (2007). Petrographic classification of mid-Ordovician fossil meteorites from Sweden. Meteorit. *Planet. Sci.* 42, 1781-1789.

Brownlee D. E. Bate B. A. and Wheelock M. (1984). Extraterrestrial platinum group nuggets in deep sea sediments. *Nature* 309, 693-695.

Chen J. -Y. and Lindström M. (1991) Cephalopod septal strength indices (SSI) and depositional depth of Swedish Orthoceratite limestone. *Geol. Paleontol.* 25, 5-18.

Chen C., Taylor S. and Sharma M. (2005) Iron and osmium isotopes from stony micrometeorites and implications for the Os budget of the ocean. *LPSC* XXXVI, 2134 (abstract).

Cohen A. S., Coe A. L., Bartlett J. M. and Hawkesworth C. J. (1999) Precise Re-Os ages of organic-rich mudrocks and the Os isotopic composition of Jurassic seawater. *Earth Planet. Sci. Lett.* 167, 159-173.

Colodner D. C., Boyle E. A., Edmond J. M. and Thomson J. (1992) Post-depositional mobility of platinum, iridium and rhenium in marine sediments. *Nature* 358, 402-404.

Cronholm A. and Schmitz B. (2009) Extraterrestrial chromite distribution across the Puxi River section, central China: Evidence for a global major spike in flux of L-chondritic matter during the mid-Ordovician. *Submitted*.

Dalai T. K. and Ravizza G. (2006) Evaluation of osmium isotopes and iridium as paleoflux tracers in pelagic carbonates. Geochim. Cosmochim. Acta **70**, 3928-3942.

Dalai T. K., Ravizza G. E. and Peucker-Ehrenbrink B. (2006) The Late Eocene 187Os/188Os excursion : Chemostratigraphy, cosmic dust flux and the Early Oligocene glaciation. Earth Planet Sci. Lett. **241**, 477-492.

Dia A. N., Cohen A. S., Onions R. K. and Shackleton N. J. (1992) Seawater Sr isotope variation over the past 300 kyr and influence of global climate cycles. *Nature* **356**, 786-788.

Dyer B. D., Lyalikova N. N., Murray D., Doyle M., Kolesov G. M. and Krumbein W. E. (1989) Role of microorganisms in the formation of iridium anomalies. Geology **17**, 1036-1039.

Esser B. K. and Turekian K. K. (1988) Accretion rate of extraterrestrial particles detemined from osmium isotope systematics of Pacific pelagic clay and manganese nodules. Geochim. Cosmochim. Acta **52**, 1383-1388.

Esser B. K. and Turekian K. K. (1993) The osmium isotopic composition of the continental crust. Geochim. Cosmochim. Acta **57**, 3093-3104.

Faure G. (1986) Principles of Isotope Geology, 2nd edn. Wiley, New York, 608pp.

Greenwood R. C., Schmitz B., Bridges J. B., Hutchison R. and Franchi I. A. (2007) Disruption of the L-chondrite parent

body: New oxygen isotope evidence from Ordovician relict chromite grains. *Earth Planet. Sci. Lett.* **262**, 204–213

Haack H., Farinella P., Scott E. R. D. and Keil K. (1996) Meteoritic, asteroidal, and theoretical constrains on the 500 Ma disruption of the L-chondrite parent body. *Icarus* **119**, 182-191.

Häggström T. and Schmitz B. (2007) Distribution of extraterrestrial chromite in Middle Ordovician Komstad Limestone in the Killeröd quarry, Scania, Sweden. *Bull. Geol. Soc. Denm.* **55**, 37-58.

Hassler D. R., Peucker-Ehrenbrink B. and Ravizza G. (2000) Rapid detemination of Os isotopic composition by sparging OsO4 into a magnetic-sector ICP-MS. *Chem. Geol.* **166**, 1-14.

Heck P. R., Schmitz B., Bauer H., Halliday A. N. and Wieler R. (2004) Fast delivery of meteorites to Earth after a major asteroid collision 480 Myr. *Nature* **430**, 323-325.

Heck P. R., Schmitz B., Baur H. and Wieler R. (2008) Noble gases in fossil micrometeorites and meteorites from 470 Myr old sediments from southern Sweden, and new evidence for the L-chondrite parent body breakup event. *Meteorit. Planet. Sci.* **43**, 517-528.

Hodell D. A., Mead G. A. and Mueller P. A. (1990) Variation in the strontium isotopic composition of seawater (8 Ma to present): implications for chemical weathering rates and dissolved fluxes to the oceans. *Chem. Geol.* **80**, 291–307.

Koeberl C. and Shirey S. B. (1997) Re-Os isotope systematics as a diagnostic tool for the study of impact and distal ejecta. *Palaeogeo. Palaeoclim. Palaeoeco.* **132**, 25-46.

Korochantseva E. V., Trieloff M., Lorenz C. A., Buykin A. I., Ivanova M. A., Schwarz W. H., Hopp J. and Jessberger E. K. (2007) L-chondrite asteroid breakup tied to Ordovician meteorite shower by multiple isochron ^{40}Ar-^{39}Ar dating. *Meteorit. Planet. Sci.* **42**, 113-130.

Korochantsev A. V., Lorenz C. A., Ivanova M. A., Zaytsev A. V., Kononkova N. N. Roshina I. A., Korochantseva E.V. and Sadilenko D. A. (2009) Sediment-dispersed extraterrestrial chromite in Ordovician limestone from Russia. *Lunar. Planet. Sci.* **XL**, 1101 (abstract).

Lal D. and Jull A. J. T. (2003) Extraterrestrial influx rates of cosmogenic isotopes and platinum group elements: Realizable geochemical effects. *Geochim. Cosmochim. Acta* **67**, 4925–4933.

Levasseur S., Birck J.-L. and Allègre C. J. (1998) Direct measurement of femtomoles of osmium and the 187Os/186Os ratio in seawater. *Science* **282**, 272-274.

Levasseur S., Birck J. –L. and Allègre C. J. (1999) The osmium riverine flux and the oceanic mass balance of osmium. *Earth Planet. Sci. Lett.* **174**, 7-23.

Lindström M. (1971) Vom Anfang, Hochstand und Ende eines Epikontinentalmeeres. *Geologische Rundschau* **60**, 419–438.

Lindström M. (1979) Diagenesis of Lower Ordovician hardgrounds in Sweden. *Geol. Paleont.* **13**, 9-30.

Löfgren A. (2003) Conodont faunas with Lenodus variabilis in the upper Arenig to lower Llanvirnian of Sweden. *Acta Palaeont.* **48**, 417-436.

Love S. G. and Brownlee D. E. (1993) A direct measurement of terrestrial mass accretion rate of cosmic dust. *Science* **262**, 550-553.

Meisel T., Biino G. G. and Nägler T. F. (1996) Re-Os, Sm-Nd, and rare earth element evidence for Proterozoic oceanic and possible subcontinental lithosphere in tectonized ultramafic lenses from the Swiss Alps. *Geochim. Cosmochim. Acta* **60**, 2583–2593.

Meisel T., Walker R. J., Irving A. J. and Lorand J-P. (2001) Osmium isotopic compositions of mantle xenoliths: A global perspective. *Geochim. Cosmochim. Acta* **65**, 1311–1323.

Oxburgh R. (1998) Variations in the osmium isotope composition of sea water over the past 200,000 years. *Earth Planet. Sci. Lett.* **159**, 183-191.

Peucker-Ehrenbrink B. (1996) Accretion of extraterrestrial matter during the last 80 million years and its effect on the marine osmium isotope record. *Geochim. Cosmochim. Acta* **60**, 3187-3196.

Peucker-Ehrenbrink B. (2001) Iridium and osmium as tracers of extraterrestrial matter in marine sediments. In *Accretion of extraterrestrial matter throughout Earth's history* (eds. B. Peucker-Ehrenbrink and B. Schmitz). Kluwer Academic/Plenum Publishers, New York, pp. 163-178.

Peucker-Ehrenbrink B. and Ravizza G. (2000a) The effects of sampling artifacts on cosmic dust flux estimates: A reevaluation of nonvolatile tracers (Os, Ir). *Geochim. Cosmochim. Acta* **64**, 1965-1970.

Peucker-Ehrenbrink B. and Ravizza G. (2000b) The marine osmium isotope record. *Terra Nova* **12**, 205-219.

Peucker-Ehrenbrink B. and Jahn B. –M. (2001) Rhenium-Os-

mium isotiope systematics and platinum group element concentrations: leoss and the upper continental crust. *Geochem. Geophys. Geosys.* **2**, paper 2001GC000172.

Peucker-Ehrenbrink B., Ravizza G. and Hoffmann A. W. (1995) The marine $^{187}Os/^{186}Os$ record of the past 80 million years. *Earth Planet. Sci. lett.* **130**, 155-167.

Peucker-Ehrenbrink B., Bach W., Hart S. R., Blusztajn J. S. and Abbruzzese T. (2003) Rhenium-osmium isotope systematics and platinum group element concentrations in oceanic crust from DSDP/ODP Sites 504 and 417/418. *Geochem. Geophys. Geosys.* **4**: art. No. 8911.

Qing H., Barnes C., Buhl D. and Veizer J. (1998) The strontium isotopic composition of Ordovician and Silurian brachiopods and conodonts: Relationships to geological events and implications for coeval seawater. *Geochim. Cosmochim. Acta* **62**, 1721-1733.

Ravizza G. (2007) Reconstructing the marine $^{187}Os/^{188}Os$ record and the particulate flux of meteoritic osmium during the late Cretaceous. *Geochim. Cosmochim. Acta* **71**, 1355-1369.

Ravizza G. and Turekian K. K. (1992) The osmium isotopic composition of organic-rich marine sediments. *Earth Planet. Sci. Lett.* **110**, 1-6.

Ravizza G., Martin C. E., German C. R. and Thompson G. (1996) Os isotopes as tracers in seafloor hydrothermal systems: metalliferous depositis from the TAG hydrothermal area, 26°N Mid-Atlantic Ridge. *Earth Planet. Sci. Lett.* **138**(1-4), 105-119.

Schmitz B. and Häggström T. (2006) Extraterrestrial chromite in Middle Ordovician marine limestone at Kinnekulle, southern Sweden – Traces of a major asteroid breakup event. *Meteorit. Planet. Sci.* **41**, 455-466.

Schmitz B., Lindström M., Asaro F. and Tassinari M. (1996) Geochemistry of meteorite-rich marine limestone strata and fossil meteorites from the lower Ordovician at Kinnekulle, Sweden. *Earth Planet. Sci. Lett.* **145**, 31-48.

Schmitz B., Peucker-Ehrenbrink B., Lindström M. and Tassinari M. (1997) Accretion rates of meteorites and cosmic dust in the Early Ordovician. *Science* **278**, 88-90.

Schmitz B., Tassinari M. and Peucker-Ehrenbrink B. (2001) A rain of ordinary chondritic meteorites in the early Ordovician. *Earth Planet. Sci. Lett.***194**, 1-15.

Schmitz B., Häggström T. and Tassinari M. (2003) Sediment-dispersed extraterrestrial chromite traces a major asteroid disruption event. *Science* **300**, 961-964.

Schmitz B., Peucker-Ehrenbrink B., Heilmann-Clausen C., Åberg G., Asaro F., and Lee C. -T. A. 2004. Basaltic explosive volcanism, but no comet impact, at the Paleocene–Eocene boundary: highresolution chemical and isotopic records from Egypt, Spain and Denmark. *Earth Planet. Sci. Lett.* **225**, 1–17.

Sharma M. and Wasserburg G. J. (1997) Osmium in the rivers. *Geochim. Cosmochim. Acta* **61**, 5411-5416

Sharma M., Papanastassiou D. A. and Wasserburg G. J. (1997) The concentration and isotopic composition of osmium in the oceans. *Geochim. Cosmochim. Acta* **61**, 3287-3299.

Sharma M., Wasserburg G. J., Hoffman A. W. and Chakrapani G. J. (1999) Himalayan uplift and osmium in oceans and rivers. *Geochim. Cosmochim. Acta* **63**, 4005-4012.

Sharma M., Balakrishna K., Hofmann A. W. and Shankar R. (2007a) The transport of Osmium and Strontium isotopes through a tropical estuary. *Geochim. Cosmochim. Acta* **71**, 4856-4867.

Sharma M., Rosenberg E. J. and Butterfield D. A. (2007b) Sea Search for the proverbial mantle osmium sources to the oceans: Hydrothermal alteration of mid-ocean ridge basalt. *Geochim. Cosmochim. Acta* **71**, 4655-4667.

Smoliar M. I., Walker R. J. and Morgan J. W. (1996) Re–Os ages of group IIA, IIIA, IVA and IVB iron meteorites. *Science* **271**, 1099– 1102.

Tinn O. and Meidla T. (2001) Middle Ordovician ostracods from the Lanna and Holen limestones, south-central Sweden. *GFF* **123**, 129–136.

Villumsen J., Nielsen A. T. and Stouge S. (2001) The trilobite and conodont biostratigraphy of the upper Volkhov-lower Kunda deposits at Hällekis quarry, Västergötland, Sweden. Working group on the Ordovician geology of Baltoscandia-2001. Copenhagen: Geological Museum. pp. 30–31 (abstract).

Widom E., Gaddis S. J. and Wells Jr. N. E. (2004) Re-Os isotope systematics in carbonates from Serpent Mound, Ohio: Implications for Re-Os dating of crustal rocks and the osmium isotopic composition of Ordovician seawater. *Geochem. Geophys. Geosys.* **5**, Q03006.

Woodhouse O. B., Ravizza G., Kenison-Falkner K. and Peucker-Ehrenbrink B. (1999) Osmium in seawater: Vertical profiles of concentration and isotopic composition in the eastern Pacific Ocean. *Earth Planet. Sci. Lett.* **173**, 223-233.

Yamashita Y., Takahashi Y., Haba H., Enomoto S. and Shimizu

(2007) Comparison of reductive accumulation of Re and Os in seawater-sediment systems. *Geochim. Cosmochim. Acta* **71**, 3458-3475.

Zhang J. (1998) Middle Ordovician conodonts from the Atlantic Faunal Region and the evolution of key conodont genera. Thesis, *Meddelanden från Stockholms Universitets Institution för Geologi och Geokemi* 298, 1-27.